THE ISOMERIZATION AND STEREOCHEMISTRY OF SOME IRIDIUM HYDRIDE COMPLEXES

by

© William John Yorke
B.Sc., Saint Joseph's University, 1973

A Thesis submitted to the Faculty of Graduate Studies and Research in partial fulfillment of the requirements for the degree of Doctor of Philosophy

Department of Chemistry
McGill University
Montreal, Quebec

November 1979

Chemistry Ph.D.

THE ISOMERIZATION AND STEREOCHEMISTRY OF SOME IRIDIUM HYDRIDE COMPLEXES

William John Yorke

ABSTRACT

Samples of fac and mer carbonyltrihydridobis(triphenylphosphine)iridium (III) were prepared and fully characterized by i.r., ^{1}H and ^{31}P n.m.r. spectroscopies. Isomeric interconversion at 25°C was demonstrated. The rates of isomerization and hydrogen loss from each isomer were independently measured. The similarity of these rates strongly supports a mechanism by which isomerization occurs through the oxidative addition and reductive elimination of molecular hydrogen. The results of deuterium labelling experiments were consistent with the isomerization mechanism, and further suggest that either trans-oxidative addition of hydrogen or intramolecular hydride interchange in the mer isomer may occur. Various partially deuterated analogues of the fac and mer isomer were formed by further reaction in solution and identified in the ^{1}H n.m.r. spectrum. An unusual downfield isotope shift occurred when deuterium was in a position trans to hydride.

Chimie Ph.D.

L'ISOMERISATION ET LA STEREOCHIMIE DE QUELQUES COMPLEXES HYDROGENO IRIDIUM

William John Yorke

RESUME

Des échantillons des isomères fac et mer du trihydrogéno-carbonylbis(triphénylphosphine)iridium(III) ont été préparés et entièrement caractérisés par spectroscopies infra-rouge et r.m.n. (^{1}H et ^{31}P). La conversion isomérique a été démontrée à 25°C. Les vitesses de l'isomérisation et de la perte d'hydrogène ont aussi été mesurées indépendamment pour chaque isomère. La similitude de ces vitesses corroborent parfaitement un mécanisme par lequel l'isomérisation se produit par l'addition oxydante et l'élimination réductrice de l'hydrogène moléculaire. Les résultats des expériences utilisant le deutérium comme traceur sont en accord avec ce mécanisme d'isomérisation et suggèrent en plus qu'il peut être dû, ou bien à, l'addition oxydante trans de l'hydrogène, ou bien à l'échange intramoléculaire d'un hydrure dans l'isomère mer. Divers autres analogues deutérés des isomères fac et mer sont aussi formés par de subséquentes réactions en solution et ont été identifiés sur le spectre r.m.n. (^{1}H). Un déplacement isotopique inhabituel vers un plus faible champ se produit lorsque le deutérium était en position trans par rapport à l'hydrure.

To Louise

ACKNOWLEDGEMENTS

The financial support received from the Dow-Corning Corporation in 1973-74 and from McGill University in subsequent years is gratefully acknowledged.

I would like to thank my research director, J.F. Harrod, for his advice and patience throughout the course of this work. I am also grateful to Doctors Alan Shaver, Ian Butler, D.F. Gilson, Russ Hughes and J. Paul Fawcett for helpful discussions and guidance. I am especially indebted to Doctors Gordon Hamer and Bill Dawson for obtaining many n.m.r. spectra under difficult conditions, and for much help in the interpretation of the spectra.

I am thankful for the friendship and encouragement of all the members of lab 435. For help in preparing and proof-reading this thesis, I am particularly grateful to Michel Drouin, Susan Quinn, Rabin Lai, Jim McCall, Paul Fitzpatrick, Ann English and Jacqueline Svedman. The expert typing of Assunta Cerrone is likewise appreciated.

I am very grateful to my parents for unfailing encouragement and understanding over many years.

I would like most of all to thank my wife Louise for constant and indispensable support, given in many ways and in many forms.

La raison agit avec lenteur, et avec tant de vues, sur tant de principes, lesquels il faut qu'ils soient toujours présents, qu'à toute heure elle s'assoupit ou s'égare, manque d'avoir tous ses principes présents.

- Pascal

TABLE OF CONTENTS

APPENDICES

LIST OF FIGURES

LIST OF TABLES

LIST OF SCHEMES

LIST OF ABBREVIATIONS

P	triphenylphosphine
fac	facial
mer	meridional
ϕ	phenyl
dp	1,2-bis(diphenylphosphine)ethane
S	solvent molecule
Et	ethyl
DMF	N,N-dimethylformamide
i.r.	infra-red (spectroscopy)
n.m.r.	nuclear magnetic resonance (spectroscopy)
D	deuterium
THF	tetrahydrofuran
NR	no reaction

CHAPTER I

GENERAL INTRODUCTION

Although the subject of this thesis, the formation and interconversion of two isomers of $IrH_3(CO)\ P_2$* is itself a rather limited one, the results reported herein bear some relation to three important areas of research: the behavior of transition metal hydrides, the interaction of molecular hydrogen with metal centers, and the stereochemistry of key steps in homogeneous catalytic processes. In order to examine this relation and so put this research in perspective, a general overview of the fields of transition metal hydrides and the oxidative addition of hydrogen to metal centers is given. A brief introduction to these large and much-studied fields cannot be complete even in outline; I have merely tried to mention those aspects which I felt to be interesting, important, or relevant. However, the concluding section gives a fairly complete history of the particular compounds that I have studied.

---

*Here and throughout this thesis, P = $P(C_6H_5)_3$

A. TRANSITION METAL HYDRIDES

1. General Comments

Transition metal hydrides comprise an area of chemistry that presently is receiving a great deal of attention among researchers. This is due to both the diversified and interesting chemistry that has been reported in this field, much of it in the last twenty years, and also to the proven or potential value of metal hydrides in areas of technological importance, such as catalysis and energy storage.

Two sorts of compounds containing hydrogen-transition metal bonds may be distinguished. One type, which here will be called metal hydrides, are also known as primary or binary hydrides (of formula MH_x), or ternary hydrides (of formula $M'MH_x$, with M' often an alkali metal). They are often formed directly by reaction of hydrogen with the metal, contain metal hydrogen bonds, and exist in molecular aggregates of indefinite size and, sometimes, indefinite stoichiometry. A second type, here called hydride complexes, consists of discrete molecular units, which may be isolated, fully characterized, and systematically and reproducibly investigated with regard to their chemistry and structure by the standard chemical and physical techniques[1]. The latter type, then, is more amenable to detailed scientific study.

Metal hydrides are of great current interest to technology

in various applications, such as nuclear reactor applications, powder metallurgy, surface coating, metal-ceramic bonds[2], and energy storage. Hydride complexes are also technologically useful in themselves as homogeneous catalysts and as reagents in chemical synthesis.

2. Historical Survey

The first compound containing a transition metal-hydrogen bond was reported in 1844 by Wurtz[3], who isolated the unstable binary hydride CuH. Hydrides of non-transition metals were developed in subsequent years; for example, CaH_2 was patented as early as 1902 for use as a portable hydrogen source for filling gas balloons, an application for which it was used extensively during the Second World War[4]. The ability of palladium to absorb large amounts of hydrogen has been known since 1866[5,6].

The first transition metal hydride complexes were prepared in the early 1930's by Heiber and co-workers, who isolated the unstable $FeH_2(CO)_4$ and $CoH(CO)_4$[7]. Hydrides were reported with increasing frequency after cyclopentadienyl hydrides[8] and tertiary phosphine hydrides[9] were prepared in the mid-fifties. The rapid development of this field is illustrated by the fact that in 1965, there were about 200 hydride complexes known; by 1970, 500 additional complexes were reported[10].

Interest in these compounds has been sustained by their availability, structural features, and by their applicability to many chemical processes, especially catalysis. Many more complexes have since appeared. A recent (1977) review[11] of three metals important to catalysis (Ru, Rh and Ir), for example, listed over 2000 hydride complexes[12]. At least that number of complexes in addition can be expected for the remaining transition metals. Besides increasing in number, transition metal hydride complexes have shown an increasing variety of structures, with cluster compounds, hydride-bridged structures, and metallocyclic structures among the hydrides now commonly reported.

3. Transition Metal Hydrides

Metal hydrides of the transition elements are usually metallic or semi-metallic solids. They resemble metals in thermal and electrical conductivity, but are often non-lustrous and brittle[13,14]. In some cases, particularly among the lanthanides and actinides, the hydrides are black powders. There are examples of binary hydrides of formula MH_x, with x not necessarily an integer, for most elements of the periodic table. They are generally formed by direct interaction of the metal with hydrogen. Examples include nearly all the rare earth metals, and most of the early transition elements[14],

such as the scandium, titanium and vanadium subgroups, as well as chromium, although the latter system has not been definitively characterized[15,16]. The later, more electron-rich transition metals, however, do not form binary hydrides with hydrogen (with the exception of palladium and possibly nickel[17]), despite the fact that many of these metals can activate hydrogen, and are useful in catalytic hydrogenations[15]. Nonetheless, many of the later transition metals will form ternary hydrides[18]. Some gaseous diatomic hydrides, although unstable in the massive state, have been detected spectroscopically; among these are Mn-H, Fe-H and Co-H[15].

The nature of the bonding in binary transition metal hydrides is still not completely clear. Internuclear distances are sufficiently close to allow covalent bonding, with a bond polarity in the direction of M^+-H^- [15]. Nevertheless, the bonding in transition metal hydrides is more often described in terms of metallic conduction bands, with the hydrogen present interstitially in the metal lattice either as H^+ (the metal hydrides are in this case described as metallic or alloys) or H^- (often called ionic hydrides). Some experimental measurements of the mobility of hydrogen, magnetic susceptibility, and the migration of hydrogen toward the cathode in an electric field favor the protonic description, whereas internuclear M-H distances, heats of formation of the hydrides, and the co-existence of hydrogen and oxygen simultaneously in metal

hydrides suggest that the hydridic description is preferable. Of the two, the latter model appears to be the more successful in accounting for experimental results. It has been pointed out[15], however, that a covalent description of the M-H bond (given a certain amount of $M^{+}-H^{-}$ polarity) accounts for the physical properties of the hydrides as well as an ionic model.

The indefinite nature of bonding theories for metal hydrides arises in part from the fact that they cannot be isolated and characterized as discrete units, as hydride complexes can be. For this reason, hydride complexes can serve as model compounds to aid in the understanding of reactivity and bonding in the less-tractable metal hydrides. This is particularly true for metal cluster hydrides, which often have features such as bridged hydride ligands, or hydrides encaged in metal atoms[20]. The similarity to metallic hydrides has recently been pointed out in studies of the oxidative addition of hydrogen[15,21] to a solid complex, molecular orbital studies on polyhydride ions[22], and structural studies of cluster complexes[23]. In a recent article, many parallels have been drawn between coordination chemistry and surface chemistry[24]. It is hoped that a unified view of the two areas will soon be available for transition metal hydrides.

4. Hydride Complexes of the Transition Metals

Most hydride complexes that have so far been isolated have

been mono-nuclear metal complexes, although there is a large and rapidly growing number of binuclear, hydride-bridged, and cluster complexes as well. Hydride complexes are generally diamagnetic solids, often highly colored (depending to some extent on the oxidation state), and of variable stability towards light, air, and heat; some complexes can only be isolated at low temperature under nitrogen, while others are stable indefinitely in air at elevated temperatures. The hydride ligand is usually identified by the M-H stretching frequency in the infrared spectrum (ν_{M-H}, 1700-2300 cm^{-1}; $\nu_{M-D} = \nu_{M-H}/1.4$; ν_{M-H-M} (bridged) = ca. 1000-2000 cm^{-1}; δ_{M-H}, 700-950 cm^{-1})[25], and by the high field chemical shift in the proton n.m.r. spectrum (δ 0 to -50 ppm [τ 10 to 60 ppm]; the usual range is δ -5 to -20 ppm [τ 15 to 30 ppm]). The structures of transition metal hydrides are usually assigned by the use of one or both of these techniques.

Transition metal hydride complexes have received a great deal of attention in the last twenty years, paralleling the development of organometallic preparative techniques, the widespread use of i.r. and n.m.r. spectroscopies, and structural determinations by the various diffraction techniques. Molecular hydride complexes containing only hydride ligands are unusual, and, with the exception of the $[ReH_9]^{2-}$ and $[TcH_9]^{2-}$ systems[26], are unstable. However, thousands of transition metal hydride complexes, many of which are air-stable at room

temperature, have been prepared containing other ligands. Particularly useful in this regard are ligands of the "π-acid" type (such as tertiary phosphine, carbonyl, nitrosyl, cyclopentadienyl, etc.) which stabilize low oxidation states. A recent review[11], for example, listed over five hundred hydride complexes for iridium alone. There have been several reviews of hydride complexes in the last fifteen years[1,10,11,26-31].

Mono-nuclear hydride complexes of the transition metals exhibit more or less similar structural characteristics to other complexes. They often adopt octahedral or other common geometries and usually have normal metal-hydrogen bond lengths. They differ structurally from other complexes in a tendency to distort in the presence of larger ligands, to have unusually high coordination numbers (e.g., $IrH_5(P\phi_3)_2$, or $[ReH_9]^{2-}$), and to be stereochemically non-rigid. Recent structural studies[32] on bridged hydrides have located the hydride ligands by neutron-diffraction methods, and shown that they exert considerable stereochemical influence on the molecules. Species where the hydride is doubly or triply bridging have been isolated: doubly bridging binuclear compounds (e.g., $[Pt(\underline{\mu}_2\text{-H})(SiEt_3)\{P(C_6H_{11})_3\}]_2$[33]) or cluster compounds (e.g., $Os_3(\underline{\mu}_2\text{-H})(H)(CO)_{11}$[34]) have been prepared, as well as triply-bridging hydrides, such as one having μ_3-hydride ligands occupying the face of an Ru_6 octahedron, $Ru_6(\underline{\mu}_3\text{-H})_2(CO)_{18}$[34].

The position of the hydride as a ligand has undergone

various interpretations through the years[34]. Before 1960, the hydride ligand was generally regarded as unlike other ligands and as having a very short metal-hydrogen bond length. It was even viewed as a proton floating in a sea of metal electrons, and not occupying a regular site in the coordination sphere. This model was discarded when structural studies showed that the hydride ligand did occupy a regular coordination position, and that the metal-hydride bond length was entirely normal. Recently, this viewpoint was further modified to accommodate findings that in the presence of many bulky ligands, the stereochemical influence of the hydride ligand on the coordination polyhedron is almost nil. In $RhHP_4$, for example, the phosphine ligands adopt a nearly tetrahedral coordination around the metal atom[35]. Similarly, in the "monocapped" octahedron, $MoH(CO)_2dp_2$,[36] the carbonyl and phosphine ligands form an octahedron, whereas the hydride ligand migrates from face to face, and exerts little stereochemical influence. Indeed, the fluxionality that is often observed in these complexes and in polyhydride complexes may derive to some extent from distortions from a regular geometry brought about by the presence of other, invariably larger ligands in the coordination sphere. In any case, the status of hydride as a ligand still may be regarded as similar to that of other ligands, even though more compressible and prone to migrate.

5. Applications of Transition Metal Hydrides

a) Metal Hydrides

Metal hydrides in general are useful in nuclear reactor applications due to their ability to absorb neutrons. Other applications include deoxidation agents for molten alloys and portable hydrogen sources, as well as uses in powder metallurgy, alloying, surface coating on metals, and in forming metal-ceramic bonds. Titanium and zirconium hydrides find the most use in these fields.

On both a laboratory and industrial scale, hydrogenations using heterogeneous transition metal catalysts have become commonplace. They are usually a platinum group metal, especially platinum or palladium, with nickel and copper chromite also used, particularly for high-pressure hydrogenations. The metals are generally used in a finely divided form, often supported on an inert carrier, either in elemental form or reduced in situ from their salts. The catalysis is largely a surface phenomenon and probably involves an unsaturated organic compound adsorbed on the surface in the proximity of hydrogen activated by interaction with the metal. Most common unsaturated organic groups, such as alkenes, carbonyls, esters, nitriles and nitro compounds, as well as aromatic groups, may be hydrogenated under certain conditions using heterogeneous catalysts[37].

b) Hydride Complexes

Two of the most important aspects of transition metal hydride complexes are their use as homogeneous catalysts, and their role as intermediates in catalytic processes involving hydrogen and hydro-functional compounds, such as hydrogenation, hydrosilation and hydroformylation of olefins, as well as other catalytic processes[38]. The ability of transition metal complexes to function as catalysts for these processes is largely a result of their ability to coordinate unsaturated compounds, to activate molecular hydrogen, or to form metal hydrides as intermediates. Consequently, it is not surprising that so many homogeneous catalytic processes involve metal hydride complexes. Examples of catalytic processes involving the oxidative addition of hydrogen and metal-hydride intermediates follow.

i) Hydrogenation of olefins[39,40]:

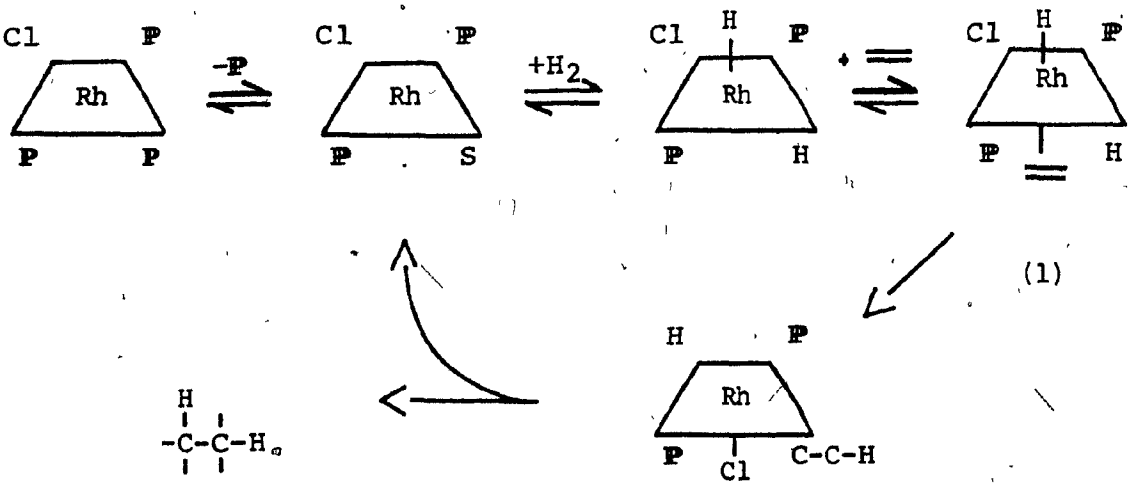

Here, molecular hydrogen adds oxidatively to an unsaturated molecule to form a metal dihydride complex. The coordination of an alkene follows, and the subsequent hydrogenation of the alkene and regeneration of the catalyst apparently involve intramolecular rearrangement of various transition metal hydride intermediates. The stereochemistry of the oxidative addition, as well as that of the subsequent rearrangement, is obviously important in determining the course of the reaction. This fact has been exploited in order to effect the stereospecific hydrogenation of certain substrates. For example, hydrogenations employing asymmetric analogues of Wilkinson's catalyst have led to the synthesis of α-amino acids and other biologically important materials in high optical yields[40]. Catalysts used in these reactions are similar to Wilkinson's catalyst (equation 1), but contain chiral phosphine ligands. This and similar applications of asymmetric catalysis represent an extremely active field of current research, and present a clear example of the importance of stereochemistry to catalysis.

ii) Hydroformylation of olefins[43]: In the example shown below, in which hydrogen, carbon monoxide, and an olefin react to form an aldehyde, the oxidative addition of hydrogen again plays an essential role in activating hydrogen in the form of a metal dihydride. Five of the eight metal complexes thought to be involved in this catalytic cycle are metal hydride complexes.

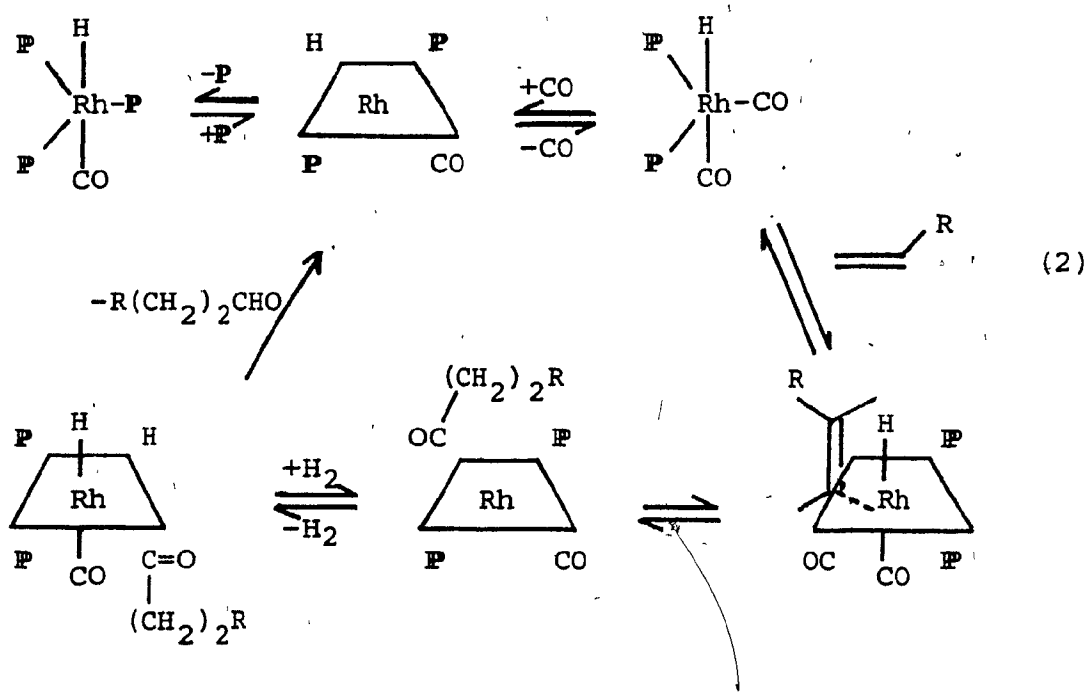

Other reactions involving homogeneous catalysis which do not include activation of hydrogen by metals, but do involve hydrido-species as intermediates, are mentioned below.

iii) Hydrosilation of olefins: The hydrosilation of olefins is a process in which a silyl group may be added catalytically to an olefin[38,41,42]. It is in many ways similar to the hydrogenation of olefins, the main difference being the fact that an Si-H bond is activated by oxidative addition to the metal center, rather than an H-H bond. There has been considerable work done on the mechanism and energetics involved in the reaction using model systems[44,45].

iv) Alkene isomerization: The isomerization of alkenes can be catalyzed by transition metal complexes through a process of reversible olefin coordination to a coordinatively unsaturated metal hydride complex, followed by the formation of a metal alkyl species. Isomerization also occurs by hydride abstraction from an olefin to yield an allyl metal hydride complex. In either case, the reverse reaction can result in hydrogen-atom exchange, double-bond migration, and cis/trans isomerization[38].

v) Other applications: Other industrially important processes involve metal hydride intermediate complexes. The Dupont synthesis of 1,4-hexadiene, an ingredient in rubber manufacture, is accomplished via hydride intermediates formed when ethylene and butadiene react in the presence of a nickel or rhodium catalyst. The Wacker Process, in which ethylene is catalytically converted to acetaldehyde by a palladium/copper system, is believed to involve a metal hydride as an unstable intermediate. The water-gas shift, in which carbon monoxide and water react to produce hydrogen and carbon dioxide through catalysis by ruthenium clusters, probably involves metal-hydride intermediates[63]. In short, many, if not most, of the homogeneous catalytic cycles of proven or potential importance have a transition metal hydride complex present at some stage[38].

c) Energy Production and Storage

i) Reversible reaction of hydrogen with metals: Many metals react with molecular hydrogen exothermically, but the reaction can be reversed by heat at reasonable temperatures. The hydrides formed can contain more hydrogen per unit volume than liquid or solid hydrogen. These facts have resulted in a widespread interest in binary or ternary metal hydrides[47]. Properties considered necessary for a metal hydride to be useful in a practical energy storage system[48] include a high hydrogen to metal ratio, a low hydrogen-metal dissociation temperature (< 100°C) , high rates of hydrogen absorption and desorption, low enthalpy of formation, and air-stability. Also, they should be of low density and cost. Because no binary hydride possesses all of these qualities, recent research has attempted to find a more complex material that does[49]. Two main types[47] of hydrides have been investigated in this regard. One is simply an alloy or solid solution of two binary hydrides which would be expected to have properties intermediate between those of the two constituents. The other type of compound, the ternary hydrides, are reversibly formed from intermetallic compounds (which may or may not originally contain some hydrogen) and molecular hydrogen, and have properties that are quite different from substituent hydrides. In this group, one or both of the metals generally is a transition metal. There are many examples of ternary hydrides, and many metal combinations

have been studied, despite the fact that most transition metals do not themselves react with hydrogen to form binary hydrides. The inertness of some transition metals in this regard may result in desirable qualities in a ternary system, since when combined with a metal which forms hydrides easily, it serves to destabilize the system, and impart reversibility toward hydrogen absorption[50]. Among systems which have been studied[49] in this regard are Mg_2Cu, TiFeH, TiCuH, R_2Co_7, RCo_3, RFe_3, $LaNi_5$, $LaNi_{5-x}Al_x$, TiMoH, R_2RuH_6, $RRuH_6$, and $RIrH_x$, where R is a rare earth element.

ii) Transition metal complexes as models for hydrogen storage: Transition metal hydride complexes have been studied as models for binary and ternary hydride systems, often with a view toward application as energy storage systems. The oxidative addition of hydrogen to unsaturated complexes exhibits many similarities to the reversible adsorption of hydrogen by metals, as many workers have recognized[21,51]. Muetterties has recently drawn attention to the close parallel between the surface chemistry occurring when small molecules are adsorbed on metals, and traditional coordination chemistry[24]. Geoffroy et al. have made a series of studies[12,52,53] into the photochemistry of hydride complexes of Ir, Ru, and Mo that lose molecular hydrogen upon irradiation, and they have briefly reviewed the subject[12]. Green and co-workers also have conducted several studies[54,55,56] on the effects of irradiation

of cyclopentadienyl tungsten hydrides.

iii) Fuel production: The production of fuel from inexpensive feedstocks is of large and growing importance. Transition metal hydride complexes may play a central role in the development of this area in the future. One area in which they already play a large role is Fischer-Tropsch catalysis[57]. By this process, gasoline and related products are produced from a hydrogen/carbon monoxide mixture derived from coal. In South Africa, over two hundred thousand tons per year of primary products, much of it gasoline, have been produced by this process since 1957. Currently, heterogeneous iron-based catalysts are employed. The reaction is believed to involve metal hydridocarbonyl intermediates.

The water-gas shift (see above) is often used in tandem with the Fischer-Tropsch reaction to increase the hydrogen/carbon monoxide ratio in the feed gas. For both reactions, metal hydrocarbonyl complexes, similar to the ones that are the subjects of this thesis, have been studied as model compounds for key intermediates[57].

There are other areas of fuel production of unproven value but potential importance that are currently of interest to researchers. One such area is the transition metal catalyzed photolysis of water. The production of hydrogen and oxygen have been separately realized in homogeneous catalytic systems that use light as the source of energy. However, a system

where both reactions are part of a catalytic cycle has not yet been reported[58,59]. A heterogeneous system in which both hydrogen and oxygen were produced has been reported, but could not be reproduced[60,61]. The mechanisms of these reactions are thought to involve metal hydride complexes[62].

Another area of potential importance is the activation of water by transition metal complexes. The species $Pt[P(isopropyl)_3]_2$ is active in catalyzing a water-gas shift under mild conditions[63]. The key intermediate, $PtH(OH)-[P(isopropyl)_3]_2$, was later isolated and characterized[64]. Since metal complexes are capable of both activating water and eliminating molecular hydrogen, one may expect continued interest in these complexes as catalysts in energy-related fields.

6. Chemistry of Transition Metal Hydride Complexes

a) Preparation of Transition Metal Hydride Complexes

The various preparations of transition metal hydride complexes may be classified into the five types outlined and exemplified below. More complete details may be found in many reviews[1,10,11,26-31].

i) Reactions with molecular hydrogen: There are several ways in which transition metal complexes may react with molecular hydrogen. Direct hydrogenation is possible at high temperatures and pressure, with metal, ligand and hydrogen

combining to form a hydride complex. The complex $CoH(CO)_4$ can be synthesized in this way[65].

Hydrogen may also react with metal complexes at less extreme conditions by ligand substitution, or by oxidative addition of molecular hydrogen to unsaturated metal complexes. The role of the latter reaction in catalytic cycles has already been mentioned. The following example illustrates the two processes occurring in the same reaction[39]. Here, prior dissociation of the ligand forms a coordinate unsaturated complex (S represents a solvent molecule in the structure below), which then undergoes oxidative addition.

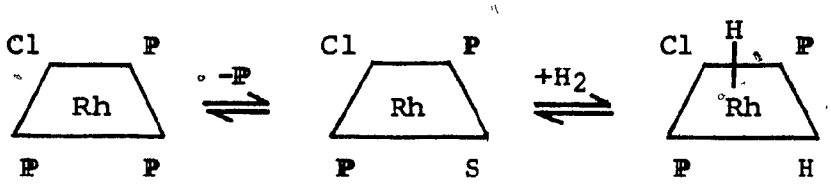

(3)

Other methods involving hydrogen are the reaction with metal salts, cleavage of metal-metal bonds, and cleavage of anionic ligands by hydrogen[66].

ii) Reaction with hydriding agents: The reaction of metal complexes with hydriding agents such as sodium borohydride or hydrazine to produce hydride complexes is probably the most useful preparative method[67]. The reactant metal complex is usually a halide, although other anionic ligands such as alkoxides, also react. Cationic metal complexes form hydrides

under these conditions also. Examples of this reaction may be found for nearly all the transition metals. A reaction of this type was used to prepare the trihydrides studied in this thesis.

Reactions employing hydriding agents are often convenient because, when carried out in the presence of excess ligand, they allow a one-step synthesis of hydridometal-ligand complexes. The use of $NaBH_4$ can result in the formation of metal-boro-hydride complexes; such complexes often exhibit structurally interesting features, such as bridging hydrides and fluxionality[68].

iii) Hydrogen transferred from other sources: Transition metal hydride complexes may be formed by hydrogen transfer from solvent, particularly alcohols[69]; organometallic reagents, such as metal alkyl or Grignard reagents[70]; oxidative addition of various groups of formula HL, such as Group IV hydrides[46], protonic acids[71] or hydrogen-sulfur compounds; or by intramolecular hydride transfer, such as the oxidative addition of a ligand C-H bond[72]. The addition of water to some transition metal anion, cation[73,74], or neutral complexes[64] can result in the formation of a hydride complex.

The addition of H^+ to coordinatively unsaturated complexes can also form hydrides. Depending on the nature of the counterion and the number of electrons and empty coordination sites on the metal complex, the counterion may coordinate as

well. This reaction then formally corresponds to the oxidative addition of HL.

b) Reactions of Transition Metal Hydrides Complexes

i) Comments on the stability and chemical reactivity of transition metal hydride complexes: Transition metal hydride complexes, particularly those of the "late" transition metals, are usually fairly stable with respect to temperature, oxygen, and water, presumably due to the covalent nature of the M-H bond. Many of these compounds are light sensitive, however[12]. Hydride complexes generally exhibit increasing stability down a triad. The most stable examples usually have 18-electron configurations stabilized by π-acid ligands[11].

ii) Trans-effect: The hydride ligand exhibits a high trans effect, and so increases the rate of dissociation, isomerization and substitution of trans ligands. For example, it has been shown[75] in $IrHX_2L_3$ complexes (where X = halogen and L = phosphine), the ligand trans to hydride will exchange preferentially to other ligands. According to one scale of the strength of the trans-effect[76], the hydride ligand is much higher than the halogens and many other common ligands: it is comparable to tertiary phosphine, and surpassed only by C_2H_4, CN^-, and CO. Unlike the latter group of ligands, however, the hydride ligand is unable to participate in π-bonding. It transmits its effect solely through σ-bonding,

which presumably polarizes and weakens the trans ligand-metal bond. One study[77] which attempts to separate π- and σ-influence in the trans effect lists hydride as the ligand with the largest σ-induced trans-effect of any common ligand.

iii) Elimination of hydrogen: Hydrogen is often reductively eliminated from di- or poly-hydride complexes. The reaction may be facilitated by heating , irradiation[53], an inert gas purge , or by the presence of excess free ligand[80]. For labile hydrides, any of these methods may be sufficient for hydrogen elimination; others require special conditions. Some complexes, for example, retain hydrogen upon heating but eliminate it upon irradiation[53]. Systems which can reversibly add and eliminate hydrogen have been studied as models for energy storage[12,51-56]. The elimination of molecular hydrogen is also essential for some catalytic processes, such as the water-gas shift[63]. The intramolecular metallation of a coordinated ligand may occur through M-H bond cleavage and elimination of hydrogen[72].

iv) Hydride transfer to coordinated ligand: The ability of transition metal hydride complexes to facilitate the attachment of hydrogen atoms onto coordinated ligands accounts for the importance of these compounds in catalysis. Various examples of hydride transfer in catalysis have been mentioned above.

v) Reaction with halides: Metal hydrides commonly react

with halogen-containing species, including halocarbon solvents. In some cases involving the latter, the result is exchange of H for Cl, Br and I. The reactivity of chloromethanes with metal hydrides increases in the order $CH_3Cl < CH_2Cl_2 < CHCl_3 < CCl_4$[78]. Besides exchange of halide, the oxidative addition of the solvent can occur as well[79].

Both hydrogen halides and halogens react with transition metal hydride complexes and generally exchange a halogen for a hydride ligand, thereby producing a metal halide complex, along with molecular hydrogen and hydrogen halide, respectively. The reaction with hydrogen halide is usually quantitative, and results in complete substitution by halide[82], although there are exceptions[81].

vi) Other reactions: Hydride complexes can undergo many other reactions, including thermolysis; intermolecular hydrogen exchange with solvents, especially water and alcohol, hydrogen or deuterium, and olefins; various acids and bases; alkali metals; and, of course, a variety of reactions which do not affect M-H bonds. The reactions of hydride complexes are covered more completely in several reviews[1,10,11,26-31].

B. OXIDATIVE ADDITION OF HYDROGEN TO TRANSITION METAL COMPLEXES

1. The Oxidative Addition Reaction

In oxidative addition reactions, all or part of a molecule

is added to the coordination sphere of a metal complex. The result is an increase in both the formal oxidation state of the metal, and the coordination number of the complex. Although reactions of this type have been known for a long time (for example, halogenation of a metal complex often is an oxidative addition), it is only in the last twenty years that this class of reactions has been systematically studied. The discovery of the reversible hydrogen and oxygen carrier, $Ir(CO)ClP_2$ by Vaska in 1961[83], and the realization that this and similar complexes displayed diverse chemistry, interesting stereochemistry and applications to biology and catalysis, resulted in widespread attention to the preparative and mechanistic aspects of oxidative addition. Several reviews now exist which report and classify examples, mechanisms and reactivity trends in oxidative addition[21,84-88].

The oxidative addition reaction is relevant to several areas of chemistry. In homogeneous catalysis, for example, the oxidative addition of a neutral molecule, such as hydrogen (see section A, part 5b), is often the single most important step, since it provides a means whereby a molecule with a high bond energy can react under mild conditions[86]. Some addition reactions of covalent molecules to transition metals, including reactions which are not formal oxidations, can be considered as models for certain biochemical reactions, such as the reversible binding of oxygen to haemoglobin[89-91]

and nitrogen-fixation[92,93]. An interesting example involving hydrides is the following reaction in which nitrogen is reversibly bound[94].

$$CoH(N_2)\,P_3 + H_2 \rightleftharpoons CoH_3\,P_3 + N_2 \qquad (4)$$

Attention has also been drawn to the similarity between the absorption of small molecules on a metal surface, and the oxidative addition of these molecules to metal complexes[95]. This relationship has been observed from the points of view of both coordination chemistry and surface chemistry. Accordingly, the resemblance between the reversible addition of hydrogen gas by Vaska's complex, and hydrogen chemisorption on metals has been noted[96]. On the other hand, the surface properties of metals containing adsorbed gases have been regarded in terms of metal-ligand coordination[24].

The simultaneous occurrence of oxidation and addition can be regarded as a reflection of the tendency of organometallic complexes to retain a set number of electrons in their coordination sphere[84]. Accordingly, the loss of electrons by oxidation is compensated by a gain of electrons through a rise in coordination number. For the same reason, the early transition metal complexes, with one to four d electrons, tend to have a larger coordination number than the later metal complexes of d^7-d^{10} electronic configuration.

Because its coordination number is already high, and steric factors preclude further increase, the former group shows little tendency to undergo oxidative addition. Consequently, metal complexes involved in oxidative addition usually have a d^7 to d^{10} electronic configuration, and so tend to be Group VIII metals.

The oxidative addition reaction is promoted by low initial oxidation state, high metal basicity, and unsaturation in the coordination sphere. While steric effects account for the third tendency, the other two simply reflect the fact that complexes with the greatest electron density are the most likely to undergo reactions which decrease it. For any given series of complexes, the rate of oxidative addition is increased by the substitution of basic, electron-donating ligands. It follows that the ideal candidates for oxidative addition are Group VIII metal complexes in low oxidation states, having both strongly-bound, electron-donating ligands, such as alkyl phosphines, and either empty coordination sites, or loosely-bound, labile ligands, such as a solvent molecule.

Kinetic studies have been carried out on a number of complexes in order to determine the effects of various electronic and steric factors on the rate of oxidative addition. The usual approach has been to compare the rate of reaction observed upon the systematic variation of a ligand in a series of analogous compounds. The kinetics and thermodynamics of

analogues of Vaska's compound, $Ir(CO)XL_2$, with X = halogen or other electronegative group, and L = tertiary aryl or alkyl phosphine or arsine, have been particularly well-studied[97-102,84]. The effects of varying the oxidative addend[97,51], the steric[98-100] and donor[101] properties of L and the electronegativity of X[97] have all been examined, and the results are generally consistent with the model described above: reactivity increasing with metal basicity, and decreasing with ligand size[102]. An equation relating enthalpy and the electronic and steric properties of the ligands has recently been advanced[102].

Some well-known examples of complexes which furnish oxidative addition products are $Ir(CO)Cl\,P_2$, $RhCl\,P_3$, $Pt\,P_3$, $Pt\,P_4$, $Ni[P(OEt)_3]_4$ and $IrH(CO)\,P_3$. Covalent molecules which can be added to complexes such as these include H_2, O_2, CO, Cl_2, alkyl halides[51,103-104], olefins, (particularly activated olefins, such as $(CN)_2C{=}C(CN)_2$)[105], and Group IV hydrides[46]. The oxidative addition of C-H bonds has been observed in aryl compounds[107], more recently, alkyl C-H addition has been reported[108]. In both cases, intramolecular addition is most often encountered[109]. The similarity between oxidative addition and classical donor coordination has been pointed out[45].

2. Reaction Mechanisms of Oxidative Addition

For an oxidative addition of the general form

$$L_nM + XY \rightarrow L_nM(X)(Y) \qquad (5)$$

the following models may be considered as limiting mechanisms:

Scheme 1. Concerted Addition

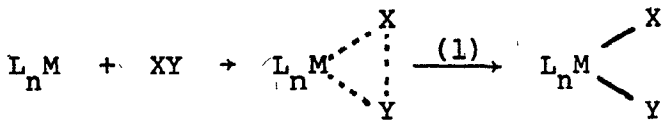

Scheme 2. Stepwise Addition

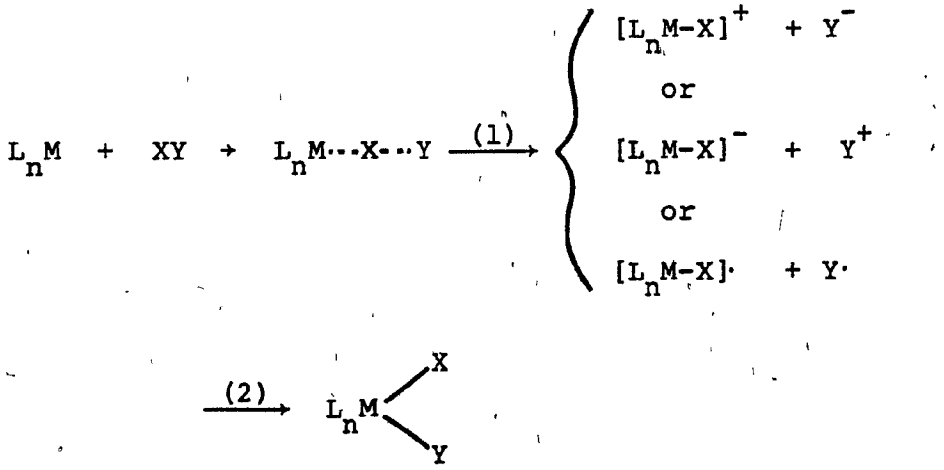

Scheme 3. Predissociation of addend

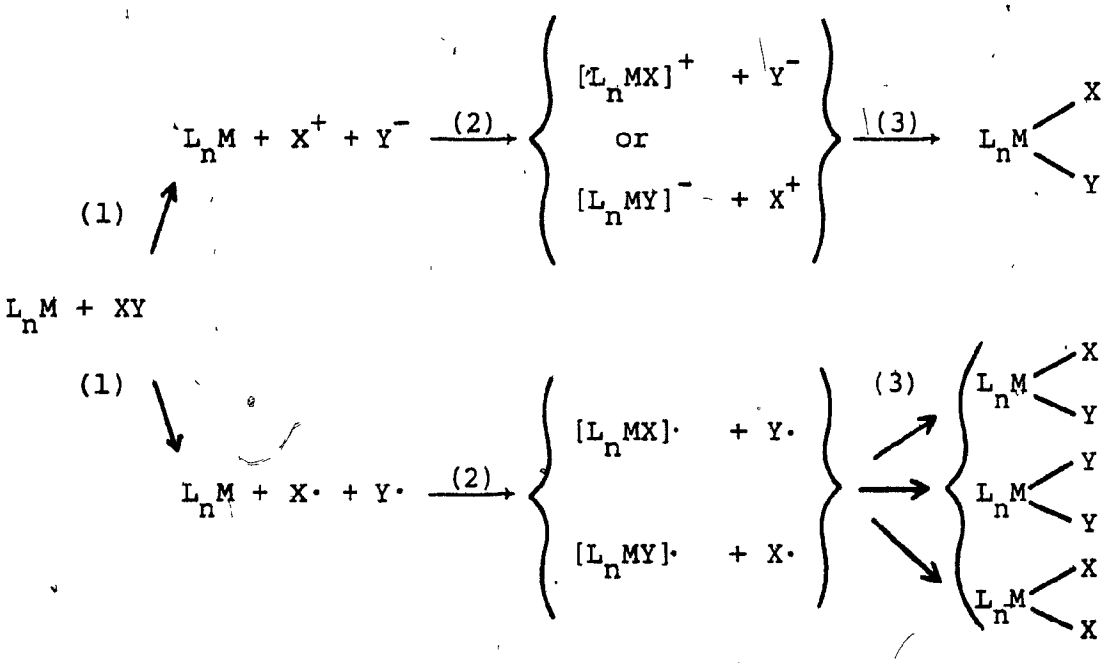

The concerted mechanism for oxidative addition is depicted in Scheme 1 as passing through a three-center transition state where both ligands approach the metal center in an edge-on manner, and attach themselves simultaneously. The reaction therefore must take place in a single step and exhibit second-order kinetics, in the absence of complicating side reactions. Other characteristics of this model are the requirement of coordinative unsaturation and, given an optically active oxidative addend (for example, if XY is $(CH_3)(C_2H_5)CHI$), retention of configuration around the asymmetric center. Reactions of this sort are common when the addends are small covalent molecules having little or no polarity about the X-Y

bond; for example, H_2, O_2 or SiH, or when the formation of ionic or radical molecular fragments is unlikely.

In stepwise addition, Scheme 2, one envisions a linear transition state giving rise to an intermediate complex and a molecular fragment of the addend. The intermediate complex may be charged, in which case the fragment will also be ionic, or uncharged, which would leave the remaining fragment a free radical. Since the second step in the sequence, which would involve the reaction between oppositely charged ions, or else involve a free radical, would in most cases be rapid compared to the first, one would expect second-order kinetics to be observed for this reaction, if other reactions do not occur to further complicate the rate law.

An asymmetric oxidative addend which reacts according to Scheme 2 may undergo either inversion of configuration or racemization. Inversion will occur if the asymmetric part (in this case, X in Scheme 2) is added first. If the asymmetric fragment (in this case, Y in Scheme 2) is added as part of the second step, then racemization will occur.

Stepwise additions are most likely in polar molecules where the electronegative end forms a good leaving group. Such a reaction resembles an S_N2-type nucleophilic substitution, where, for example, the electropositive end of a polar oxidative addend forms a linear transition state with a basic transition metal complex. In this regard, the stereochemistries

of the oxidative addition products of polar addends, such as asymmetric alkyl halides, are of interest (see below).

Reactions in which the addends predissociate (Scheme 3) are three-step processes, involving the dissociation of the addends as a first step to form ionic or radical fragments, which can further react to form intermediate species similar to those formed in the stepwise addition. If ionic species are formed, the products should resemble those resulting from a concerted or stepwise addition, while several species may result from radical formation. The overall reaction is likely to be rapid, and first order in either the metal complex or the oxidative addend, but not both. Racemization would be expected of any asymmetric addend.

For those reactions in which a ligand is lost from the starting complex, as in reaction 6,

$$L_nM + XY \rightarrow L_{(n-1)}M(X)(Y) + L \qquad (6)$$

there is the additional problem of determining when in the reaction sequence is the ligand lost. Since the ligand may be lost before, during, or after the oxidative addition occurs, the mechanistic possibilities are in this case greatly increased.

The mechanistic models presented above must be recognized as extreme limits: any actual mechanism may be a modification of one or a combination of several. Even so, the models given

above represent many possible mechanisms. The nature of the reactants often limits the mechanistic options, however, and renders certain theoretical possibilities implausible. The oxidative addition of hydrogen to Vaska's complex most likely occurs through a concerted process, for example, since the alternatives involve H· free radicals, H^- ions, hydrido-metal anions, or other species unlikely to exist in solution. While neither these nor more complex mechanisms can be ruled out, they appear much less likely. The oxidative addition of HCl, on the other hand, may easily be envisioned as proceeding through any one of the three general types of mechanisms: e.g., by a concerted addition in the solid state or non-polar solvent; or else a stepwise addition (through $[L_nM\text{-}H]^+ + Y^-$) or a predissociation into H^+ and Cl^- in a polar solvent. Indeed, there is evidence that this reaction can proceed by different pathways that depend on the reaction conditions[110].

Besides variability of the reaction mechanism with experimental conditions, there is the more basic problem that any actual reaction may proceed by a mechanism in-between the extremes that were initially thought likely, as well as by a mechanism completely different, such as solvent-assisted reactions, or the intervention of a third reagent. The result in the case of oxidative addition is that while reactions of the three types presented here are distinguishable by the

combination of an accurate determination of reaction order, studies with asymmetric reagents, and the use of techniques to detect free radicals, the mechanisms of many important oxidative addition reactions remain unclear.

The stoichiometry and, to some extent, the mechanisms of oxidative addition reactions generally depend on the electronic configuration of the starting complex[84]. Five-coordinate d^7 complexes, initially 17-electron systems, oxidatively add a single (one-electron donor) ligand to become 18-electron, six-coordinate d^8 complexes. The reaction proceeds via a free radical mechanism in most cases. Four-coordinate d^8 complexes, 16-electron systems of square planar geometry, typically will oxidatively add two single-electron ligands to form six-coordinate, d^6 complexes. The mechanism of addition to d^{10} complexes, as exemplified by Pt(0) phosphine complexes, involves dissociation to form a 14-electron, two-coordinate system which can oxidatively add two ligands (to form four-coordinate d^8 complexes). Examples of oxidative additions to representative complexes are given below.

An example of oxidative addition to d^7 complexes is provided by the reactions of $Co(CN)_5^{3-}$ with a variety of reagents[84].

$$2Co(CN)_5^{3-} + XY \rightarrow Co(CN)_5^{3-}X + Co(CN)_5^{3-}Y \qquad (7)$$

(XY = H_2O_2, NH_2-OH, I-CN, some organic halides).

The second-order kinetic behavior of this reaction, as well as the detection of free radicals, indicate a stepwise, free-radical mechanism, analogous in part to Scheme 2. This is in contrast to the reaction with hydrogen, where third-order kinetics indicate a concerted mechanism of an unusual type takes place, to yield $CoH(CN)_5^{3-}$. These products are otherwise analogous to those obtained from the hydrogen peroxide addition. The formation of a monohydride product by such an unusual route perhaps reflects the tendency for hydrogen to react by a concerted mechanism, even when straightforward stepwise mechanisms can be conceived and are in fact followed by other reagents.

Oxidative addition to Vaska's complex, as in the reaction,

$$IrCl(CO)P_2 + XY \rightarrow IrCl(CO)P_2(X)(Y) \qquad (8)$$

(XY = H_2, O_2, halogens, inorganic or organic acids, and alkyl halides),

represents addition to a four-coordinate d^8 complex, and yields an octahedral d^6 complex. Reactions of this type have been extensively studied with respect to their chemistry, kinetic behavior, stereochemistry, and spectral properties. A variety of mechanisms can operate, depending on reagent and reaction conditions[21,84,88].

A concerted mechanism prevails for the addition of small,

covalent molecules such as hydrogen. Evidence for a concerted mechanism includes second order kinetics, a small kinetic isotope effect, and the stereochemistry of the product[21,97]. When the reaction involved alkyl halides, however, a different pattern of kinetic behavior was observed, and the mechanism was a matter of considerable controversy for some years. A stepwise addition of the alkyl halide through a polar transition state to yield an ionic intermediate complex and free halide ion was first proposed, on the basis of the second-order kinetics of the reaction (like the hydrogen addition) and its large, negative activation entropy[97]. Experiments with optically active organic halides were employed to distinguish between a concerted and stepwise mechanism. Both retention[111,112] and inversion[113] of configuration were reported but later questioned[114,115]. More recently, it has been reported that racemization occurs, and that the reaction proceeds by a free radical mechanism[116]. Furthermore, it has been suggested that a large negative activation entropy need not indicate highly polarized transition state or ionic intermediates, but may occur even in concerted reactions[45,117]. Although a stepwise addition involving an ionic intermediate is still plausible for some alkyl halides, such as methyl iodide, and adequately explains some experimental results, it is probable that for other alkyl halides, as well as other reagents[51], a mechanism somewhere between the two extremes of

concerted and stepwise addition can apply.

Platinum (O) complexes provide a well-studied example of oxidative addition reactions to d^{10} species[84,86]. The first stage is generally dissociation of the starting 3 or 4 coordinate platinum complex (such as Pt P_3, Pt $P_2(C_2H_4)$, Pt $[P(isopropyl)_3]_3$ or Pt P_4) to form a reactive two-coordinate intermediate. The detailed mechanism of oxidative addition of alkyl halides to the latter complex may be similar to that of the d^8 analogues of Vaska's complex. Platinum (O) complexes containing alkyl phosphines will add molecular hydrogen[118], and recently, the oxidative addition of water to $Pt[P(isopropyl)_3]_2$ to form $PtH(OH)\ [P(isopropyl)_3]_2$ has been reported[64].

3. Stereochemistry of Oxidative Addition

The stereochemistry of the products of oxidative addition has been the focus of many studies[119]. Interest in this subject does not only stem from a desire to fully characterize reaction products, but also because the stereochemistry of the product can provide information on the intimate reaction mechanism.

Furthermore, when oxidative addition is part of a larger process, such as a catalytic cycle, the stereochemistry of this reaction has implications for the further reaction of the complex with other coordinated groups. Although product

stereochemistry is often a guide to reaction mechanism, it cannot be regarded as definitive: isomerization may occur after the initial oxidative addition reaction. Therefore, the final isomeric composition may be determined by the thermodynamic stability of each isomer and the barrier to their interconversion, rather than by the kinetic factors involved in their formation. Consequently, the isomeric composition of the products may be sensitive to reaction conditions, particularly temperature and solvent.

The oxidative addition of two ligands to a square planar complex yields an octahedral product, in which the added ligands may be cis or trans. It is reasonable as well as customary to associate a stereospecific cis addition with a concerted mechanism, and a trans addition or a mixture of cis and trans with a stepwise mechanism. From the viewpoint of orbital-symmetry, however, cis or trans addition is possible for either a concerted or stepwise mechanism[120].

Sketches of each type of addition, adapted from Pearson[120], are shown for reaction 5 (n=4) in Figure I-1. The interacting orbitals of the complex and the addend are in the plane of the paper, and the non-participating orbitals are omitted. It can be seen from the sketches that cis and trans addition result from the overlap of X-Y orbitals with the same metal d orbital. Cis and trans products are formed when X-Y is parallel (a) or perpendicular (b) to the metal-ligand plane,

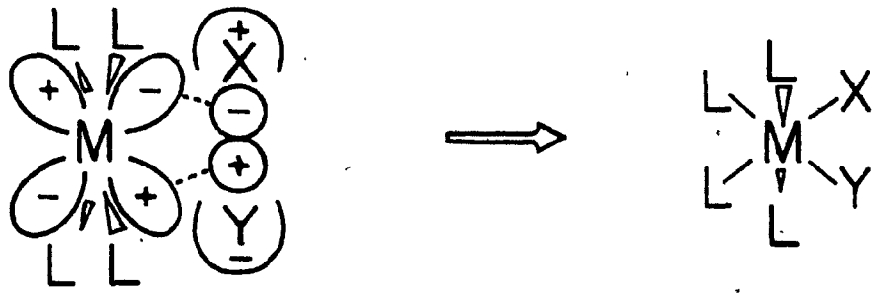

a) Concerted Cis Addition

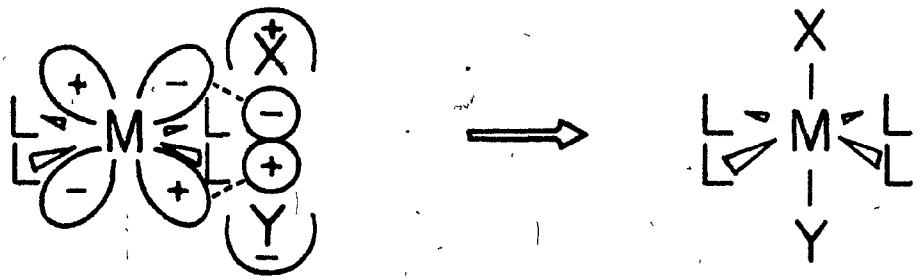

b) Concerted Trans Addition

Figure I-1. Orbital symmetry of concerted oxidative addition.

respectively.

Stepwise addition in complexes of this type occurs through a five-coordinate intermediate. If this intermediate is trigonal bipyramidal, both cis and trans products can result. A square pyramidal intermediate, on the other hand, would result in stereospecific trans addition, assuming a rigid pyramid with the first-added ligand in the apical position[121]. Figure I-2 illustrates these possibilities for a stepwise nucleophilic displacement. The same products would result for a stepwise free radical or pre-dissociative mechanism.

Although symmetry allowed, there has been no unambiguous demonstration to date of a concerted trans addition to a square-planar complex. Indeed, the case for which it had been originally proposed, that of the assymmetric alkyl halide addition with reported retention of configuration (see above), was later shown to operate by a free radical mechanism, rather than a concerted one[116]. The addition of methyl halides[122] and halogens[104] to planar complexes in a gas/solid interaction, or with the complex suspended or dissolved in non-polar solvents, results in stereospecific trans addition; in polar solvents, however, a mixture of cis and trans products occur in both cases. While an ionic stepwise mechanism is unlikely in the gas phase, a radical mechanism remains an alternate possibility to a concerted process. The observation of isomeric mixtures

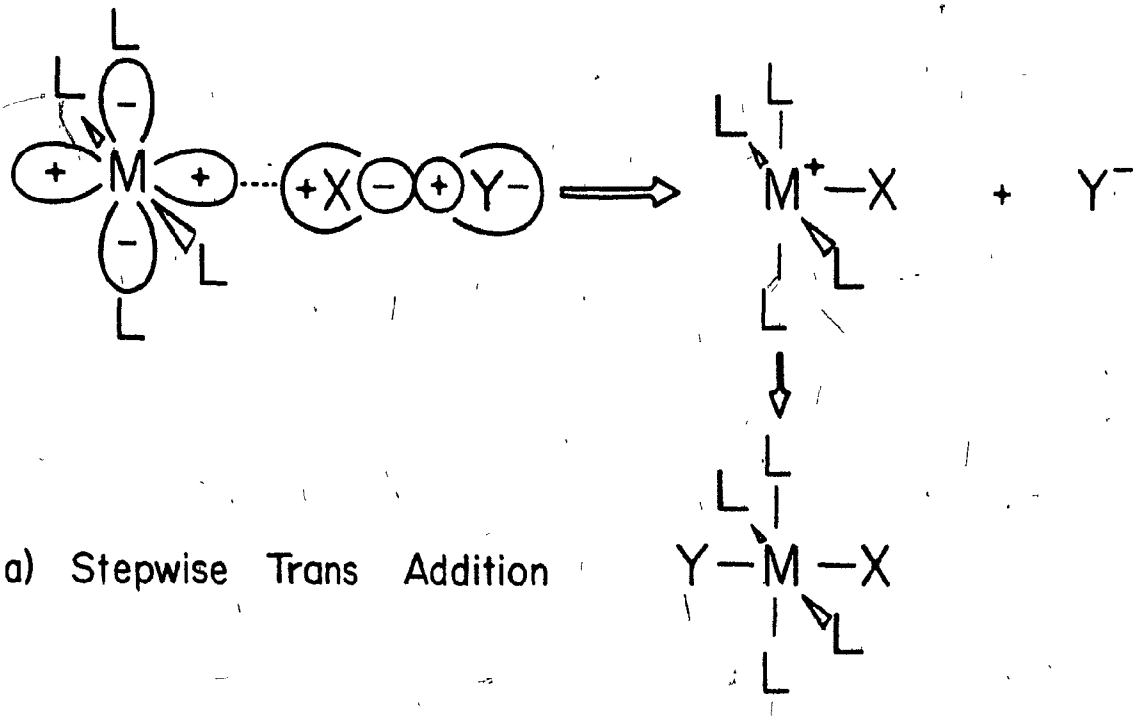

a) Stepwise Trans Addition

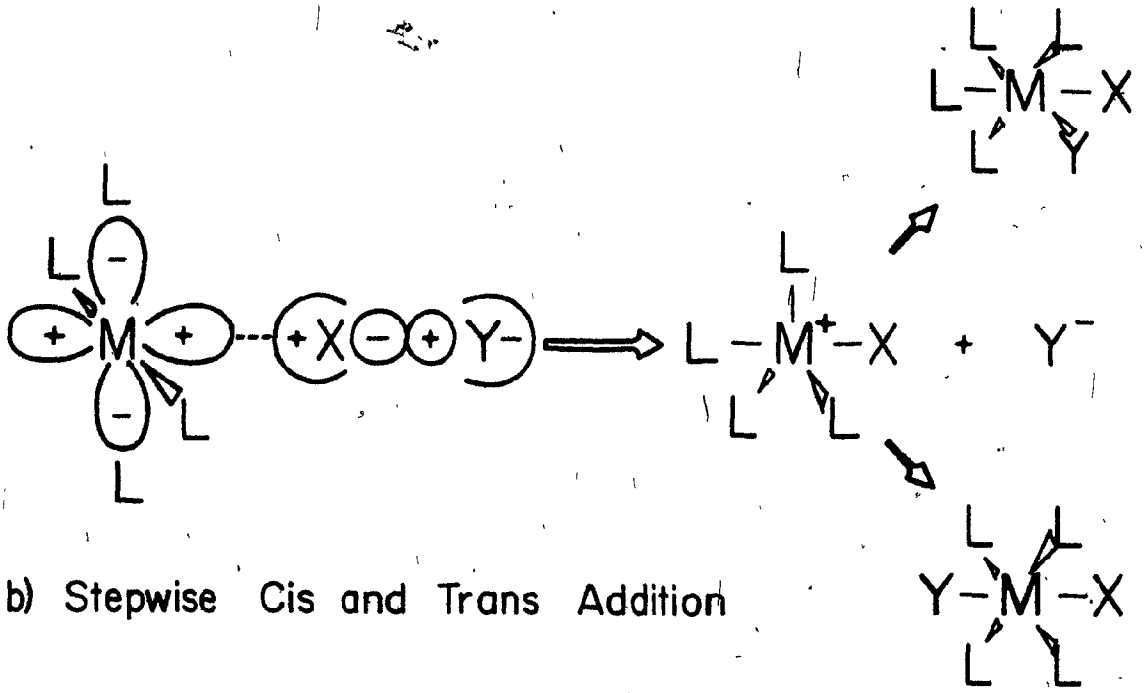

b) Stepwise Cis and Trans Addition

Figure I-2. Orbital symmetry of stepwise oxidative addition.

in polar solutions is most easily explained by an ionic mechanism which passes through either a five-coordinate cationic trigonal bipyramidal intermediate, or a five-coordinate square pyramid intermediate that rearranges in polar solution[121]. Methyl halide additions apparently are not radical processes in solution[116].

Hydrogen halides add to solid Vaska's complex stereospecifically to form cis products[71]. Like the examples of trans addition mentioned above, however, stereospecificity is limited to heterogeneous systems and non-polar solvents; both cis and trans isomers are found in polar solvents[110]. For hydrogen, the addition is stereospecifically cis in all cases reported, regardless of solvent[51]. The same can be said for the oxidative addition of Si-H bonds[123]. It is interesting to note that for H_2 and R_3SiH additions, where a concerted, three-centered process is the most likely reaction mechanism, only stereospecific cis addition has yet been reported.

There is some indication that the steric properties of a substrate may affect the stereochemistry of the products. In a study using an analogue of $Ir(CO)X\,P_2$, with X a very bulky carborane cage, isomers were observed from the addition of hydrogen[124]. It is unclear whether the variety of products is the result of various modes of hydrogen addition, or the subsequent isomerization of a single addition product.

4. Oxidative Addition of Hydrogen

The oxidative addition of hydrogen to transition metal complexes may provide a means of obtaining insight on some mechanistic and stereochemical aspects of concerted oxidative addition. Hydrogen is non-polar and unlikely to pre-dissociate, react heterolytically, or be affected by polar media, and thus is likely to react in a concerted manner. Information of this sort would be particularly relevant to the field of asymmetric hydrogenation, where the stereochemistry of catalytic intermediates (formed by oxidative addition of hydrogen to metal complexes with chiral ligands) is directly related to the stereochemistry of the hydrogenation products[125].

The oxidative addition of hydrogen at ambient temperature is remarkable considering the high bond energy of hydrogen (450 kJ/mol). It has been suggested that the reaction is facilitated by metal d-electrons entering the 1 s* antibonding orbitals of the hydrogen molecule, resulting in bond weakening[126]. The metal-hydride bonds together must have at least as much bond energy as hydrogen alone, since the overall reaction enthalpy is usually negative[51]. Nevertheless, each metal-hydride bond may have less bond energy. The fact that metal complexes can activate hydrogen toward further reaction is partly the result of this relationship: that is, it is not necessary to supply all of the hydrogen dissociation energy at once to initiate a

reaction between, for example, hydrogen and an olefin, but only that energy necessary to break a single M-H bond.

The preference for concerted mechanisms in the oxidative addition of hydrogen may be another consequence of the high dissociation energy of hydrogen. It has already by pointed out in connection with the addition of hydrogen to $Co(CN)_5^{3-}$ complexes (see section B, part 2) that a concerted mechanism is apparently followed even when two metal complexes are involved in the transition state. One explanation for this behavior would be that the formation of a single M-H bond does not provide sufficient energy to allow the reaction to proceed, but the formation of two M-H bonds does. Whether the two metal-hydrogen bonds are formed to the same metal-complex (as in the concerted oxidative addition given in Scheme 1), or to two adjacent metal complexes (as in activation on a metal surface, a metal cluster, or, perhaps, a four-center transition state in the cobalt case) may not be of primary importance. The "activation" of hydrogen in all these cases may be due to the ability of each to form two M-H bonds simultaneously. It is interesting to note that water reacts with $Co(CN)_5^{3-}$ in the same manner as hydrogen[127]. Perhaps activation of water operates in ways similar to the activation of hydrogen, as indeed has been reported with platinum complexes[64], where two-ligand oxidative addition to a single metal center has been proposed, and with metal clusters[128],

where adjacent metal centers may be involved.

Hydrogen adds to mononuclear complexes in a cis fashion that is usually stereospecific. No examples of the trans-addition of hydrogen have been so far reported.

C. A SURVEY OF THE SYNTHESIS AND PROPERTIES OF SOME RELEVANT IRIDIUM COMPLEXES

1. $IrH_3(CO)[P(C_6H_5)_3]_2$

The iridium trihydride complex $IrH_3(CO)\ P_2$, 1, was first prepared by Malatesta et al. and fully reported in 1965[80] along with a series of phosphine-containing iridium carbonyl hydrides. It was prepared through the action of sodium borohydride or lithium aluminium hydride on $IrCl(CO)\ P_2$, 2, or $IrHI_2(CO)\ P_2$. The addition of sodium borohydride, or molecular hydrogen, to a complex identified as $IrH(CO)\ P_2$ (actually $IrH(CO)_2\ P_2$, see below, part 3) also resulted in the formation of the iridium trihydride, 1. Two isomers of this compound were isolated which had different i.r., m.p., and electric dipole moments. On the basis of these data, the following structures were assigned.

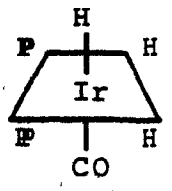

3

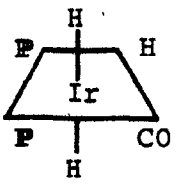

4

In solution, 3 was reported to change rapidly into 4, and so was considered an unstable isomer of 4. An excess of triphenylphosphine added to the trihydride, 1, resulted in an equimolar amount of H_2 plus $IrH(CO)\ \mathbb{P}_3$, 5, according to reaction 9.

$$\underset{1}{IrH_3(CO)\ \mathbb{P}_2} + \mathbb{P} \rightarrow \underset{5}{IrH(CO)\ \mathbb{P}_3} + H_2 \qquad (9)$$

The trihydride, 1, was later reported by Wilkinson et al.[129] as part of a study of Ir and Rh allyl complexes. The complex $Ir(\pi\text{-allyl})CO\ \mathbb{P}_2$ reacts with molecular H_2 to give the trihydride, 1. The sequence given below was proposed for the reaction, where $R = C_3H_5$, although the intermediate $IrH(CO)\mathbb{P}_2$, 6, was neither isolated nor observed spectroscopically.

$$IrR(CO)\ \mathbb{P}_2 + H_2 \rightarrow \underset{6}{IrH(CO)\ \mathbb{P}_2} + RH \xrightarrow[+H_2]{-RH} \underset{1}{IrH_3(CO)\ \mathbb{P}_2} \qquad (10)$$

The infra-red spectrum of the trihydride, 1, reported in this study corresponds to the mer isomer, although a stereochemistry was not assigned. The complex was also prepared by bubbling hydrogen through $IrH(CO)_2\ \mathbb{P}_2$ in refluxing benzene, and by addition of sodium borohydride to Vaska's complex, 2, in ethanol. Both methods gave the product, 1, in high yield. There was no mention of more than one isomer present.

Another study by Wilkinson et al.[130] first suggested that the trihydride, 1, could be formed from the tris(phosphine) complex, 5. These workers noted that solutions of $IrH(CO)_2\,\mathbb{P}_2$, when heated under hydrogen, formed an isomeric mixture of hydrides, while warming the solutions with triphenylphosphine resulted in $IrH(CO)\,\mathbb{P}_3$. The implication of these reactions is that $IrH(CO)\,\mathbb{P}_3$, $IrH(CO)_2\,\mathbb{P}_2$ and $IrH_3(CO)\,\mathbb{P}_2$ all dissociate via a common intermediate, $IrH(CO)\,\mathbb{P}_2$.

An earlier study by Vaska et al.[131] had characterized the product of hydrogen addition to the tris(phosphine) complex, 5, as a seven-coordinate species, $IrH_3(CO)\,\mathbb{P}_3$. As others have suggested[130,132], the correct formulation is undoubtedly the bis(phosphine) complex, 1. The same report also stated that ethylene formed an adduct with the tris-(phosphine) complex, 5, at atmospheric pressure. This has been disputed by Burnett et al.[132], who found no olefin-complex formed with ethylene alone, or ethylene in the presence of hydrogen.

The interaction of the trihydride, 1, with hydrogen and triphenylphosphine, and its role in the hydrogenation of olefins was examined in a series of papers by Burnett et al.[132-135]. It was found that the following equilibrium was established, with K = 5.6 at 25°C in dimethylformamide[132].

$$IrH(CO)\,P_3 + H_2 \rightleftharpoons IrH_3(CO)\,P_2 + P \qquad (11)$$

The reaction kinetics suggested that equilibrium occurred through the dissociation of triphenylphosphine, followed by the addition of hydrogen to a four-coordinate intermediate.

$$IrH(CO)\,P_3 \underset{k_{+P}}{\overset{k_{-P}}{\rightleftharpoons}} IrH(CO)\,P_2 + P \qquad (12)$$

$$IrH(CO)\,P_2 + H_2 \underset{k_{-H}}{\overset{k_{+H}}{\rightleftharpoons}} IrH_3(CO)\,P_2 \qquad (13)$$

Because of the complex equilibria involved, the kinetic results could only be expressed as ratios of rate constants*. At 25°C,

$$\frac{k_{-P}k_{+H}}{k_{+P}} = 1.5 \times 10^{-3}\ sec^{-1}$$

In these studies, the trihydride, 1, was reported as a

---

*The ratio $k_{-p}k_{+H}/k_{-H}$ appears in the abstract of Ref. 132. It is apparently a misprint. The form given above appears later in the text, and is the only possible quantity in view of related reactions.

mixture of two isomers, fac and mer, with the following structures.

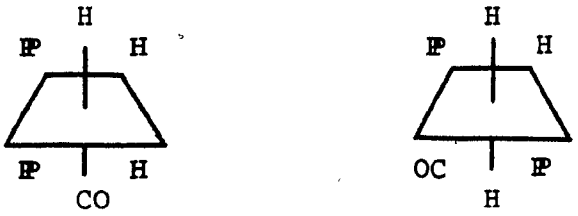

fac 3 mer 7

It should be noted that the mer isomer is given a different structure than in the original work of Malatesta et al.[80], 4, although the discrepancy is neither acknowledged nor explained in the later paper[132]. Equilibrium between the two isomers was assumed on the basis of similar values for the equilibrium constant of equation 9 over a large range of reactant concentrations, along with the observed constant proportion of the isomers in solid-state spectra of the trihydride, 1. These indications of isomeric equilibrium are indefinite, however, since the range of equilibrium "constants" is large (± 35%), and solid-state measurements do not necessarily represent equilibrium proportions. In any case, a discrete equilibrium between isomers was not shown directly. Thus, the nature of the isomerization and stereochemistry of the isomers of the trihydride, 1, remained ambiguous.

Further studies on these iridium compounds, 1 and 5, were undertaken by Burnett et al. to determine the mechanism

of the catalytic hydrogenation of olefins, and the manner in which the overall rate of catalysis depends on individual equilibria between the various reagents[133-135]. The iridium species were chosen for study because their slower reaction rates render them more convenient than the otherwise more useful rhodium species. The initial study[132] of the catalytic hydrogenation of ethylene with hydrogen, the tris(phosphine) complex, 5, and triphenylphosphine indicated that the active species was the four-coordinate species, 6, present in a low concentration, and that the rate of hydrogenation decreased as the trihydride, 1, accumulated. The following catalytic cycle was proposed, involving coordination of ethylene to an active intermediate, 6, formation of an alkyl species, and subsequent oxidative addition of H_2 and regeneration of the intermediate, 6.

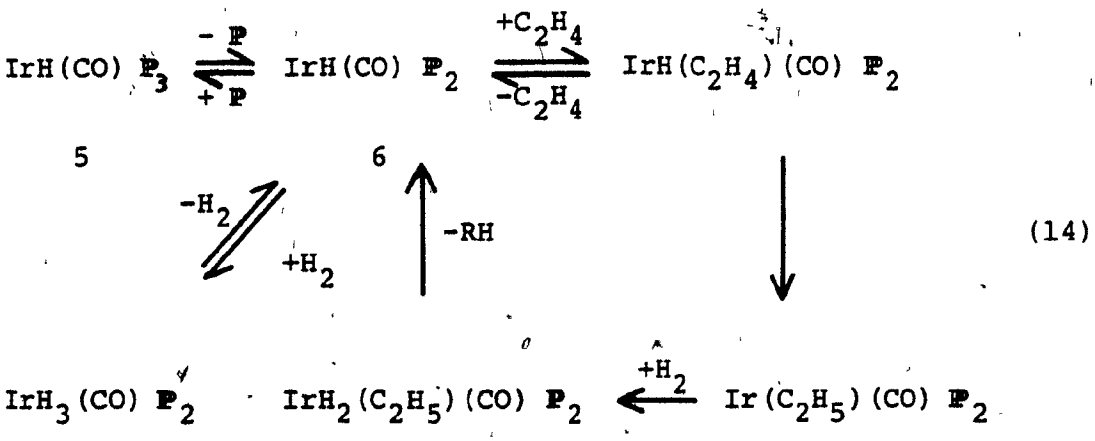

(14)

The trihydride, 1, was considered only indirectly involved in the catalytic cycle. An analogous process had been previously proposed[136] for catalysis by $RhH(CO)P_3$, except that a trihydride species is not formed with rhodium.

Subsequent papers by Burnett's group examined the stoichiometric and catalytic hydrogenation of ethylene and butadiene with the trihydride, 1,[134] and Vaska's complex, 2 [133]. Earlier conclusions regarding the mechanism of hydrogenation catalysis were modified, and it was suggested that the catalysis was controlled not through equilibria involving iridium hydride species (equations 12, 13) but through competitive reactions of an intermediate complex. The active species in catalysis was considered to be the trihydride, 1 , rather than the four-coordinate intermediate, 6, since the latter was thought to be present in too low a concentration. The catalysis apparently proceeds through a bimolecular reaction of the trihydride, 1, and ethylene. A recent paper[135] on the hydrogenation of dimethyl maleate proposed a complex catalytic cycle in which the crucial alkyl-metal intermediate is formed by a bimolecular attack on 1, 5, or a metal-olefin complex.

The trihydride complex, 1, has been mentioned in several other papers. Vaska et al. included this compound in a study of the catalytic formation of water from hydrogen and oxygen[137]. The trihydride, characterized as the mer form,

functioned as a catalyst for the reaction, although it was not as efficient as some other compounds tested. The products in a study of deuterium exchange with metal hydrides were not fully characterized[138]; however, $IrD_2H(CO)\ P_2$ was undoubtedly formed by addition of deuterium to $IrH(CO)\ P_3$, 5.

The trihydride complex, 1, was one of a series of compounds examined in a more recent polarographic study[139]. Half-wave potentials decreased regularly in going from $IrCl_3$ to IrH_3 when compounds of the formula $IrH_xCl_{3-x}(CO)\ P_2$, ($x = 3,2,1,0$) were reduced. This trend was related to increased covalency in the molecules. The linear correlation of the half-wave potential with the C-O stretching frequency indicated to the authors that both parameters "reflect the polarity of the molecular orbital". The fact that the trihydride, 1, was consistent with this trend may indicate, it was suggested, that the trihydride, 1, is isostructural (i.e., phosphines trans) with the other members of the series; accordingly, the "unknown" structure of the trihydride, 1, would be that of the mer isomer, 7. This study is another case where a knowledge of the structure and isomeric nature of trihydride, 1, would have been beneficial to the discussion.

More recent studies[140-141] by van Doorn et al. have shown that both isomers of the trihydride, 1, were formed by oxidative addition of carboxylic acids to analogues of Vaska's compound, 2, over several days at room temperature. The isomers were

regarded as the products of disproportionation or decarboxylation of carbonylbis(formato)hydridobis(triphenylphosphine)-iridium(III), and were characterized by proton n.m.r. as the fac, 3, and mer (trans P), 7, structures. This report[141] is the first detailed n.m.r. of the two compounds. Even in this report, the fac isomer is not completely analysed, and some peaks are unreported. The fac/mer ratio is reported as 1 to 3, although the method of arriving at this figure is not mentioned.

Analogues of trihydride, 1, have also been reported. Shaw et al. have studied carbonyltrihydridoiridium(III) complexes with the alkyl phosphines $P(C_6H_5)(C_2H_5)_2$[142,143] and $P(t\text{-}C_4H_9)_2(n\text{-}C_3H_7)$[144]. Crystalline solids were not obtained in either case, although the products were well-characterized by proton n.m.r. in solution and the latter compound was isolated as a yellow oil. These trihydrides were prepared by addition of carbon monoxide to solutions of the appropriate pentahydridobis(organophosphine) complex. As in the case of the triphenylphosphine complexes, care must be taken to use only one equivalent of CO, since the formation of the dicarbonyl-hydridobis(organophosphine) complex is possible. Both alkylphosphine complexes had the mer configuration (analogous to 7) in solution; little or no fac isomer was detected.

An attempt to prepare the thiocarbonyl analogue of the trihydride, 1, resulted in the formation of a thiomethoxy

complex, 11, apparently as a result of complete hydrogenation of the thiocarbonyl carbon atom to CH_3[145]. The reactants are otherwise similar to those involved in equation 11, namely, IrH(CS) P_3 (structurally analogous to 5) plus hydrogen. The authors suggested that the reaction proceeds through the following intermediates.

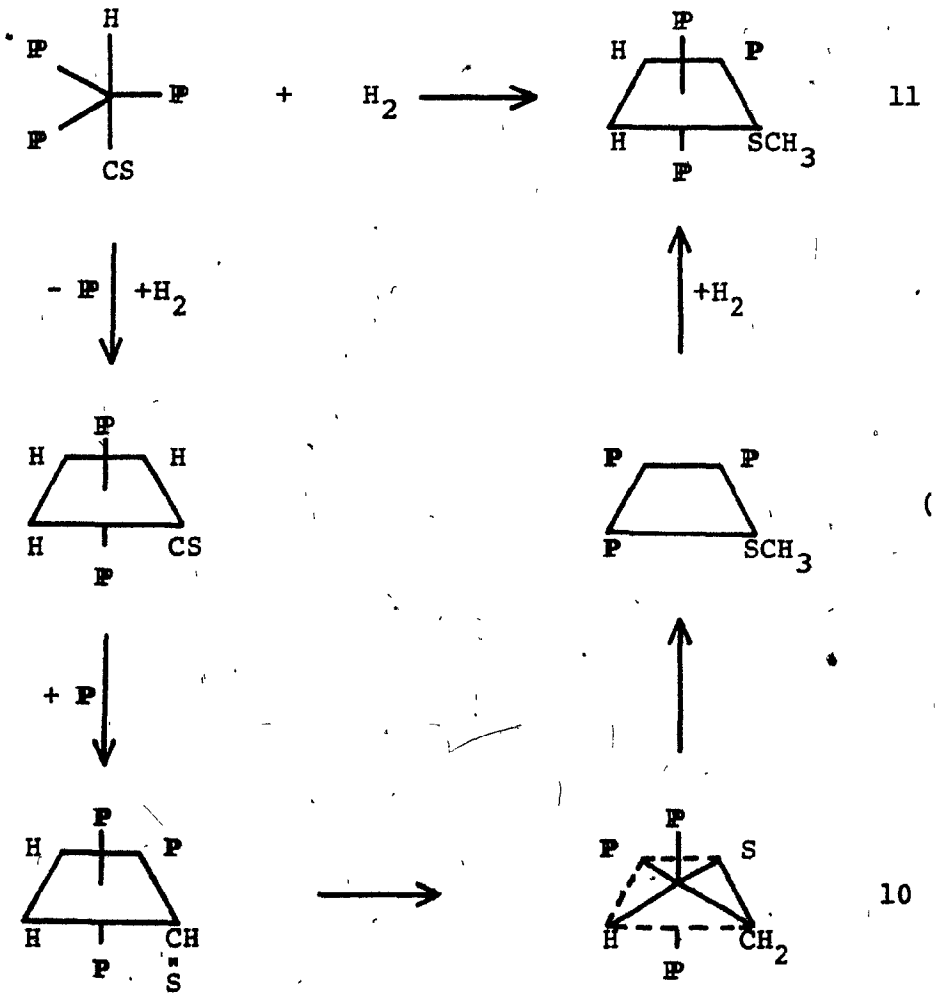

Only the final product, 11, was isolated and characterized, although other compounds with thioformyl[145], as in 9, or thioformaldehyde[146], as in 10, ligands were isolated soon afterward. Neither of the compounds reported later were metal hydride complexes. Although the scheme shown remains a plausible one, a fac trihydride (8', analogous to 3) could be proposed as an alternative to 8, with the advantage that a concerted intramolecular two-atom hydrogen transfer to the thiocarbonyl carbon might then be envisioned, obviating intermediate 9.

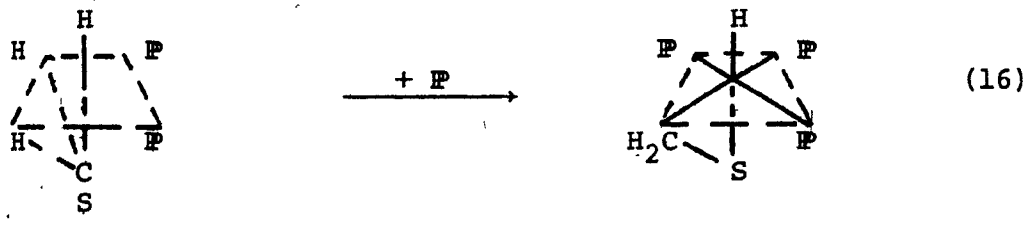

8' 10 (16)

Such an alternative is not possible with the mer trihydride, 8, where the hydrogens adjacent to the thiocarbonyl group are trans to one another. Although the proposed alternative scheme is highly speculative, it is no more so than the original proposal, and must be considered a possibility if it can be shown that the addition of hydrogen to the carbonylhydridotris-(triphenylphosphine) complex, 5, results in the formation of both the fac, 3, and the mer, 7, trihydride complexes.

Many other iridium trihydrides have been prepared of

the formulae IrH_3L_3 or IrH_3L_2Q, where L is a tertiary phosphine or arsine ligand, and Q is a π-acid ligand. Of the former group, isomers of both fac and mer configurations have been isolated for L = $P(C_6H_5)(C_2H_5)_2$[69], $\mathbb{P}$[69,146-148], $P(C_6H_5)_2(CH_3)$,[149] $P(C_6H_5)_2(C_2H_5)$,[149] and $As(C_6H_5)_3$[150]. Structural studies have been carried out on both isomers of $IrH_3\mathbb{P}_3$[148] and on fac-$IrH_3[P(CH_3)_2(C_6H_5)]_3$[151]. The effects of ultraviolet light on both fac and mer $IrH_3\mathbb{P}_3$ have also been examined[12]. The interconversion of the fac and mer has been reported in benzene solution at room temperature with L = $P(C_6H_5)(C_2H_5)_2$, and with heating for several hours in tetrahydrofuran with L = $\mathbb{P}$[69]. The complexes $IrH_3[P(C_6H_5)(CH_3)_2]_3$[151] and $IrH_3[As(C_6H_5)(C_2H_5)_2]_3$[69] have been reported in only the fac configuration. The latter did not isomerize even when heated to its melting point[69]. In contrast, the mer isomer was predominant in a solution of $IrH_3[P(C_2H_5)_3]_3$[143].

Two groups of trihydrides of the formula IrH_3L_2Q have been studied, and exhibit contrasting behavior. With L = $P(C_6H_5)(C_2H_5)_2$ and Q = $\mathbb{P}$, $P(OCH_3)_3$, $As(C_6H_5)(CH_3)_2$, $Sb(C_6H_5)_3$, CH_3CN, $S(CH_3)_2$ and $P(C_6H_5)(OCH_3)_2$, as well as L = $P(C_2H_5)_3$ and Q = $As(C_6H_5)(CH_3)_2$, the major product (≥ 90%) was in all cases the mer isomer of the trans-L configuration[142,143] (analogous to 7). The fac isomer was in most cases undetected, and approached 10% only in the cases where Q = $Sb(C_6H_5)_3$ and $S(CH_3)_2$. With L = $As(C_6H_5)_3$, and Q a series of isocyanide

ligands (Q = CNC_2H_5, $CN(C_6H_{11})$, CN-p-tolyl, CN-p-anisyl)[152], on the other hand, only fac isomers were isolated. (In this case, the assignment of stereochemistry rests on i.r. data alone). It is possible that arsine ligands favor a fac configuration for octahedral trihydrides; however, the data are yet very incomplete in this regard. In no case has fac/mer isomerization in octahedral trihydrides been studied in detail.

2. $IrH(CO)[P(C_6H_5)_3]_3$ (5)

The title compound was first synthesized by Vaska and Bath[153]. A more convenient preparation was reported by Wilkinson et al.[130,154], who obtained the compound by heating the chloride, 2, with sodium borohydride and excess ligand in ethanol. Harrod et al.[155] have prepared it, 5, by the dehydrohalogenation of $IrH_2Cl(CO)P_2$ with strong base in the presence of excess triphenylphosphine. The reactions of primary importance in the present study, however, are the preparation of the tris(phosphine) complex, 5, through the reaction of $IrH_3(CO)P_2$, 1, with excess phosphine, first reported in 1965 by Malatesta[80], and the equilibrium established between the trihydride, 1, and tris(phosphine), 5, complexes.

The tris(phosphine) complex, 5, is a pale yellow solid, stable for long periods in air at room temperature, and exists in two interconvertible[156] crystalline forms, differentiable

by solid-state i.r. and m.p.[80]. A structural study of the rhodium analogue showed a trigonal bipyramid, with the hydride and carbonyl ligands in the axial position, and the phosphine ligands in an equatorial plane[157]. The n.m.r. spectrum of a solution of the complex has been measured up to 100°C[130]. At 35°C, the spectrum showed only a high field quartet, but line broadening was observed at higher temperatures, and coalescence occurred above 100°C. These observations indicate that little dissociation of the complex occurs in solution at room temperature, and the following equilibrium lies far to the left.

$$\underset{5}{IrH(CO)\,P_3} \rightleftharpoons \underset{6}{IrH(CO)\,P_2} + P \qquad (16)$$

The behavior at higher temperatures indicates either fluxionality in complex 5 at high temperatures, or rapid dissociation and exchange of the phosphine ligands. The nature of the high-temperature coalescense was not specified; however, only the latter alternative (dissociation to the four-coordinate species, 6) was suggested by the authors[130]. Dissociation is indeed consistent with patterns of chemical reactivity and kinetic behavior.

The reactions of $IrH(CO)\,P_3$ may in general be characterized as substitution reactions of a two-electron ligand A or two

one-electron ligands B and C (often from the molecule BC, in an oxidative-addition reaction) to form IrH(CO)(A) $\mathbb{P}_2$ or IrH(CO)(B)(C) $\mathbb{P}_2$, respectively. Besides the addition of H_2 mentioned earlier[129,132], reagents such as SO_2[158], R_3SiH[44,45,117,159], R_3GeH[117], R_3SnH[117], and activated alkenes (for example, $(CN)_2C = C(CN)_2$)[105,106] undergo reactions of this sort. Ethylene apparently only forms a complex with the trisphosphine, 5, at elevated pressures[130,132], contrary to an early report[131] which claimed the facile formation of IrH(CO) $\mathbb{P}_3(C_2H_4)$, a seven-coordinate, twenty-electron system. The tris(phosphine), 5, can exchange phosphine ligands in the presence of excess L to form IrH(CO)L $\mathbb{P}_2$ complexes, where L is a stronger base than $\mathbb{P}$[160]. When heated in an inert solvent, the tris(phosphine) complex can eliminate hydrogen as well as phosphine to form a P-bridged dimer, 12[161,162].

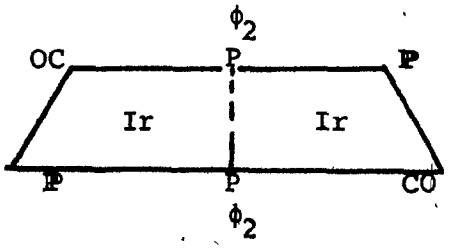

12

Kinetic studies on systems involving the tris(phosphine) complex, 5, indicate a stepwise mechanism of substitution, in which the dissociation of phosphine from complex 5 forms a reactive intermediate, 6, which readily undergoes oxidative

addition[45,117,132].

$$IrH(CO)\,\mathbb{P}_3 \underset{+\,\mathbb{P}}{\overset{-\,\mathbb{P}}{\rightleftharpoons}} IrH(CO)\,\mathbb{P}_2 \underset{-BC}{\overset{+BC}{\rightleftharpoons}} Ir(H)(CO)(B)(C)\,\mathbb{P}_2 \qquad (17)$$

A system of this sort, where BC = H_2, has been mentioned in the previous section (equations 12 and 13). The intermediate, 6, is apparently too reactive to isolate (see below), and undergoes oxidative addition reactions quite readily. A system utilizing the above equilibrium has been studied[45], in which a classical donor ($\mathbb{P}$) and the oxidative addend R_3SiH were both competing for addition to the intermediate, 6. In this case, measurements of the activation parameters led to the conclusion that the largest effect on the reaction rate was deformation of the square-planar complex by the addend, rather than the processes of bond-making and bond-breaking. Consequently, it was suggested that oxidative-addition and classical donor coordination are energetically similar processes, at least in those cases where the oxidative addition is concerted.

3. $IrH(CO)[P(C_6H_5)_3]_2$ (6)

The title complex was first reported[80,163] and

characterized by Malatesta, Angoletta, and Caglio in the mid-sixties. Since that time, it has been cited in several places, mainly reviews[164], as well as a more recently reported synthesis by another method[146]. In contrast, the failure to isolate this complex by a variety of methods has also been reported[155], as well as numerous indications from kinetic[45,132-135] and spectroscopic[130] studies that the complex is highly reactive and unstable in solution.

In the original study[80], the complex in question was prepared by bubbling CO through IrH_3P_2, and the product characterized on the basis of i.r., elemental analysis, and the following reactions:

$$\text{"}IrH(CO)P_2\text{"} + P \longrightarrow \underset{5}{IrH(CO)P_3} \qquad (18)$$

$$\text{"}IrH(CO)P_2\text{"} \underset{+N_2}{\overset{+H_2}{\rightleftharpoons}} \underset{1}{IrH_3(CO)P_2} \qquad (19)$$

In the later report of Zanella et al.[146], a compound identical to the one mentioned above in color, m.p. and i.r. was isolated and identified as $IrH(CO)P_2$ by reference to the original work.

The dicarbonyl complex $IrH(CO)_2P_2$, 13, has been prepared

by several methods[130,165,166], including bubbling CO through a solution of the tris(phosphine) complex, 5. The dicarbonyl has been very well characterized by i.r. and n.m.r. at various temperatures[130], and by crystallographic structure determination[167]. The physical properties of the dicarbonyl complex correspond closely to those of the compound isolated by Zanella and Malatesta, as can be seen in the following table.

Table I-1. Reported Data on $IrH(CO)\ P_2$.

	"$HIr(CO)\ P_2$"	"$HIr(CO)\ P_2$"	$HIr(CO)_2\ P_2$
ref.	80	146	130
mp (°C)	132	128	135
color	pale yellow	pale yellow	yellow
i.r. (cm^{-1})	2040	2037 (nujol)	2029 (nujol)
	1980	1975	1970
	1920	1913	1915

In view of this striking similarity and the widespread evidence of the instability of $IrH(CO)\ P_2$, the compounds isolated by Malatesta[80] and Zanella[146] should undoubtedly be characterized as the dicarbonyl, $IrH(CO)_2\ P_2$. Indeed, Wilkinson has already suggested[130] an early claim[163] of $IrH(CO)\ P_2$ was actually the dicarbonyl, 13. It is not surprising that the chemistry of the dicarbonyl, 13, should

mimic that of monocarbonyl, 6, since the former complex reacts via CO dissociation, to form the monocarbonyl, 6, as a highly reactive intermediate. Most of the preparations[80] of the putative $IrH(CO)\,P_2$ involve excess CO, and so are also consistent with a dicarbonyl formulation. The only remaining curiosity is the production of "$IrH(CO)\,P_2$" by bubbling nitrogen through a solution of the trihydride, $IrH_3CO\,P_2$[80]. Here it is likely that either a compound other than the dicarbonyl was formed (but having a band at 1985 cm^{-1}, similar to the products of a nitrogen purge reported in Chapter 2), or a reaction with the precipitating solvent, ethanol, occurred to form the dicarbonyl, as indeed occurred in the report of Zanella[146]. In any case, it is clear that $IrH(CO)\,P_2$ has not yet been isolated and characterized, and that all previous claims to its existence, other than as a reactive intermediate, are erroneous.

It might be pointed out here that the other "unsaturated" hydride isolated in the study by Malatesta et al., $IrH_3\,P_2$, has been shown to be the pentahydride, $IrH_5\,P_2$[168]. Since many of the compounds in this study have been characterized by a network of interlocking reactions, it is likely that many of the others have been mischaracterized as well. In particular, $IrHI_2L_2$, $[IrH_2L_2]ClO_4$, IrH_2IL_2 and $[IrH_2(CO)L_2]ClO_4$ should probably be identified, respectively, as $IrH_3I_2L_2$, $[IrH_4L_2]ClO_4$,

IrH_4IL_2 and $[IrH_2(CO)_2L_2]ClO_4$ instead. By the same token, the five-step reaction scheme proposed by Zanella for the reaction of $IrH_3\,\mathbb{P}_2$ (or $IrH_5\,\mathbb{P}_2$) with ethanol must likewise be considered invalid, since it was largely based upon the characterization of the reaction product as "$IrH(CO)\,\mathbb{P}_2$".

Although $IrH(CO)\,\mathbb{P}_2$, 6, has not been isolated, there is a large amount of chemical and kinetic evidence indicating that it is an intermediate in the substitution reactions of saturated iridium species of the formula $IrH(CO)(XY)\,\mathbb{P}_2$, where XY is a classical donor or oxidative addend. The chemical evidence includes the repeated demonstration of the reversibility of the following equilibria, and the interconvertibility of many of the possible XY/AB combinations.

$$IrH(CO)(XY)\,\mathbb{P}_2 \underset{+XY}{\overset{-XY}{\rightleftharpoons}} IrH(CO)\,\mathbb{P}_2 \underset{-AB}{\overset{+AB}{\rightleftharpoons}} IrH(CO)(AB)\,\mathbb{P}_2 \qquad (20)$$

XY or AB = $\mathbb{P}$[80,132], R_3SiH[45], R_3SnH[117], R_3GeH[117], SO_2[158], CO[130], H_2[80,132]

Reactions where XY or AB is gaseous are convenient in this regard in that they may be readily initiated (by bubbling the gas through the solution) or reversed (by heating, or purging with inert gas). Kinetic measurements are consistent with a dissociation mechanism to form an unsaturated intermediate, 6, when XY = $\mathbb{P}$, AB = R_3MH, (R_3 is a variety of organic and

electronegative groups, M is a group IV element)[45,117], and XY = P, AB = H_2[132]. These kinetic studies are consistent with a n.m.r. study which indicates complex 6 is in a very low concentration when in the presence of a free ligand[130].

There has been no definite spectroscopic evidence for the existence of complex 6, and so the stereochemistry is unknown. The high-temperature spectrum of the tris(phosphine) complex, 5, indicated only rapid exchange of the ligand, not the spectrum of the dissociated species[130]. The rhodium analogue, RhH(CO) P_3, which is much more highly dissociated in solution than the iridium complex, 5, has been studied spectroscopically at various temperatures[169]. Evidence for a high degree of dissociation comes from cryoscopic and osmometric molecular weight measurements. Also, n.m.r. data indicate that rapid P exchange occurs at room temperature, but at -30°C, the complex exists as an undissociated trigonal bipyramid. Because both n.m.r. chemical shifts (^1H in Rh-H) and infra-red stretching frequencies (ν_{Rh-H}, ν_{C-O}) were unchanged over a range of temperature and solvents for which the degree of dissociation was known to be different, it was concluded that the H and CO ligands were trans to one another in the dissociated and undissociated species. Therefore, RhH(CO) P_2 has a square planar, P-trans geometry.

By analogy to the rhodium case, it is reasonable to assign to IrH(CO) P_2, 6, a square planar, trans- P geometry as well.

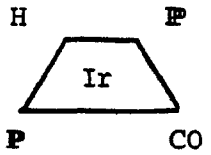

14

This geometry is reasonable from the viewpoint of the comparative steric properties of the phosphine ligands. Also, this complex, 14, is an analogue of Vaska's complex, 2, which has trans phosphines. A large and well-studied group of analogues to Vaska's complex, 2, of formula $IrXYZ_2$, where X is a variety of electro-negative species, Y = CO or CS, and Z any of a large number of tertiary phosphines or arsines, all have a planar geometry with Z in the trans position. This geometry is even observed when the Z ligands are connected by a long alkyl chain[99]. The sole exception appears to be a chelating diarsine complex, which is reportedly of cis configuration[170]; this complex has not been definitively characterized, however.

The stereochemistry of oxidative addition to complex 14, generated by the use of the tris(phosphine) complex, 5, can be compared to that observed for analogues of Vaska's complex. The addition of hydrogen to Vaska's analogues has been studied in detail[51], and it was found that products in which the phosphorus ligands remain trans are formed stereospecifically.

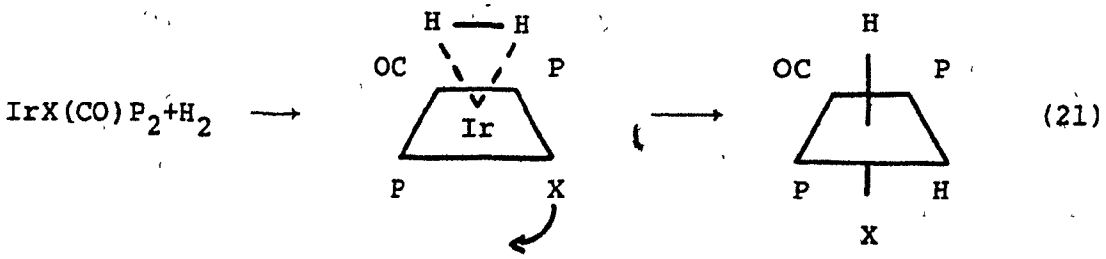

(21)

The stereochemistry of the products when X = H has not yet been reported; much of the present thesis deals with this subject. The addition of silicon hydrides to analogues of Vaska's complex has been studied for cases where X is a hydride or halogen. These studies are related to those of hydrogen addition, because both represent concerted oxidative additions. Addition to complexes under mild conditions yield products analogous to the above reaction, when X = Cl[123].

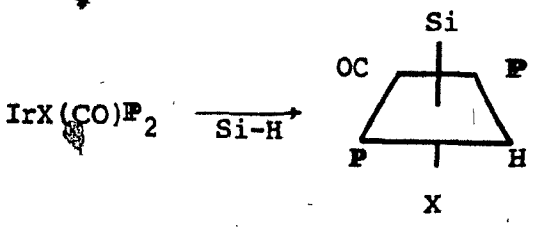

(22)

15

In solution, however, the dihydride, 16, was isolated with an entirely different stereochemistry[171] through a process

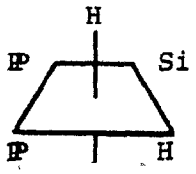

16

apparently involving reductive elimination of a Si-Cl compound. The same product was observed for the addition of Si-H compounds to the tris(phosphine) complex, 5, suggesting that the intermediate 14 was involved in both cases[159]. An experiment using a silicon deuteride complex indicated that both ligands added trans to phosphine[172].

CHAPTER II

STRUCTURE AND ISOMERIZATION OF $IrH_3(CO)[P(C_6H_5)_3]_2$

A. INTRODUCTORY REMARKS

The structure of $IrH_3(CO)P_2$ and the nature of its isomerization are reported in this Chapter. Two isomers of the title complex have been isolated in pure form and fully characterized by i.r. and n.m.r. spectroscopies. The nature of the equilibrium between isomers, and the conditions under which it is established have been studied. Ambiguities in the literature regarding the structure and isomerization of the title complex, referred to in the Introduction (Chapter I), have been resolved. After the completion of this work, the structures of the two isomers were determined by n.m.r. and reported[140], although isomerization behavior was not discussed.

B. EXPERIMENTAL PROCEDURE

1. Preparation and Purification of fac and mer $IrH_3(CO)P_2$

The following procedure is a variation of a published method[80]. A suspension of trans-$IrCl(CO)P_2$[154] (.50 g, .64 mmol) and sodium borohydride (.15 g, 3.9 mmol) was stirred in freshly distilled acetonitrile (5 ml) for 24 h under an

atmosphere of hydrogen. The solution was then evaporated to dryness in a stream of hydrogen. The iridium complex was extracted into toluene (6 ml) by stirring the residue in toluene for one hour at 40°C under hydrogen, and filtering the resulting suspension. The mer isomer was precipitated from the filtrate by the careful addition of hexane (6 ml) and filtered from the solution. As soon as possible after removal of the mer isomer (< 5 min), the fac isomer was obtained by addition of more hexane (ca. 10 ml), cooling the solution to ca. -20°C, and filtering the solution under nitrogen. Although the trihydride was produced in high yield (ca. 80%) the total amount of pure isomers obtained was less, usually 20-30% each. The relative proportion of the mer isomer could be increased by leaving the initial toluene/hexane solution under hydrogen for 24 h. Under these conditions, a 53% yield of pure mer isomer was obtained.

2. Measurement of Spectra

Infra-red spectra were recorded on a Perkin-Elmer 257 Grating Infra-red Spectrophotometer. All spectra were calibrated by reference to the 1601 and 1583 cm^{-1} peaks of polystyrene, and are believed accurate to $\pm$ 2 cm^{-1}.

Solid-state spectra were obtained from samples dispersed in KBr disks, or Nujol mulls between NaCl plates. Solution

spectra were measured using matched 1 mm pathlength solution cells with NaCl windows. Samples were transferred to the cells with a syringe from a standard methylene chloride solution (ca. 7 mM). Atmospheric gases were not rigorously excluded during the transfer process. Spectra were recorded within five minutes of transfer. Stock solutions were kept in a constant temperature bath under a static atmosphere of hydrogen or nitrogen. In experiments done with a nitrogen purge, a constant total concentration of iridium in solution was maintained by periodic restoration of the sample volume with solvent.

Proton n.m.r. spectra were measured at 90.023 MHz on a Bruker WH-90 Fourier-Transform Spectrometer equipped with a liquid nitrogen variable temperature probe capable of ± 2°C temperature stability. Chemical shifts were measured electronically from the solvent-reference ($CHDCl_2 \equiv 4.65$ τ, or $C_6D_5\text{-}CHD_2 \equiv 7.91$ τ), and are accurate to ± .01 ppm. Coupling constants and relative chemical shifts are accurate to ± .5 Hz, except where noted.

The ^{31}P n.m.r. spectra were measured on the same instrument at 36.442 MHz. Chemical shifts were measured electonically from an external reference (85% $H_3PO_4 \equiv 0.00$ δ), and are accurate to ± .02 ppm. Since coupling with the phenyl protons on the tertiary phosphine ligands results in very

broad signals, spectra were recorded with these protons decoupled. In some cases, it was possible to selectively decouple the phenyl protons; the remaining hydride-phosphorus coupling, however, was diminished by residual decoupling [$J_{H-P}(^{31}P$ spectra) = $.66J_{H-P}(^{1}H$ spectra)]. The reported coupling constants are corrected for partial decoupling and are accurate to ± 2 Hz.

Spectra were measured in CD_2Cl_2 solution (ca. 20 mM). Samples run at low temperature were cooled soon (< 5 min) after dissolution. Vortex plugs were used in the samples run at room temperature, and these isolated the solutions to some extent with respect to gaseous interchange within the n.m.r. tube. Solutions were filtered and put in tubes under nitrogen but not sealed rigorously, nor was the solvent degassed prior to dissolution.

Second-order spectra were analyzed according to an AA'XX' spin system. Coupling constants were determined by repeated simulations until a suitable fit with the experimental spectrum was obtained. A calculator program was written to facilitate this, and is given in Appendix III.

C. RESULTS

1. Infra-Red Spectra

The infra-red spectra of both isomers in the solid state

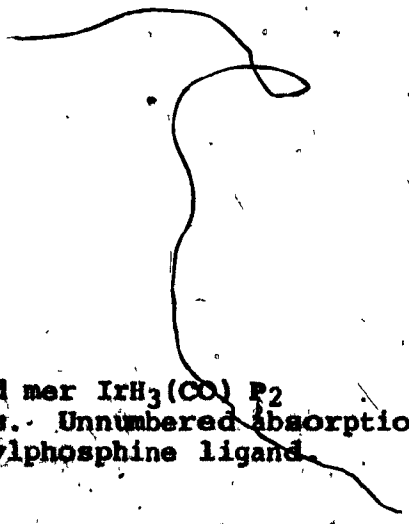

Figure II-1. I.R. spectra of fac and mer $IrH_3(CO)P_2$ measured as nujol mulls. Unnumbered absorptions are due to the triphenylphosphine ligand.

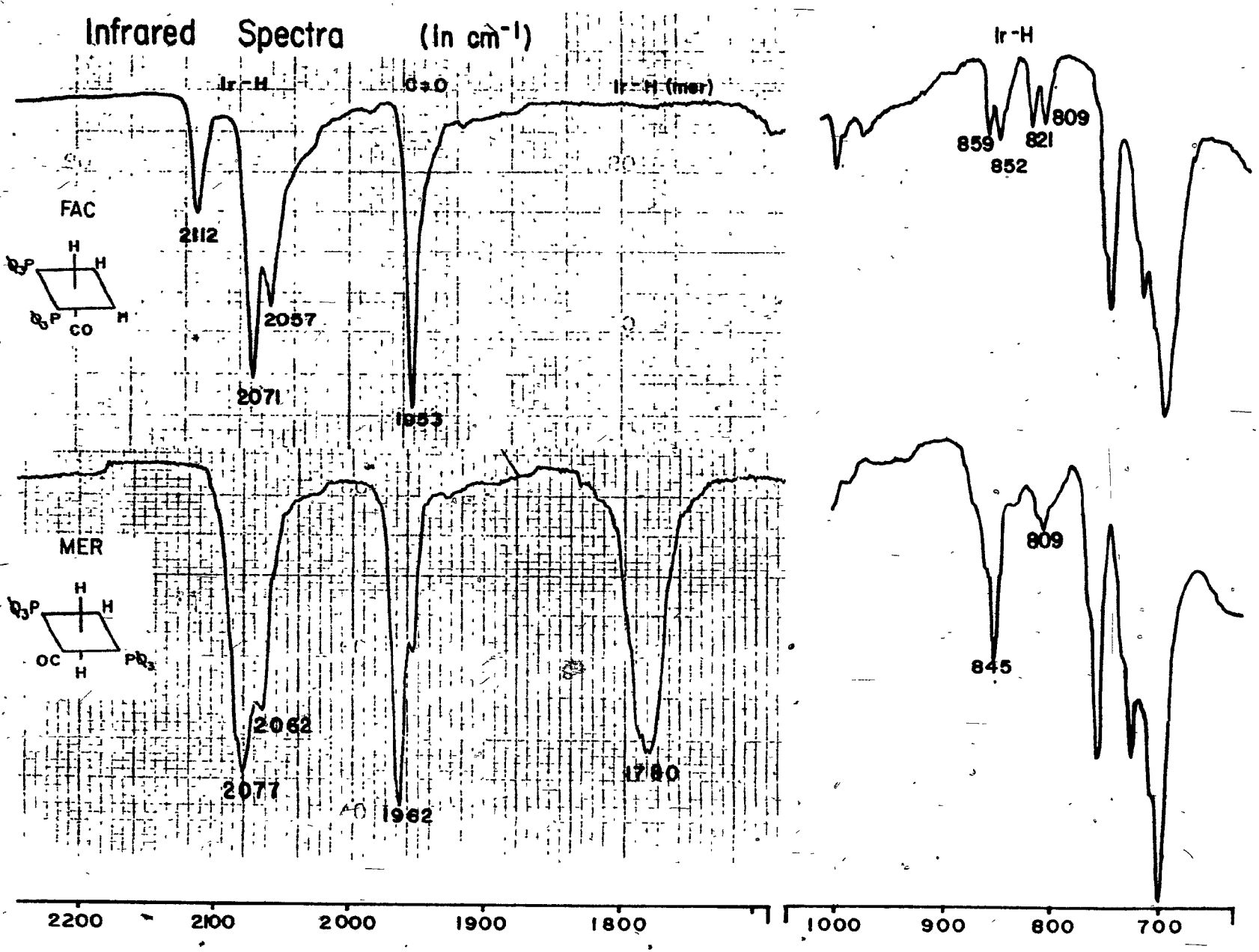
Infrared Spectra (In cm⁻¹)
Ir-H
C=O
Ir-H (mer)
FAC
2112
2057
2071
1953
MER
2062
2077
1962
1780
Ir-H
859
852
821
809
809
845
2200
2100
2000
1900
1800
1000
900
800
700

Table II-1. Infra-red spectra of fac and mer $IrH_3(CO)P_2$.

isomer (pt. group)	Absorption wavenumbers (cm^{-1}) (nujol)	(CH_2Cl_2 soln)	(literature)[80]	Assignments (mode)	(group-trans ligand)
	2077 s 2062 m	2086 s	2080	$2A_1$	ν_{Ir-H} (CO)
mer C_{2v}	1962 s 1953 sh	1969 s	1965		ν_{CO} (H)
	1780 s,br	1785 s	1785	B_1	ν_{Ir-H} (H)
	845 m 809 w		845 802		δ_{Ir-H}
	2112 m	-	2118	A'(2)	ν_{Ir-H} (P)
fac C_s	2071 s 2057 m	2083 s	2080	A'(1) A"	ν_{Ir-H} (CO,P)
	1953 s	1972 s	1960		ν_{CO} (H)
	859 w 852 w 821 w 809 w		850 840 820 800		δ_{Ir-H}

are shown in Figure II-1. Corresponding infra-red wavenumbers in the region 2200-1700 cm^{-1} are listed in Table II-1, and compared with literature values. It can be seen from Figure II-1 that complete isomeric separation has been achieved: peaks characteristic of one isomer are absent in the spectrum of the other. For example, there is no peak at 2112 cm^{-1} in the spectrum of the mer isomer, nor any at 1780 cm^{-1} in that of the fac isomer. The wavenumbers reported here agree well with published values[80]. The assignments are discussed in detail below. Solution spectra are listed in Table II-1, and are further described below, and in Figures II-7 to II-9.

2. The N.M.R. Spectra of the Isomers

The ^1H n.m.r. spectra of both isomers of $IrH_3(CO)P_2$ were measured at 25°C in methylene chloride-d_2, and are presented in Figures II-2 and II-3. The spectrum of the mer isomer may be analyzed and assigned in a first-order manner. The parameters agree closely with those of analogous compounds in the literature, as can be seen in Table II-3. The fac isomer is not amenable to first-order analysis; a computer simulation* using literature values[142,143] was performed

*This simulation was done by Dr. Gordon Hamer of Dr. Perlin's laboratory, McGill University, as were most of the ^1H spectra. The ^{31}P spectra were measured by Dr. William Dawson, of that laboratory. All other calculations of spectra and spectral parameters were done by the author.

Figure II-2. The ^{1}H n.m.r. spectrum of mer-$IrH_3(CO)P_2$, measured at 25°C 0.2 h after dissolution in CD_2Cl_2. Peaks due to the fac isomer are hatched. The frequencies of numbered peaks are listed in Appendix II.

Proton NMR Spectrum

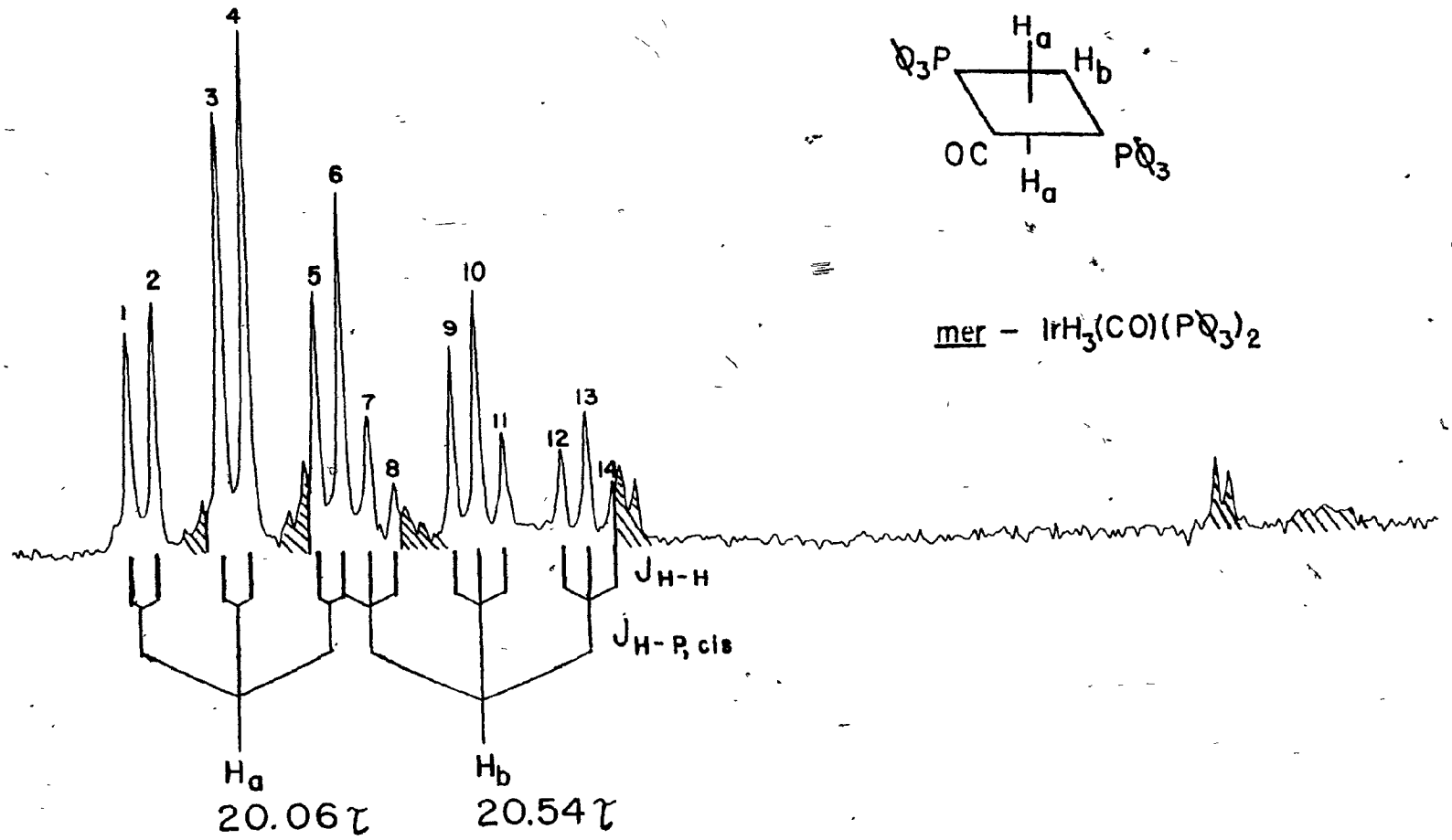

mer – $IrH_3(CO)(PR_3)_2$

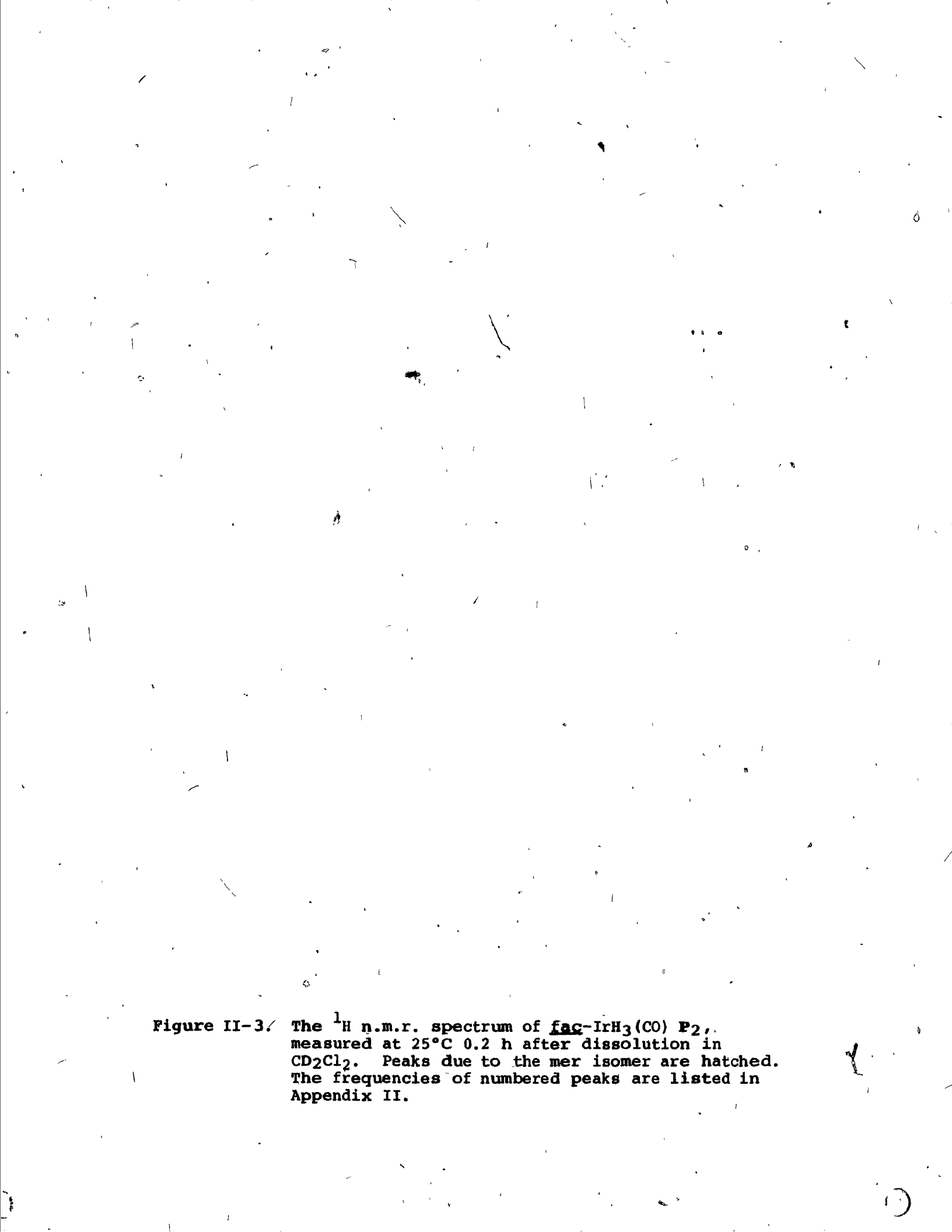

Figure II-3. The ^1H n.m.r. spectrum of fac-$IrH_3(CO)P_2$, measured at 25°C 0.2 h after dissolution in CD_2Cl_2. Peaks due to the mer isomer are hatched. The frequencies of numbered peaks are listed in Appendix II.

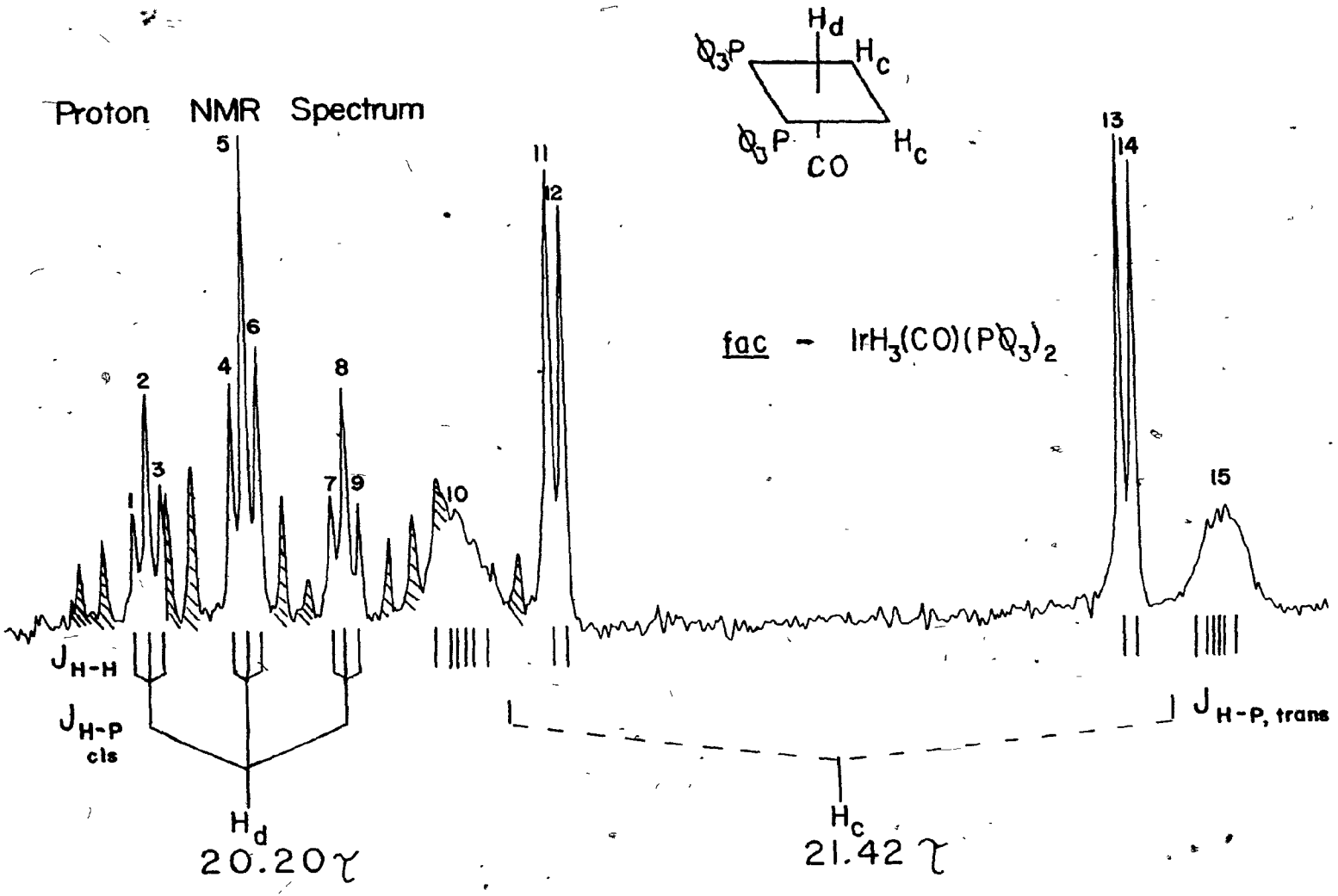
Proton NMR Spectrum
Q_3P
H_d
H_c
Q_3P
CO
H_c
fac - $IrH_3(CO)(PQ_3)_2$
1
2
3
4
5
6
7
8
9
10
11
12
13
14
15
J_{H-H}
J_{H-P} cis
$J_{H-P, trans}$
H_d
20.20 τ
H_c
21.42 τ

Table II-2.** ^{1}H and ^{31}P n.m.r. parameters for fac and mer $IrH_3(CO)\,\mathbb{P}_2$*.

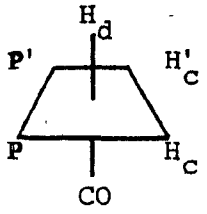

3

fac isomer

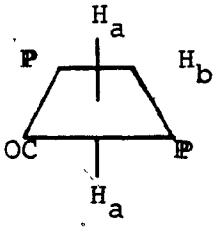

7

mer isomer

Chemical shifts†

H_d	-10.20 δ (20.20 τ)	H_a	-10.06 δ (20.06 τ)
H_c	-11.42 δ (21.42 τ)	H_b	-10.54 δ (20.54 τ)
P	6.55 δ	P	15.48 δ

Coupling constants, ^{1}H spectra‡

$J_{H_d-H_c}$	(cis) 2.4 Hz	$J_{H_{a,a}-P,P}$	(cis) 16.6 Hz
J_{H_d-P}	(cis) 18.1	$J_{H_b-P,P}$	(cis) 19.5
$J_{H_c-P'}$	(trans) 123.1	$J_{H_{a,a}-H_b}$	(cis) 4.6
J_{H_c-P}	(cis) -18.1		
$J_{H_c-H'_c}$	2-5		
$J_{P-P'}$	4-8		

continued/

Table II-2 continued.

	fac isomer		mer isomer	
Coupling constants, ^{31}P spectra[ʃ]				
J_{H_d-P}	(cis) 18 Hz	(12.0; .66)	J_{H_a-P} 17 Hz	(11.0; .66)
$J_{H_c-P'}$	(trans) 123	(81.2; .66)	J_{H_b-P} 20	(12.9; .66)
J_{H_c-P}	(cis) -18	(-12.0; .66)		
$J_{PP'}$	-	(12.0; 1.5-3)		
$J_{H_cH_{c'}}$	-	(0; 0)		

---

[*] All spectra measured in CD_2Cl_2.

[**] The chemical shifts are recorded throughout the thesis in τ units, in common with most of the literature. Both δ and τ units are given in this table. The units may be interconverted by the formula δ shift = 10 - τ shift.

[†] ^1H measured at 25°C, ± .01 ppm error; ^{31}P measured at 25°C, relative to 85% H_3PO_4, ± .02 ppm error.

[ǂ] Coupling constants measured and calculated from hydride spectra; ± .5 Hz error.

[ʃ] Coupling constants calculated from $^{31}P\{$phenyl protons$\}$ spectra and are corrected for partial decoupling; ± 2 Hz error. Values in parentheses are the apparent coupling constant, and the ratio J(^1H spectra)/J(^{31}P spectra).

Table II-3. Proton n.m.r. parameters for analogous mer-$IrH_3(CO)L_2$ complexes.

L	reference	H_a (τ)	H_b (τ)	J_{P-H_a} (Hz)	J_{P-H_b} (Hz)	$J_{H_a-H_b}$ (Hz)
$P(C_6H_5)_3$*	present study	20.10	20.53	16.7	19.3	4.6
$P(C_6H_5)_3$‡	140	19.2	19.9	16	20	5
$P(C_2H_5)_2(C_6H_5)$†	143	20.79	21.58	16.5	20.7	4.8
$P(t\text{-}C_4H_9)_2(n\text{-}C_3H_7)$†	144	21.58	22.39	14.6	19.2	4.8

*Measured at 0°C in CD_2Cl_2; ± .01 ppm error.

‡Measured at 28°C in C_6D_6; ± .2 ppm error.

†Measured at 28°C in C_6D_6; ± .02 ppm error.

(Figure II-4), and closely matches the experimental spectrum. The spectra, assignments, and analyses are further discussed in the next section. Parameters for both the fac and mer isomers are summarized in Table II-2. A complete tabulation and analysis of these spectra may be found in Appendix II.

The ^{31}P n.m.r. spectra of the trihydrides were recorded as well. A completely decoupled $^{31}P\{H\}$ spectrum of a mixture of the isomers showed only two singlets at 15.48 δ and 6.55 δ. The inclusion of phosphorus - hydride coupling in the spectrum resulted in the appearance of a quartet and a symmetrical multiplet in the $^{31}P\{$phenyl proton$\}$ spectrum (Figure II-5). These signals are assigned to the mer and fac isomers, respectively. Simulated spectra were calculated to extract values of the coupling constants, and a calculated spectrum which agrees closely with the experimental spectrum is shown in Figure II-6. Numerical values for calculated spectra are listed in Appendix II. Apparent coupling constants, used to calculate the spectrum in Figure II-6, are listed in Table II-2, along with coupling constants corrected for partial decoupling. The spectra are further discussed in the next section.

3. Isomeric Equilibrium in Solution

a) Infra-Red Spectra

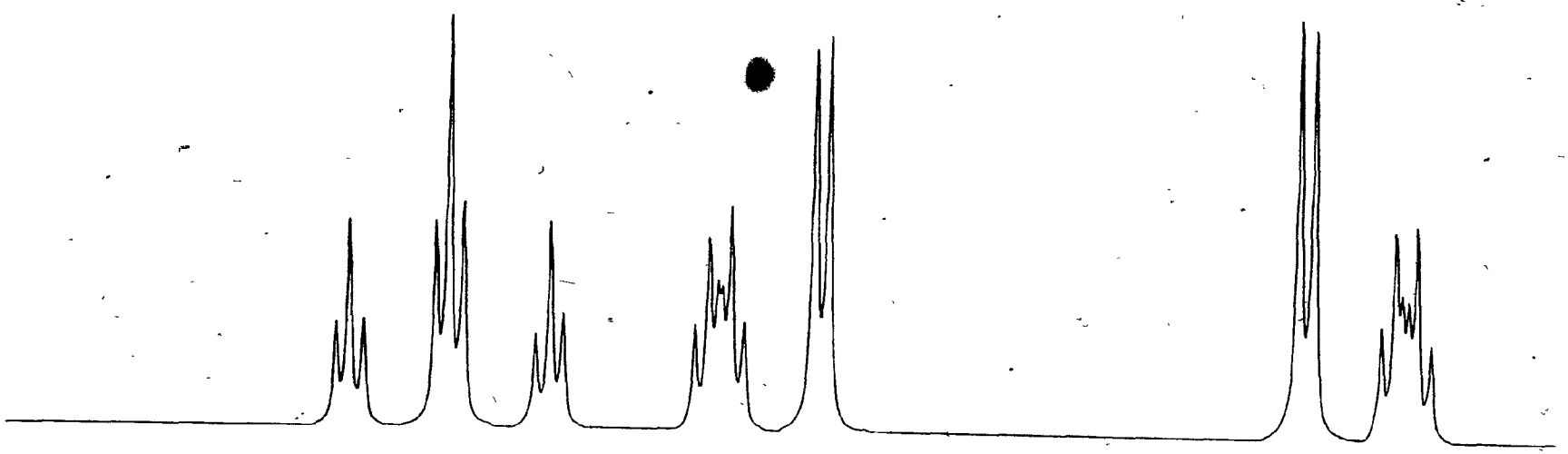

Figure II-4. A simulated ^{1}H spectrum of fac-$IrH_3(CO)P_2$. The experimental spectrum is shown in Figure II-3.

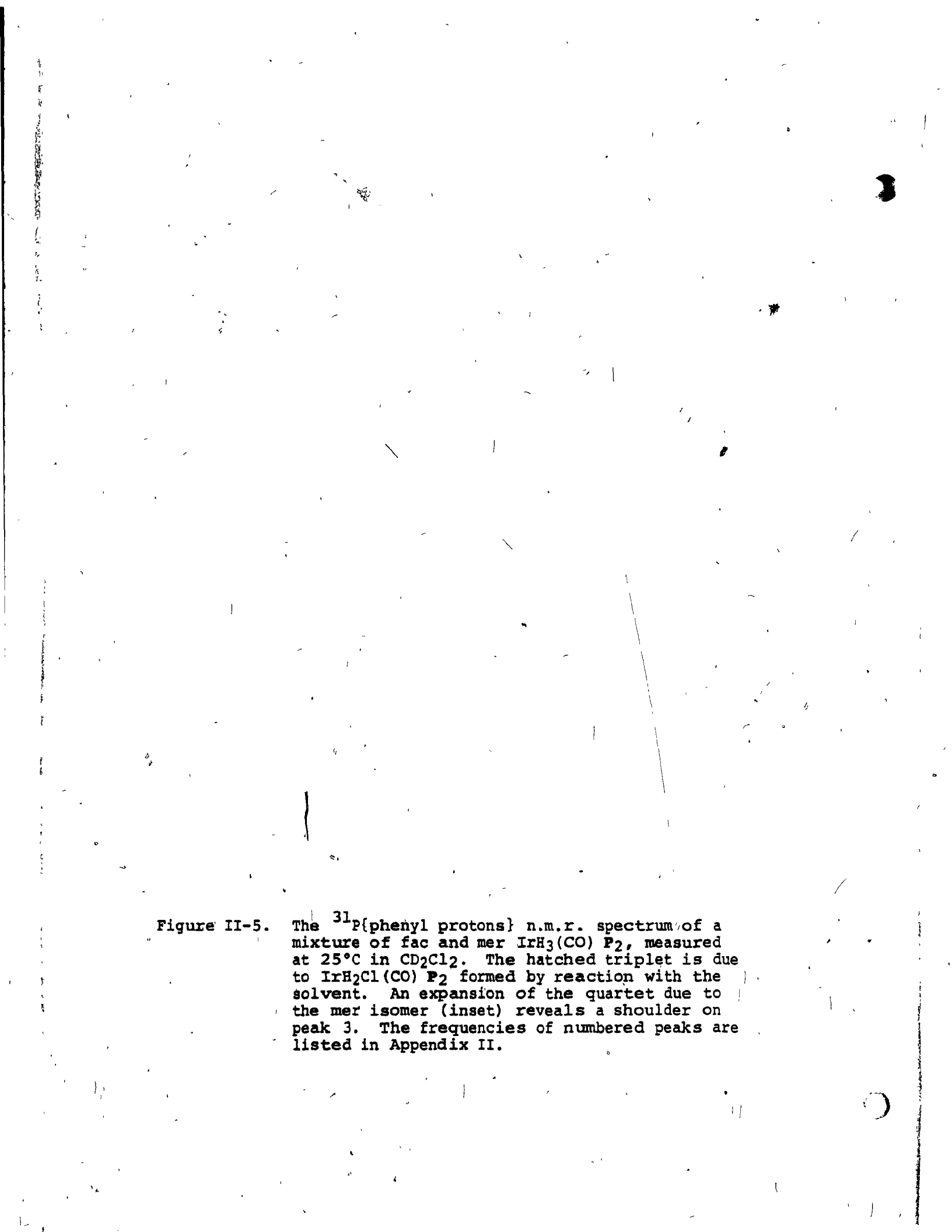

Figure II-5. The $^{31}P\{phenyl\ protons\}$ n.m.r. spectrum of a mixture of fac and mer $IrH_3(CO)\ P_2$, measured at 25°C in CD_2Cl_2. The hatched triplet is due to $IrH_2Cl(CO)\ P_2$ formed by reaction with the solvent. An expansion of the quartet due to the mer isomer (inset) reveals a shoulder on peak 3. The frequencies of numbered peaks are listed in Appendix II.

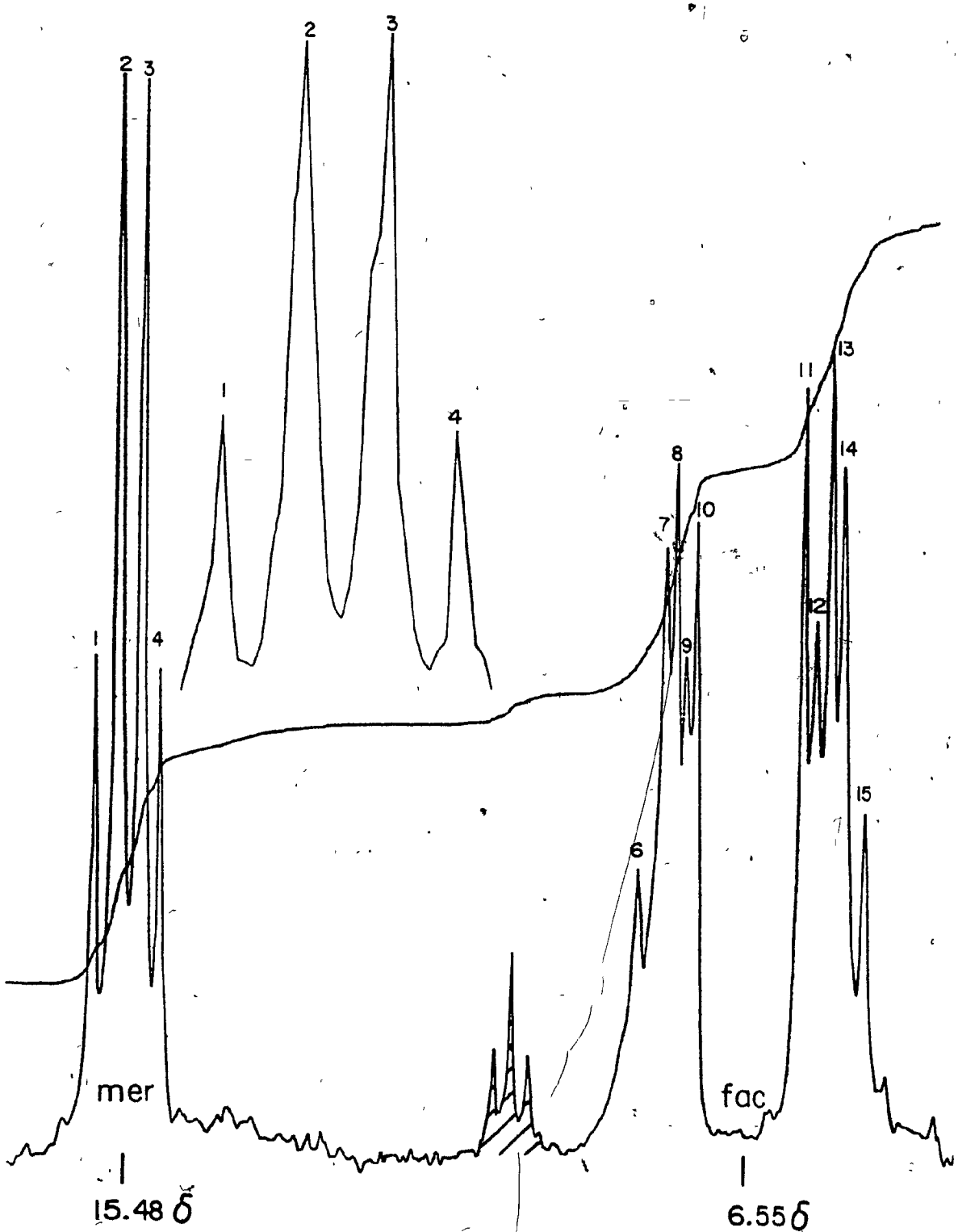
1
2
3
4
mer
15.48 δ
fac
6.55 δ

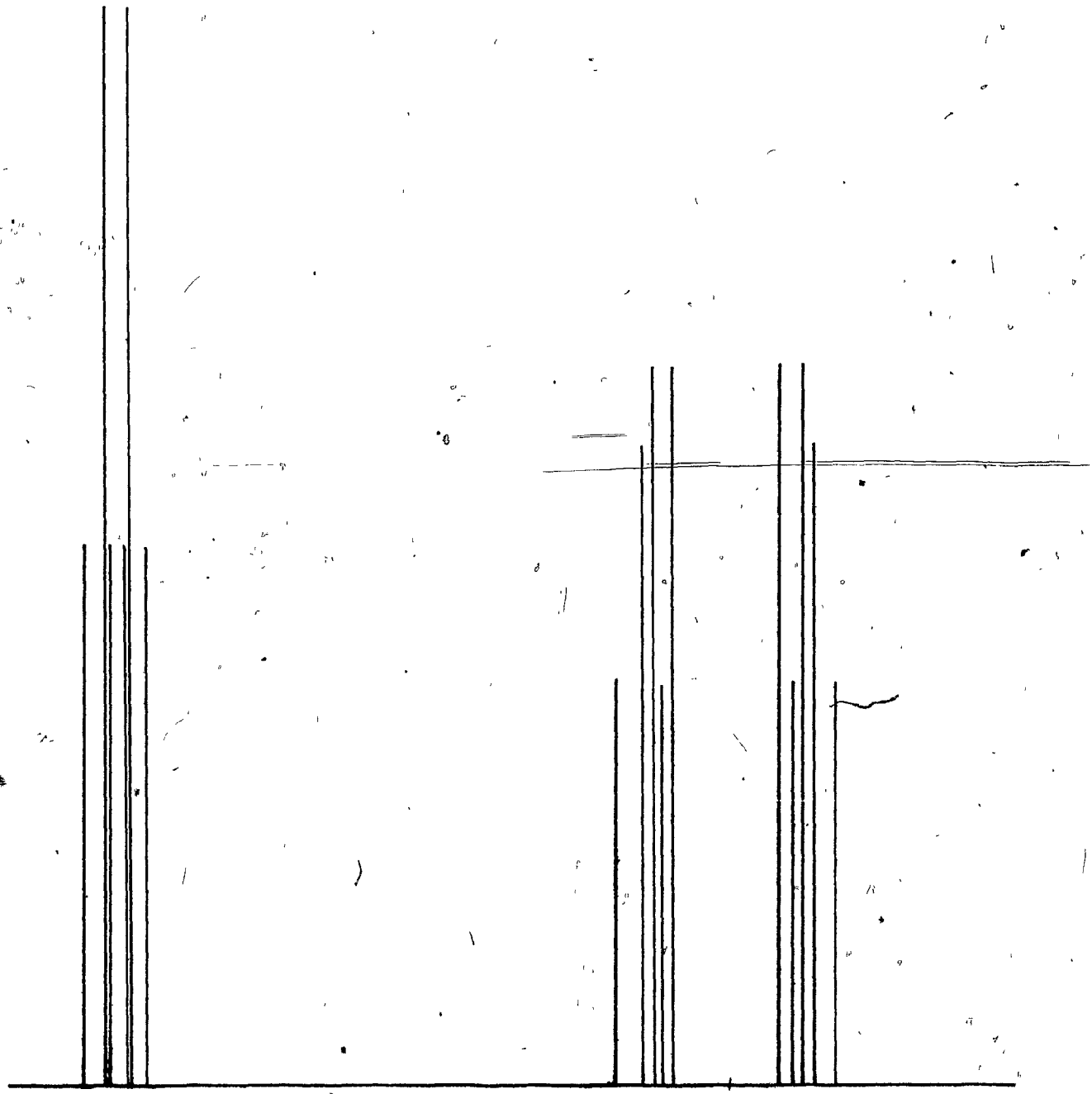

Figure II-6. A simulated $^{31}P\{phenyl\ protons\}$ spectrum of a mixture of fac and mer $IrH_3(CO)P_2$. The experimental spectrum is shown in Figure II-5.

Spectra of solutions of the fac and mer isomers in methylene chloride, initially both in pure form, were recorded under a hydrogen atmosphere at 25°C, and are shown in Figure II-7. Although the Ir-H and C-O stretching wavenumbers are similar to those measured in the solid state, solution spectra exhibit broader, less-resolved bands. The high-wavenumber peak in the spectrum of the fac isomer is not resolved in solution; consequently, the band at 2080 cm^{-1} is more intense in the solution spectrum of the fac isomer than that of the mer isomer.

Solutions that initially contained only the fac or mer isomer showed an approach to an equilibrium mixture of both isomers when kept under an atmosphere of hydrogen at 25°C, as illustrated in Figure II-7. Spectra of a solution of the mer isomer showed an increase in the Ir-H (H-trans-CO, or -P) peak at 2080 cm^{-1}, a diminution of the Ir-H (H-trans-H) peak at 1780 cm^{-1}, and constancy of the CO peak with time. Such behavior demonstrates an isomerization to an equilibrium amount of the fac isomer. Analogous behavior was seen in the variation with time of the spectra of solutions that contained initially only fac isomer. After about six hours, the spectra of both solutions were identical, with both fac and mer isomers present in the same proportion regardless of the starting isomer (Figure II-7b). The solution composition remained unchanged after 24 h under a hydrogen atmosphere,

Figure II-7. I.r. spectrum of solutions of mer and fac $IrH_3(CO)P_2^t$, under a hydrogen atmosphere, at 25°C in methylene chloride. The solutions were initially pure mer or fac isomer, but show interconversion with time in spectra a, b, and c.

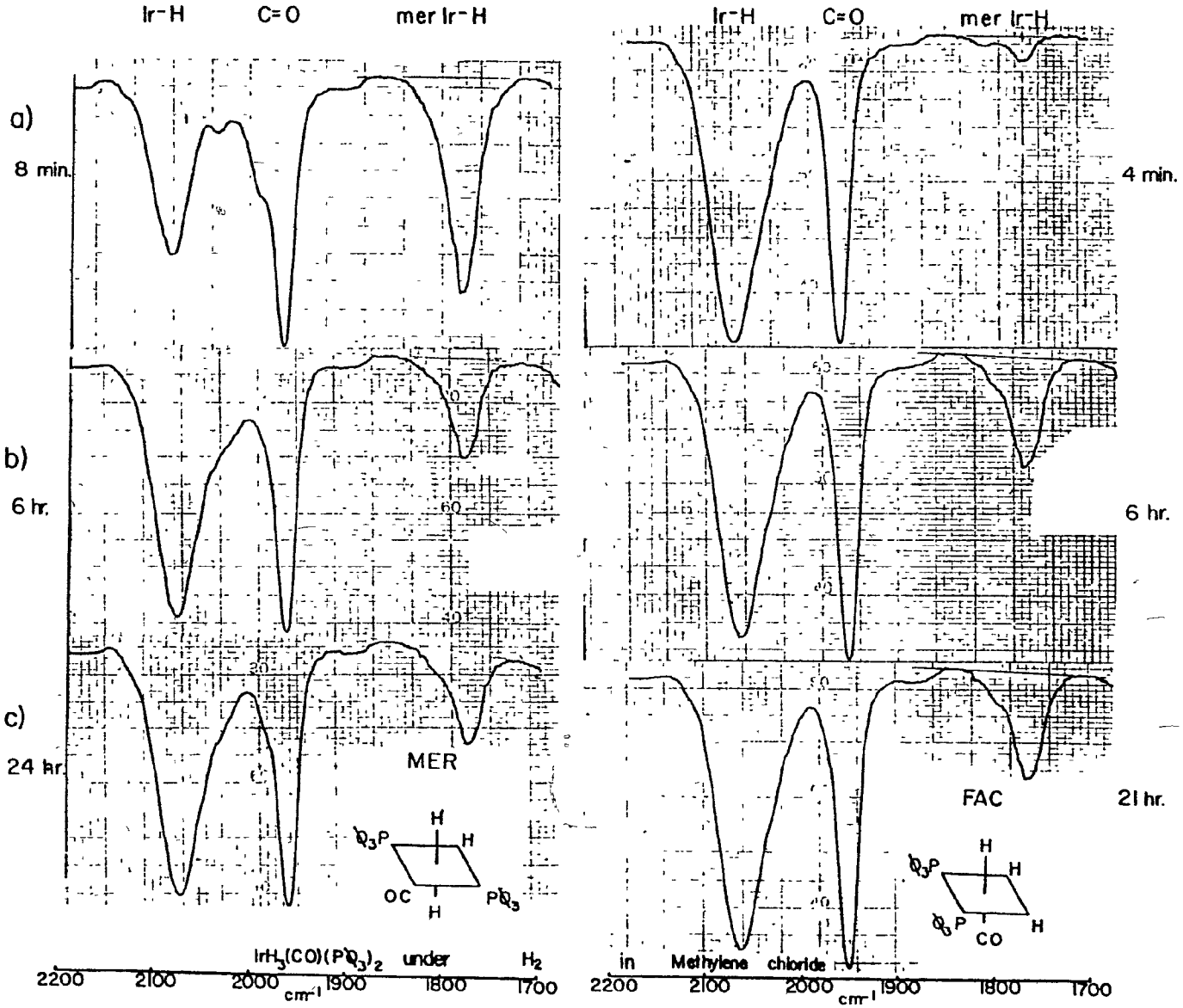
Ir-H
C=O
mer Ir-H
a)
8 min.
b)
6 hr.
c)
24 hr.
MER
H
H
OC
H
IrH3(CO)(PQ3)2 under H2
2200
2100
2000
1900
1800
1700
cm-1
Ir-H
C=O
mer Ir-H
4 min.
6 hr.
FAC
21 hr.
H
H
CO
H
in Methylene chloride
2200
2100
2000
1900
1800
1700
cm-1

with neither a departure from equilibrium nor degradation of the complexes having occurred (Figure II-7c).

Solutions of both isomers were studied under a nitrogen atmosphere, under conditions otherwise similar to the previous experiments under hydrogen. Typical spectra are given in Figure II-8. The same behavior was observed in this case as under hydrogen for the first hour; at longer reaction times, however, the spectra differed. Similar peaks due to Ir-H (2080 cm^{-1}, 1780 cm^{-1}) can be seen in the case of both the fac and mer isomers (Figure II-8b), when compared with corresponding spectra recorded under hydrogen after six hours. Peaks due to Ir-H continued to diminish when left 20 hours under nitrogen for both isomers (Figure II-8c). Although the fac sample apparently contained somewhat more hydrogen bound to iridium than the mer sample, both solutions contained considerably less than equivalent solutions under hydrogen. These spectra suggest, then, that one or both of the trihydride isomers degrade through loss of hydrogen bound to iridium, and that this loss can be prevented or reversed by the presence of molecular hydrogen in the solution.

An even greater loss of hydrogen from the system was observed when a methylene chloride solution containing the fac or mer isomers was purged with nitrogen for several hours. Experiments indicated that there is a reaction with solvent that does not occur under static nitrogen (see below).

Figure II-8. I.r. spectra of solutions of mer and fac $IrH_3(CO)P_2$, under a nitrogen atmosphere, at 25°C in methylene chloride. The solutions were initially pure mer or fac isomer, but show interconversion and loss of hydrogen with time in spectra a, b, and c.

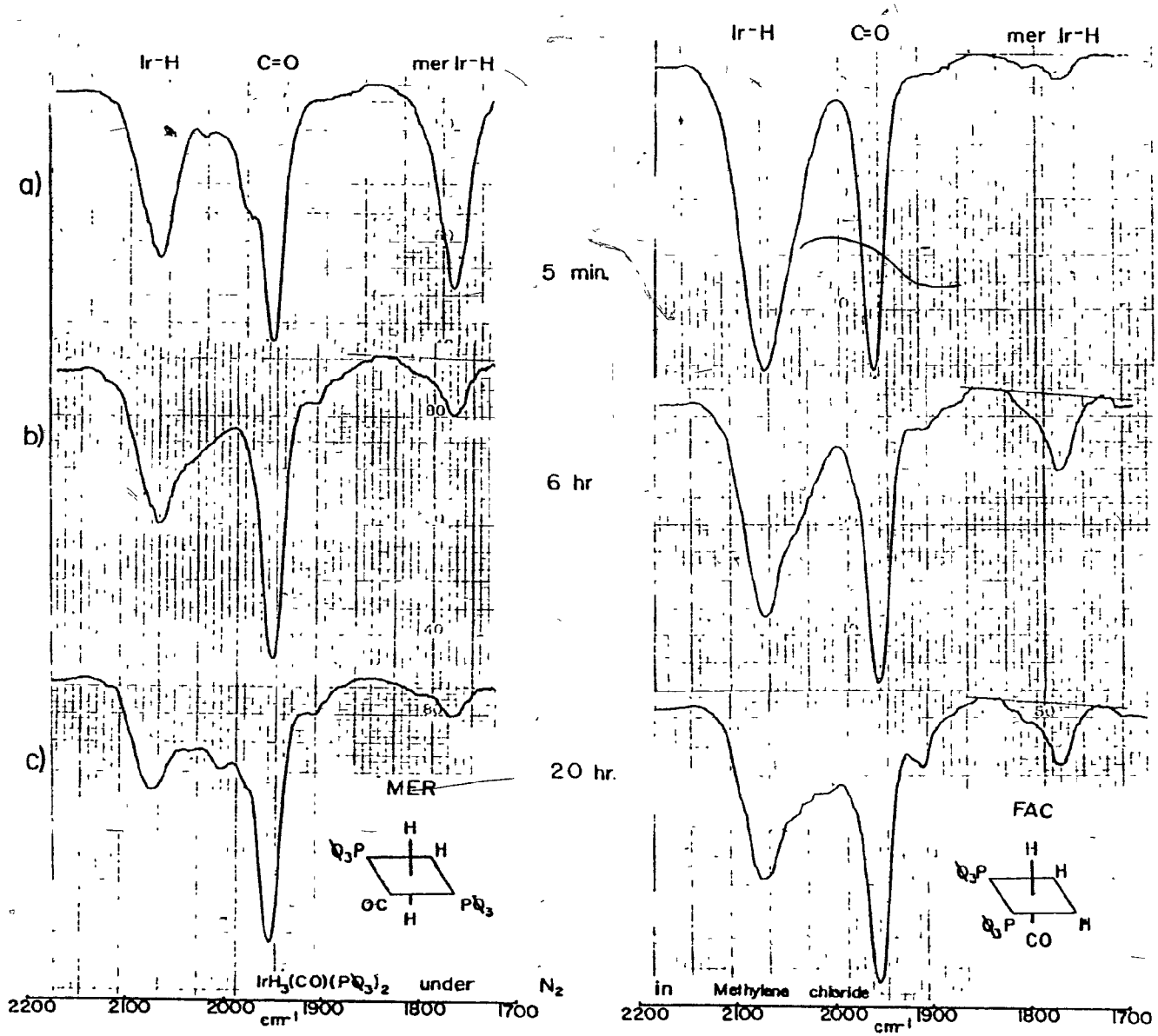
Ir-H
C=O
mer Ir-H
a)
b)
c)
5 min.
6 hr
20 hr.
MER
FAC
$IrH_3(CO)(PPh_3)_2$ under N_2
in Methylene chloride
2200
2100
2000
1900
1800
1700
cm⁻¹

b) N.M.R. Spectra

Figure II-8 shows the proton spectrum of a solution that initially contained only the mer isomer, after 4.2 h in a relatively concentrated methylene chloride-d_2 solution that was isolated from the atmosphere. Interconversion between isomers can again be observed by the appearance of peaks corresponding to the fac isomer. Spectra taken as a function of time clearly indicate a gradual diminution of all peaks associated with the mer isomer, and a corresponding increase in those of the fac isomer. In solutions of initially pure fac isomer, the opposite situation prevails. The rate of interconversion is relatively rapid soon after dissolution: a noticeable change in the spectra can be observed after only a few minutes. A few hours later, however, further change ceased; spectra obtained starting from either isomer were virtually superimposable, with all peaks in the same proportion. All peaks observed in any of these spectra may be attributed to either the fac or mer isomer of $IrH_3(CO)\ P_2$: no third species was observed.

c) Interconversion at 0°C

The interconversion of the isomers of $IrH_3(CO)\ P_2$ at 0°C was studied by infra-red and n.m.r. spectroscopies. Spectra were in all cases similar in appearance to those obtained at room temperature. The only difference between the two cases

Figure II-9. The ^{1}H n.m.r. spectrum of fac (a) and mer (b) $IrH_3(CO)P_2$, measured in CD_2Cl_2 at 25°C ca. 0.2 h after dissolution, where peaks due to the other isomer are hatched. After 4.2 h, a rerun of (b) yielded spectrum (c). An identical spectrum was obtained from a rerun of (a).

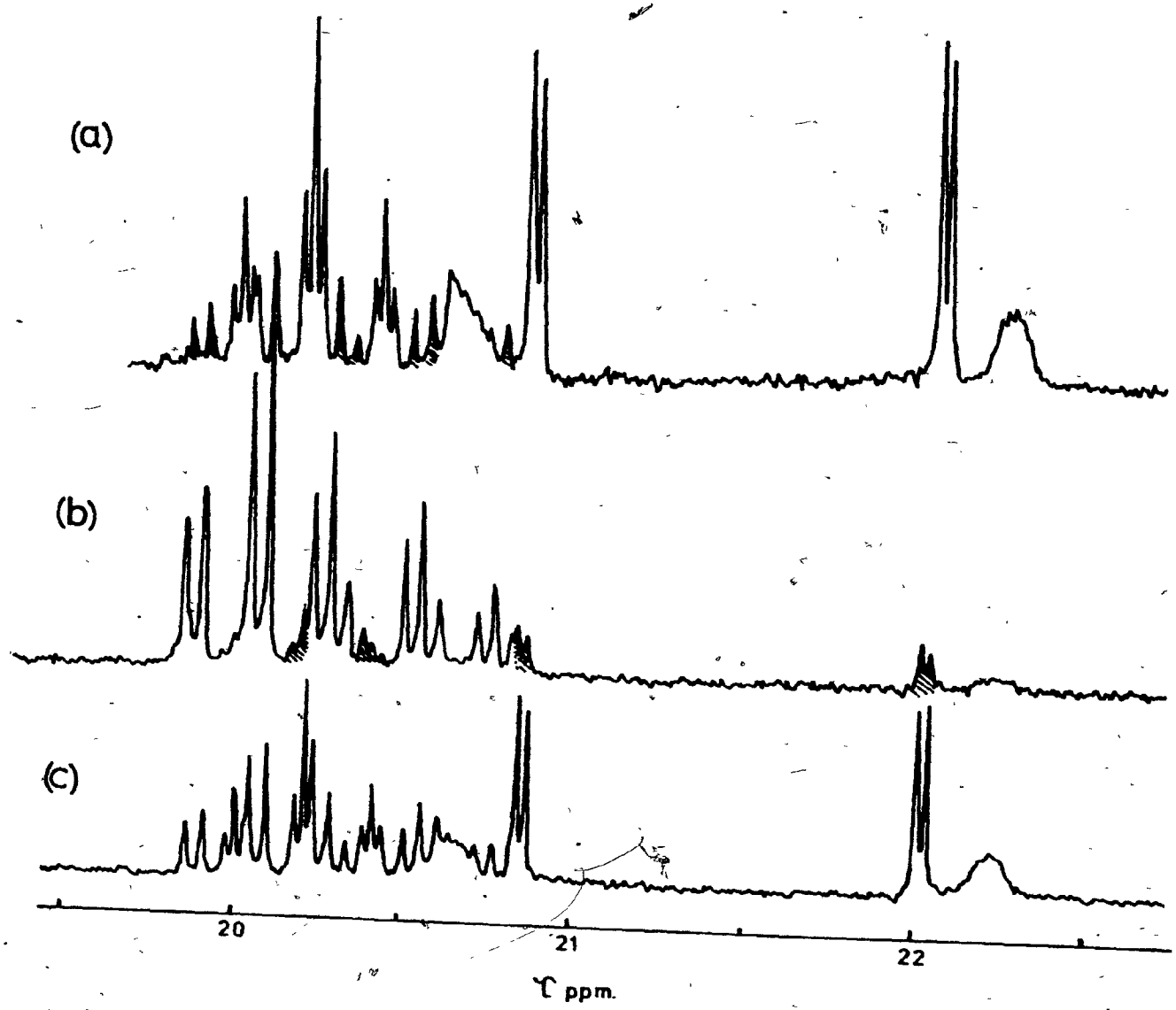
(a)
(b)
(c)
20
21
22
δ ppm.

was the much slower rate of interconversion at the lower temperature. At 0°C, samples starting from either isomer were far from equilibrium after 10 h, in contrast to the case at 25°C, where equilibrium is achieved after only ca. 3 h. Measurements of the extent of interconversion are presented in the following section.

d) Extent of Isomerization

The relative amounts of fac and mer isomer in a sample may be measured from infra-red spectra by comparing the absorbance at 1780 cm^{-1} in initial and final spectra. At equilibrium, the fac/mer ratio represents the equilibrium constant for the isomerization reaction. The n.m.r. spectra may also be used to estimate fac/mer ratios from a measurement of the relative peak heights of each isomer; details on this procedure are given in the experimental section and in Chapter V.

Values for the extent of isomerization determined in this way are given in Table II-4, where the percentages cited represent the relative amounts of the sample which have isomerized in the indicated time interval. In all cases, the isomeric purity of the initial sample exceeded 90%. At 25°C, the equilibrium mixture of isomers has been reached after 3-4 h; the concentration of the fac isomer exceeds that of the mer isomer at this temperature. At 0°C, by contrast,

Table II-4. Extent of isomerization[a].

Reaction temp (°C)		fac[b]	mer[b]	K[c]
0°C	i.r.	5-15% (6.8 h)	5-15% (6.8 h)	-
	^{1}H n.m.r.	5-15% (8.4 h)	15-25% (9.5 h)	-
25°C	i.r.	30-50% (6 h)	55-65% (6 h)	1.5
	^{1}H n.m.r.	25-30% (6.3 h)	70-75% (4.2 h)	2.8

[a]Table gives the percent of the isomer which has isomerized in comparable time intervals for methylene chloride solutions that were initially pure fac or mer $IrH_3(CO)P_2$.

[b]Isomer at start of reaction.

[c]fac/mer ratio.

there was little isomerization in comparable time periods. The mer isomer, for example, as measured by n.m.r., isomerizes up to 75% in 4 h at 25°C, while at 0°C, only up to 25% isomerization was observed in twice that time.

There is a discrepancy between the values obtained by n.m.r. and i.r. This is especially evident for the mer isomer at 25°C, where a higher value was obtained by n.m.r. than by i.r. The infra-red result is regarded as more accurate for two reasons: a) the infra-red measurements were carried out under a hydrogen atmosphere, whereas the n.m.r. experiments were not, and therefore might be subject to partial oxidation or non-equilibrium conditions; b) the infra-red measurements are straightforward applications of Beer's law, while the n.m.r. measurements are based on peak heights. The use of the latter parameter involves a variety of assumptions regarding the theoretical splitting patterns and the proportionality of peak height to peak area. While the n.m.r. measurements are thus subject to systematic error, conclusions based on comparison of n.m.r. spectra measured under the same conditions (cf. Chapter V) remain valid.

4. Decomposition Products of the Trihydrides

a) Solid-State Decomposition of the mer Isomer

The mer isomer of the trihydride decomposes upon standing

for more than two hours in air. Decomposition is apparently the result of oxidation, since the compound is stable in a vacuum even if heated (65°C, 2 h), and for long periods under hydrogen at room temperature. Decomposition occurs even in dry air[134]. The decomposition product does not add molecular hydrogen readily in toluene or methylene chloride solution, but slowly reacts in the latter solvent. The compound can be identified by a peak at 1982 cm^{-1} (Nujol) in the i.r., which increases upon standing in air as peaks characteristic of the mer trihydride decline. The product contains hydride, and has a five-line multiplet apparently consisting of two triplets of equal intensity in the high field region (^{1}H n.m.r., CD_2Cl_2, 25°C, triplets centered at 25.35 τ and 25.67 τ, with J_{P-H}(cis) 14.0 Hz both cases). The proton-decoupled ^{31}P n.m.r. spectrum indicates two signals of equal intensity ($^{31}P\{H\}$, in CD_2Cl_2 at 25°C, 7.60 δ and 2.98 δ, relative to external 85% H_3PO_4). A ^{31}P spectrum exhibiting hydride-phosphorus coupling indicates that the latter signal is a doublet (J_{H-P} ca. 15 Hz, after correction for partial decoupling). The former signal is obscured by a larger multiplet in the coupled spectrum; in view of the hydride spectrum, the signal at 7.60 δ must also be a doublet. Consistent with these data are complexes with two equivalent phosphines and one hydride per iridium atom, such as the following structures:

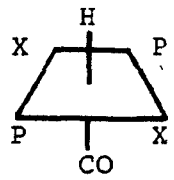

and

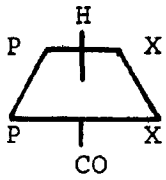

where X is a one-electron ligand without spin (other than chloride). Other possibilities include intrametallated products, dimeric species, or two conformers of a single product. A more definite structural determination must await isolation of this material. Although the decomposition product itself reacts slowly with methylene chloride, the presence of a significant portion of the same decomposition material in recovered n.m.r. samples ensure that the n.m.r. data discussed above are not the results of a further reaction with the solvent.

b) Reactions of the Trihydrides in a Nitrogen Purge in Methylene Chloride

A methylene chloride solution containing the fac and mer isomers was purged with nitrogen for several hours (Figure II-10). After only 2.5 h (Figure II-10b), identical spectra were obtained from both fac and mer isomers. Both showed a diminution of the peaks characteristic of the trihydride, and the appearance of an absorbance at 2012 cm^{-1} which became quite intense after 6 h (Figure II-10c). No trihydride was apparent after 24 h. A comparison with solution spectra measured under static nitrogen (Figure II-8) under otherwise

Figure II-10. I.r. spectra of solutions of mer and fac $IrH_3(CO)P_2$ under a nitrogen purge, measured at 25°C in methylene chloride. The solutions were initially pure mer or fac isomer, but show the formation of a reaction product with time in spectra a, b, and c.

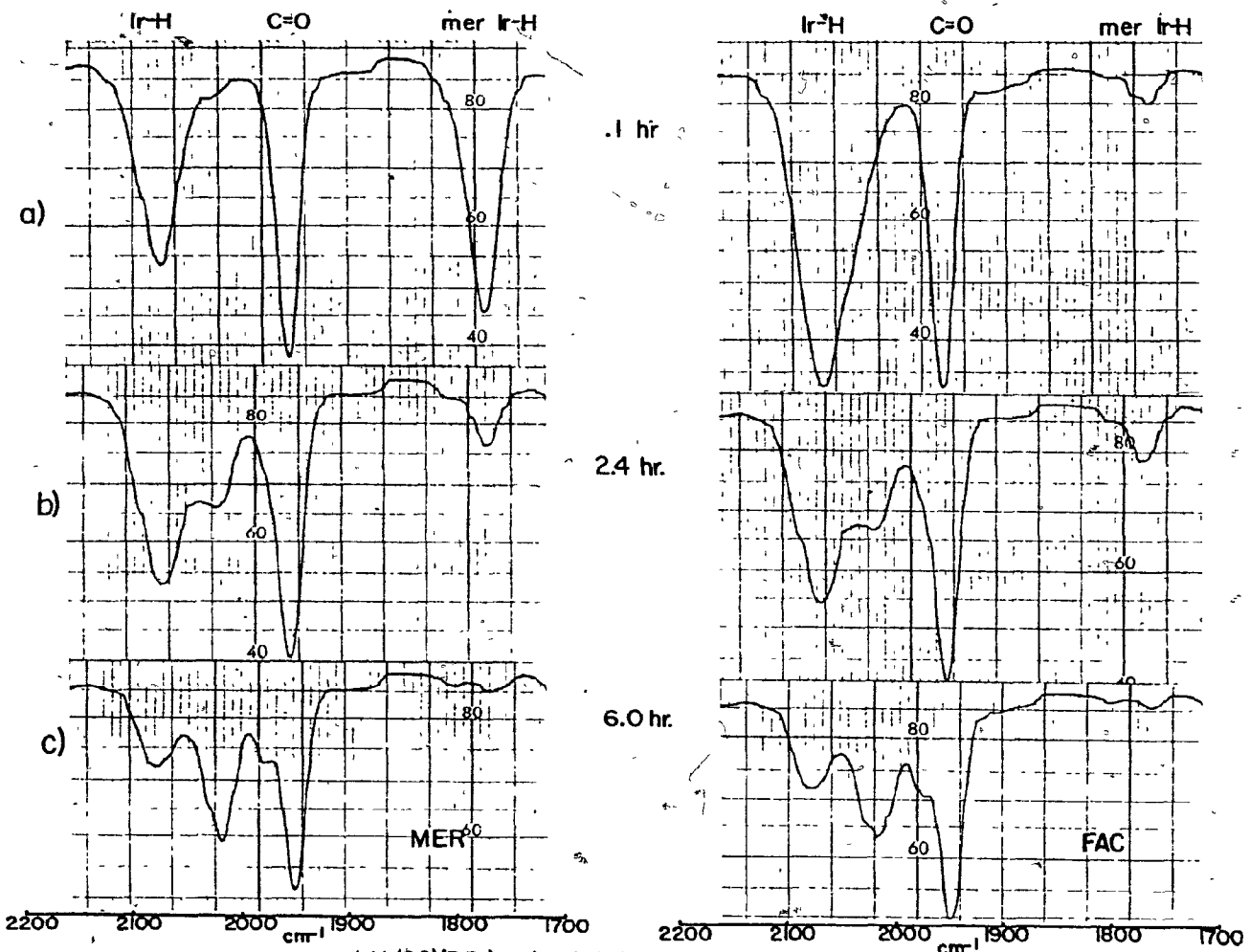

$IrH_3(CO)(PO_3)_2$ in Methylene Chloride with an N_2 Purge

similar conditions suggests that a nitrogen purge results in a faster loss of hydrogen from the iridium trihydride, less fac to mer interconversion, and the formation of a reaction product (observed at 2012 cm^{-1}) that is not observed under static hydrogen or nitrogen.

The interaction between methylene chloride and the trihydrides was further investigated by ^{1}H and ^{31}P n.m.r. Under a nitrogen purge, a more concentrated methylene chloride solution of the trihydride precipitated a yellow solid upon slight heating to 30°C for four hours (ca. 20% yield). The precipitate was identified as Vaska's complex, $IrCl(CO)\ P_2$, by its i.r. spectrum (1948 cm^{-1}, Nujol), and its ability to add hydrogen gas in toluene solution to form $IrH_2Cl(CO)\ P_2$ (i.r., 2187, 2103, 1999, 1974 cm^{-1}, Nujol; lit.[175], i.r. 2196, 2108, 1997, 1983 cm^{-1}, Nujol). The supernatent methylene chloride solution, after solvent evaporation and dissolution in CD_2Cl_2, contained primarily $IrH_2Cl(CO)\ P_2$ (^{1}H n.m.r., 2 triplets of doublets, H_a, 17.28 τ, J_{H-P} = 17.6 Hz, J_{H-H} = 5.1 Hz; H_b = 28.40 τ, J_{H-P} = 14.0 Hz, J_{H-H} = 5.1 Hz; $^{31}P\{$phenyl protons$\}$ n.m.r., triplet, 9.95 δ, J_{H-P} = 16 Hz). The above data is in close accord with the literature values[175], and leaves little doubt that the species appearing in the infra-red spectrum is the dihydride (i.r., 2010 cm^{-1} in $CHCl_3$, ^{1}H n.m.r., CH_2Cl_2, 17.3 τ, J_{H-P} = 15 Hz, 28.4 τ, J_{H-P} = 15 Hz; ^{31}P n.m.r. not previously reported).

Also identified in the methylene chloride solution is the dichloride complex, $IrHCl_2(CO)\ P_2$ (^1H n.m.r., triplet 27.10 τ, J_{H-P} = 12.5 Hz; $^{31}P\{phenyl\ protons\}$ n.m.r. doublet, -.70 δ, J_{H-P} = 15 Hz). Although the ^1H n.m.r. parameters for this complex have not been reported[11], published values for tertiary phosphine analogues support the dichloride assignment (e.g., for $IrHCl_2(CO)[P(CH_3)_3]_2$, configuration 18, 26.6 τ, J_{P-H} = 12.9 Hz in CH_2Cl_2)[176]. The structures of the complexes are given below.

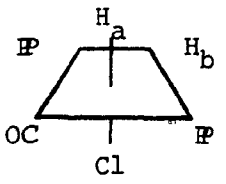

17

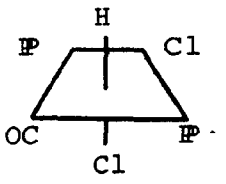

18

There are no other species containing iridium-hydride bonds in the methylene chloride solution according to ^1H and ^{31}P n.m.r. spectroscopy. The ^{31}P chemical shifts of other species present containing phosphorus, along with a rough estimate of the relative intensity of the signal, are: 27.20 δ (.8), 24.18 δ (.3), 3.95 δ (.1), -9.04 δ (.1) and -13.83 δ (.2). By comparison, the relative intensities of $IrH_2Cl(CO)\ P_2$ and $IrHCl_2(CO)\ P_2$ are 1.01 and .6, respectively.

It is likely that the formation of Vaska's complex

through reaction of methylene chloride occurs through $IrH_2Cl(CO)\ P_2$, which can reductively eliminate hydrogen[96]. The following scheme accounts for the production of the observed species.

$$IrH_3(CO)\ P_2 + CH_2Cl_2 \xrightarrow{N_2\ purge} IrH_2(CO)Cl\ P_2 \xrightarrow[-H_2]{N_2\ purge} IrCl(CO)\ P_2$$

$$IrH_2(CO)Cl\ P_2 \xrightarrow[purge]{N_2} IrHCl_2(CO)\ P_2 \quad (-CH_3Cl)$$

Scheme 4. Interaction of $IrH_3(CO)\ P_2$ with CH_2Cl_2

Since both methyl chloride and hydrogen are gaseous, Scheme 4 also accounts for the reaction being driven by a nitrogen purge. The fact that little dihydride is formed in static solutions suggests that the initial reaction proceeds through the unsaturated intermediate $IrH(CO)\ P_2$.

D. DISCUSSION

1. Preparation of $IrH_3(CO)\ P_2$

The preparation of the title complex was carried out by a method similar to those of Malatesta et al.[80] and Burnett et al.[132]. The separation of the fac and mer isomers of the

trihydride is fully described for the first time, although the isolation of the mer isomer has been previously reported[132].

The mechanism of the synthesis of the trihydrides is not clear. One possibility is the production of the intermediate $IrH(CO)P_2$ by reaction with sodium borohydride (the other products being, for example, sodium chloride and diborane), followed by the oxidative addition of hydrogen.

$$IrCl(CO)\ P_2 \xrightarrow{+NaBH_4} IrH(CO)\ P_2 \xrightarrow{+H_2} IrH_3(CO)\ P_2 \qquad (23)$$

In reactions done under nitrogen, hydrogen necessary for the second step might be supplied by a separate reaction of sodium borohydride with, for example, trace amounts of moisture. The reaction does in fact proceed under nitrogen, but with lower yields than the reaction under a hydrogen atmosphere. A high-yield synthesis of $IrH_3(CO)\ P_2$ has been reported with the same reagents under nitrogen in the presence of excess p-toluidine[132]. It has been suggested that the synthesis of metal hydrido complexes by reaction with $NaBH_4$ may proceed through metal hydroborato intermediates[184].

2. The Structure and Spectra of fac and mer $IrH_3(CO)\ P_2$

The infra-red and n.m.r. spectra conclusively establish

the structures of the two isomers. As mentioned in Chapter I, some ambiguity regarding the structure of each isomer exists in the literature. The present structural assignments are in agreement with all previous reports of the fac isomer, and all previous reports of the mer isomer except for those of Malatesta et al.[80] The structure of the mer isomer proposed in the present study also corresponds to analogous trihydrides with different tertiary phosphines[142,143]. Both isomers have been recently identified and characterized by proton n.m.r. as reaction products of organic acids and Ir(I) species[141]. In the latter report, the ^1H n.m.r. spectrum of the mer isomer has been fully reported and analyzed for the first time, in complete agreement with the present assignments; however, the spectrum of the fac isomer was not fully analyzed in that report.

a) Analysis of the Infra-Red Spectra

The assignments of infra-red absorption wavenumbers to iridium-hydride stretching modes, shown in Table II-1, are in agreement with the original report of the isomers[80]. Also, they are consistent with data reported for other iridium polyhydride species[11]. For example, mer-$IrH_3[P(C_6H_5)_3]_3$ absorbs at 2110, 1771, and 1750 cm^{-1}, corresponding to iridium-hydride stretches with hydride trans to phosphorus (2110 cm^{-1}) and hydride ligands. Fac-$IrH_3[P(C_6H_5)_3]_3$, with all

hydride ligands trans to phosphorus, absorbs at 2106, 2094 and 2083 cm^{-1}.

The infra-red absorptions in the hydride stretching region may be interpreted according to group theory. From a comparison to other metal hydridocarbonyls[185], the peak at 1962 cm^{-1} in the mer isomer, and 1953 cm^{-1} in the fac isomer, may be assigned to the C-O stretch (trans to H). The remaining peaks in that wavenumber range (2200-1700 cm^{-1}) may therefore be assigned to Ir-H stretches. The mer isomer is of point group C_{2v}, and will result in three Ir-H stretching vibrational modes, two A_1 and a B_1 mode. The latter mode corresponds to anti-symmetric stretching of H-trans-H, and may be assigned to the peak at 1780 cm^{-1}, in keeping with many other examples of H-trans-H in mer trihydrides in the literature[69].

The remaining A_1 modes correspond to the symmetric stretching of hydrides trans to hydride and carbonyl. Under strict local symmetry, the intensity of the symmetric H-trans-H mode would be negligible, due to the lack of a net change in dipole moment. However, mode mixing often occurs with ligand vibrational modes of the same symmetry and similar energy[185] (which in this case includes the carbonyl stretch), and thus the wavenumber and intensity of these modes are unpredictable. The two peaks at 2077 and 2062 cm^{-1} are therefore tentatively assigned to the two A_1 modes. The shoulder apparent on the carbonyl peak at 1962 cm^{-1} is presumably due to a solid-state effect.

The fac isomer is of point group C_s, and therefore three infra-red active vibrational modes are expected, an A" and two A' modes. The A'(1) mode, corresponding to an Ir-H stretch trans to carbonyl, is assigned to the peak at 2071 cm^{-1}, by analogy with the literature[185] and by comparison to the spectrum of the mer isomer, in which a similar A_1 mode occurs near that wavenumber. The symmetric A'(2) and antisymmetric A" stretch of Ir-H trans to phosphorus are assigned to the peaks at 2112 and 2057 cm^{-1}, respectively. The assignment of these peaks to the A'(2) and A" stretching modes is supported by the absence of similar peaks in the spectrum of fac-$IrD_2H(CO)P_2$ (see Chapter V). The peak at higher wavenumber is assigned to the symmetric stretch in view of the expectation that in-phase stretching requires more energy than out-of-phase stretching, since competition for the same orbitals is involved. Symmetric stretching generally occurs at higher wavenumber than antisymmetric stretching in octahedral carbonyl complexes[38].

b) Analyses of the ^1H Spectra

A first-order analysis of the hydride spectrum of a solution of the mer isomer yields a triplet of doublets, centered at 20.10 τ, and an overlapping triplet of triplets centered at 20.53 τ, with the coupling constants listed in Table II-2. Chemical shift and coupling constants for the mer isomer are in line with analogous values in the literature, as illustrated in Table II-3. The small difference in the chemical shift for $L = P(C_6H_5)_3$ in this study and that of van Doorn et al.[140] may be attributed to temperature and solvent effects. The trend observed in hydride chemical shifts with various tertiary phosphines is probably due to greater shielding

of the hydride with increased basicity of the phosphines. In all cases, the coupling constants agree closely.

The spectrum of the fac isomer, Figure II-3, measured under the same conditions, is not amenable to first-order analysis, due to the magnetic inequivalence of the hydrogens trans to phosphorus, H_c, although both have equivalent chemical shift. The spectrum can be interpreted according to an AA'MXX' analysis, in which H_d (spin M) is in a first-order relationship with two hydrogen (H_c, spins AA') and two phosphorus atoms (spins XX'). This results in a triplet of triplets for H_d, from which δ_{H_d} (the chemical shift of H_d), $J_{H_c-H_d}$ and J_{H_c-P} may be directly obtained. The rest of the spectrum may be interpreted as the "A" portion of an AA'XX' spectrum[173,174] in which all peaks are symmetrically doubled by the $J_{H_c-H_d}$ coupling. Values for δ_{H_c}, $J_{H_c-H_c}$, $J^{cis}_{H_c-P}$, $J^{trans}_{H_c-P}$, and J_{P-P} were found by repeatedly varying the various parameters until the calculated line frequencies and intensities agreed with the measured spectrum. Exact values for $J^{cis}_{H_c-P}$ and $J^{trans}_{H_c-P}$ were eventually obtained from partially deuterated analogues (cf. Chapter V) of the fac isomer; exact values for $J^{cis}_{H_c-H_c}$ and J^{cis}_{P-P}, cannot be obtained, however, due to the overlapping nature of the spectrum and the difficulty of varying two parameters simultaneously. Ranges for these parameters are given in Table II-2. A computer-generated simulation of the fac isomer, using approximate values for the coupling constants,

is shown in Figure II-4, and closely resembles the measured spectrum. Trihydrides of both configurations have been previously analyzed by Mann, Masters, and Shaw[143,144], and values reported there for the mer isomer, as well as the recently reported partial analysis of van Doorn et al.[140], are compared with the present results in Table II-3.

c) Analysis of the ^{31}P Spectra

The $^{31}P\{H\}$ and $^{31}P\{$phenyl protons$\}$ spectra confirm the assignments. The quartet at 15.48 δ in the ^{31}P spectrum (Figure II-5), assigned to the mer isomer, agrees well with a spectrum (Figure II-6) calculated from corrected values of J_{H-P} obtained from the hydride spectrum. All six lines in the calculated spectrum are not apparent in the experimental spectrum due to natural line width and instrumental resolution. An expansion of the experimental spectrum does reveal a shoulder which corresponds to line 4 in the calculated spectrum. The multiplet at 6.55 δ, assigned to the fac isomer, is in excellent agreement with the calculated spectrum. In this case, the apparent lack of hydride-hydride coupling in the second order spectrum allowed discrete values of the coupling constants to be obtained. Numerical values for the calculated and experimental spectrum are given in Appendix II.

The apparent values of all five H-P coupling constants used to calculate the ^{31}P spectra of both isomers are decreased

by the same amount due to partial decoupling (Table II-2). It is interesting to note that the other apparent coupling constants, $J_{H_CH_C}$ and J_{PP}, are not affected to the same degree in the second-order spectrum of the fac isomer. The apparent value of $J_{H_CH_C}$ goes to zero, while that of J_{PP} actually increases upon weak irradiation of the hydride nuclei. The latter relation was surprising, since only couplings involving hydrogen were expected to change upon weak irradiation of hydrogen. Presumably, this phenomenon is a result of the fact that the energies of most of the transitions in the AA'XX' spin system are functions of all four coupling constants[177]. As a consequence, alteration of the energy levels of the hydride nuclei by weak irradiation also alters the apparent values of all four coupling constants. The exact degree by which the apparent values of J_{HH} and J_{PP} differ from the true value of these coupling constants cannot be measured, since discrete values for the latter parameters cannot be determined from the coupled hydride spectrum.

3. Equilibrium

It is clear from both the i.r. and n.m.r. experiments that an equilibrium exists in solution between the two isomers of $IrH_3CO[P(C_6H_5)_3]_2$. Starting with either the fac or the mer isomer, an equilibrium mixture results. The rate of interconversion is rapid initially: a noticeable change

occurred after only a few minutes. After ca. six hours, further change ceased and spectra obtained starting with either isomer are virtually superimposable. External hydrogen is necessary for the maintenance of equilibrium, and no degradation of the solution is observable up to 24 h after the start of reaction. Although only the fac and mer isomer, and no other iridium hydride, were detectable by i.r. or n.m.r. spectroscopy when the solution was kept under hydrogen, a third species formed under static nitrogen, which contained few if any iridium-hydrogen bonds. The identity of this species has not been determined.

The fact that an equilibrium mixture is formed in each case, regardless of the starting isomer, demonstrates conclusively that a true, dynamic equilibrium between the two isomers occurs in solution. This is contrary to an early proposal[80] which suggested that the two isomeric forms of the trihydride were the result of the conversion of an unstable isomer to a more stable form. A mixture resulting from partial isomeric conversion by reaction with an impurity may likewise be eliminated.

Although the present study is the first to explicitly show isomeric equilibrium between fac and mer $IrH_3(CO)[P(C_6H_5)_3]_2$, indirect evidence for equilibrium in this system has been reported by Burnett et al.[132]. In the latter study, a system which contained both isomers of the trihydride, triphenyl-

phosphine, $IrH(CO)[P(C_6H_5)_3]_3$ and dihydrogen was found to be near equilibrium over a wide range of concentration values. ($K = 3.55$ to 7.54 at 25°C in DMF, for the reaction $IrH(CO)\,\mathbb{P}_3 + H_2 \leftrightarrow IrH_3(CO)\,\mathbb{P}_2 + \mathbb{P}$. This was taken as evidence for the equilibrium between isomers of the trihydride. In addition, solid-state infra-red spectra of product mixtures suggested that the fac and mer isomers were present in constant proportions. In view of the lack of precision of the values for the equilibrium constants, the complexity of the system, and the qualitative nature of the infra-red spectra, these results do not demonstrate clearly a discrete equlibrium between the fac and mer isomers of $IrH_3(CO)[P(C_6H_5)_3]_2$. The present study clarifies the situation by confirming an equilibrium in solution between two distinct, isolable isomers of established stereochemistry, and by providing an equilibrium constant for the isomerization. The failure of a number of workers to recognize the existence of this dynamic equilbrium leaves the physical parameters measured on one or the other of the supposed isomers open to question[80,139,141].

There is slightly more of the fac isomer than the mer isomer at equilibrium, in contrast to the recent report of van Doorn et al.[141], in which the mer/fac ratio as three to one. The discrepancy between the two values may be due to an interaction with other reagents present in van Doorn's system. The present

results also do not conform with analogous iridium trihydride carbonyl complexes having different phosphine ligands[142-144] in which the mer configuration was predominant, and little or no fac isomer detected. With iridium trihydride complexes containing three tertiary phosphine or arsine ligands, however, many examples of both fac and mer configurations have been reported, and interconversion has been noted in some cases (see Chapter 1).

The importance of dihydrogen in the equilibrium is demonstrated by the fact that an equilibrium is achieved and maintained for long time periods under hydrogen, but loss of hydrogen from the complexes occurs under nitrogen. The most obvious explanation is that one or both of the complexes lose molecular hydrogen in solution. Such behavior is not uncommon for metal-hydride complexes[11,53].

E. CONCLUSIONS

1. $IrH_3(CO)[P(C_6H_5)_3]_2$ occurs in two forms, which have been fully characterized by i.r. and n.m.r.

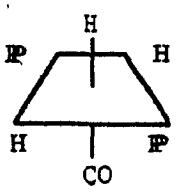

mer

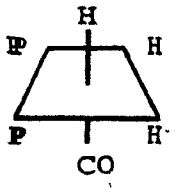

fac

2. These two species are in equilibrium in solution under H_2 at 25°C. At lower temperatures (0°C), equilibrium is approached only very slowly (several days); at 25°C, it is achieved within four hours.

3. For IrH_3 mer $\leftrightarrow$ IrH_3 fac, K = 1.5-2.0 at 25°C in methylene chloride.

4. In the absence of external dihydrogen, the isomeric solution degrades with loss of hydrogen.

5. Only the two isomers of $IrH_3(CO)P_2$ can be detected under hydrogen; a third species is formed under nitrogen.

6. Methylene chloride reacts with $IrH_3(CO)P_2$ in a nitrogen purge to form various chloroiridium complexes.

CHAPTER III

KINETIC STUDIES OF THE ISOMERIZATION OF $IrH_3(CO)[P(C_6H_5)_3]_2$

A. INTRODUCTION

In the previous chapter, it was demonstrated that both fac and mer $IrH_3(CO)\ P_2$ can be isolated in pure form, and isomerized to equilibrium in solution under a hydrogen atmosphere. In order to investigate quantitatively the isomerization reaction and perhaps gain some insight into its mechanism, kinetic studies of this reaction were undertaken.

In view of the dependence of the equilibrium on external hydrogen, a likely mechanism for the isomerization was thought to involve a square-planar intermediate as in the following reaction.

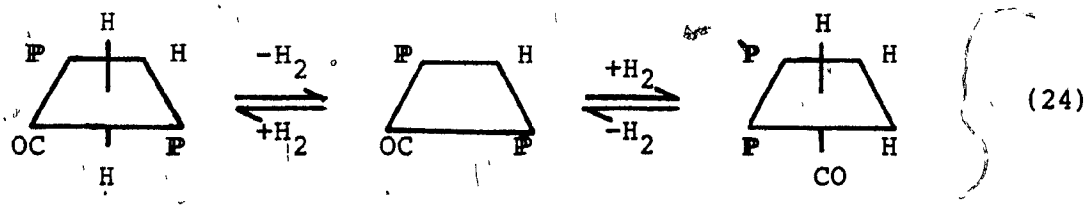

(24)

mer 7 — 14 — fac 3

Such an intermediate has been proposed in synthetic[130,172] and kinetic[45,132] studies of reactions of $IrH(CO)\ P_3$ and the

trihydride complex. The existence of such an intermediate is also consistent with the following known reaction[129].

$$IrH(CO)\,P_3 + H_2 \rightleftharpoons IrH_3(CO)\,P_2 + P \qquad (11)$$

Consequently, a rate study was carried out to determine the dependence of the isomerization reaction on the hydrogen concentration.

For an isomerization process in which equilibrium is achieved by first-order reactions in both directions, expressions for both rate constants may be obtained by a straightforward application of the rate laws and the equilibrium expression[178]. Using integrated rate expressions together with the results of an experimental determination of the concentration of one of the reactants versus time, values for both rate constants may be obtained. Expressions obtained in this way are given below for the case of a first order fac/mer interconversion, where k_F and k_R are rate constants for the forward and reverse reactions, and A is the concentration of the mer isomer at time t, at the start of the reaction (A_o), or at equilibrium (A_{eq}). It is assumed that there is initially none of the fac isomer present.

$$\text{mer} \underset{k_R}{\overset{k_F}{\rightleftharpoons}} \text{fac} \qquad (25)$$

$$\ln\left[\frac{A_o-A_{eq}}{A-A_{eq}}\right] = (k_F+k_R)t \qquad (26)$$

$$\frac{A_o-A_{eq}}{A_o}\ln\left[\frac{A_o-A_{eq}}{A-A_{eq}}\right] = k_F t \qquad (27)$$

With k_F and (k_F+k_R) known, a value for k_R may then be obtained by difference. The equilibrium constant, K_{eq}, for equation 25 is equal to k_F/k_R. A similar expression may be obtained for the sum (k_F+k_R) in the case where there is initially no mer isomer present, and the concentration of the mer isomer is measured with time. In this case,

$$\ln\left[\frac{A_{eq}}{A_{eq}-A}\right] = (k_F+k_R)t \qquad (28)$$

Under these circumstances, it is not possible to obtain an expression for k_F alone.

A measure of the concentration of the mer isomer is conveniently provided in the infra-red spectrum by an absorption at 1780 cm^{-1}. Values for k_F and k_R may be obtained by measuring the absorbance at various times in solutions containing only the mer isomer, and plotting the left-hand-sides of equations 26 and 27 versus t. Since there is no isolated peak specific for the fac isomer, these equations

cannot be employed for solutions initially containing only the fac isomer; a value for the sum (k_F+k_R) in this circumstance may be obtained, however, through an application of equation 28.

The rate expressions to be expected from the processes involving a coordinatively unsaturated intermediate, as in equation 24, are somewhat more complicated. If A, B and C represent the concentrations of the mer isomer, the intermediate, and the fac isomer, respectively, then the following rate laws may be written. The significance of the rate constants is illustrated in Scheme 5.

$$-\frac{dA}{dt} = (k_{m-})A - (k_{m+})B[H_2] \qquad (29)$$

$$\frac{dB}{dt} = (k_{m-})A - (k_{m+})B[H_2] \qquad (30)$$

$$- (k_{f+})B[H_2] + (k_{f-})C$$

$$\frac{dC}{dt} = (k_{f+})B[H_2] - (k_{f-})C \qquad (31)$$

These equations may be solved if one makes the "steady-state" assumption and sets the quantity dB/dt equal to zero. This assumption is valid only when B is small compared to A or C.

Scheme 5. The relationship between the individual and overall rate constants.

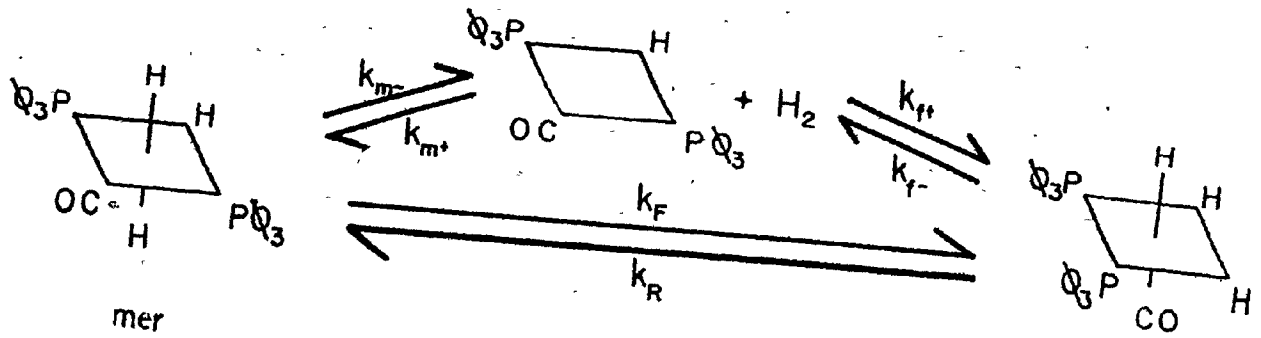

$$k_F = \frac{(k_{m-})(k_{f+})[H_2]}{(k_{m+})[H_2] + (k_{f+})[H_2]} = \frac{k_{m-}\, k_{f+}}{k_{m+} + k_{f+}} \qquad (32)$$

$$k_R = \frac{(k_{f-})(k_{m+})[H_2]}{(k_{m+})[H_2] + (k_{f+})[H_2]} = \frac{k_{f-}\, k_{m+}}{k_{m+} + k_{f+}} \qquad (33)$$

In fact, no intermediate has been detected spectroscopically in the high-field n.m.r. or infra-red spectra of solutions of the isomers at equilibrium (cf. Chapter II).

Equations 29, 30, and 31 are solved in detail in Appendix I. The resulting expressions have the same form as those obtained for the overall rate constants k_F and k_R (equations 26, 27, and 28). The relationships between the overall rate constants and the individual rate constants k_{m+}, k_{m-}, k_{f+} and k_{f-} are given in Scheme 5. The presence of a term for hydrogen concentration in both the numerator and denominator of both expressions results in expressions independent of hydrogen concentration. Thus, the rate of an isomerization which proceeds through an unsaturated intermediate by loss and re-addition of hydrogen will be independent of hydrogen concentration in both directions.

Consequently, a system which behaves according to equation 24 will exhibit the following kinetic and equilibrium behavior:

a) K_{eq}, k_F and k_R will all be independent of hydrogen concentration;

b) plots of the functions of A in equations 26, 27 and 28, versus time will be linear;

c) nonequilibrium in the absence of external hydrogen will occur;

d) there will be agreement in values for (k_F+k_R), when starting with both fac and mer isomer; and

e) agreement in the values of K_{eq} determined from the rate constants (k_F/k_R) and from independent spectroscopic measurements (i.r. and n.m.r.) of concentration will be observed.

Experiments which test these points are reported in this chapter.

B. EXPERIMENTAL PROCEDURE

1. Materials

Fac and mer $IrH_3(CO)P_2$ were prepared as described above, and stored at -20°C under hydrogen. The mer isomer contained a measurable amount of decomposition product in a few experiments; parallel experiments with freshly prepared material showed little or no difference in kinetic behavior. Solvents were dried, freshly distilled, and degassed before use.

2. Kinetic Measurements

An apparatus was constructed (see Appendix IV) which allowed the isomerization kinetics to be studied under an atmosphere in which the relative amount of hydrogen present

was known. Since, by Henry's law, the concentration of a gas in solution is proportional to the partial pressure of that gas above the solution, the relative concentration of hydrogen in solution can be varied by changing the proportion of hydrogen above the solution. Accordingly, the kinetic and equilibrium parameters involved in the isomerization of $IrH_3(CO)\ P_2$, and their dependence on the hydrogen concentration, were examined.

The rates of isomerization of $IrH_3(CO)\ P_2$ were measured at 25°C in methylene chloride under various concentrations of hydrogen. The concentration of the mer isomer was determined from the absorbance at 1780 cm^{-1} in the infra-red region. Spectra were obtained on a Perkin-Elmer 257 spectrophotometer from solutions in 1 mm-pathlength cells between sodium chloride windows, and were measured versus a pure solvent reference. The solvent was distilled before use, and saturated with a hydrogen/nitrogen mixture immediately prior to dissolution of the complex. Reactions were carried out at a total pressure of one atmosphere at constant temperature. The stock solution (25 mg of iridium complex per 5 ml of solution, 6.7 mM) was periodically sampled by pressurizing the solution with a mercury pump, and filling solution cells through stainless steel tubing. In this way, a gas mixture of constant proportion was maintained over the solution.

A sketch of the apparatus used is given in Appendix IV.

Solutions were exposed to the atmosphere only for the time necessary to measure their spectra, and were sealed in all-glass vessels at atmospheric pressure between measurements. The spectrum between 2200 and 1700 cm^{-1} was recorded for each measurement to monitor the total iridium concentration and the appearance of decomposition products, as well as the concentration of the mer isomer.

The relative proportion of hydrogen above the solution is expressed as the percentage of hydrogen in a hydrogen/nitrogen mixture that was introduced over the reaction solution. The actual amount of hydrogen present in the isolated system at vapor/liquid equilibrium is less, due to the high vapor pressure of the solvent, methylene chloride. Since all measurements were recorded at the same temperature, however, the contribution of the solvent to the total pressure is constant. The partial pressure of hydrogen above the solution, and concentration of hydrogen in solution, are both proportional to the parameter reported.

3. Treatment of Experimental Data

All calculations are based on measurements of A, the absorbance of the mer isomer, obtained from the i.r. spectra of reaction solutions using the expression

$$A = \log \left[\frac{\%T \text{ (baseline)}}{\%T \text{ (measured)}} \right]$$

The conformity of the system to Beer's law was established by separate experiments. Absorbance values were used directly to express concentration. Values of A_o, the initial concentration, were determined by extrapolation of a plot of A *versus* time to t = 0. These values were used for all calculations. A value for A_o was also obtained by fitting the data to a polynomial by computer*, and evaluating at t = 0. The equilibrium concentration, A_{eq}, was taken as the value of the absorbance at a reaction time of six hours, after which little change occurred. The quantity A_{eq} was measured in all but two cases, where interpolated (C_o = 0, 50% H_2) or extrapolated (C_o = 0, 75% H_2) values were used to estimate the value of A_{eq} at six hours. The equilibrium constant K_{eq} was calculated from the expression

$$K_{eq} = \frac{C_{eq}}{A_{eq}} = \frac{A_o - A_{eq}}{A_{eq}} \qquad (34)$$

Initial rates were calculated for all reactions. This was achieved in two ways: a) graphically, by plotting A *versus* time, extrapolating to t = 0, and finding of the line tangent at that point; and b) numerically, by computer-

*CURVFT, a FORTRAN subprogram on file at the McGill Computing Centre, was used.

fitting the data to a polynomial* and evaluating the derivative at t = 0. Only values of t less than three hours were used.

The rate constants k_F and k_R were obtained as the slope of a function of A versus t. These functions, X and X', are taken from equations 27 and 28, and are defined as

$$X = \frac{A_o - A_{eq}}{A_o} \ln \left[\frac{A_o - A_{eq}}{A - A_{eq}} \right] \qquad (35)$$

$$X' = \ln \left[\frac{A_{eq}}{A_{eq} - A} \right] \qquad (36)$$

A value for k_F was obtained as the slope of X versus t when $C_o = 0$, and $(k_F + k_R)$ as the slope of X' versus t with $A_o = 0$. Another value for $(k_F + k_R)$ was calculated with $C_o = 0$ from k_F and K_{eq} values. Because erratic values of X and X' resulted as A approached A_{eq}, only measurements at a reaction time less than 130 min, when $C_o = 0$, and 100 min, when $A_o = 0$, were used to calculate slopes.

Values for the absorbance of the mer isomer, upon which all the results in this chapter are based, are given in Appendix VI along with associated statistical information.

---

*CURVFT, a FORTRAN subprogram on file at the McGill Computing Centre, was used.

C. RESULTS

1. Qualitative Observations

The spectra of solutions of the mer and fac isomers of $IrH_3(CO)\ P_2$ kept under an atmosphere of either hydrogen or nitrogen have been described in Chapter II. The spectra of both isomers under hydrogen showed that isomerization to equilibrium occurs without the formation of other species within 24 h. In the experiments considered in this chapter, solutions were kept under mixtures of hydrogen and nitrogen, and the isomerization rates were measured under these conditions. The spectra obtained from solutions kept under gas mixtures from 100% to 25% hydrogen were qualitatively identical. Equilibria were in these cases maintained for 24 h. The concentration of hydrogen in solution, therefore, does not affect the isomerization equilibrium, although an equilibrium is not achieved in the absence of hydrogen.

Due to the instability of the mer isomer in the solid state, some of the samples of the mer isomer contained an estimated 15% decomposition product. The nature of this product has been discussed in Chapter II. The presence of this material, however, did not appear to affect the rate of isomerization. Separate studies have indicated that while the decomposition product is reactive under the conditions of the kinetic measurements, it does not form one of the

isomers in question, and so would not be expected to affect the reaction rate. Burnett et al. have observed, however, that the presence of some decomposition product in samples stored for long periods (weeks) in air resulted in an increase in the rate of hydrogenation[132,134].

2. Initial Reaction Rates

Table III-1 gives the initial rates of reaction for the isomerization of the mer (C_o=0), obtained graphically (second column) and by a numerical method (fifth column). The two methods gave values in close agreement. Although the initial rates vary considerably at different hydrogen concentrations (± 30%), there is no systematic variation with hydrogen concentration. The same is true for reactions starting with the fac isomer (A_o=0, last column). Hydrogen concentration therefore does not appear to be a factor in determining initial rates of reaction. Values for A_o obtained graphically (column two) or numerically (column six), are in close agreement for each value of the hydrogen concentration. Values of k_F (initial), like those of initial rate, are independent of hydrogen concentration. A value for k_R (initial), using an estimated equivalent to C_o, is also given in the last column of Table III-1.

3. Equilibrium Values

Equilibrium constants are given in Table III-2, along

Table III-1.* Initial rates of reaction [Initial rate = $(dA/dt)_o$].

	$C_o = 0$					$A_o = 0$
H_2 conc. (%)	10^2 x Initial Rate[a]	A_o[b] (absorbance)	$10^2 k_F$ (initial)[c] min^{-1}	10^2 x Initial Rate[d]	A_o[d] (absorbance)	10^2 x Initial Rate[d]
100	-.21	.254	.83	-.23	.254	.18
75	-.23	.200	1.2	-.29	.198	.16
50	-.35	.210	1.7	-.53	.220	.35
25	-.32	.228	1.4	-.32	.227	.29
0	-.36	.254	1.4	-.32	.254	.22
average	-.29	.229	1.3	-.34	.231	.24

average "initial rate constants": $k_F = 1.3 \times 10^{-2} min^{-1}$ $= 2.2 \times 10^{-4} sec^{-1}$; k_R[e] $= 9.4 \times 10^{-3} min^{-1}$ $= 1.6 \times 10^{-4} sec^{-1}$

*Rates of reaction in this and subsequent experiments were measured in minutes, and so individual rate constants are reported in min^{-1}. Where average values for several rate constants were computed, rate constants in sec^{-1} are also quoted.

[a]Slope of tangent at t = 0, on A vs t. [b]Intercept from tangent line, A vs t. [c]k_F = (initial rate)/A_o. [d]From CURVFT. [e]k_R = (initial rate)/C_o, with C_o = .254.

Table III-2. Equilibrium and associated values of solutions initially containing only mer isomer ($C_o = 0$).

% H_2	A_o[a] (absorbance)	A_{eq}[b] (absorbance)	K_{eq}
100	.254	.101	1.5
75	.200	.085	1.3
50	.210	.080	1.6
25	.228	.090	1.5
0	.254	(.050)[c]	(4.1)[c]
average (100-25% H_2)			1.5

[a] Initial absorbance of the mer isomer, obtained by graphical extrapolation.

[b] Equilibrium absorbance, either measured (100, 25, and 0% H_2) or estimated (75, 50% H_2) at t = 6 h.

[c] System not at equilibrium.

with values for the initial concentration of the mer isomer, A_o, and the equilibrium concentration of the mer isomer, A_{eq}. The K_{eq} values are reasonably constant in all solutions containing externally applied hydrogen at a relative concentration of 25% to 100%. For the purposes of comparison, a value for "K_{eq}" was calculated at a relative concentration of 0% hydrogen, with "A_{eq}" taken as the value of A after six hours, even though the system was not at equilibrium. The value obtained, 4.1, is much higher than values of the equilibrium constants determined at non-zero hydrogen concentration. The latter have an average value of 1.5.

Equilibrium values for the isomerization reaction under hydrogen starting with the fac isomer cannot be accurately determined, due to the fact that C_o cannot be evaluated from the spectra. However, the i.r. spectra of isomerization under various hydrogen concentrations leave little doubt that similar equilibrium behavior occurs. Measurements of the n.m.r. spectra (cf. Chapter II) indicate , moreover, that the same concentration of each isomer occurs at equilibrium by starting with either the fac or mer isomer.

4. Evaluation of k_F and k_R

Plots of X versus t, when $C_o = 0$, and X' versus t, when $A_o = 0$, were calculated and are given in Figures III-1 and

III-2, respectively. Both sets of plots are fairly linear, although some scattering and line curvature can be observed, particularly in the reaction starting with the mer isomer (Figure III-1). Numerical values in support of these figures are given in Appendix VI, along with statistical parameters derived from line-fitting by the least squares method of X versus t and X' versus t.

Values for k_F and (k_F+k_R) were obtained as slopes of the plots shown in Figures III-1 and III-2 and are listed in Table III-3. These values do not vary with hydrogen concentration for k_F, k_R, or for either determination of (k_F+k_R). Values of (k_F+k_R) are in close agreement, regardless of whether the starting material was the mer isomer ($C_o = 0$) or the fac isomer ($A_o = 0$). Finally, values of k_F and k_R are in quantitative agreement with values of k_F (initial) and k_R (initial).

D. DISCUSSION

The results reported in this and the previous chapter indicate that an equilibrium occurs between isomers of $IrH_3(CO)P_2$ which can only be maintained under hydrogen. With external hydrogen present in the system, there was no relationship observed between the hydrogen concentration in solution, and any of the following quantities: initial

Figure III-1. Plots of X versus time for solutions originally containing only the mer isomer, at 100% (a), 50% (b), and 0% hydrogen in the feed gas. X is defined in equation 35.

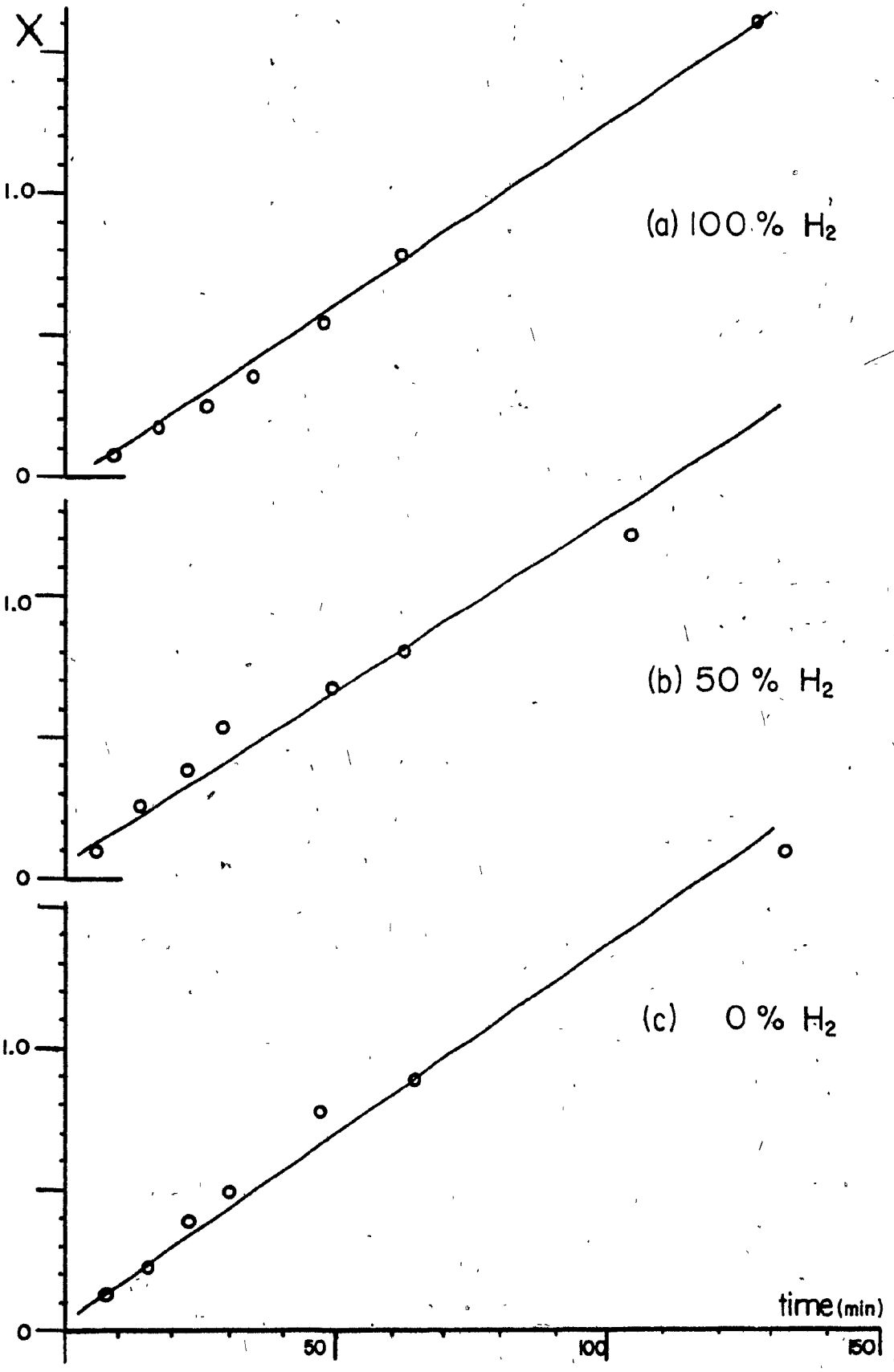
X
1.0
0
(a) 100 % H_2
1.0
0
(b) 50 % H_2
1.0
0
(c) 0 % H_2
time (min)
50
100
150

Figure III-2. Plots of X' versus time for solutions originally containing only the fac isomer, at 100% (a), 50% (b), and 0% hydrogen in the feed gas. X' is defined in equation 36.

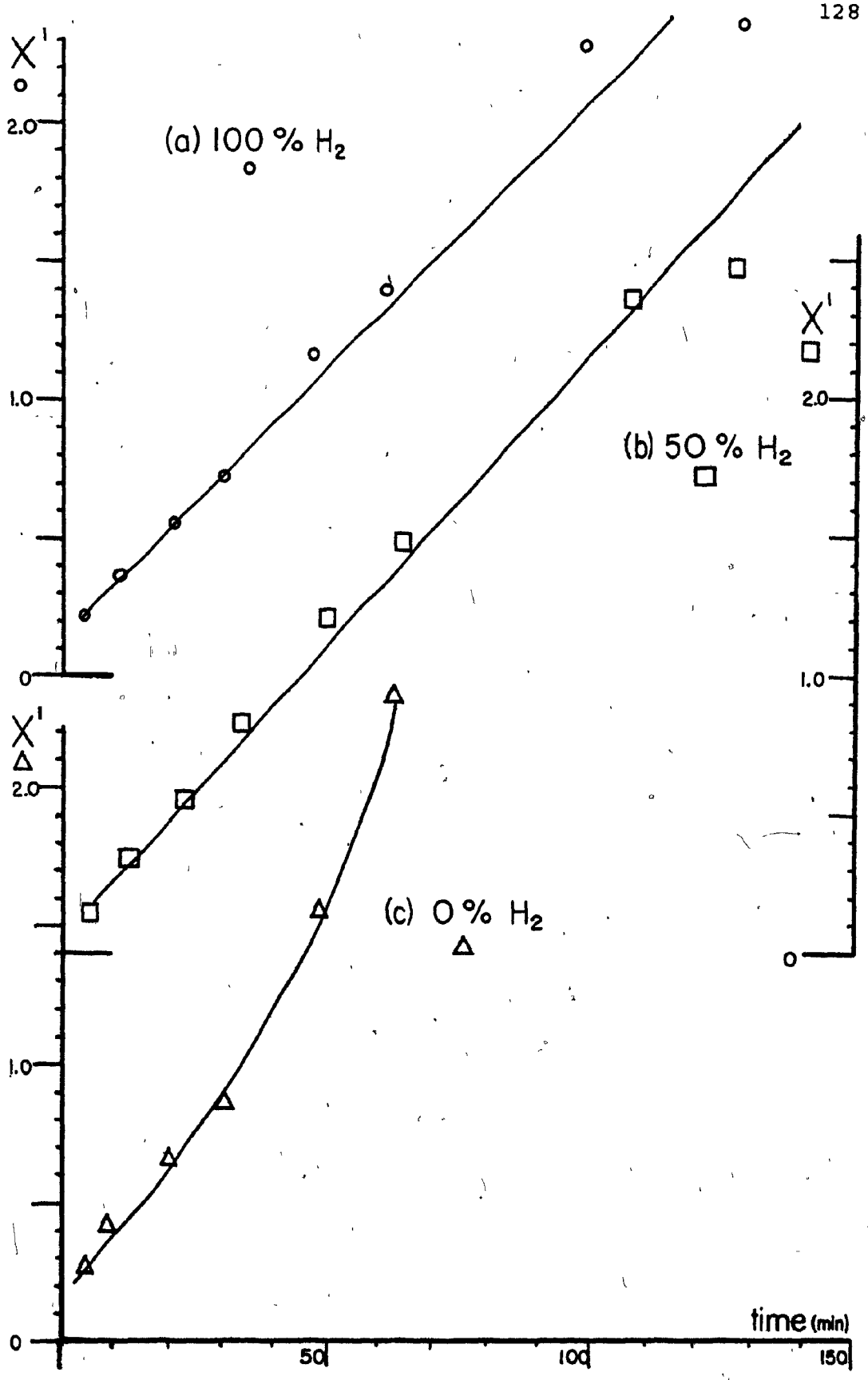
X'
2.0
1.0
0
(a) 100 % H2
(b) 50 % H2
(c) 0 % H2
time (min)
50
100
150

Table III-3. Values for k_F and k_R[a].

$$\text{mer (A)} \underset{k_R}{\overset{k_F}{\rightleftharpoons}} \text{fac (C)}$$

	$C_o = 0$[b]				$A_o = 0$[c]	
Concentration[d] of Hydrogen	N[e]	$10^2 k_F$[f,g], min^{-1}	$10^2(k_F+k_R)$[g,h], min^{-1}	k_R[i], min^{-1}	N[e]	$10^2(k_F+k_R)$[j,g], min^{-1}
100	7	1.27 ± .03	2.11 ± .05	.84 ± .05	7	2.16 ± .05
75	6	1.04 ± .09	1.80 ± .16	.76 ± .16	6	1.67 ± .18
50	7	1.07 ± .06	1.73 ± .10	.66 ± .10	7	2.17 ± .05
25	7	1.15 ± .08	1.93 ± .13	.78 ± .13	7	1.96 ± .09
0	7	(1.5)[l,n]			6	(1.9)[m,n]
average[k]		1.13 ± .16	1.89 ± .25	.76 ± .11		1.99 ± .37
		$(1.88\pm.27)\times10^{-4}$ sec^{-1}	$(3.15\pm.42)\times10^{-4}$ sec^{-1}	$(1.27\pm.18)\times10^{-4}$ sec^{-1}		$(3.3\pm.6)\times10^{-4}$ sec^{-1}

[a]All values from data measured in methylene chloride at 25°C. Experimental Data in Appendix VI. [b]Solutions initially contained only the mer isomer. [c]Solutions initially contained only the fac isomer. [d]Percentage of hydrogen in the initial hydrogen/nitrogen mixture. [e]Number of points in the plot. [f]Plot of X vs t (equation 35). [g]Slope of a line fit by the method of least-squares. Error limits quoted are the standard deviation of the slope. [h]$k_F x[A_o/(A_o-A_{eq}]$. [i]Col. 4-Col. 3. [j]Plot of X' vs t (equation 36). [k]Mean of values for 100%-25% H_2, ±95% confidence limits, N = 4. [l]Using "A_{eq}" = .050 (value at 360 min). [m]Using "A_{eq}" = .081 (value at 360 min). [n]System not at equilibrium; estimated slope.

reaction rates, equilibrium constant, or any of the derived rate constants k_F (initial), k_F and (k_F+k_R). All reactions measured under hydrogen followed the integrated rate laws derived from equation 24 or 25.

These results are all consistent with the hydrogen-dissociation mechanism via an unsaturated intermediate, as shown in equation 24. Indirect evidence consistent with this mechanism includes chemical evidence that these iridium trihydrides react by dissociation of hydrogen to add a variety of classical donor ligands and oxidative addends[80,129,130]. The common intermediate in all these reactions is believed to be $IrH(CO)[P(C_6H_5)_3]_2$. Furthermore, kinetic studies of the five-coordinate iridium species, $IrH(CO)\ P_3$, have established that oxidative addition occurs through the same intermediate as the one expected in a hydrogen-dissociation mechanism of isomerization[45,132-135]. Finally, there are known examples of oxidative addition to square-planar complexes which form structural analogues of both the fac isomer (e.g., Si-H and $IrH(CO)\ P_3$)[159] and the mer isomer (e.g., H_2 and $Ir(CO)Cl\ P_2$)[179] of the trihydride.

Alternate mechanisms of ~~isomeriz~~ation are shown in Scheme 6, where equations 37a and b represent the isomerization model already discussed (equation 24), under conditions where the rate constants for the addition and loss of hydrogen have different relative values.

Scheme 6. Alternate Mechanisms for the Isomerization of $IrH_3(CO)P_2$.

$$A \underset{k_{m+}}{\overset{k_{m-}}{\rightleftharpoons}} B + H_2 \underset{k_{f-}}{\overset{k_{f+}}{\rightleftharpoons}} C \qquad (37)$$

$$k_{m-},\ k_{f-} \geq k_{m+},\ k_{f+} \qquad (37a)$$

$$k_{m-},\ k_{f-} \ll k_{m+},\ k_{f+} \qquad (37b)$$

$$H_2 + B \underset{k_{m-}}{\overset{k_{m+}}{\rightleftharpoons}} A \underset{k_R}{\overset{k_F}{\rightleftharpoons}} C \qquad (38)$$

$$A \underset{k_R}{\overset{k_F}{\rightleftharpoons}} C \underset{k_{f+}}{\overset{k_{f-}}{\rightleftharpoons}} B + H_2 \qquad (39)$$

In equations 38 and 39 of that scheme, plausible alternatives are given where one of the isomers is in equilibrium with hydrogen and an unsaturated intermediate. The isomerization reaction in these cases occurs by a process apart from hydrogen dissociation, such as intramolecular isomerization, dissociation of triphenylphosphine or carbonyl, or a process involving dimeric species. There are many examples in the literature of intramolecular isomerizations among octahedral transition metal dihydride[180] and polyhydride species[181], octahedral chelate[182] and monodentate complexes[183]. Also, dissociative and dimeric mechanisms, including a recent proposal of hydrogen-bridged dimers in a similar reaction of iridium hydrides[140] have been described.

All of the isomerization mechanisms mentioned above, except possibly the dimerization mechanism, can be regarded as first-order equilibrium processes. Consequently, they all would behave in the manner outlined in the introduction and are in accord with the rate and equilibrium results discussed above.

The initial rates of reaction may be examined to distinguish between the alternatives in Scheme 6. One would expect the same initial rate (equal to $k_R C_o$) when starting with the fac isomer ($A_o=0$) by both equation 38 and 39, regardless of the initial concentration of hydrogen. When starting with

the mer isomer ($C_o = 0$), however, one would expect, by equation 38, a different initial rate [equal to $-(k_{m-}+k_F)A_o$] when the initial hydrogen concentration is zero than when it is non-zero (initial rate = $-k_F A_o$ when $[H_2]_o \neq 0$). By equation 39, the initial rate is the same (equal to $-k_F A_o$) regardless of the initial concentration of hydrogen. Since no difference in initial rate was observed experimentally under zero and non-zero initial concentrations of hydrogen, it is not likely that the isomerization proceeds by equation 38.

Equation 37a implies that the initial rate when $A_o = 0$ would be zero. Since a non-zero initial rate was observed, this mechanism is also unlikely. Also, the failure to observe B experimentally in the infra-red or n.m.r. studies of the isomerization also does not support this mechanism.

Equation 37b would be expected to give the same initial rates as equation 39 (see above). Both agree with experimental results (Table III-1) in their indifference to hydrogen concentration, and in the measured values of k_F and k_R. Additional experiments are necessary to distinguish between the two alternatives, as well as to provide more precise measurements than can be made from initial reaction rates. Consequently, experiments were carried out in which the individual rate constants k_{m-} and k_{f-} could be measured. These are reported in the next chapters, where the mechanism of isomerization is further discussed.

E. CONCLUSIONS

The interconversion of the mer and fac isomers of $IrH_3(CO)P_2$ was found to obey first-order equilibrium kinetics under a hydrogen atmosphere at 25°C in methylene chloride for the reaction

$$\text{mer} \underset{k_R}{\overset{k_F}{\rightleftharpoons}} \text{fac} \qquad (25)$$

$$K_{eq} = 1.5$$

$$k_F = (1.88 \pm .27) \times 10^{-4} \text{ sec}^{-1}, \ [\text{fac}]_o = 0$$

$$(k_F + k_R) = (3.15 \pm .42) \times 10^{-4} \text{ sec}^{-1}, \ [\text{fac}]_o = 0$$

$$k_R = (1.27 \pm .18) \times 10^{-4} \text{ sec}^{-1}, \ [\text{fac}]_o = 0$$

$$(k_F + k_R) = (3.3 \pm .6) \times 10^{-4} \text{ sec}^{-1}, \ [\text{mer}]_o = 0$$

The parameters listed above were found to be independent of hydrogen concentration. From initial rates and chemical evidence, the most likely isomerization mechanism is considered to be the following

$$\text{mer} \underset{k_{m+}}{\overset{k_{m-}}{\rightleftharpoons}} IrH(CO)P_2 + H_2 \underset{k_{f-}}{\overset{k_{f+}}{\rightleftharpoons}} \text{fac} \qquad (37)$$

This mechanism is kinetically equivalent to equation 25 when

$$k_F = \frac{k_{m-}\ k_{f+}}{k_{m+} + k_{f+}},\ k_R = \frac{k_{m+}\ k_{f-}}{k_{m+} + k_{f+}}$$

and

$$k_{m-}, k_{f-} \ll k_{m+}, k_{f+}$$

Since other mechanisms are still plausible, additional experiments must be carried out to confirm this mechanism.

CHAPTER IV

KINETIC STUDIES OF THE REACTION OF TRIPHENYLPHOSPHINE AND $IrH_3(CO)[P(C_6H_5)_3]_2$

A. INTRODUCTION

The rate of displacement of hydrogen by triphenylphosphine was studied to obtain additional evidence for the isomerization of $IrH_3(CO)\ \mathbf{P}_2$. Triphenylphosphine is known to add to the trihydride by the following reaction[80].

$$\underset{1}{IrH_3(CO)\ \mathbf{P}_2} + \mathbf{P} \rightarrow \underset{5}{IrH(CO)\ \mathbf{P}_3} + H_2 \qquad (9)$$

If it is established that the reaction of both isomers of the trihydride proceeds through the dissociation of hydrogen to form an intermediate complex, then the rate constants of dissociation are equal to k_{m-} or k_{f-} in the isomerization rate expression (Scheme 5, Chapter III). Useful comparisons between the rates of substitution and isomerization may then be made.

B. EXPERIMENTAL PROCEDURE

1. Materials

Fac and mer $IrH_3(CO)\ P_2$ were prepared and stored as described in the previous chapters. Triphenylphosphine was recrystallized from methanol. ^1H n.m.r. spectra were prepared and measured as described in Chapter II.

2. Kinetic Measurements

The rates of substitution of triphenylphosphine with fac and mer isomers of $IrH_3(CO)\ P_2$ were determined in the presence of excess ligand in methylene chloride and in toluene at 25.4°C. The absorbance of the reaction product, $IrH(CO)\ P_3$, at 330 nm was measured on a Perkin-Elmer/Coleman 124 double-beam spectrometer, equipped with a Hitachi 124 thermostated cell-compartment accessory in conjunction with a Haake K-41 temperature controller.

Since the reaction product was found to be sensitive to oxygen, solutions were prepared under nitrogen from degassed solvents. Reactions took place in quartz UV cells of 1 cm pathlength that were fitted with glass stopcocks. The cells were flushed with nitrogen (ca. 5 min) prior to introduction and mixing of the reagents in the cell by syringe transfer. The cells were then sealed from the atmosphere.

Three samples of different concentrations were measured concurrently. Since the same stock solution was used for each series of measurements, the relative concentrations were known within 10% for each series. Triphenylphosphine concentrations were in 200, 100 and 50 fold excess of the iridium complex (.050 mM) in those series where the rate dependence on the ligand was examined. The concentration of the iridium complex was varied in the ratio 1:2:3, in a constant concentration of triphenylphosphine (5.0 mM), in 300 fold excess of the most dilute sample of the iridium complex.

Preliminary experiments indicated that the reaction product obeyed Beer's law in the presence of excess phosphine, and that the iridium trihydride complexes did not absorb at the wavelength of interest. Samples were removed from the constant temperature bath only for the brief interval necessary to measure their absorbance.

A u.v. spectrum of a solution of IrH(CO) P_3 exhibited, besides the absorption due to the tris (phosphine) complex, additional peaks at 330, 384 and 442 nm which are suppressed in the presence of excess triphenylphosphine. The additional peaks are presumably due to the dissociation of the tris-(phosphine) to form IrH(CO) P_2. The extent of dissociation, however, is not great. A n.m.r. spectrum at 25°C in methylene chloride showed less than 1% dissociation for a 40 mM solution.

The reaction cells were impermeable to the

atmosphere, and contained ca. 2 ml of solution under ca. 2 ml of nitrogen and solvent vapor. Under these conditions, along with dilute solutions and excess triphenylphosphine, re-addition of hydrogen to reform the trihydride is believed to be negligible. In selected experiments, the cells were covered with metal foil, to investigate the effect of incidental light on the sample.

3. Treatment of Experimental Data

The substitution of P for hydrogen by a dissociative mechanism can be represented by the following equations, where D, B and E are the concentrations of the iridium complexes indicated.

$$\underset{D\text{(fac or mer)}}{IrH_3(CO)\,P_2} \xrightarrow{k_D} \underset{B}{IrH(CO)\,P_2} + H_2 \qquad (40)$$

$$\underset{B}{IrH(CO)\,P_2} + P \underset{k_{-P}}{\overset{k_{+P}}{\rightleftharpoons}} \underset{E}{IrH(CO)\,P_3} \qquad (41)$$

Equation 40 yields the following rate expression in the absence of the back reaction.

$$-\frac{dD}{dt} = k_D D \qquad (42)$$

In the presence of a large excess of ligand, the equilibrium indicated in equation 41 lies far to the right. Consequently, equation 42, after integration between D and D_o and substitution for D, results in the following expression, where E is the product concentration when the reaction is complete.

$$-\ln(E_{eq}-E) = k_D t - \ln E_{eq} \qquad (43)$$

In these experiments, the dissociation rate constant k_D was obtained from plots of $-\ln(E_{eq}-E)$ versus t over two to three half-lives. The validity of equations 40 and 41 was investigated for each isomer by an analysis of the initial reaction rates, as well as the linearity of the plots of equation 43.

Although solutions containing the tris (phosphine) complex were stable in oxygen-free solutions of toluene, the concentration of the complex in methylene chloride solution was found to decline over several hours, presumably through reaction with the solvent. The result was severe curvature in plots of equation 43 with methylene chloride. Because the rate constant for decomposition, k' was found to

be first order and much smaller than the dissociation rate constant, k_D, it was possible to correct for decomposition. The following expression, equation 44, was therefore used to calculate the dissociation rate constant for experiments done in methylene chloride, in place of equation 43. The derivation of equation 44 is given in Appendix I.

$$-\ln\left[e^{-k't} - \frac{E}{E'_{eq}}\right] = k_D t \qquad (44)$$

In this expression, E'_{eq} is the value of E_{eq} which would be obtained in the absence of decomposition.

To facilitate the use of equation 44, the computer program KINCOR was written. The complete program is given in Appendix III. The program functions in the following manner: i) an estimate of k_D is obtained through the application of equation 43, where "E_{eq}" is the largest value of E; ii) from k_D, a value of t is calculated where the initial reaction is 99% complete; iii) values of E at larger t values are then used to calculate k'; iv) equation 44 is applied to find a corrected value of k_D; and v) the 99% completion point is recalculated and, if necessary, steps iii and iv repeated one or more times with improved values of k' and E'_{eq}.

The computer output for a typical experiment is given in

Appendix V. The final plots of the data plotted according to equation 44 gave very good straight-line fits. The values of k_D are believed to be as accurate as those obtained under conditions where decomposition did not occur.

The decomposition of IrH(CO) $\mathbf{P}_3$ in methylene chloride was further examined in separate experiments. Assuming equation 41 and a first-order decomposition through intermediate IrH(CO) $\mathbf{P}_2$, the decomposition rate constant will be pseudo first-order in excess ligand, and inversely proportional to the ligand concentration. Accordingly, the following expressions may be written.

$$\text{IrH(CO) } \mathbf{P}_3 \xrightarrow{k'} \text{decomposition products} \qquad (45)$$

where

$$k' = \frac{k'' k_{-P}}{k_{+P}[\mathbf{P}]} \qquad (46)$$

In these equations, k' is the apparent decomposition rate, k" is the reaction rate of IrH(CO) $\mathbf{P}_2$ to give decomposition products, and k_{-P} and k_{+P} are as shown in equation 41. The derivation of these relationships is shown in Appendix I.

Initial reaction rates were determined to find the order of the triphenylphosphine substitution reaction of $IrH_3(CO)\ \mathbf{P}_2$ (equation 9) with respect to the iridium complex and

triphenylphosphine, in methylene chloride and toluene. Values for the instantaneous rates of reaction were obtained using CURVFT (see Chapter III). It was found that reaction rates evaluated at t = 10 min gave more reliable results than those evaluated at t = 0. This is presumably due to the fact that the latter value is derived from an extrapolation of a non-linear expression, while the curve at t = 10 min is still within the range of the experimental data. Consequently, the "initial" reaction rates are those at a reaction time of 10 min. Since the reaction is only 10 to 15% complete at this time, such an approximation is not likely to lead to significant error.

Initial rates were also calculated to an initial concentration of zero. These rates were found to be quite erratic, and are not reported.

As a check on the initial rates, rate constants were calculated from initial rate vales by dividing the latter by E_{eq} or, for reactions in methylene chloride, E'_{eq}. These initial rate "constants" are generally in good agreement with the rate constants obtained from the integrated rate expressions.

In a few cases, erratic points near t = 0 caused unreasonable values of the initial rate. Hand-drawn tangents of E versus t were used in these cases, which are marked "estimated values" in Table IV-1.

C. RESULTS

The initial rates of reaction and reaction rate constants determined for the substitution of triphenylphosphine for both isomers of $IrH_3(CO)\ P_2$ are summarized in Table IV-1. A computer analysis of typical experiments in each solvent is shown in Appendix V. Tables of data for all experiments follow in Appendix VII.

1. Initial Reaction Rates

The initial rates of reaction for both isomers are listed in Table IV-1. Since the experiments were done in groups of three samples taken from a stock solution, and there was variation in concentrations between solutions, initial rates and concentrations were calculated from measured values, with the intermediate value of concentration and the corresponding rate taken as unity.

The initial reaction rates change very little when the concentration of ligand is varied relative to the fac isomer in methylene chloride. The mer isomer under these conditions shows more variation in initial rates with ligand concentration, although the results do not indicate any systematic dependence on triphenylphosphine. The initial rates are directly proportional to the starting concentration of the fac isomer, indicating a first-order dependence. The

Table IV-1. Initial Rates of Reaction of the fac and mer isomers of $IrH_3(CO)P_2$, with triphenylphosphine, at 25°C. Values of the concentration and initial rates are relative to the experiment at intermediate concentration.
i) Ligand concentration varied: [Ir] = .050 mM; [P] = 10.0, 5.0 and 2.5 mM.
ii) Metal concentration varied: [Ir] = .075, .050 and .025 mM; [P] = 5.0 mM.

	Expt. #	Initial Rate	Relative Rate	Expt. #	Initial Rate	Relative Rate	Expt. #	Initial Rate	Relative Rate
				A. in methylene chloride					
i)[P]				fac isomer					
2.0	34	.0041	0.9	43	.0050	1.1			
1.0	55	.0044	1.0	44	.0047	1.0			
0.5	36	.0036	0.8	45	.0042	0.9			
				mer isomer					
2.0	31	.0103	1.4	37	.0098	1.0	55	.0070	1.3
1.0	32	.0075	1.0	38	.0100	1.0	56/57	.0052[b]	1.0
0.5	33	.0090	1.2	39	.0052	0.5	58	.0041[a]	0.8
ii)[Ir]				fac isomer					
1.5	46	.0071	1.5	69	.0095	1.5			
1.0	47	.0047	1.0	68/70	.0064[b]	1.0			
0.5	48	.0017	0.4	67	.0038[a]	0.6			
				mer isomer					
1.5	49	.0119	1.5	59	.0135	1.4			
1.0	50	.0078	1.0	60	----[c]	--[c]			
0.5	51	.0026[a]	0.3	62	.0048	0.5			
				B. in toluene					
i)[P]		fac isomer			mer isomer				
2.0	22	.0113	1.0	40	.0146	1.2			
1.0	23	.0107	1.0	41	.0117	1.0			
0.5	24	.0102	1.0	42	.0130	1.1			
ii)[Ir]		fac isomer			mer isomer				
1.5	27	.0163	1.6	54	.0127	1.4			
1.0	26	.0103	1.0	53	.0089	1.0			
0.5	25	.0057	0.6	52	.0042	0.5			

[a] Estimated value.

[b] Average of two values.

[c] Accidental oxidation; rates relative to .0048 (E.5).

initial rates of the mer isomer also are roughly proportional to the concentration of the metal complex, although, again, somewhat less regular than with the fac isomer.

All results obtained in toluene are in good agreement with the trends suggested by the methylene chloride results; that is, zero-order dependence on triphenylphosphine, and a first-order dependence on the iridium complex for both isomers. The more regular results obtained in toluene probably reflect the non-participation of that solvent in the reaction.

The order of the reaction in both reagents is clear from a double logarithmic plot of the initial rate versus reagent concentration, Figure IV-1. In this plot, the slope of the line indicates the reaction order. Although there is considerable scatter in both plots, the best fit for either isomer correspond to the reaction orders described above.

2. Reaction Rate Constants

Rate constants obtained from plots of integrated rate laws are listed in Table IV-2. All plots of the experimental results were quite linear, whether or not they were corrected for solvent-induced decomposition. This linearity is reflected in the statistical parameters calculated from the plots of equations 43 and 44. The correlation coefficient generally exceeded .99, and the standard deviation in the

Figure IV-1. The concentration dependence of the initial reaction rate is shown in double logarithmic plots of the initial rate versus the concentration of triphenylphosphine (a) or the concentration of the iridium complex (b). Because all values are relative to intermediate values of the initial rate and concentration, all lines pass through the origin. Initial rates were measured for the mer (filled symbols) and fac (unfilled symbols) isomers in methylene chloride (circles) and toluene (squares).

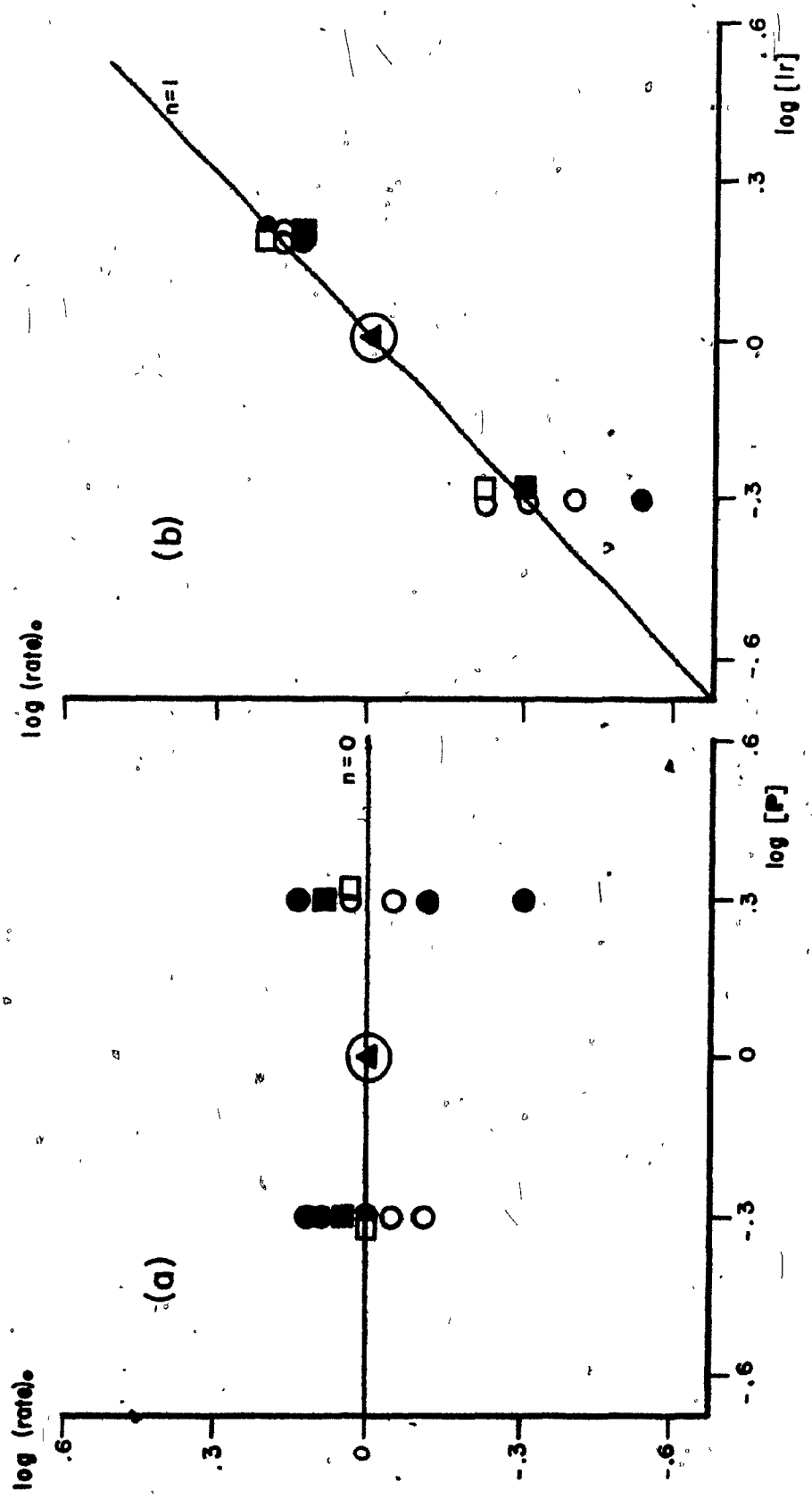
log (rate)
log [P]
n=0
(a)
log (rate)
log [Ir]
n=1
(b)
.6
.3
0
-.3
-.6

Table IV-2. Reaction Rate Constants for Equation 40 at 25°C.

A. Methylene Chloride

10^2[Ir] mM	[P] mM	[P]/[Ir]	MER $10^2 k_D$, [b] min^{-1}	MER Expt. #	FAC $10^2 k_D$, [b] min^{-1}	FAC Expt. #
5.0	10.0	200	1.17	31	1.21	34
			1.12	37	1.22	43
			1.28	55		
2.5	5.0	200	.97±.01	59	1.01±.01	67
			1.40±.03	63		
5.0	5.0	100	1.36	32	1.11±.01	35
			1.20	38	1.75±.03	44
			1.46±.02	56	1.00±.01	68
			1.39±.01	57[a]	1.03±.01	70[a]
			1.19±.01	64		
			1.12±.01	66[a]		
7.5	5.0	67	1.30±.01	62	1.02±.01	69
			1.27±.01	65		
5.0	2.5	50	1.66	33	1.57	36
			1.31	39	1.65	45
			1.56	58		
Average values[c]			(1.30±.09)x10^{-2} min^{-1}		(1.26±.20)x10^{-2} min^{-1}	
			(2.17±.15)x10^{-4} sec^{-1}		(2.10±.33)x10^{-4} sec^{-1}	

B. Toluene

2.5	7.5	300			1.91	25
5.0	10.0	200	1.61	40	1.85±.02	22
5.0	7.5	150			2.06	26
7.5	7.6	100			2.09	27
5.0	5.0	100	1.46	41	1.80±.02	23
5.0	2.5	50	1.41	42	1.76	24
Average values[c]			(1.49±.17)x10^{-2} min^{-1}		(1.91±.14)x10^{-2} min^{-1}	
			(2.48±.28)x10^{-4} sec^{-1}		(3.18±.22)x10^{-4} sec^{-1}	

[a] Samples protected from the light.

[b] Error limits are the standard deviation of the slopes, computed for typical experiments.

[c] Mean of values, ±95% confidence limits, N = 16 and 10 in Section A, N = 3 and 6 in Section B.

slope was less than 2%. The variation in rate constants obtained in experiments under similar conditions, however, is considerably greater. There appears to be systematic error due to some variation in reaction conditions between experiments. Daily temperature fluctuations are a possible cause; although the samples were kept in a constant-temperature bath, measurements involved periodic removal from the bath. Consequently, the error limits given on average values are 95% confidence limits based on the precision of several experimental values.

There is no large variation of the rate constant with ligand concentration. Slightly higher values appear at low phosphine concentrations in methylene chloride, although the tendency is not clear-cut. The effect may be solvent-induced, since it does not appear in toluene.

There is no significant difference between the rate constants of the fac and mer isomers in methylene chloride. The fac isomer reacts slightly faster than mer isomer in toluene.

The effect of the solvent is small in these reactions, consistent with a dissociative process. The reaction rate constants are virtually the same in the two solvents for the mer isomer, and slightly faster in toluene for the fac isomer. A previous kinetic study had found that the rate constant for dissociation of P from $IrH(CO)P_3$ was slightly slower in

toluene than in methylene chloride[117].

In reports in the literature, ultraviolet radiation was found to greatly increase the elimination of hydrogen in some iridium polyhydrides[53]. To protect against this, some samples were protected from the light, as indicated in Table IV-2. These samples showed the same rate of reaction as the exposed sample, indicating that accidental irradiation is not a factor in the reaction rates reported here.

3. Decomposition of IrH(CO) $\mathbb{P}_3$ in Methylene Chloride

a) Decomposition in the IrH(CO) $\mathbb{P}_3$/IrH(CO) $\mathbb{P}_2$ System

The rate constants measured in methylene chloride, listed in Table IV-2, were corrected for anaerobic decomposition of the product, IrH(CO) $\mathbb{P}_3$. A first-order decomposition at a rate that generally decreases with increasing ligand concentration was observed. The results, however, were not inversely proportional to the ligand concentration to an extent that would give reliable results if a single decomposition rate constant, k", were to be used in all experiments. Consequently, individual apparent rate constants, k', were calculated for each measurement.

b) The Rate of Decomposition of $IrH(CO)\,\mathbb{P}_3$

The rate of anaerobic decomposition of $IrH(CO)\,\mathbb{P}_3$ in methylene chloride was measured in separate experiments starting with that complex in the presence of excess ligand. For three concentrations of triphenylphosphine, plots of the integrated rate expression (see Appendix Ic) versus time are very linear, and the apparent rate constant is inversely proportional to the phosphine concentration. The decomposition rate constants are given in Table IV-3.

Table IV-3. Reaction Rate Constants for the Decomposition of $IrH(CO)\,\mathbb{P}_3$ in Methylene Chloride at 25°C.

[Ir] mM	[ℙ] mM	[ℙ]/[Ir]	$10^3 k'$, min^{-1}	$10^5 k'' k_{-P}/k_{+P}$ min^{-1}
.05	10.0	200	1.4	1.4
.05	5.0	100	3.5	1.7
.05	2.5	50	6.4	1.6
average values				1.6×10^{-5} min^{-1}
				2.6×10^{-7} sec^{-1}

These results are all in accord with decomposition of $IrH(CO)\,\mathbb{P}_3$ <u>via</u> the intermediate $IrH(CO)\,\mathbb{P}_2$, according to equation 45. The apparent decomposition rate constants, k',

in Table IV-3, generally are of the same order of magnitude as the values of k' obtained in the experiments with the trihydride at similar phosphine concentrations. Variability in k' values for the latter case may be the result of trace impurities, or of the formation of reaction products which affect the decomposition rate at long reaction times in the more complicated trihydride system.

c) The Oxidation of IrH(CO) $\mathbb{P}_3$

Solutions of IrH(CO) $\mathbb{P}_3$ in methylene chloride that were left open to the atmosphere, but under otherwise similar conditions to the decomposition experiments, reacted by a process strictly first-order in the complex at a rate almost one hundred times that of anaerobic decomposition, to give an apparent rate constant of 3.7×10^{-3} sec^{-1} ([Ir] = .075 mM, [$\mathbb{P}$] = 7.5 or 5.5 mM, at 25°C). Since this represents a half-life of ca. three minutes, the need for rigorously anaerobic conditions in measurements involving this complex is apparent. It is expected that, like anaerobic decomposition, oxidation proceeds through the square-planar intermediate.

d) The Products of Decomposition

The long-term stability of a CD_2Cl_2 solution of IrH(CO) $\mathbb{P}_3$ was also investigated. After a week at room temperature, a ^1H n.m.r. spectrum of the solution showed that other iridium

hydride species had formed in the n.m.r. tube. Besides the quartet characteristic of the tris(phosphine), in a relative concentration of ca. 85%, there was evidence of a dihydride species, indicated by H-H coupling, whose chemical shifts and splitting patterns suggested H trans to P and Cl. Structure 19 is consistent with the observed spectrum (H_a = 18.46 τ, J_{HP} (trans) = 148.7 Hz, J_{HP} (cis) = 23.2 Hz, J_{HH} = 4.7 Hz; H_b = 37.55 τ, J_{HP} (cis) = 11.2 Hz, J_{HP} (cis) = 17.2 Hz, J_{HH} = 5.2 Hz), and corresponds to a species present in ca. 12%. This structure has not been previously reported in

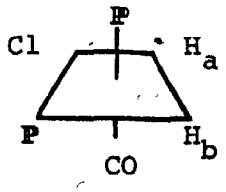

19

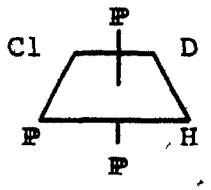

20

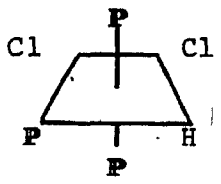

21

the literature, presumably due to the preferential formation of the trans P isomer by the usual synthetic route (addition of hydrogen to Vaska's complex). A quartet can also be observed at 30.32 τ (J_{HP} = 18.0 Hz), corresponding to a monohydride species present in ca. 3%. Structure 20 is in close agreement with literature values (for $IrH_2Cl P_3$ in CH_2Cl_2, configuration 20, ν_H = 30.2 τ, J_{HP} = 15 Hz)[175]. The formation of 20 would be remarkable in being stereospecifically produced;

none of its isotopomer is present in the spectrum. Structure 21 is also considered possible, since its reported chemical shift, while outside the reported error range (± .1 ppm), is nonetheless close to the observed value (lit. 29.2 τ, J_{HP} = 15 Hz in CH_2Cl_2)[175].

D. DISCUSSION

1. The Mechanism of Triphenylphosphine Substitution in $IrH_3(CO)\ P_2$

The results presented above show that the addition of triphenylphosphine to both isomers of $IrH_3(CO)\ P_2$ is first-order in the iridium complex, and zero-order in triphenylphosphine. Initial rate studies of each isomer, and the high degree of linearity of plots of integrated rate expressions clearly indicate these reaction orders. Furthermore, the absence of solvent effects on the reaction rate, and evidence for decomposition through a coordinately unsaturated intermediate all suggest a dissociative process.

The reaction mechanism given in equations 40 and 41 is consistent with all these results. Accordingly, hydrogen is lost from the starting trihydride complex in a rate-controlling step to give a four-coordinate intermediate. The ligand adds relatively quickly to form the product, $IrH(CO)\ P_3$ through a reaction which goes to completion in the presence

of excess ligand.

Previously reported systems involving $IrH(CO)\,P_3$ also give results consistent with a dissociative process (equation 41). The square-planar complex formed by dissociation of the tris(phosphine) complex has frequently been cited as an intermediate in reactions of the latter complex (see Chapter I, section c). Kinetic studies of the reactions of Group IV hydrides with the tris(phosphine) complex concluded that the reaction proceeds according to equation 41[45,117]. Chemical evidence first led researchers to propose that the iridium trihydride reacts through loss of hydrogen, to form the intermediate $IrH(CO)\,P_2$[80]. Of particular relevance to the present work is a kinetic and equilibrium study in which the same reaction mechanism (equations 40 and 41) was proposed for a mixture of the isomers of $IrH_3(CO)\,P_2$[132]. The present study, besides verifying the measurements by a different procedure, adds to information already in the literature mainly in establishing that a dissociative mechanism is valid for each isomer individually.

Besides the direct and indirect evidence mentioned above, the lack of a suitable alternative mechanism also lends support to reaction <u>via</u> pre-dissociation of hydrogen. A displacement of hydrogen by free ligand, for example, cannot occur given the zero-order dependence of the reaction on free ligand. Conceivable associative mechanisms, besides involving

species of greater than the usual 18 electrons and six ligands, generally would not result in the rate laws observed.

The results obtained in the present study are compared with literature values in Table IV-4. In particular, the results of Burnett et al.[132] on the $IrH_3(CO)\ P_2/IrH(CO)\ P_3$ system in DMF are of interest. Since the isomers of the trihydride were not isolated, individual rate constants for each were not determined. An average rate constant for hydrogen dissociation from the isomeric mixture, k_{-H}, although not given in the work cited, may be calculated from reported values of K (equation 9) and $k_{-p}k_{+H}/k_{+p}$ given in Chapter I. The calculated value of k_{-H} is in close agreement with the results obtained in the present study in both toluene and methylene chloride.

Although the solvent may influence the rate constant for hydrogen addition, the values in Table IV-4 suggest that it does not greatly affect hydrogen elimination. The absence of a large solvent effect is characteristic of dissociative processes, where the ligating ability of the solvent is not a major factor in the reaction. The literature values suggest that the rate of hydrogen addition is faster than that of hydrogen elimination, consistent with the failure to observe the intermediate in the isomerization reactions. It also can be seen that the rate constant for hydrogen elimination from $IrH_2X(CO)\ P_2$ is an order of magnitude larger when X is hydride,

Table IV-4. Comparative values of rate constants k_{+Y} and k_{-Y}.

$$IrX(CO)P_2 + Y \underset{k_{-Y}}{\overset{k_{+Y}}{\rightleftharpoons}} IrXY(CO)P_2$$

X	Y	product structure	solvent	temp °C	$10^5\ k_{-Y}$ (sec^{-1})	k_{+Y} ($sec^{-1}M^{-1}$)	reference
H	H_2	mer H	H_2CCl_2	25	22±2		present work
H	H_2	fac H	H_2CCl_2	25	21±3		present work
H	H_2	mer H	$C_6H_5CH_3$	25	25±3		present work
H	H_2	fac H	$C_6H_5CH_3$	25	32±2		present work
H	H_2	mer H/fac H[a]	DMF	25	27	.3	132[d]
NCO	H_2	trans P	C_6H_5Cl	30	1.4	.022	51
Cl	H_2	trans P	C_6H_5Cl	30	4.0	1.2	51
I	H_2	trans P	C_6H_5Cl	30	1.0	430	51
Cl	H_2	trans P	C_6H_5Cl	25	1.7	.88	51
Cl	H_2	trans P	$C_6H_5CH_3$	25	1.7	.45	51
Cl	H_2	trans P	DMF	25	1.7	1.4	51
H	P	tbp	H_2CCl_2	25	10^4	>10^4[e]	117[d]
H	P	tbp	$C_6H_5CH_3$	25	5,700		117
H	P	tbp	DMF	25	>1000		132
H	R_3SiH[b]	cis P	$C_6H_5CH_3$	20	2.2		117[d]
H	R'_3SiH[c]	cis P	$C_6H_5CH_3$	20	41		45[d]
H	R'_3SiH[c]	cis P	$C_6H_5CH_3$	30	210		45[d]

[a] Isomeric mixture.

[b] $(CH_3)(C_2H_5O)_2SiH$

[c] $(C_6H_5)_3SiH$

[d] Calculated from reported values.

[e] k_{+P} estimated from n.m.r. spectrum indicating $IrHCOP_3$ less than 1% dissociated (see Chapter 2).

than when X is a halogen or pseudohalogen. Such a relationship is consistent with the large trans effect of hydride, in the case of the mer trihydride, compared with a halogen or pseudohalogen[121]. The fac trihydride has a different structure, and cannot be compared.

The rate constants for the dissociation of triphenylphosphine, shown in Table IV-4, are much larger than comparable values for hydrogen. The large rate constant for triphenylphosphine addition, however, results in a complex that is largely undissociated in solution, even though the ligand exchanges rapidly with the complex. The rate of triphenylphosphine addition is much faster than even hydrogen addition, which itself is sufficiently fast to prevent accumulation of the intermediate $IrH(CO)\ P_2$. The rate of dissociation of silicon hydrides are given as examples of compounds which, like hydrogen, react with $IrH(CO)\ P_2$ by a concerted mechanism of oxidative addition and reductive elimination. The range of reaction rate constants for silicon hydrides is very large, and may be much faster or slower than the analogous elimination of hydrogen, depending on the substituents on the silicon atom.

2. The Mechanism of $IrH_3(CO)\ P_2$ Isomerization

In view of the foregoing results and discussion, it is

clear that $IrH_3(CO)P_2$ reacts with triphenylphosphine through a dissociative process. The rate constants obtained represent the rate at which hydrogen is lost from the trihydride, independent of other reagents. Dissociation rate constants are compared with isomerization rate constants in Table IV-5.

Table IV-5. A Comparison of Isomerization and Dissociation Rate Constants in Methylene Chloride at 25°C (10^4 k, sec^{-1}).

Isomerization	Dissociation
mer $\underset{k_R}{\overset{k_F}{\rightleftharpoons}}$ fac	mer $\xrightarrow{k_{m-}}$ IrH + H_2
	fac $\xrightarrow{k_{f-}}$ IrH + H_2
k_F 1.88 ± .27	k_{m-} 2.17 ± .15
k_R 1.27 ± .18	k_{f-} 2.10 ± .33

It can be seen that the dissociation rate constants are as large or larger than the isomerization rate constants. This is consistent with an isomerization which proceeds through dissociation and re-addition of hydrogen, as in equations 40 and 41. Accordingly, the rate constants for dissociation of hydrogen are identical to k_{m-} and k_{f-} in Scheme 5 and equations 32 and 33, and are indicated as such

in Table IV-5. The values of k_{m-} and k_{f-} are quite reasonable in view of the relationship between the rate constants and k_F and k_R (equations 32 and 33). For example, if the ratio k_{m+}/k_{f+} is defined as x, substitution into equation 32 yields the following expression

$$k_{m-} = k_F(1+x) \qquad (47)$$

Thus, the dissociation rate constant, k_{m-}, can be equal ($k_{m+} < k_{f+}$), slightly larger ($k_{m+} \sim k_{f+}$), or much larger ($k_{m+} > k_{f+}$), than the isomerization rate constant, but cannot be smaller. A similar argument holds for the dissociation rate constant k_{f-}, which is accordingly equal to $k_R(1 + 1/x)$.

The comparative values of the isomerization and dissociative rate constants are also reasonable from the point of view of the total reaction mechanism (Scheme 5). For example, k_{f-} can be larger than k_R, because not all instances of dissociation from the fac isomer result in isomerization; addition of hydrogen can occur to reform the fac isomer.

Thirdly, there is independent chemical and rate evidence for each step of the isomerization mechanism. That both isomers of $IrH_3(CO)P_2$ can lose hydrogen has been amply demonstrated in Chapter II. The addition of hydrogen to $IrH(CO)P_2$ is indicated by the known reversibility of equation 9. Experiments described below demonstrate that

hydrogen adds to IrH(CO) P_3 to form both isomers of the trihydride by a mechanism other than isomerization. In view of the well-documented dissociation of the tris(phosphine) complex to form IrH(CO) P_2[45,117], one can conclude that hydrogen adds to the latter complex.

Finally, it is clear from the zero-order dependence of the substitution reaction on triphenylphosphine that both isomers of $IrH_3(CO)$ P_2 would lose hydrogen at rates at least as fast as isomerization even in the absence of ligand. To propose that isomerization can only occur by a mechanism other than dissociation would necessitate the establishment of separate equilibria of both isomers with hydrogen, to avoid net loss of hydrogen. This in turn implies two different intermediates; for example, cis and trans IrH(CO) P_2. These structures do in fact appear in the literature to account for hydride exchange in the products of silicon hydride addition to the tris(phosphine) complex[10].

In the present case, at least, the postulation of two intermediates is an unnecessary complication. So too is the postulation of isomerization by more than one mechanism. Isomerization by loss and re-addition of hydrogen, equation 24, is the simplest and most likely mechanism, and is in accord with all experimental results.

Isomerization <u>via</u> loss and re-addition of hydrogen, coupled with the fact that hydrogen is lost at equal rates

from both isomers, implies that the prevalence of the fac isomer at equilibrium is a result of a somewhat faster rate of hydrogen addition to form that isomer, compared with the mer isomer. In terms of equation 47, an isomerization constant of 1.5, therefore, implies x = .66. Use of this factor to calculate k_{m-} and k_{f-} from measured values of k_F and k_R in fact results in higher values [$k_{m-} = k_{f-} = (3.15 \pm .45) \times 10^{-4}$ sec^{-1}] than obtained experimentally (Table IV-5). The difference is likely due to an undetermined systematic error in one or both methods of measurement, and can be expected when comparing kinetic parameters obtained by entirely different methods. Given these uncertainties, x may be estimated to range from .3 to 1.0. Consequently, the rate constant of hydrogen addition to form the fac isomer is from one to three times as fast as that for the formation of the mer isomer.

The mechanism of isomerization of $IrH_3(CO)P_2$ proposed in equation 24 implies that there are two different modes of addition to the square-planar complex, $IrH(CO)P_2$. The addition of hydrogen to square-planar iridium (I) species in nearly all other cases is stereospecific. For species of the formula $IrX(CO)L_2$, where X is an anionic ligand and L is a tertiary phosphine ligand, the resulting six-coordinate species has hydride ligands cis and phosphine ligands trans, as in species 22. In the present experiments,

where X = H, addition in this mode would form the mer trihydride.

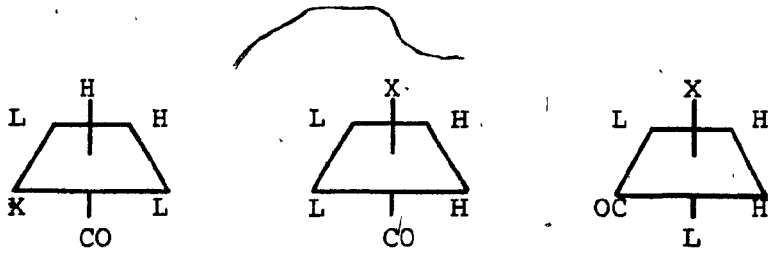

22 23 24

The formation of the fac isomer represents a mode of hydrogen addition in which the product has the phosphine ligands in a cis configuration. Addition of reagents to $IrX(CO)L_2$ to give products of a cis-phosphine configuration, 23, although unusual, is not without precedent. The addition of silicon hydrides to $IrH(CO)\,\mathbb{P}_2$ to give products of this stereochemistry has been mentioned above (Chapter I)[172]. Although the addition of hydrogen to $IrCl(CO)[P(CH_3)_2(C_6H_5)]_2$ results in the conventional trans-phosphine structure, 22, the addition of allyl halides[186] and tetracyanoethylene[104] forms products having cis phosphines, analogous to 23.

More to the point in the present case are the stereochemistries of the hydrogen addition products to complexes of the formula $IrX(CO)\,\mathbb{P}_2$[124], where X is a σ-carborane, $R\text{-}B_{10}C_2H_{10}^-$. Depending upon the nature and position of R, hydrogen adds stereospecifically to the solid complex to form either 23 or 24. In solution with the complex IrX(CO)dp,

where dp = 1,2-bis(diphenylphosphino)ethane, and the ligands are restricted to the cis configuration, the addition of hydrogen results only in structure 24[187]. In methylene chloride solution, however, structures 22 and 23 were produced in proportions of 60% and 40%, respectively, along with small amounts of 24 (ca. 2%). If X = H, the production of 22 and 23 corresponds to the fac and mer trihydrides of the present work, formed in the same solvent and in the same proportions.

In the carborane case, the complex 23 isomerizes quantitatively to 22 in solvents such as methylene chloride and benzene. Further experiments indicated that the production of 22, 23 and 24 is entirely the result of direct addition of hydrogen, not subsequent isomerization. In acetonitrile and other highly polar solvents, 24 is formed stereospecifically. The addition of acetonitrile to solutions containing 22 and 23 induces isomerization of 23 to 24, but does not affect 22[124].

The mechanism of these isomerization was not determined. Preliminary measurements indicate that the conversion of 23 to 22 is first-order in the starting complex, and occurs about ten times slower than the isomerization described in the present experiments ($t_{1/2}$ = 460 min at 25°C in 1,2-dichloroethane). The appearance of several isomers was thought to be the result of steric crowding of the large carborane and phosphine ligands. Distortions induced in the square-planar

starting complex, it was suggested, result in formation of the cis phosphine complex, 23, in addition to the complex of conventional configuration, 22[124].

In view of the isomerization mechanism of $IrH_3CO\,\mathbb{P}_2$ proposed above (equation 24), it is interesting that a similar mechanism fits all the information on the production and isomerization of the carborane dihydrides of structures 22, 23 and 24. Thus, in non-polar solvents, if one ignores the minor product, 24, the following mechanism for the isomerization may be suggested, where X is a carborane ligand.

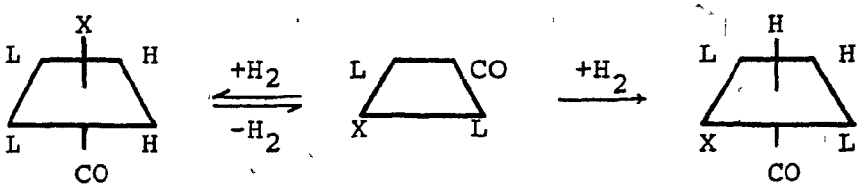

23 25 22 (48)

In this mechanism, hydrogen oxidatively adds to 25 by two stereochemical modes at nearly equal rates. The dihydride, 23, loses hydrogen at a much slower rate to reform 25, while dihydride, 22, is stable towards hydrogen loss. The isomerization is identical to that of $IrH_3(CO)\,\mathbb{P}_2$, except for the stability of 22. The ratio of rates of hydrogen addition to 25 is similar to the equivalent ratio, k_{m+}/k_{f+} in the trihydride case. As in the latter case, the magnitude of the addition rate constants to 25 must be much greater than that for hydrogen elimination from 23.

A similar mechanism may be proposed for the reaction in acetonitrile and other very polar solvents.

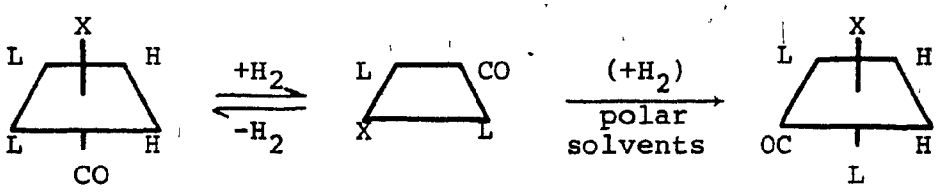

23 25 24 (49)

The isomerization in this case is similar to that in less-polar solvents (equation 48), except that the reaction of 25 along the reaction pathway leading to the dihydride, 24, must be much faster than the addition to form dihydride, 23.

The above mechanisms (equations 48 and 49) provide an explanation for the fact that both the addition of hydrogen and the isomerization of 23 are solvent-dependent, and both exhibit a tendency to form species 24 in the presence of very polar solvents. Further elucidation of the pathway 25 to 24 (equation 49) is provided in a very recent report by the same authors[107]. The reaction, at least in the case of acetonitrile and benzonitrile, apparently proceeds through intermediate complexes formed by reaction with the solvent, as in equation 50.

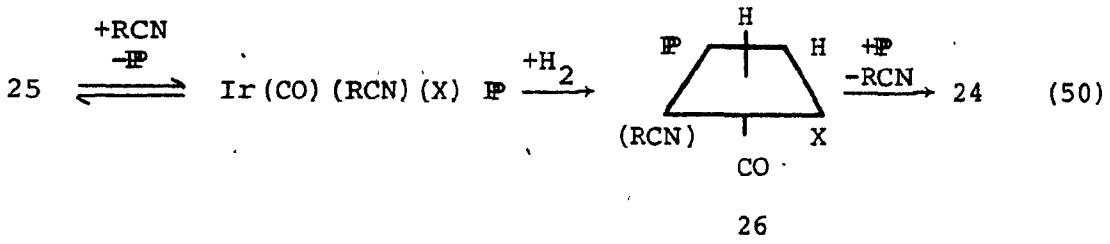

25 $\overset{+RCN}{\underset{-\mathbb{P}}{\rightleftharpoons}}$ $Ir(CO)(RCN)(X)\,\mathbb{P}$ $\xrightarrow{+H_2}$ 26 $\xrightarrow[-RCN]{+\mathbb{P}}$ 24 (50)

Isomerization by reductive elimination of hydrogen from the dihydride, 23, provides a pathway for the formation of the square-planar complex, 25, from which isomer 24 can be produced through equation 50.

All the evidence cited above indicates that there are at least two cases where the oxidative addition of hydrogen to square-planar Ir(I) complexes, $IrX(CO)\,\mathbb{P}_2$, is not stereospecific. The reason why these cases, where X is a hydride or carborane, differ from others, where X is a halogen or pseudohalogen, is not clear. It does not seem to be the electronic influence of X, since the electron-withdrawing ability of the carborane is comparable to that of the chloride ligand[188]. The suggestion advanced in the case of the carborane complexes, that the requirements of a very large ligand (X) result in unusual modes of hydrogen addition[124], is also inconsistent with the fact that very similar behavior occurs when X is the smallest size possible.

In the formation of the two isomers of $IrH_3(CO)\,\mathbb{P}_2$, there are at least two modes of addition of hydrogen. It is not clear which two of the three hydride ligands are the added

ligands. To answer this question, the labeling experiments described in the next chapter were carried out.

E. CONCLUSIONS

The rates of reaction for the substitution of triphenylphosphine for hydrogen in both isomers of $IrH_3(CO)\ \mathbb{P}_2$ were measured in toluene and methylene chloride, and are listed in Table IV-2. The reaction is first-order in the iridium complex and zero-order in triphenylphosphine. The kinetic behavior strongly suggests a mechanism by which both isomers react by the reductive elimination of hydrogen to form the intermediate complex, $IrH(CO)\ \mathbb{P}_2$.

A comparison with the rate of isomerization (Table IV-5) indicates that isomerization also proceeds by the reductive elimination of hydrogen. The implication is that non-stereospecific oxidative addition of hydrogen to $IrH(CO)\ \mathbb{P}_2$ is occurring. Because the addition of hydrogen to square-planar iridium (I) species is generally stereospecific, this form of isomerization is unusual. However, it is likely that a similar isomerization occurred in some iridium (I) carborane complexes, and had not been recognized.

CHAPTER V

SPECTROSCOPIC STUDIES OF $Ir(D/H)_3(CO)[P(C_6H_5)_3]_2$

A. INTRODUCTION

The labelling experiments described in this chapter were carried out to determine the stereochemical mode or modes of hydrogen addition to the square-planar intermediate, $IrH(CO)P_2$, to form the title complex. In these studies, deuterium or hydrogen gas was added to the iridium (I) hydride or deuteride, and the resulting mixture analyzed by infra-red and proton n.m.r. spectroscopies. It was possible to distinguish between primary products formed by reaction with the feed gas, and secondary products resulting from intermolecular exhange in static solution.

The reaction examined here is the reverse of the one studied kinetically in Chapter IV.

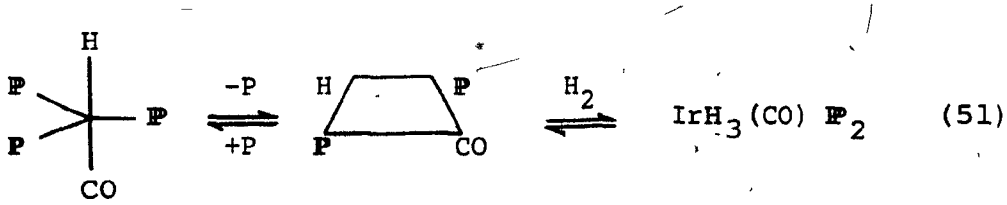

Evidence for an intermediate was found in the u.v. spectrum of 27 (see Chapter IV); moreover, the kinetic behavior of

$IrH_3(CO)P_2$[132] and $IrH(CO)P_3$[117] toward oxidative addition leave little doubt that the intermediate $IrH(CO)P_2$ is involved. The stereochemistry of the intermediate is suggested by i) analogy with $IrX(CO)P_2$[51] (X = halogen, P = aryl or alkyl phosphines), ii) steric grounds, since the bulky phosphine are expected to assume trans positions, and iii) the spectroscopic observation of a trans-P structure in the rhodium analogue, $RhH(CO)P_2$[169]. It is therefore assumed that the intermediate also has trans-P as in 14.

B. EXPERIMENTAL PROCEDURE

1. Synthetic Methods and the Sources of Reagents

Deuterated reagents were purchased from the following sources, and used without further purification: methylene chloride-d_2 (99.5%), toluene-d_8 (99.5%) and deuterium oxide (99.6%), Stohler Isotope Chemicals; deuterium (99.5%), Linde/Union Carbide, Ltd.; sodium borodeuteride (98%) and lithium aluminum deuteride (99%), Merck, Sharp, and Dohme (Canada), Ltd. The synthesis of $IrH_3(CO)P_2$ is described in Chapter II and those of $IrCl(CO)P_2$[154], $IrClH_2(CO)P_2$[96], $IrH(SO_2)(CO)P_2$[147] and $[IrH_2(CO)P_3]ClO_4$[80] appear in the literature.

a) IrH(CO) P_3

$IrH(CO)P_3$ was prepared according to literature methods[154]

and recrystallized from hot ethanol to give pale yellow crystals, i.r. 2087, 1930 cm^{-1} in Nujol.

b) $IrD(CO)\ P_3$

$IrD(CO)\ P_3$ was prepared by a modification of literature methods[80,130]. A suspension of $IrCl(CO)\ P_2$ (.25 g, .33 mmol) was stirred with $LiAlD_4$ (.042 g, 1.0 mmol) and excess triphenylphosphine (.26 g, 1.0 mmol) for two hours in freshly distilled, dry tetrahydrofuran (25 ml) under nitrogen. Excess $LiAlD_4$ was destroyed with a few drops of D_2O, and the grey mixture evaporated to dryness. The residue was stirred in toluene (25 ml), filtered, and the filtrate was left for 12 h at 25°C under nitrogen. Following evaporation of the solution to 1 ml, the crystallization of product was induced by the slow addition of hexane (10 ml) and cooling to -10°C. The product was filtered, washed with hexane, and dried. Yield: .25 g (71%), isotopic purity > 95%.

c) $IrD_3(CO)\ P_2$

$IrD_3(CO)\ P_2$ was also prepared by a modified literature method[80]. $IrCl(CO)\ P_2$ (.25 g, .33 mmol) was stirred with $LiAlD_4$ (.042 g, 1.0 mmol) in freshly distilled tetrahydrofuran (10 ml) for six hours at 25°C under nitrogen. Excess $LiAlD_4$ was destroyed with a few drops of D_2O, and the mixture was evaporated to dryness. The residue was extracted in toluene

(15 ml) by stirring 30 min under D_2 and filtered. The fac and mer isomers were separated in the same way as the trihydride isomers. Total yield: .10 g (41%).

d) Attempted Stereospecific Synthesis of mer-$IrH_3(CO)\,\mathbf{P}_2$

In typical experiments, small amounts (ca. 20 mg) of an iridium complex, $IrH_2Cl(CO)\,\mathbf{P}_2$, $IrH(SO_2)(CO)\,\mathbf{P}_2$, or $[IrH_2(CO)\,\mathbf{P}_3]ClO_4$, were mixed with an excess of hydriding agent (ca. 10 mg), briefly at 25°C, or longer at low temperature, in ca. 2 ml of solvent. The suspension was then evaporated to dryness in a stream of nitrogen and quickly extracted into ca. 1 ml methylene chloride, filtered, and again evaporated. After trituration in hexane, the resulting powder was analyzed by i.r. as a Nujol mull. Further details of these reactions are given in Table V-6.

2. Interaction of H_2 or D_2 with $Ir(D/H)(CO)\,\mathbf{P}_3$

a) I.r. studies

The iridium complex (ca. 100 mg) was dissolved in 25 ml of freshly distilled methylene chloride (4 mM) in a flask fitted with a serum cap and needle for the release of pressure. A continuous stream of H_2 or D_2 was passed through the solution via a syringe needle. The yellow solution faded as the reaction progressed. The reaction was monitored by periodic

withdrawal of 1 ml of solution, rapid evaporation (< 2 min) to dryness in a stream of nitrogen, and trituration in hexane (1 ml). The i.r. spectrum of the resulting powder was taken as a Nujol mull or a KBr disk. In these experiments, the effects of intermolecular H/D exchange were minimized by constantly purging the solution with reactant gas, and solid-state sampling.

b) N.m.r. Studies

The reaction products were analyzed by solution-state n.m.r. spectroscopy in a manner similar to that described above (part a), but on a smaller scale (10 mg Ir(I) complex), in deuterated solvents (ca. 1 ml of CD_2Cl_2 or toluene-d_8) and at somewhat higher concentrations (10 mM). The gas was bubbled for ca. one hour at 25°C or ca. five hours at 0°C. The solutions were then quickly filtered into n.m.r. tubes and stoppered under nitrogen. In some cases, the samples were then cooled. Only a short time passed between the cessation of bubbling and cooling (< 5 min). Further details of the i.r. and n.m.r. spectral measurement are given in Chapter II, section B.2.

C. RESULTS AND ANALYSIS OF SPECTRA

Spectral data and structural assignments of the

$Ir(D/H)_3(CO)\ \mathbb{P}_2$ reaction products are described below, as well as the effects of varying the reagent, the temperature, and the solvent. The range over which the reaction temperature could be varied was limited: much above ambient temperature, the loss of hydrogen from the complexes was too fast, while at temperatures below 0°C, no reaction at all occurred, even after six hours.

Structures referred to in the text are listed in Table V-1. Isotopomers with complementary H/D substitution patterns are indicated by superscript primes, and hydrogen atoms having the same relationship to the tertiary phosphine and carbonyl ligands are indicated by subscript letters.

1. Infra-Red Spectra

Solid-state spectra were measured on Nujol mulls obtained from methylene chloride solutions of the tris-(phosphine) complex, 27, treated with hydrogen at room temperature. These spectra are compared to partially deuterated products, obtained under similar conditions, in Figure V-1.

Assignments of the peaks in these spectra may be made with the aid of the trihydride spectra and Vaska's study of some partially deuterated hydrido-carbonyl complexes[185,189]. In those studies, a resonant interaction between metal-hydrogen

Table V-1. Isotopomers of $IrH(CO)P_3$, $IrH(CO)P_2$, and $IrH_3(CO)P_2$.

IrH	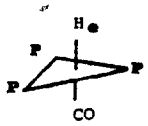	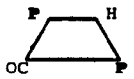
	27	14
IrD	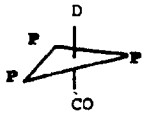	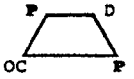
	27'	14'
IrH_3	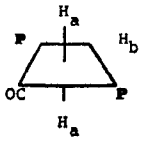	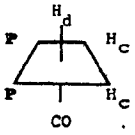
	7	3
IrH_2D	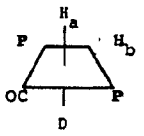	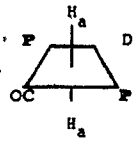 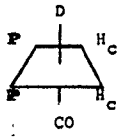 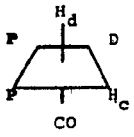
	28	29 30 31
IrD_2H	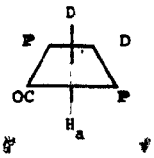	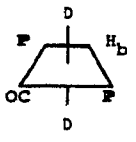 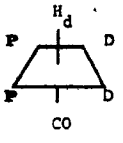 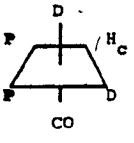
	28'	29' 30' 31'

Figure V-1. I.r. spectra of $Ir(D/H)_3(CO)\ P_2$ reaction products in the Ir-H and CO stretching regions, measured in nujol mulls. In (a), the spectrum of $IrH(CO)\ P_3$ treated with hydrogen is shown before the reaction (a.i), after ca. 1 h (a.ii), and after ca. 4 h (a.iii). In (b), the spectrum of $IrH(CO)\ P_3$ is shown before reaction (b.i), and after bubbling D_2 for 1 h (b.ii) and 2.5 h (b.iii). In (c), the spectrum of $IrD(CO)\ P_3$ is shown before reaction (c.i), and after bubbling hydrogen for 0.8 h (c.ii), and 1.5 h (c.iii).

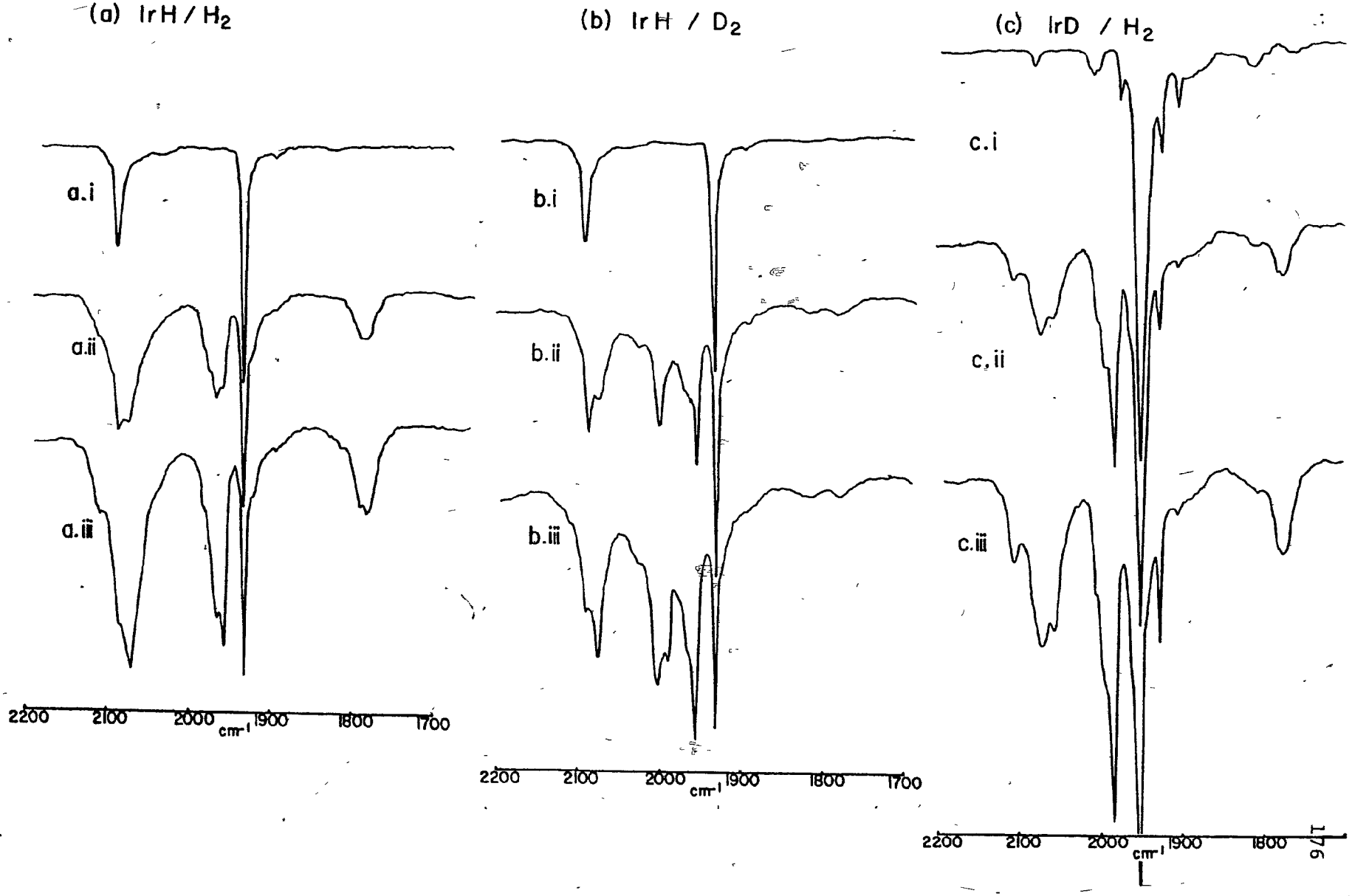
(a) IrH / H2
(b) IrH / D2
(c) IrD / H2
a.i
a.ii
a.iii
b.i
b.ii
b.iii
c.i
c.ii
c.iii
2200
2100
2000
1900
1800
1700
cm-1

and carbonyl stretching vibrations was noted in complexes where the hydrogen and carbonyl ligands are trans to one another. This interaction would in the present case result in an increase of 20 to 30 cm^{-1} in ν_{CO} upon the substitution of deuterium for hydrogen trans to carbonyl. Furthermore, the ratio ν_{Ir-H}/ν_{Ir-D} for a similar H/D substitution cis to the carbonyl ligand was found to be 1.39. Accordingly, for ν_{Ir-H} trans to H, one would expect an absorption at 1281 cm^{-1} upon substitution with deuterium.

These relationships were verified by the preparation of fac and mer $IrD_3(CO)$ $\mathbf{P}_2$. Both isomers had the same ν_{CO} (1986 cm^{-1}), but the mer isomer exhibited a broad, weak absorption at 1280 cm^{-1} that was missing in the fac isomer. The absorption due to ν_{Ir-D} trans to D is much weaker than its trihydride counterpart, possibly due to a lack of resonant interaction in the former case.

a) $IrH(CO)$ $\mathbf{P}_3/H_2$

Both fac and mer $IrH_3(CO)$ $\mathbf{P}_2$ are clearly present after one hour of treatment with hydrogen (Figure V-1, a.ii). Further growth of absorptions due to trihydride species ceases after a reaction time of ca. 4 h. The spectrum at this time indicates that only the three species 27, 3 and 7 are present.

b) IrH(CO) P_3/D_2

After 60 min (Figure V-1, b.ii), absorptions characteristic of H trans to CO (2073, 1965 cm^{-1}) and D trans to CO (1998 cm^{-1}) are apparent. All these peaks continued to grow with time (Figure V-1, b.iii). Very weak, broad absorptions are tentatively assigned to ν_{Ir-H} trans to D and H, respectively. A weak absorption appeared at 1285 cm^{-1}, and is assigned to ν_{Ir-D} trans to D. In view of the relatively low extinction coefficient of this stretching mode, the presence of this absorption suggests that appreciable amounts of a compound with trans D ligands was formed.

c) IrD(CO) P_3/H_2

After a reaction time of 45 min (Figure V-1, c.ii) several peaks appear which are assigned to ν_{Ir-H} trans to P (2110, 2061 cm^{-1}) ν_{Ir-H} trans to CO (2076 cm^{-1}), and ν_{CO} trans to D (1986 cm^{-1}). It is expected that the substitution of deuterium for hydrogen in a position trans to hydrogen will result in an increase in ν_{Ir-H}. Consequently, the large absorption at 1780 cm^{-1} is assigned to ν_{Ir-H} trans to H. No evidence of ν_{Ir-D} (trans to H or D) was apparent in the region 1200-1350 cm^{-1}.

d) Exchange Processes

Intermolecular H/D exchange is expected to be small under

the conditions of these experiments (i.e., constant purge of the solution by H_2 or D_2, and solid-state sampling. The relatively slow growth of ν_{CO} due to 27 (1930 cm^{-1}) in the addition of H_2 to IrD(CO) $\mathbb{P}_3$ (Figure V-1c) shows that exchange is not a major factor in these experiments. The absorbances mentioned above in sections b and c are therefore due to $IrD_2H(CO)\ \mathbb{P}_2$ and $IrDH_2(CO)\ \mathbb{P}_2$, respectively.

e) Structural Assignments

The spectra in Figure V-1 indicate that the fac isomer is formed by addition of hydrogen trans to $\mathbb{P}$, since both of these stretching modes [A'(2) and A" in Table II-1] are present in c and absent in b. The mer isomer is formed by the added hydrogen occupying trans positions in the product. This is indicated by presence of ν_{Ir-H} (trans H) in c and the absence of it in b, as well as the presence of ν_{Ir-D} (trans D) in b but not c. Also, there are indications of additional species present (i.e., H trans CO in c, and D trans CO in b which implies non-stereospecific formation of each isomer. The n.m.r. experiments described below determined the nature of these additional species.

f) $IrH(CO)\ \mathbb{P}_3/D_2$ Reaction Products in KBr Disks

Reactions with deuterium, carried out under the same conditions as in section b, were also analyzed as KBr pellets

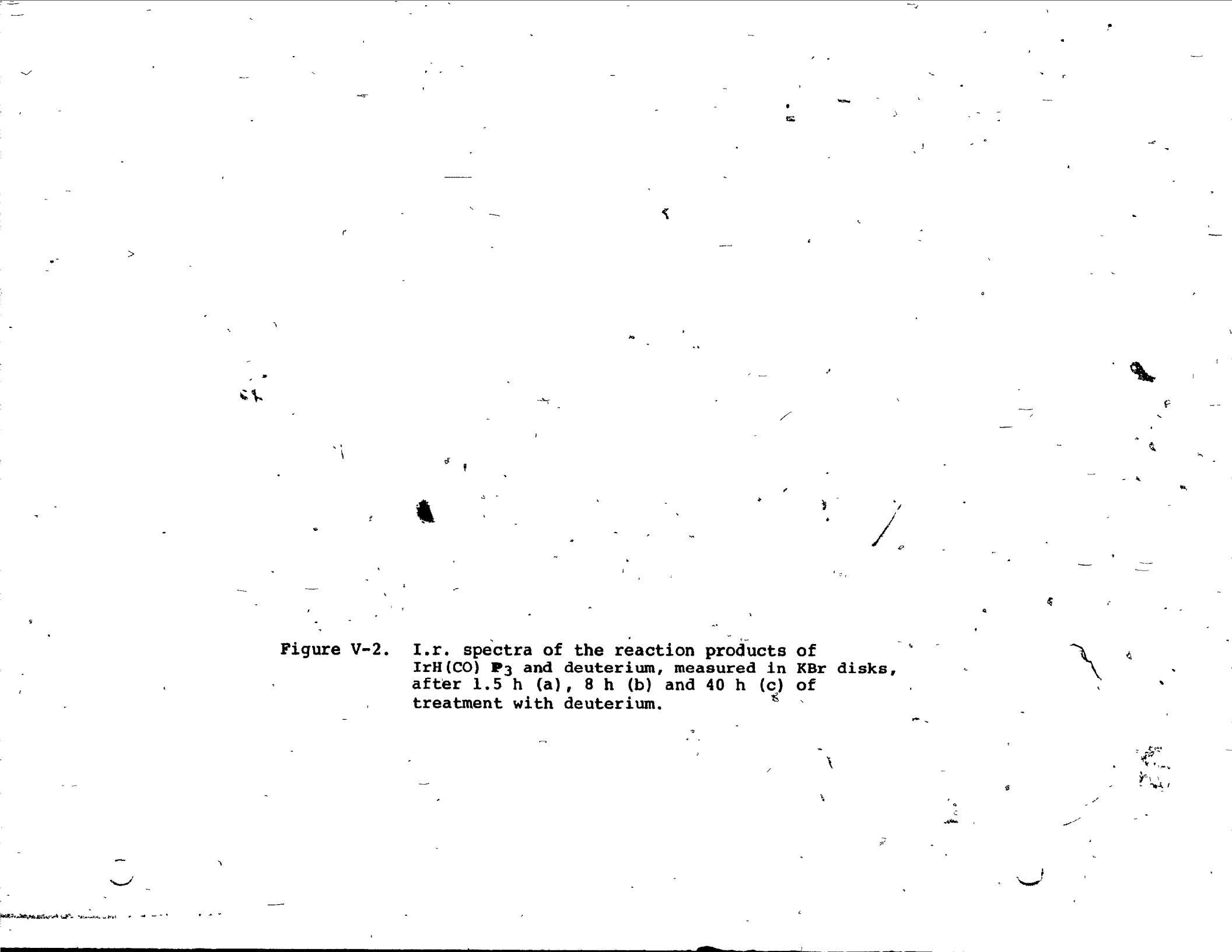

Figure V-2. I.r. spectra of the reaction products of $IrH(CO)P_3$ and deuterium, measured in KBr disks, after 1.5 h (a), 8 h (b) and 40 h (c) of treatment with deuterium.

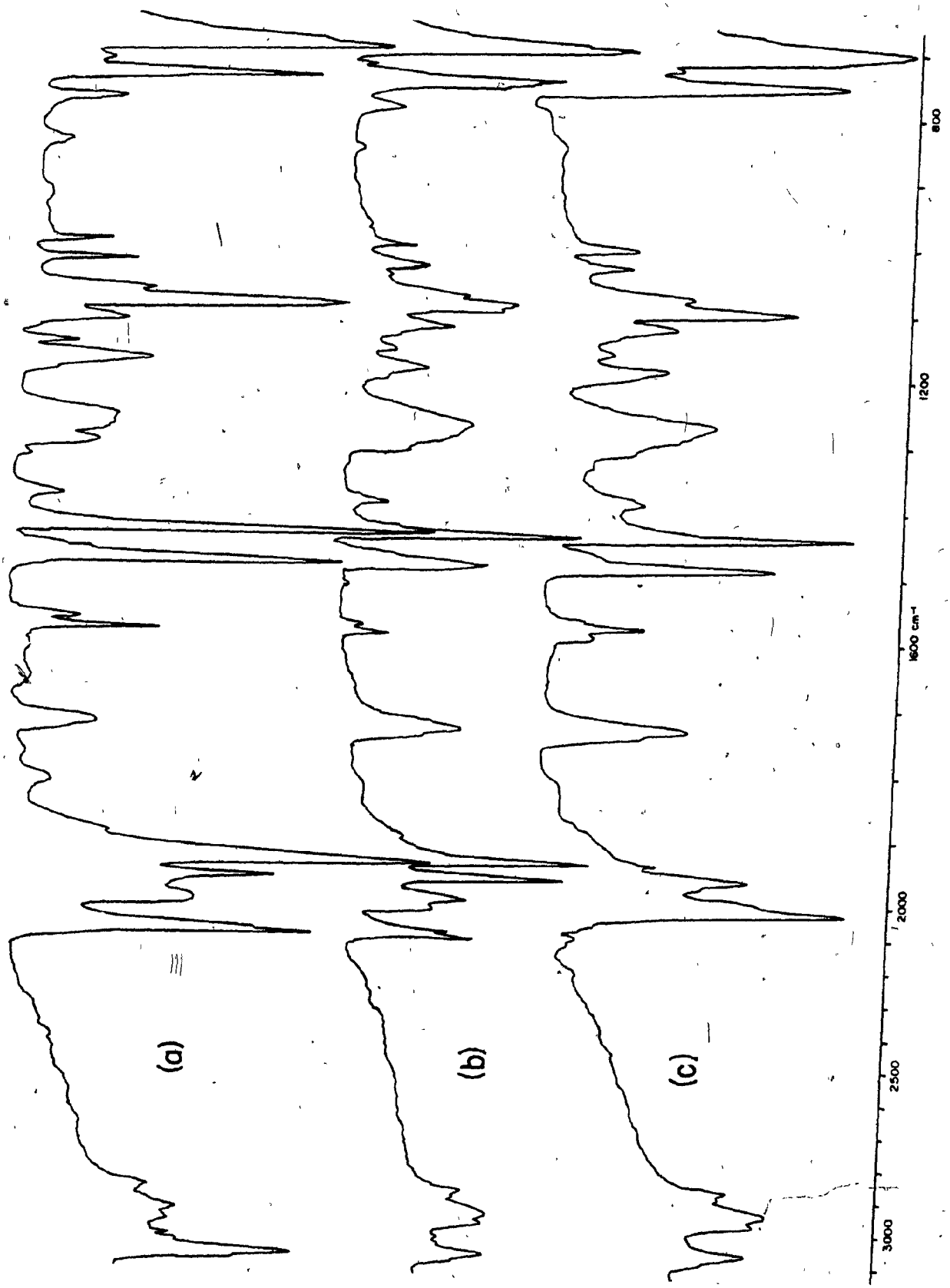
(a)
(b)
(c)
3000
2500
2000
1600 cm⁻¹
1200
800

(Figure V-2). Although all the absorptions noted in spectra taken as Nujol mulls (Figure V-1b) were also present in those taken as KBr pellets, additional peaks appeared at 1730 and 1280 cm^{-1} in the latter case. Curiously, these peaks continued to grow even after forty hours of a deuterium purge (Figure V-2c), when no other Ir-H stretches were evident. It is believed that the additional peaks are a result of a solid-state reaction which occurred during the preparation of the KBr pellets. Under these conditions (i.e., an evacuated die-press under a pressure of 7,000 kg/cm^2 exerted for ca. 15 min with the concurrent generation of heat), it appears that an intrametallated species, such as 32 or 33, was formed by transfer of a hydrogen atom from the ortho-phenyl position of the triphenylphosphine ligand of an Ir(III) species, along with the elimination of HD or D_2.

Consistent with structures 32 and 33, the rather large absorptions at 1730 and 1280 cm^{-1} are assigned to ν_{Ir-H} and ν_{Ir-D}, respectively. The relative increase in intensity of absorptions assigned to ν_{CC} (1572, with small shoulders at 1762, 1745 and possibly 705 cm^{-1}) suggest changes in the substitution pattern of the aromatic ring, and are characteristic of intrametallated compounds[53,190]. Furthermore, the intensity of ν_{Ir-H} (trans D) is roughly proportional to the amount of $Ir(D/H)_3CO\,P_2$ present in solution, regardless of whether the Ir(III) species is IrD_2H (Figure V-2b) or IrD_3

(Figure V-2c) . The source of the hydride ligand is therefore not the starting material, 27. The fact that the absorptions at 1730 and 1280 cm^{-1} are present at a reaction time of 90 min (Figure V-2a) rules out a reaction with solvent as a possible source of hydrogen.

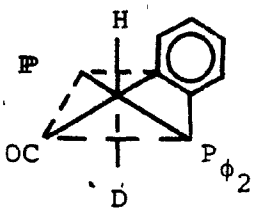

32

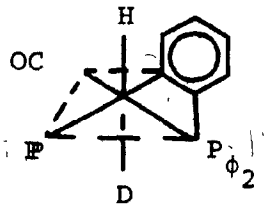

33

The above proposals should be verified by n.m.r., to fully establish intrametallation and to perhaps distinguish between 32 and 33. Isomers of 32 and 33 having cis hydride and cis phosphorus ligands have been prepared by the oxidative addition of hydrogen to $Ir(CO)[P(C_6H_4)(C_6H_5)_2]P$[190]. Since, in the present case, the compounds are formed in high yield, the preparation of intrametallated complexes by solid-state synthesis may be a useful synthetic method. The n.m.r. results presented in this chapter clearly demonstrate that a similar reaction does not occur in solution. Solid-state intrametallation at high pressure, if verified, would provide an interesting illustration of Parshall's suggestion that "any

C-H bond may be metallated if it is 'rubbed' sufficiently hard against a reactive metal atom"[191].

2. N.M.R. Spectra: Primary Reaction Products

The primary reaction products of the addition of hydrogen or deuterium to the tris(phosphine) deuteride (27') or hydride (27), respectively, may be found by carrying out the reaction at 25°C, immediately cooling the solution, and measuring the spectrum at low temperature. The very small amount of the hydride, 27, which can be found among the products of hydrogen addition to the deuteride, 27', (see Figure V-3b) demonstrates that this procedure does indeed eliminate secondary reaction products formed by further intermolecular reaction of the Ir(III) products. This hydride (27) would dominate the spectrum of a solution in which secondary processes occurred to a significant extent.

The spectra of the solutions that result from the addition of hydrogen or deuterium to 27 or 27' are shown in Figure V-3. The chemical shifts of all peaks in Figures V-3 and V-6 are listed in Appendix II. Resonance patterns are identified by a number and subscript letter which correspond to the structures listed in Table V-1.

In the following analysis, only isotopomers of the fac

Figure V-3. The ^1H n.m.r. spectra of primary $Ir(D/H)_3(CO)P_2$ reaction products, measured in CD_2Cl_2 at 25°C (a) and -20°C (b,c). The spectra indicate the products of addition of H_2 to $IrH(CO)P_3$ (a), H_2 to $IrD(CO)P_3$ (b), and D_2 to $IrH(CO)P_3$ (c) for ca. 1 h at 25°C. The resonance patterns are identified by tie-lines and numbers corresponding to structures in Table V-1. The frequencies of all numbered peaks are listed in Appendix II.

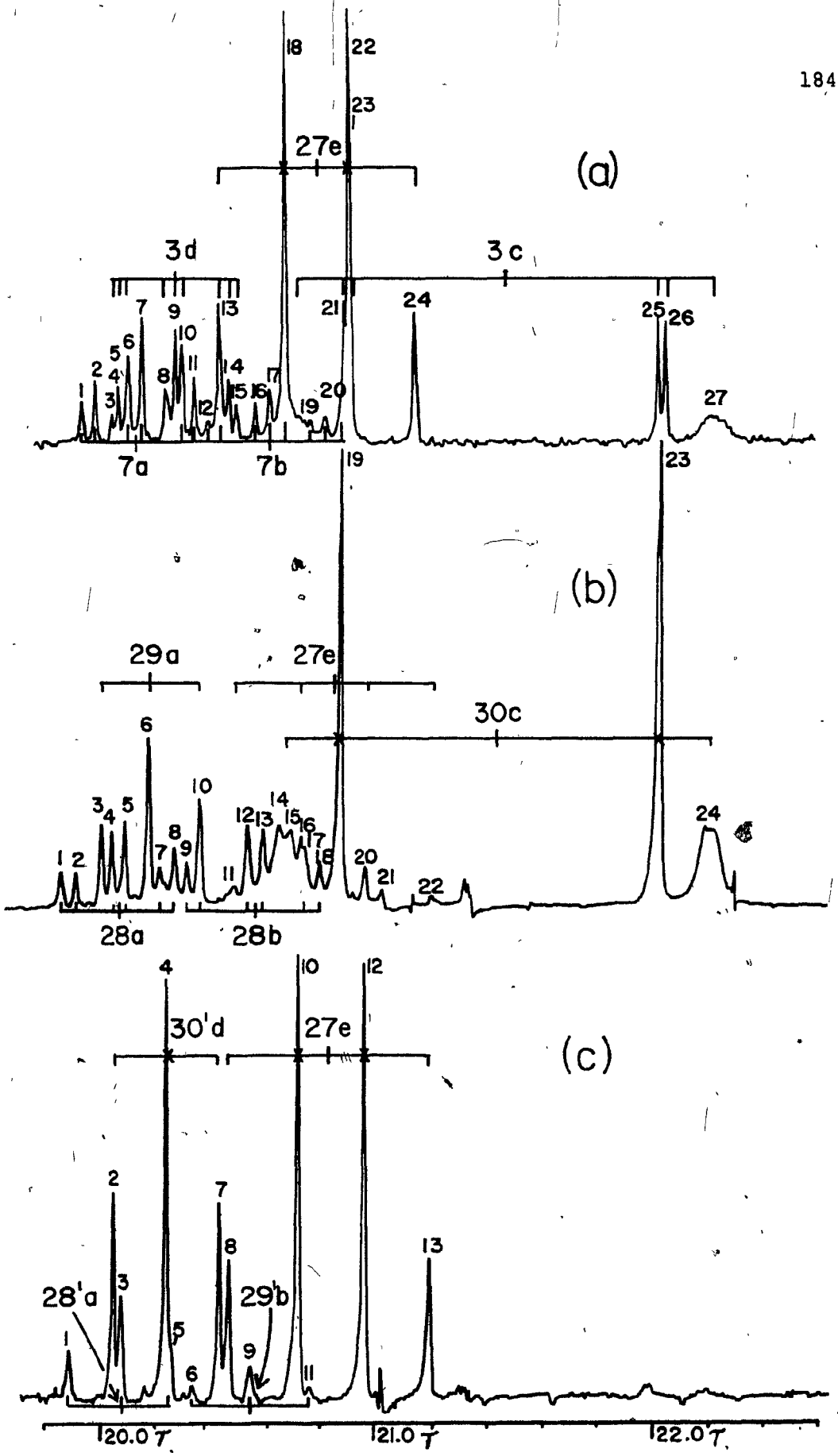
(a)
27e
3d
3c
7a
7b
(b)
29a
27e
30c
28a
28b
(c)
30'd
27e
28'a
29'b
20.0 τ
21.0 τ
22.0 τ

and mer trihydrides of structures 3 and 7 are explicitly discussed as possible reaction products. Isotopomers of 4, the mer-H, cis-P trihydride isomer which was not formed in any of the reactions previously discussed, were also considered as possible products. On the basis of the n.m.r. spectra, it was found that these isotopomers are not present in any of the deuterated samples.

a) $IrH(CO)\ P_3/H_2$

The large quartet in the center of the spectrum (Figure V-3a) is due to the starting complex, 27. A comparison to the spectrum of an equilibrium mixture of the trihydrides (Figure II-9) indicate that all other peaks in the spectrum may be attributed to the isomers, 3 and 7. The isomers of the trihydride are present in the same proportion in both cases.

b) $IrD(CO)\ P_3/H_2$

The largest peaks in Figure V-3b are singlets of nearly equal intensity at 20.85 τ (peak 19) and 22.01 τ (peak 23), and are accompanied by unresolved multiplets that are symmetric to the resonance center. This second-order pattern indicates hydrogen trans to phosphorus in a situation in which the hydrogen atoms are equivalent in chemical shift, but magnetically inequivalent. The multiplet is similar in

chemical shift and appearance to the fac trihydride, 3, but without obvious H-H coupling. Structure 30 is therefore assigned.

The next largest peaks, 3, 6, and 10, form a simple triplet centered at 6. The triplet splitting indicates hydrogen cis to equivalent phosphorus atoms. The absence of hydrogen coupling in this triplet indicates either two chemically and magnetically equivalent hydrogens, or a single hydrogen. Of the possibilities, 29, 28' and 29', the dihydride, 29, is assigned on the basis of the chemical shift, the coupling constant and the indication of trans-hydrogen in the infra-red spectrum (see Figure V-1c). Furthermore, it is unlikely that a species containing two deuterium atoms would be formed by this reaction, since other evidence indicates that H/D exchange does not occur.

The remaining lines in the spectrum may all be assigned to a species with hydrogen cis to hydrogen. If the triplet due to 29a is ignored, a triplet of doublets is apparent in the region 19.8 to 20.3 τ, centered at peaks 4 and 5. The triplet pattern is indicative of hydrogen cis to equivalent phosphorus atoms. Another doublet (peaks 12 and 13) of approximately equal intensity is apparent further upfield with the same H-H coupling constant. Only 28, of the possible isomers of formula $IrDH_2(CO)\ \mathbf{P}_2$, has the appropriate structure, chemical shifts and coupling constants. The 28a multiplet

shows clearly, although the 28b multiplet is partially obscured by other peaks.

The assigned structures, 28, 29 and 30, account for nearly every line in the spectrum. As mentioned above, the absence of significant H/D intermolecular exchange occurring through intermediate 14 is indicated by the absence of a significant amount of the tris(phosphine) complex, 27. Peaks 16 and 20, the center lines of the 27e quartet, are clearly present, although the outer peaks, 11 and 22, are barely perceptible.

c) $\underline{IrH(CO)\ P_3/D_2}$

The addition of deuterium to 27 gives rise to a spectrum that is much simpler than those described above. There is no H-H coupling apparent in Figure V-3c, suggesting the absence of $IrDH_2(CO)\ P_2$ species, and therefore the absence of intermolecular H/D exchange. Furthermore, there is no evidence of hydrogen trans to phosphorus. The spectrum may be completely analyzed in a first-order manner, and considered to be composed of symmetrical triplets and a quartet arising from hydrogen cis to two and three equivalent phosphorus atoms, respectively.

The largest peaks comprise a quartet due to the starting complex, 27. The largest triplet is assigned to a fac configuration with deuterium trans to phosphine, structure 4'. The absence of any hydrogen trans to phosphorus in the spectrum

demonstrates that this isomer is formed stereospecifically, which is again consistent with the absence of H/D intermolecular exchange.

The remaining two triplets in the spectrum are assigned to two forms of the mer isomer. The larger triplet is assigned to 28', which has deuterium in a cis configuration, and the smaller triplet to 29', having trans deuterium ligands.

d) Structural Assignments

Chemical shifts of the deuterated products of the hydrogen (28, 29 and 30) and deuterium (28', 29' and 30') addition reactions discussed above are listed in column 2 of Table V-2. The close agreement with chemical shifts of analogous trihydride resonances strongly supports the above assignments. The small differences between the trihydride shifts and those of the partially deuterated products may all be attributed to the effects, discussed systematically below, of temperature and solvent on the chemical shift. Moreover, the coupling constants are in excellent agreement with trihydride measurements in all cases (see Appendix II for spectral data).

The complementary reactions, IrD(CO) P_3 plus hydrogen, and IrH(CO) P_3 plus deuterium, both give three different primary reaction products: a fac isomer, in which the added molecule is in a cis configuration (30, 30'), and two mer

Table V-2. Chemical Shifts of Isotopomers of $IrH_3(CO)P_2$.

Structure	Chemical Shift (τ) Methylene Cloride -20°	0°	25°	Toluene 25°	$\frac{\Delta\tau}{\Delta°C}$ (x 10^3)	$\Delta[\tau_{tol}-\tau_{mc}]$* (ppm)
		resonance a				
7		20.10	20.06			
28	20.05	20.02	19.96	19.27	-2	-.69
28'	20.06	20.04	19.99	19.29	-2	-.70
29	20.17	20.14	20.08	19.38	-2	-.70
		resonance b				
7		20.53	20.54			
28	20.54	20.56	20.55	20.09	0	-.46
29'	20.54			20.10		
		resonance c				
3		21.40	21.42			
30	21.43	21.43	21.42	20.48	0	-.94
		resonance d				
3		20.22	20.20			
30'	20.23	20.22	20.19	19.57	-1	-.38
		resonance e				
27	20.82	20.79	20.72	20.42	-2	-.32

*The difference between the chemical shift measured in toluene and that measured in methylene chloride, at 25°C.

isomers, in which the added atoms are cis (28, 28') and trans (29, 29') to one another. These are entirely consistent with the products observed in i.r. spectra.

3. Secondary Reaction Products

When spectra were recorded after letting reaction solutions stand a few hours at room temperature, mixtures of $IrDH_2(CO)$ P_2 and $IrD_2H(CO)$ P_2 products were obtained. The following results indicate that intermolecular H/D exchange occurs in static solution, and the extent of exchange increases with time. Analysis of spectra containing secondary products revealed the presence of all ten isotopomers of the trihydride 3 and 7, listed in Table V-1.

Intermolecular exchange is indicated by several spectral features, identified in Figure V-4 as i to vi. Schematic representations of exchange-produced spectral features are shown in Figure V-5.

a) $IrD(CO)$ P_3/H_2

i: A decrease of the dihydride, 28, relative to the dideuteride, 28'; is indicated by the transformation in the lowest field doublet in Figure V-4a,b. Because the chemical shift of 28'a is slightly higher than 28a, due to an isotope shift, the right side of the doublet is larger than the left.

Figure V-4. The ^{1}H n.m.r. spectra of secondary $Ir(D/H)_3(CO)\,P_2$ reaction products, measured in CD_2Cl_2 at 25°C (a,b) and 0°C (c). The spectra are the products of H_2 addition to $IrD(CO)\,P_3$ after 1 h (a) and 2.5 h (b) in static solution at 25°C. The products of D_2 addition to $IrH(CO)\,P_3$ after 3.5 h in static solution at 25°C are shown in (c). Features indicating exchange are indicated by i to vi, described in the text, and illustrated in Figure V-5.

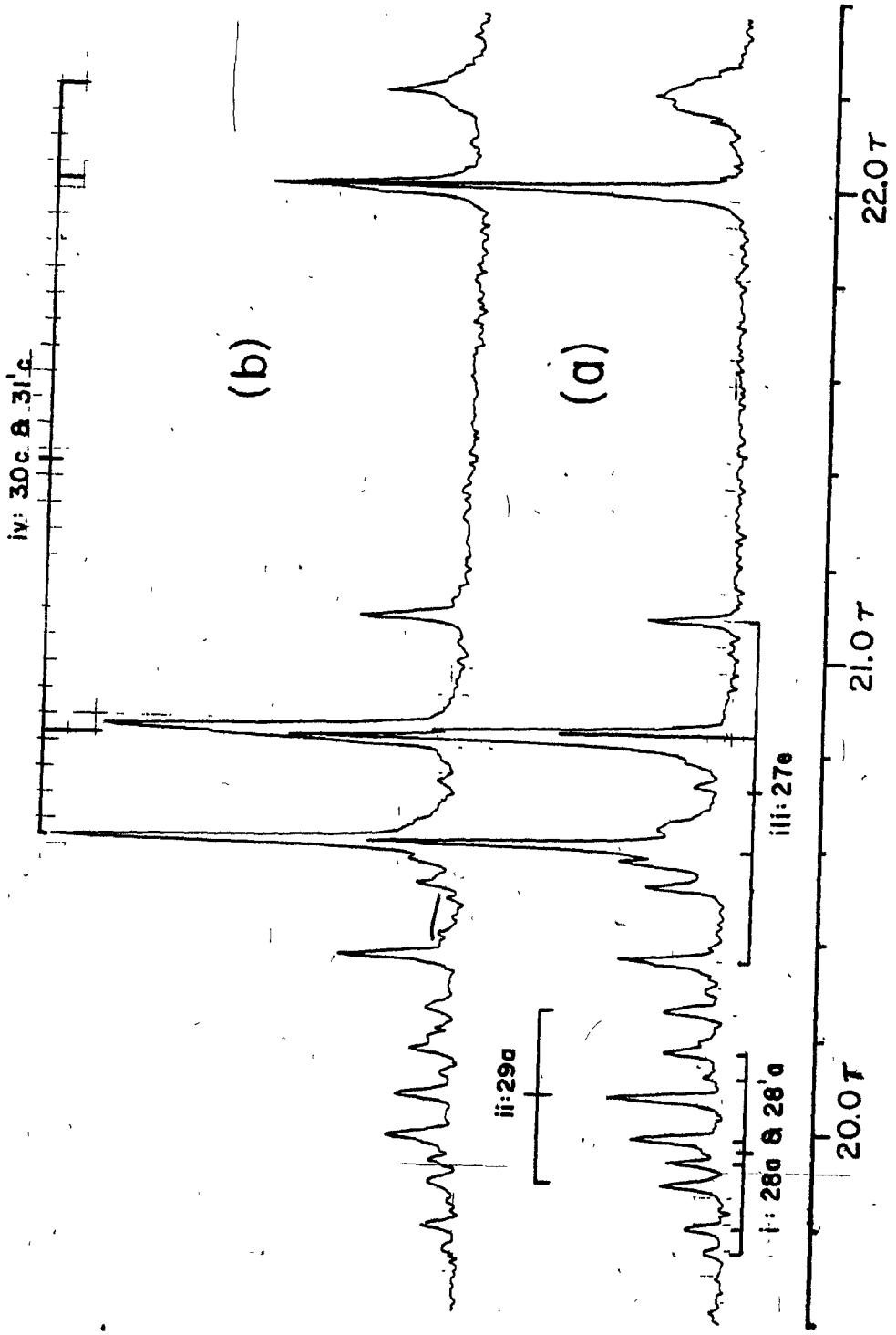
iv: 30c & 31'c
(b)
(a)
ii: 29a
iii: 27e
i: 28a & 28'a
20.0 τ
21.0 τ
22.0 τ

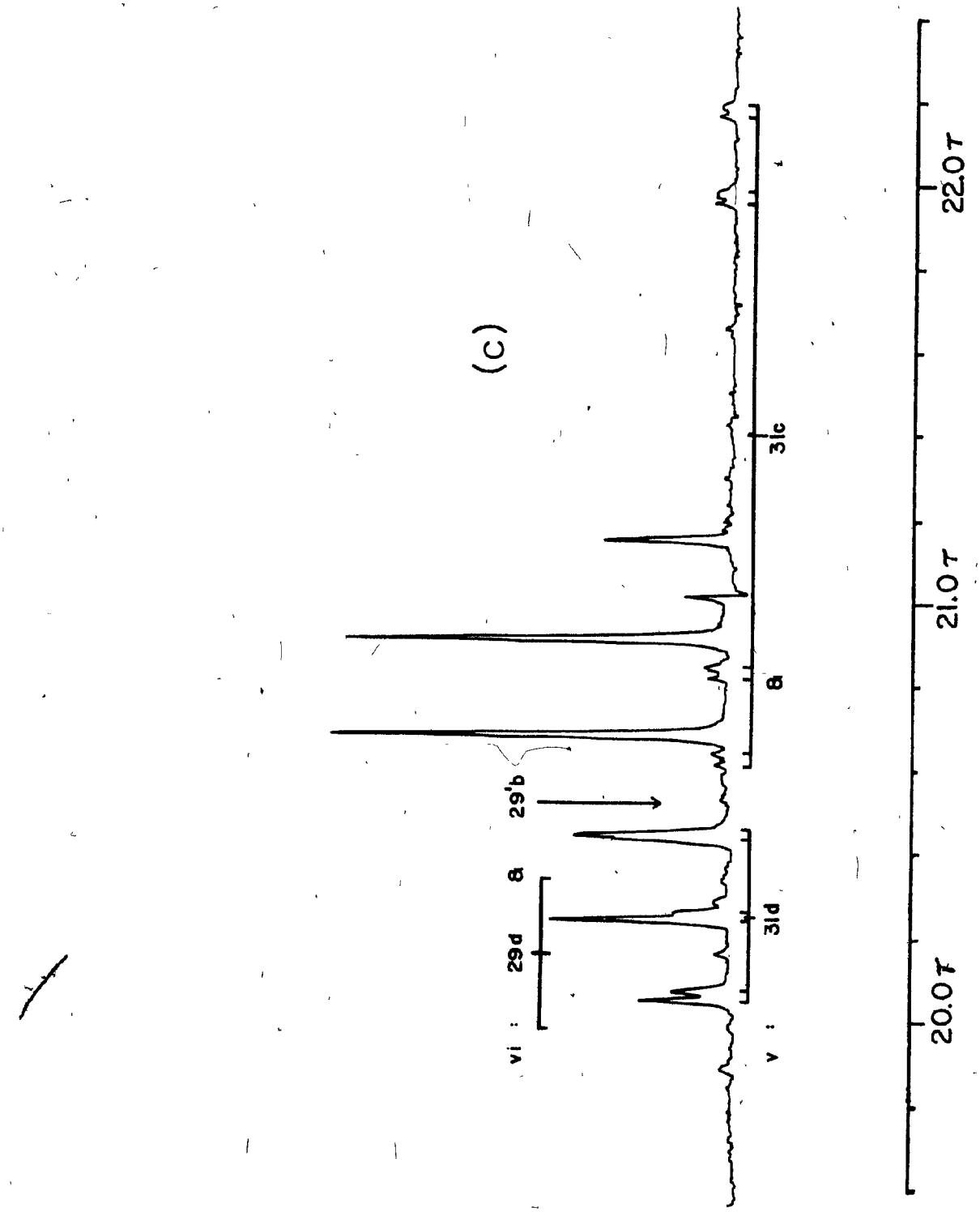
(c)
22.0τ
21.0τ
20.0τ
29'b
8
31c
8
vi :
29d
8
31d
v :

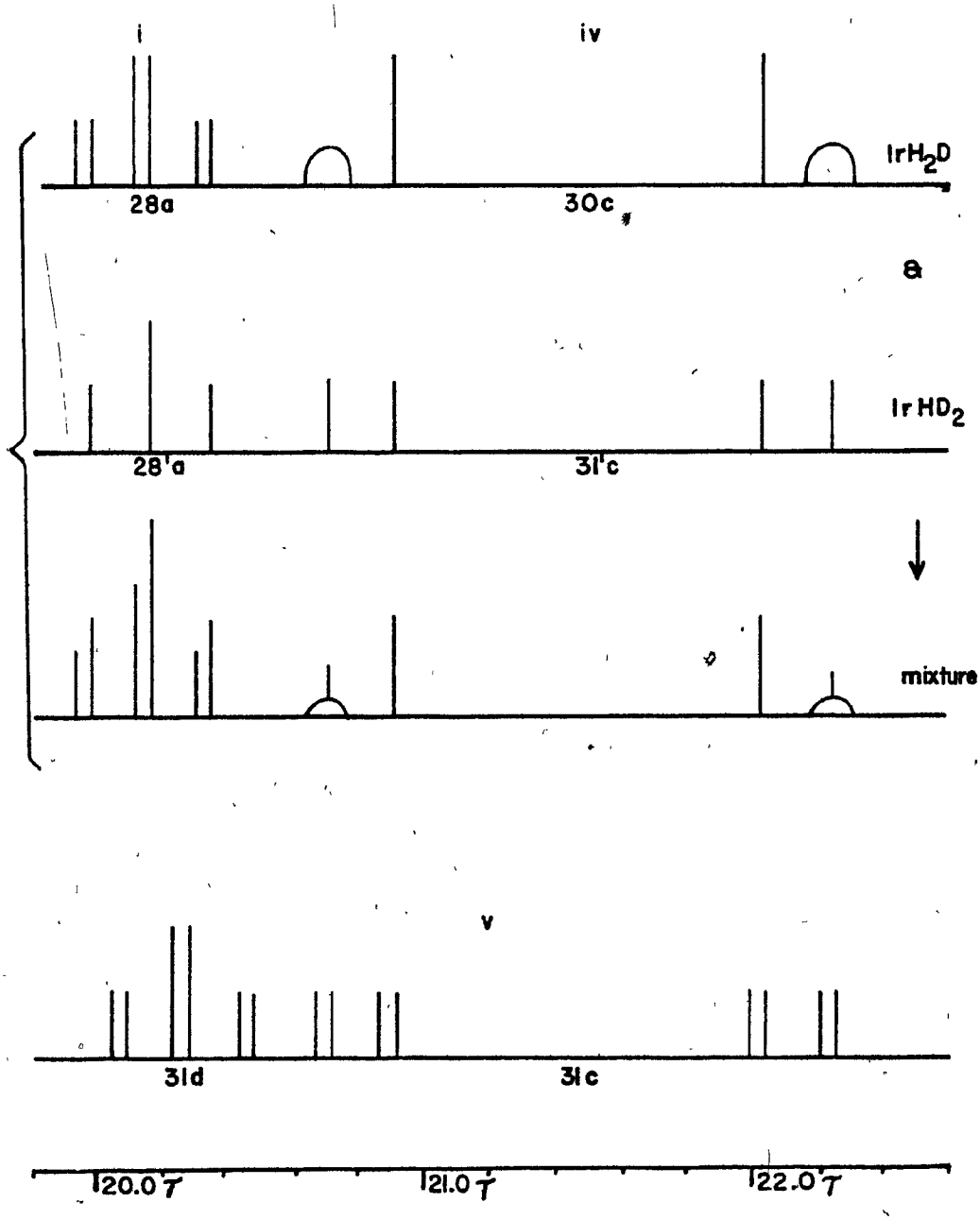

Figure V-5. Schematic representations of the spectra of some secondary reaction products indicated in Figure V-4.

ii: The largest triplet in Figure V-4a, assigned to the dihydride, 29, decreases in intensity relative to a lower-field triplet assigned to a dideuteride, 28'.

iii: The tris(phosphine) species, 27, produced by the loss of HD from a dihydride , is the dominant species in Figure 4b. Species 27 is barely detectable in the analogous low-temperature spectrum (Figure V-3b).

iv: The high-field pattern in Figure V-4b indicates clearly the formation of a species, 31', not present in any low-temperature spectrum. The doublet of doublets expected of 31' accounts for the sharp singlet growing out of the broad multiplet near 22.0 τ.

b) $\underline{IrH(CO)\ P_3/D_2}$

v: The main exchange product to be expected, 31, is indicated by a widely split quartet of doublets, all of equal intensity, assigned to 31c in Figure V-4c. The broadening apparent on the right side of the doublets may be due to small amounts of 31'. The triplet of doublets expected from 31d was presumably obscured by primary products.

vi: A small triplet was assigned to the secondary product 29 in Figure V-4c. The primary product, 29', present in the low-temperature spectrum (Figure V-3c), is not apparent in Figure V-4c.

4. The Effects of Solvent, Temperature, and Isotopic Substitution on the N.M.R. Spectra

a) Reactions in Toluene

The addition of hydrogen and deuterium to 27' and 27, respectively, was carried out at room temperature in toluene-d_8 to verify structural assignments and the absence of solvent participation in the reaction. The results in both solvents were completely analogous. All of the primary reaction products found in methylene chloride are present in toluene, and in roughly the same proportion (see Table V-4). Secondary reaction products are formed in static solution upon standing, indicating that intermolecular H/D exchange occurs in the same manner as in methylene chloride. None of the products of reactions done in methylene chloride, therefore, are a result of a reaction with solvent.

b) Effects of Solvent on the Chemical Shift

Reaction products measured in methylene chloride exhibited higher chemical shifts than those measured in toluene, as shown in Table V-2. The difference in chemical shift due to the solvent, here called the solvent effect, varies significantly from one type of proton to another (see Table V-1 for the positions of protons a to e). Solvent effects are related to structural features of the complexes in the following series:

c > a > b > d > e

1 P cis 2 P cis 2 P cis 2 P cis 3 P cis

The most likely interpretation of the observed order is that solvent-solute interaction is sterically inhibited by the presence of large triphenylphosphine groups in the cis position. Thus the largest solvent effect occurs when the proton is least sterically blocked from the surrounding environment by adjacent triphenylphosphine ligands. A solvent-solute interaction of this sort might occur if metal-methylene chloride "outer-sphere" coordination effectively shields the hydridic protons. By this interpretation, methylene chloride has the larger effect on the solute, contrary to the usual situation in organic molecules, where the shift induced by aromatic solvents is considered most important[192,193]. The interpretation of solvent effects is further complicated in the present case by the fact that neither solvent can be considered completely inert with respect to interactions with the solute.

c) Effects of Temperature on the Chemical Shift

The effects of temperature on the chemical shift, listed in Table V-2, are much less than those apparent on changing the solvent, a change of at most .1 ppm occurring over a 45 degree range. Like solvent effects, the effect of temperature

variation on the chemical shift is dependent more on the resonance type than on a particular molecular structure. For example, the chemical shift of proton 28a is temperature dependent, but 28b is not. The same temperature dependence observed in "a" resonances merely reflects the indifference of the temperature dependence to isotopic substitution. The resonances either move downfield with increasing temperature, or are unaffected by temperature . The order in which the various resonances are affected by temperature is not the same as that observed on changing solvents.

The effect of temperature on the spectrum of the IrD(CO) P_3/ H_2 system is illustrated in Figure V-6. Resonances due to the same proton are joined by lines and the extent to which each pattern is shifted can be seen. The spectra are identical with respect to splitting pattern and coupling constant, and show none of the line broadening characteristic of fluxionality.

The irreversible formation of secondary products can be seen from a comparison of Figure V-6 a and c, both recorded at -20°C. For example, a sharp peak due to 31', can be seen in the center of the multiplet to the highest field in Figure V-6c. This peak, not present in Figure V-6a, was produced by intermolecular H/D exchange occurring during the time (ca. 20 min) that the sample was at room temperature.

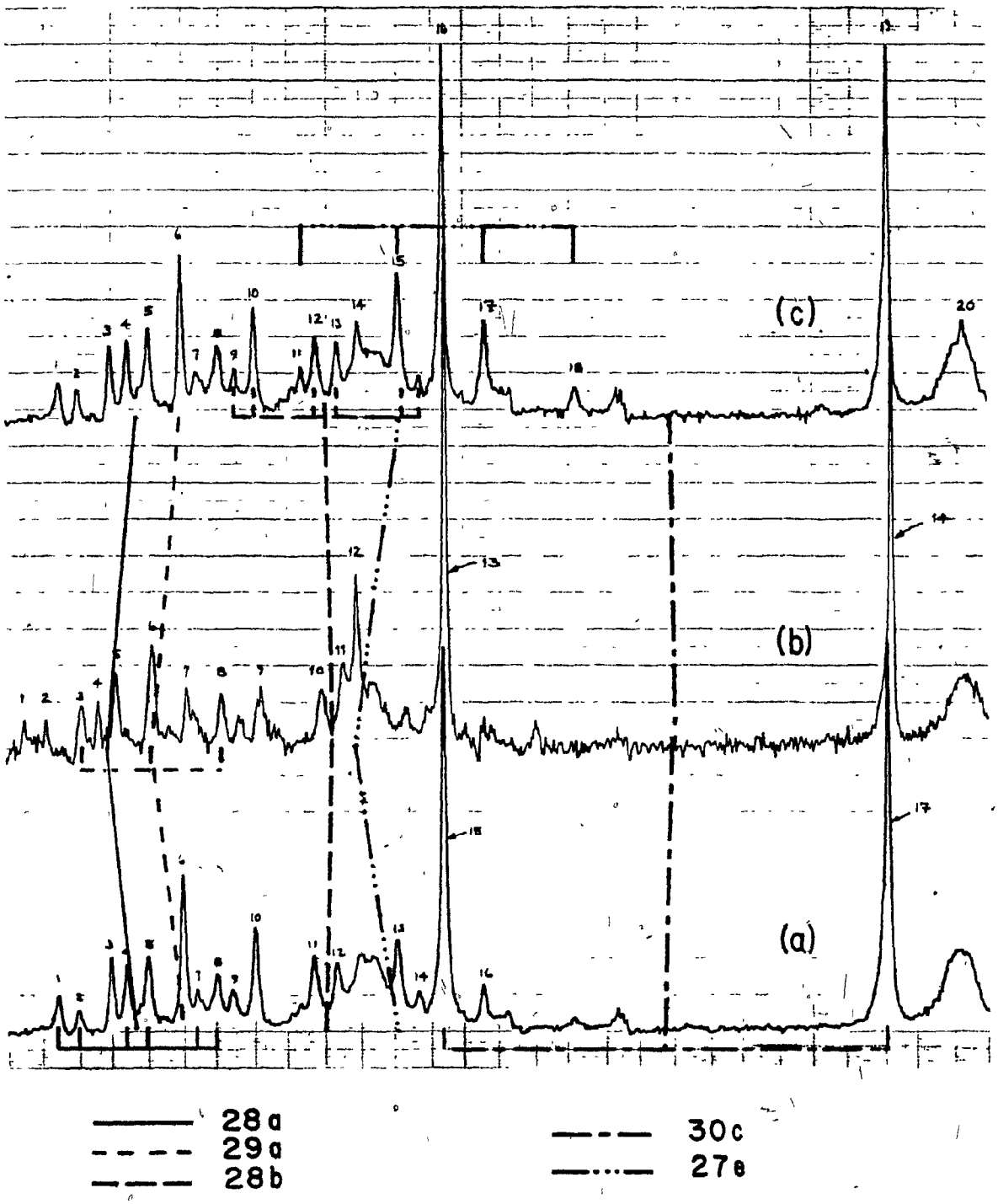

Figure V-6. The effect of temperature on the chemical shift. The same sample of IrD(CO) P_3 treated with hydrogen in CD_2Cl_2 was cooled to -20°C (a), let warm to 25°C for .4 h (b), and re-cooled to -20°C (c). Resonances of the same species are joined by lines.

d) Isotope Effects on the Chemical Shift

The chemical shifts of $Ir(D/H)_3(CO)P_2$ isotopomers are listed in Table V-3. The substitution of one or two hydrogen atoms by deuterium at positions cis to the proton being observed has little effect on the chemical shift. Protons trans to each other, however, show a marked downfield shift of .08 ppm upon changing the trans ligand from H to D.

This shift is opposite in direction to that usually found in isotopic substitution in organic molecules[194]. Downfield isotope shifts, although rare, are sometimes observed in organic compounds, and have been attributed to intermolecular effects such as hydrogen-bonding[195] or interaction with solvent[196]. Recently, large downfield, as well as upfield, isotope shifts were reported in paramagnetic metallocenes[197]. The present results are the first observation of downfield isotope shifts in diamagnetic transition-metal complexes.

In structures where the proton observed is trans to phosphorus or carbonyl (H_b or H_c), the isotope shift upon substitution of one or two deuterium atoms in a cis position is in no case greater than the experimental error inherent in comparing different spectra. Since the isotope shift is generally proportional to the degree of isotopic substitution[194], the lack of a measurable shift implies a shift of less than one Hertz. With H trans to D, a small upfield isotope shift was

Table V-3. Effects of Isotopic Substitution on the Chemical Shift*.

Resonance type	trans Ligand	cis ligand		
		cis H	cis D	
a	H	20.10 (7)	20.14 (29)	
a	D	20.02 (28)	20.04 (28')	
		cis 2H	cis H, cis D	cis 2D
b	CO	20.53 (7)	20.56 (28)	20.54† (29')
c	P	21.40 (3)	21.43 (30) 21.41 (31)	21.41‡ (31')
d	CO	20.22 (3)	20.23 (31)	20.22 (30')

*Shifts measured in methylene chloride at 0°C, unless otherwise noted, are in units of τ (ppm). Structure numbers are in parentheses.

†Shift measured at -20°C. The same shift is expected at 0°C.

‡Shift measured at 25°C. The same shift is expected at 0°C.

detected in H_a by the asymmetric overlap of the resonances of the same spectrum.

The difference in isotope shift caused by substitution of D in a cis or trans position in an otherwise identical molecule resembles the large difference in cis and trans coupling constants observed in these molecules (e.g., J_{HP} cis, 18.1 Hz; J_{HP} trans, 123 Hz). In fact, a systematic study of the isotope shift in some organofluorine compounds have shown it to be, at least in some cases, directly proportional to the coupling constant[194]. In the present case, the isotope shifts and the coupling constants J_{HH} (cis) and J_{HH} (trans) do not appear to be similarly related. The absence of noticeable J_{HD} (trans) coupling in 28'a (see Figure V-3c) suggests, since J_{HD} = ca. 1/6 J_{HH}, that J_{HH} (trans) is less than 6 Hz, which is the same range as J_{HH} (cis).

The isotope shift in n.m.r. has been interpreted according to several theoretical models, including zero-point vibrational amplitude lowering[198], isotope-induced changes in bond hybridization[194], and, recently, the result of rotational and anharmonic vibrational contributions[199,200]. According to the latter interpretation, the temperature dependence of the chemical shift is related to the isotope shift, and both are related to the variation of chemical shielding with internuclear displacement. In this context, it is noteworthy that the temperature dependence of H_a is

larger than that of H_b, H_c or H_d. The reason for the unusual downfield direction of the isotope shift, however, remains unclear. The large difference in isotopic shift for deuterium substituted in the cis and trans position may be yet another illustration of trans-influence in octahedral transition metal complexes[201].

e) Effect of Concentration on the Chemical Shift

The effect of concentration on the chemical shift has not been explicitly determined, but does not seem to be a factor in the results discussed above for the following reasons. All initial solutions had roughly the same initial concentration of the starting Ir(I) complex, 27 or 27' (ca. 20 mM). The chemical shift of 27, present in very different concentrations in Figures V-3b and c, changed only very little (ca. 20.84 τ versus 20.82 τ). Finally, the changes in temperature and solvent result in the same type (e.g., H_a in 28, 28' and 29), even when these species were present in different concentrations.

5. Relative Amounts of $Ir(D/H)_3(CO)\ P_2$ Products

Product ratios were calculated for each reaction, and are listed in Table V-4. These figures represent the molar amounts of each isomer, relative to fac isomers 3, 30 or 30'.

Table V-4. Relative Amounts of $Ir(D/H)_3(CO)P_2$ Products[a].

Reactants[c]	Conditions[d] (°C)	mer isomer			fac isomer (30,30')	tris(phosphine) (27)
		Added cis (28,28')	Added trans (29,29')	Total		
A. IrH/H_2	25/25			.47 .50	1.01 .99	2.15
B. IrD/H_2	25/25	.4	.2	.6	1.0	1.0
IrH/D_2	25/25	.2	-	.2	1.0	2.0
IrD/H_2	25/25[b]	.6	.3	.9	1.0	1.0
IrH/D_2	25/25[b]	.5	-	.5	1.0	1.8
C. IrD/H_2	25/-20	.37 .38	.21	.59	1.00	.10
IrH/D_2	25/-20	.27	.09	.36	1.00	1.42
D. IrD/H_2	0/0	.36 .30	.18	.51	1.00	.18
IrD/H_2	25/0	.34 .34	.20	.54	1.00	.15
IrD/H_2	above, after 24 h at 0°C	.40 .32	.22	.58	1.00	.29

[a]Estimated error limits B:±.1; A,C,D:±.05. Reactions and measurements in methylene chloride, unless otherwise noted.

[b]Reactions and measurements in toluene.

[c]Starting complex/gaseous reagent. IrH is 27; IrD is 27'

[d]Reaction temperature/measurement temperature.

They were obtained by measuring the peak height above the base-line, multiplying by a factor appropriate for the splitting pattern, and averaging values for several lines in the multiplet. The peak heights of individual lines of the multiplet were generally in the proportion expected for that pattern. In the case of the fac isomer, the broad, unresolved multiplet of 30c is ca. 15% lower in intensity than expected from simulated spectra, and so the average value of the resolved and unresolved part of the multiplet was used. Agreement between the two resonances due to 28 (Table V-4, column 3, sections C and D) suggests that line broadening due to deuterium coupling is not significant.

In section A of Table V-4, the product distribution for the reaction of 27 with hydrogen is given as an example of an undeuterated reaction. The effect of changing solvents is shown in B, where both hydrogen and deuterium are added to 27' or 27 in methylene chloride and toluene. Since both the reactions and the measurements were done at room temperature, these products contain a certain amount of "scrambled" or secondary products and so are only approximations. More accurate product ratios can be found in C, where the spectra were measured at low temperatures. The effect of different reaction temperatures is shown in D.

In all experiments listed in Table V-4, more fac isomer is present than mer isomer. In methylene chloride, the

mer/fac ratio is usually in the range of .4-.6, while in toluene there is slightly more of the mer isomer. Partial deuterium substitution does not have a great effect on the mer/fac ratio, since it is in the same range for the unsubstituted case, .5. Since nearly the same value, .4, was obtained for the iridium trihydrides in solution in the absence of the tris(phosphine) complex, 27 (see Chapter II), 27 does not interfere in the equilibrium between the two trihydride species. In experiments in which deuterium gas is a reactant, a smaller amount of the mer isomer is produced (see Table V-4, column 5, section C). The effect is not large, however, and it is not possible to decide from these data whether the difference is due to a kinetic isotope effect on the initial reaction or the trihydride equilibrium, or merely unanticipated experimental error. Similarly, the addition of deuterium results in relatively less mer product in which the added molecule is trans (column 4, section C) than the analogous hydrogen addition. For reasons similar to those cited above, the significance of this observation is unclear.

The most reliable figures (Table V-4, section C) for both hydrogen and deuterium addition indicate that the ratio of the amount of mer isomer in which added ligands are cis (column 3) to that in which they are trans (column 4) is approximately 2 to 1. This ratio is that expected

from a random distribution of hydrogen isotopes over the three available positions in the mer configuration.

There is no difference in the product distributions between reactions carried out at 0°C and room temperature, measured under identical conditions, as shown in section D of Table V-4. Furthermore, the distribution of Ir(III) products does not change after 24 h at 0°C. The formation of a small amount of the tris(phosphine) product, 27, indicates an equally small (ca. 10%) decrease in the concentration of $Ir(D/H)_3$ products. No other evidence for secondary reaction products can be seen in the spectrum. It may be concluded that all three reaction products are formed under conditions where further intermolecular reactions do not occur, even at long reaction times.

6. Attempted Stereospecific Synthesis of mer-$IrH_3(CO)\ P_2$

Attempts were made to produce mer-$IrH_3(CO)\ P_2$ under conditions where the effects of intramolecular positional scrambling and intermolecular hydrogen exchange are minimized. The results are shown in Table V-5. The failure of either lithium aluminum hydride or sodium borohydride to produce the trihydride from $IrH_2Cl(CO)\ P_2$ in a variety of solvents under mild conditions eliminate this route as a useful method. Attempted in situ production of $[IrH_2(CO)\ P_2]^+ClO_4^-$ (reaction 3,

Table V-5. Attempted Stereospecific Synthesis of mer-$IrH_3CO\,P_2$.

Ir Complex	Reagent	Solvent	Conditions	Result[a]
1. $IrH_2Cl(CO)\,P_2$	$LiAlH_4$	toluene	-40°, 1 h	NR
		H_2CCl_2	ca. -5°, 4 h	NR
		CH_3CN		NR
		pyridine		NR
		THF	25°, 1 min	NR
		ethanol		NR
		THF/toluene		NR
2. $IrH_2Cl(CO)\,P_2$	$NaBH_4$	H_2CCl_2	ca. -5°, 4 h	NR
		CH_3CN		NR
		pyridine		NR
3. $IrH_2Cl(CO)\,P_2$	a. $Ag(ClO_4)$	THF	25°, 5 min	
	b. $LiAlH_4$	THF	25°, 1 min	product (i.r., 2004, 1998 cm^{-1})
4. $IrH(SO_2)(CO)\,P_2$	H_2	H_2CCl_2	25°, .5 h	NR
5. $[IrH_2(CO)\,P_3]ClO_4$	NaH	H_2CCl_2	25°, 2 min	NR
6. $[IrH_2(CO)\,P_3]ClO_4$	$LiAlH_4$	THF	-15°, 10 min	NR
			25°, 1 min	$IrH(CO)\,P_3$, ca. 75%
				$IrH_3(CO)\,P_2$, ca. 25%
	$LiAlD_4$	THF	25°, 1 min	$Ir(D/H)(CO)\,P_3$
				$Ir(D/H)_3(CO)\,P_2$

[a] NR = no reaction.

Table V-5), followed by treatment by $LiAlH_4$, resulted in an unidentified product rather than the trihydride. The report of the isolation of this cation, as mentioned in Chapter I, is likely erroneous[80]. Displacement of SO_2 by gaseous hydrogen, like the displacement of CO from $IrH(CO)_2\,\mathbb{P}_2$[80,130], is not more facile than displacement of $\mathbb{P}$ from $IrH(CO)\,\mathbb{P}_3$ at 0°C, and so is not a promising route. The reaction between $[IrH_2(CO)\,\mathbb{P}_3]^+$ and lithium aluminum hydride yielded primarily $IrH(CO)\,\mathbb{P}_3$; the small amount of the trihydride produced is probably formed by a further reaction of the tris(phosphine) product (27) and molecular hydrogen. The reaction of the cation with lithium aluminum deuteride did not produce stereospecific products.

7. Summary of Results and Conclusions

a) The addition of hydrogen to $IrH(CO)\,\mathbb{P}_3$ results in fac and mer trihydrides in the proportion 2/1. The same proportion occurs in fac/mer equilibrium in solution.

b) Deuterium labelling experiments indicate that primary products of hydrogen addition to $IrH(CO)\,\mathbb{P}_3$ have three distinct stereochemistries: a fac structure, (30, 70%), and two mer structures, with added hydrogen in the cis (28, 20%), and trans (29, 10%) positions. These results are consistent with infrared measurements.

c) Changes in the added molecules (H_2 *versus* D_2) or the solvent (methylene chloride *versus* toluene) had little effect on the distribution of products.

d) In static solutions, intermolecular H/D exchange products were formed at 25°C but not at 0°C. The appearance of these products is consistent with the loss and readdition of HD.

e) The proton chemical shift varies with temperature, solvent, and isotopic substitution pattern. The variation in each case is a function of structural position.

f) A downfield isotopic shift occurred upon substituting D for H in a position trans to the observed proton. Such a shift is opposite to the direction usually found in organic molecules, and is the first of its kind observed for diamagnetic transition metal hydrides.

g) All three stereochemical reaction products are formed at 0°C, in the same proportion as at 25°C.

h) Analysis of a deuterated reaction product in a KBr die suggests that the intrametallation of a coordinated ligand has occurred.

i) Attempts to stereospecifically synthesize an isotopomer of *mer*-$IrDH_2(CO)$ P_2 were not successful.

D. THE MECHANISM OF ISOMERIZATION IN $IrH_3(CO)P_2$

Mechanisms consistent with the kinetic measurements and labelling experiments reported above are shown in Schemes 7 and 8. The stereochemical course of the reaction is indicated in terms of the fac and mer dihydrides, 28, 29 and 30; completely analogous mechanisms could of course be drawn for the dideuterides, 28', 29' and 30'. Both of the schemes shown here are adaptations of the one suggested by the kinetic measurements, equation 37, modified to account for the mer isotopomers, 28 and 29. The difference between Schemes 7 and 8 lies only in the way 28 and 29 are formed.

In Scheme 7, product 29 is formed by the trans addition of hydrogen to the planar intermediate, 14'. Trans addition has not been previously observed for hydrogen, although such a reaction does not violate orbital symmetry rules[120] (see Figure I-1). Trans addition has been reported for the oxidative addition reactions involving other addends. Alkyl halides can add trans[122]; the mechanism has been the subject of some controversy, and it now appears that a free radical one is operative, as in Schemes 2 or 3[116]. Other examples of trans addition are mentioned in Chapter I. The addition of protonic acids to Ir(I) complexes can result in trans products, but the solvent-dependency in these cases suggest ionic intermediates, again as in Schemes 2 or 3[121]. Recently, the

Scheme 7. Three Modes of Hydrogen Addition.

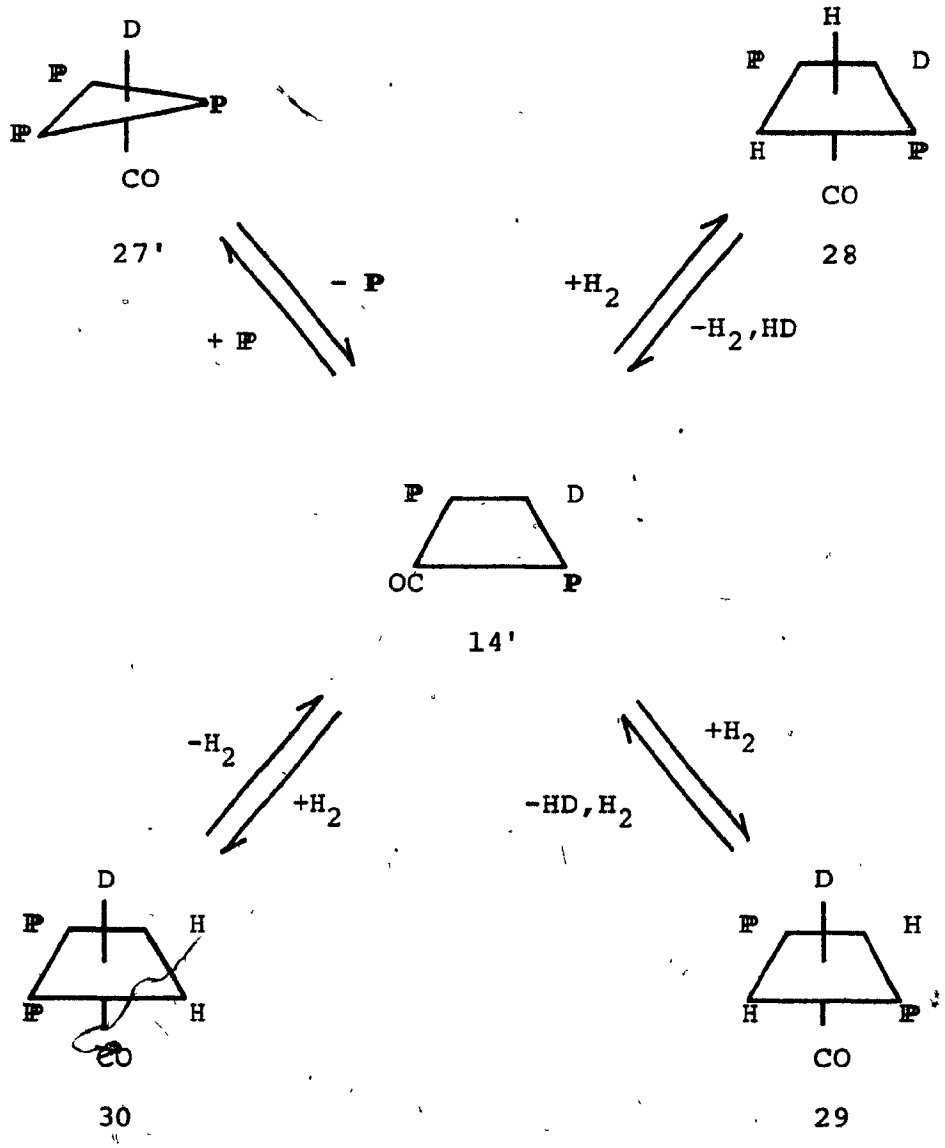

addition of protonic acids to cationic Ir(I) in a manner suggesting stepwise addition, as in Scheme 2[202], was reported. Trans addition of hydrogen in the present case would imply that a concerted addition, as in Scheme 1, can occur in a trans fashion.

Scheme 8. Two Modes of Hydrogen Addition.

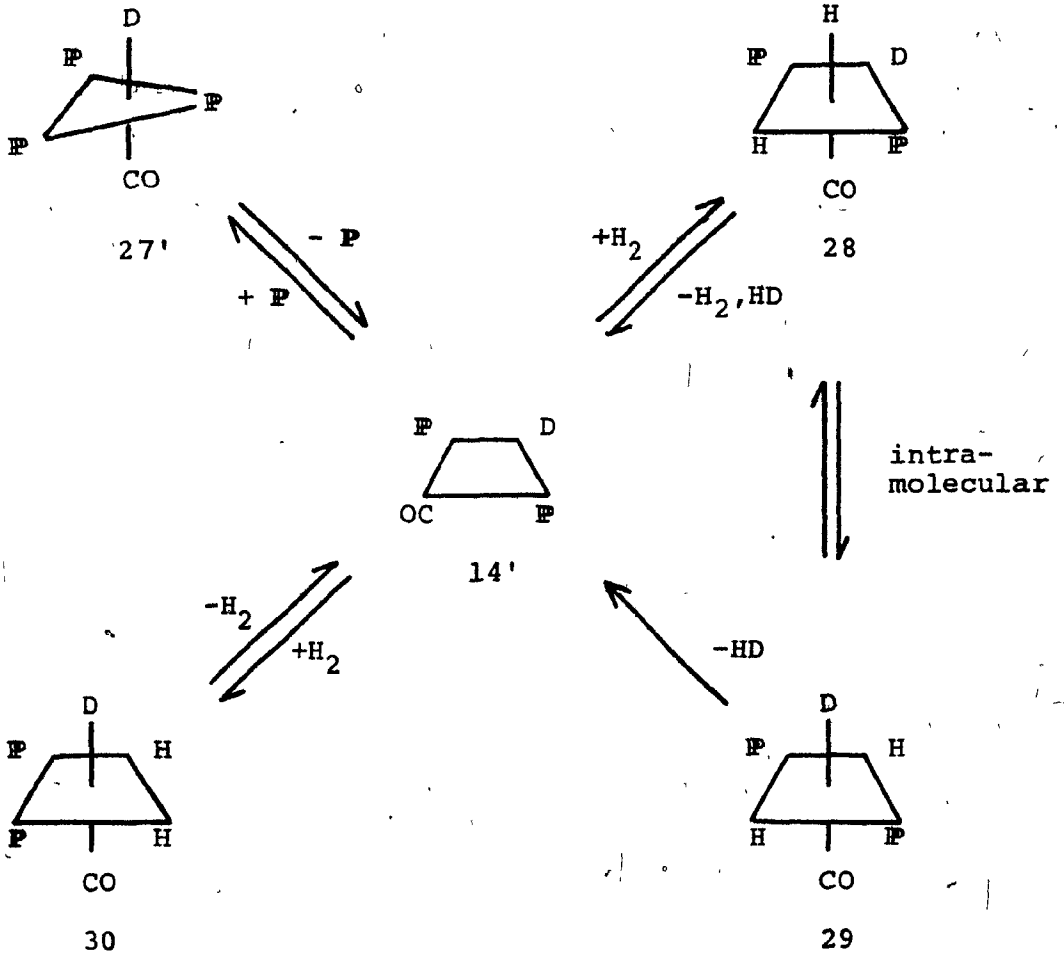

Scheme 8 shows a mechanism for isomerization which includes intramolecular positional interchange in the mer isomer. Although no line broadening attributable to fluxionality was observed in the n.m.r. spectra of the mer isomer, it is possible that such interchange occurs at a rate slow on the n.m.r. time scale, but fast enough to form both products, 28 and 29 (see below). This mechanism is strongly supported by the product distribution reported in Chapter V. The ratio of mer isomer with added hydrogen in the cis positions (28) to that with added hydrogen in the trans positions (29) is about 2:1, the same as that ratio expected when the hydrogen isotopes are randomly distributed among the three available positions.

Schemes 7 and 8 might be distinguished by the stereospecific synthesis of pure 28 or 29 by an alternate method. The absence of positional interchange after several hours in solution at 0°C would be sufficient to eliminate Scheme 8. Unfortunately, several attempts at such a synthesis, reported above, have not been successful.

It is not possible, however, to distinguish between Schemes 7 and 8 on the basis of the distribution of products among the mer isomers 28 and 29 at different reaction temperatures. Similar distributions observed may reflect either stability towards loss of H_2 or HD in Scheme 7, or the establishment of equilibrium between mer isotopomers at 0° in Scheme 8. For the latter situation to occur without line broadening in

the n.m.r. spectrum at 25°C, the rate constant of mer positional interchange, k, would be between 10^{-4} sec^{-1} and 10^{+2} sec^{-1}*. Since these limits are quite large, it is possible that rather high temperatures would be necessary to observe line broadening. High-temperature spectra would likely be further complicated by loss of hydrogen and fac/mer isomerization.

In most cases, six coordinate transition metal complexes are stereochemically rigid, probably because the regular geometry of the octahedron minimizes inter-ligand repulsion. Consequently, gross ligand movement involves a relatively high activation barrier. There are, however, examples of fluxional octahedra among chelate, low-valent carbonyl, and hydride complexes.

The tendency for chelate complexes to rearrange rapidly or isomerize[204] may be due to relatively low activation barriers in situations where the concerted movement of ligands is necessary. Chelate ring-size and ligand π-acidity may also be relevant factors in the barrier to rearrangement[182]. In the case of cis/trans isomerization in $Os(CO)_4[Si(CH_3)_3]_2$, for example, rapid migration of the trimethylsilyl group across a carbonyl carbon, via an acyl-type intermediate, was considered a possibility[183]. Other cases of intramolecular

---

*The low limit is the rate of H_2 loss from the mer isomer; the high limit was calculated from Gutowsky's formula[203] for the shortest lifetime possible for protons separated by $\Delta\nu$: $\tau^* = 1/k = \sqrt{2}/\pi\Delta\nu$.

isomerization in polycarbonyls, such as $Mo(CO)_4(PR_3)_2$, where R is an alkyl group, have been recently reported[205]. In that case, isomerization occurred very slowly (slower in fact than fac/mer isomerization in the present study), and was interpreted by a mechanism analogous to the Bailar twist through a trigonal prismatic transition state.

In metal hydride complexes, stereochemical non-rigidity has been attributed to distortions from octahedral geometry that result from the disparate sizes of the hydride and other common ligands[180,181]. Cis-MH_2L_4 complexes, where M = Fe or Ru and L = a variety of tertiary phosphine ligands, yielded temperature dependent n.m.r. spectra that were interpreted according to two mechanisms in which the phosphorus atoms moved little compared to the hydrides. The structure was regarded as a tetrahedron of phosphorus atoms around the metal with hydride ligands in the center of two faces. Fluxional processes were described by the movement of a hydride ligand across a face, the "tetrahedral jump" mechanism shown in equation 52, or through the formation of an intermediate complex, as in equation 53. The hydride ligands of the intermediate complex, 34, occupy a face and an opposite edge of the phosphorus tetrahedron, corresponding to the trans configuration in octrahedra.

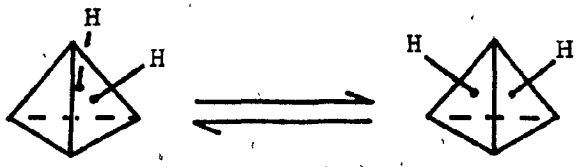

(52)

(53)

34

In the present case, an intramolecular rearrangement of mer-$IrDH_2(CO)\ P_2$ in which cis H/D ligands are transposed is consistent with experimental results. A similar "single twist" has been discussed for a bidentate complex[206], although not for monodentate complexes. Non-rigidity in the mer isomer would not be due to octahedral distortion, since one would expect, on steric grounds, greater distortion in the rigid fac isomer. Analogously, the n.m.r. spectrum of mer-$IrH_3\ P_3$ is temperature dependent and reversibly converges to a single resonance at 40°C; fac-$IrH_3\ P_3$ is rigid at room temperature[190].

Intramolecular electronic effects may be as important as steric factors in some stereochemical rearrangements.

The σ-trans effect is stronger for hydride than for any common ligand[77,207]. One expects a ligand with a high σ-trans effect to achieve a large overlap between the ligand and the p_σ orbital of the metal at the expense of the corresponding overlap in the ligand trans to it. Thus, a hydride ligand trans to hydride would be more labile than a similar M-H bond when trans to another ligand. Since the former case corresponds to mer trihydrides and the latter to fac trihydrides, intramolecular hydride exchange in mer-$IrH_3(CO)\ P_2$ and fluxional behavior in mer-$IrH_3\ P_3$, as well as the rigidity of the fac isomers of each, is consistent with the high σ-trans effect of the hydride ligand.

In view of the above discussion, the isomerization of $IrH_3(CO)\ P_2$ through two stereochemical modes of hydrogen addition, as in Scheme 8, is a more likely process than the three stereochemical modes shown in Scheme 7. Further experimental evidence is necessary, however, before either mechanism can be disproved.

The significance of elucidation of the mechanism of oxidative addition of hydrogen has been discussed in Chapter I. The demonstration of two stereochemical modes of hydrogen addition to form fac and mer $IrH_3(CO)\ P_3$ indicates that concerted oxidative addition need not be stereospecific. The possibility of trans oxidative addition of hydrogen or limited positional interchange in polyhydrides is interesting in view

of the importance of this class of compounds. Further investigation of the processes discussed in this thesis may lead to a deeper, more detailed understanding of catalytic processes.

CONTRIBUTIONS TO KNOWLEDGE

The stereochemistries of fac and mer $IrH_3(CO)\ P_2$ have been unambiguously established, and their i.r., ^1H and ^{31}P n.m.r. spectra fully analyzed and assigned. The rate of interconversion of each isomer has been measured and shown to be independent of hydrogen concentration. The rates of hydrogen substitution by triphenylphosphine have been measured for each isomer in two solvents as a function of isomer and triphenylphosphine concentration. On the basis of these measurements, a mechanism for isomerization involving molecular hydrogen is proposed. The unusual non-stereospecific hydrogen addition implicit in this mechanism is relevant to homogeneous catalysis and the general understanding of concerted oxidative addition reactions. The possibility of a trans oxidative addition of hydrogen, or a cis intramolecular hydride interchange, neither of which has been previously observed, is suggested by deuterium labelling experiments. An unusual isotope shift in the ^1H n.m.r. spectrum is noted and discussed.

SUGGESTIONS FOR FURTHER WORK

The isolation of an analogue of the proposed intermediate, $IrH(CO)\ P_2$, might be achieved through the use of tertiary phosphines large enough to inhibit further coordination. The suggestion in Chapter IV that iridium dihydride carborane complexes isomerize *via* the loss and re-addition of hydrogen could be tested by, for example, examining the behavior of 23 in a nitrogen purge.

Attempts at a stereospecific synthesis of *mer*-$IrDH_2(CO)\ P_2$ could be continued by, for example, low temperature irradiation of $IrD(CO)_2P_2$ in the presence of hydrogen, or by the *in situ* preparation of $IrDX(CO)\ P_2$, where X is easily displaced by hydrogen at low temperature. The high temperature n.m.r. spectrum of *mer*-$IrH_3(CO)\ P_2$ might be examined for line broadening by preparing a concentrated solution of the trihydride in an inert solvent under a hydrogen atmosphere in a sealed, thick-wall n.m.r. tube.

A systematic n.m.r. study of mer trihydrides might be undertaken to test the generality of fluxional behavior at elevated temperatures and, in partially deuterated samples, of downfield isotope shifts. Finally, the structure of the intrametallated species postulated in Chapter V, 32 or 33, should be established by ^1H and ^{31}P n.m.r. Solid-state intrametallation at high pressures might then be attempted on other transition metal arylphosphine hydrides that reductively eliminate hydrogen.

APPENDIX I

MATHEMATICAL DERIVATIONS

A. Derivation of Integrated Rate Expressions from the Isomerization Rate Laws

The isomerization reaction involving an unsaturated intermediate,

$$\underset{A}{\underline{mer}\text{-}IrH_3(CO)\,P_2} \underset{k_{m+}}{\overset{k_{m-}}{\rightleftharpoons}} \underset{B}{IrH(CO)\,P_2 + H_2} \underset{k_{f-}}{\overset{k_{f+}}{\rightleftharpoons}} \underset{C}{\underline{fac}\text{-}IrH_3(CO)\,P_2} \quad (37)$$

gives rise to the following rate laws, where A, B and C represent the concentration of each species.

$$-\frac{dA}{dt} = k_{m-}A - k_{m+}B[H_2] \quad (29)$$

$$\frac{dB}{dt} = k_{m-}A - k_{m+}B[H_2] - k_{f+}B[H_2] + k_{f-}C \quad (30)$$

$$\frac{dC}{dt} = k_{f+}B[H_2] - k_{f-}C \quad (31)$$

The steady-state assumption that B is small compared to A and

C implies

$$C = A_o - A \qquad \text{(A-1)}$$

where A_o is the initial concentration of the mer isomer, and

$$dB/dt = 0 \qquad \text{(A-2)}$$

By using expressions A-1 and A-2, equation 30 may be rewritten as follows.

$$B = \left[\frac{(k_{m-} - k_{f-})}{(k_{m+} + k_{f+})[H_2]}\right] A + \left[\frac{k_{f-}}{(k_{m+} + k_{f+})[H_2]}\right] A_o \qquad \text{(A-3)}$$

Substituting this expression for B into the rate law for -dA/dt (equation 29) yields

$$-\frac{dA}{dt} = k_a A - k_b A_o \qquad \text{(A-4)}$$

where

$$k_a = k_{m-} - \frac{k_{m+}(k_{m-} - k_{f-})}{(k_{m+} + k_{f+})} \qquad \text{(A-5)}$$

and

$$k_b = \frac{k_{f+}k_{f-}}{k_{m+} + k_{f+}} \qquad \text{(A-6)}$$

After cancellation, all terms for the hydrogen concentration have been eliminated from the rate expression.

Equation A-4 may be integrated to yield the expression

$$\ln(k_a A - k_b A_o) - \ln(k_a - k_b)(A_o) = -k_a t \qquad \text{(A-7)}$$

Algebraic manipulation results in the following expression for the rate law:

$$\ln\left[\frac{(k_F + k_R)A - k_R A_o}{k_F A_o}\right] = -(k_F + k_R)t \qquad \text{(A-8)}$$

where
$$k_F = \frac{(k_{m-})(k_{f+})}{(k_{m+} + k_{f+})} \qquad (32)$$

and
$$k_R = \frac{(k_{m+})(k_{f-})}{(k_{m+} + k_{f+})} \qquad (33)$$

The integrated rate expression, equation A-8, can be simplified when equations containing the equilibrium constant, K_{eq}, and the equilibrium concentrations A_{eq}, B_{eq} and C_{eq}, are introduced. Thus, from equation 37,

$$K_{eq} = \frac{C_{eq}}{A_{eq}} = \frac{C_{eq} B_{eq}}{B_{eq} A_{eq}} = \frac{(k_{m-})(k_{f+})}{(k_{f-})(k_{m+})} \qquad \text{(A-9)}$$

Substituting the constants from equations 32 and 33, one obtains the expression

$$K_{eq} = \frac{C_{eq}}{A_{eq}} = \frac{k_F}{k_R} . \qquad \text{(A-10)}$$

Since B is small,

$$A_o - A_{eq} = C_{eq}, \text{ if } C_o = 0. \qquad \text{(A-11)}$$

Equations A-10 and A-11, when substituted into equation A-8, result in the simplified expressions given below.

$$\ln \left[\frac{A_o - A_{eq}}{A - A_{eq}} \right] = (k_F + k_R)t \qquad (26)$$

and

$$\frac{A_o - A_{eq}}{A_o} \ln \left[\frac{A_o - A_{eq}}{A - A_{eq}} \right] = k_F t \qquad (27)$$

In the case where $A_o = 0$ (that is, if the starting material is pure fac isomer), an analogous derivation may be carried out from equation 31 by integrating with respect to C. The resulting equation, exactly analogous to equation 26, may be simplified to give the following equation.

$$\ln\left[\frac{A_{eq}}{A_{eq}-A}\right] = (k_F + k_R)t \qquad (28)$$

Expressions 26, 27 and 28 can be used to determine values for k_F and k_R from an experimental determination of A versus t. These expressions are identical to those obtained from a simple two-component equilibrium that is first-order in both directions. The significance of the above derivation, besides demonstrating this equivalence, is that it shows that k_F, k_R, and K_{eq} are all independent of hydrogen concentration under this model. Furthermore, the relationships between k_F and k_R and the individual rate constants (k_{m+}, k_{m-}, k_{f+} and k_{f-}) have been determined in equations 32 and 33.

B. Derivation of "Corrected" Rate Expression

In the presence of excess ligand, the primary reaction to form IrH(CO) $\mathbf{P}_3$ is a first-order decay of $IrH_3(CO)$ $\mathbf{P}_2$ (see equation 42, Chapter IV). Since the decomposition of the product is also first-order, the following consecutive reaction can be written.

$$D \xrightarrow{k_D} E \xrightarrow{k'} F \qquad (A\text{-}12)$$

In this expression, F is the concentration of decomposition

products, and the other quantities are as defined in Chapter IV. A standard first-order treatment of consecutive reactions[178] results in the expression

$$E = D_o \frac{k_D}{k'-k_D} (e^{-k_D t} - e^{-k' t}) \qquad \text{(A-13)}$$

One may define the following constant, E'_{eq}.

$$E'_{eq} = - \frac{D_o k_D}{k'-k_D} \qquad \text{(A-14)}$$

Substitution into equation A-13 yields the following expression.

$$E'_{eq} = - \frac{E}{e^{-k_D t} - e^{-k' t}} \qquad \text{(A-15)}$$

Because $k_D >> k'$, the constant E'_{eq} may be evaluated from measured values. At very long reaction times, where $t = t_L$ and $E = E_L$, the quantity $\exp(-k_D t)$ is negligible compared to $\exp(-k't)$. Therefore,

$$E'_{eq} = \frac{E_L}{e^{-k' t_L}} \qquad \text{(A-16)}$$

Rearrangement of equation A-15 yields the following expression, given in Chapter IV.

$$-\ln \left[e^{-k't} - \frac{E}{E'_{eq}} \right] = k_D t \qquad (44)$$

C. Derivation of a Rate Law for the Decomposition of IrH(CO) $\mathbf{P}_3$

Decomposition of IrH(CO) $\mathbf{P}_3$ proceeding through the intermediate IrH(CO) $\mathbf{P}_2$ may be represented by the following reaction, where k" is the rate constant of decomposition.

$$\underset{B}{IrH(CO)\ \mathbf{P}_2} \xrightarrow{k''} \underset{F}{(Ir)} \qquad (A\text{-}17)$$

From this equation and equation 41 in Chapter IV, the following rate laws are obtained.

$$-\frac{dE}{dt} = k_{-P}E - k_{+P}B[\mathbf{P}] \qquad (A\text{-}18)$$

$$\frac{dB}{dt} = -k_{+P}B[\mathbf{P}] - k''B + k_{-P}D \qquad (A\text{-}19)$$

If one makes the steady-state assumption that dB/dt = 0, then one may obtain an expression for B from equation A-19.

Substitution for B in equation A-18 and rearrangement results in the following equation,

$$-\frac{dE}{dt} = k'E, \qquad \text{(A-20)}$$

where

$$k' = \frac{k''k_{-p}}{k_{+p}[P] + k''} . \qquad \text{(A-21)}$$

The quantity k', the apparent rate constant of decomposition, will only be constant when [P] is in large excess. Since $k_{-p} >> k'$, equation A-21 may be rewritten as the following.

$$k' = \frac{k''k_{-p}}{k_{+p}[P]} \qquad (46)$$

The apparent rate constant, k', is, by equation 46, inversely proportional to the ligand concentration. Integration of equation A-20 yields

$$-\ln E = k't - \ln E_o . \qquad \text{(A-22)}$$

Consequently, a linear plot of - ln E <u>versus</u> t with a slope inversely proportional to ligand concentration provides strong support for this mechanism.

APPENDIX II

N.M.R. SPECTRA

A. ^1H N.m.r. Spectral Data in the High-Field Region.

1. Mer-$IrH_3(CO)P_2$ in CD_2Cl_2 at 25°C (see Figure II-2).

Peak Number	Chemical Shift (τ) (ppm ± .01ppm) Peak Shift	Center	Coupling Constants (Hz ± .05Hz) J_{H-H}	$J_{H-P_{cis}}$	Assignments
1	19.85		] 4.9	]16.6	
2	19.91				
3	20.04		] 4.4		
4	20.09	20.06			7a
5	20.23		] 4.4	]16.6	
6	20.28				
6	(20.28)*		] 4.4		
7	20.32		] 4.9	] 19.5	
8	20.38				
9	20.49		] 4.4		
10	20.54	20.54	] 4.9		7b
11	20.60			] 19.5	
12	20.70		] 4.9		
13	20.76		] 4.4		
14	20.81				

*In this and subsequent tables, peak shifts in parentheses indicate overlap by neighboring peaks.

2. Fac-$IrH_3(CO)P_2$ in CD_2Cl_2 at 25°C (see Figure II-3).

Peak Number	Chemical Shift (τ) (ppm ± .01ppm) Peak Shift	Center	Coupling Constants (Hz ± .05Hz) J_{H-H}	$J_{H-P_{cis}}$	Assignments
1	19.97		2.4		
2	20.00		2.4		
3	20.03			18.1	
4	20.17		2.4		
5	20.20	20.20	2.4		3d
6	20.23			19.1	
7	20.37		2.4		
8	20.40		2.4		
9	20.43				
10	ca. 20.6†				
11	20.83		2.4	105.1*	
12	20.86	21.42			3c
13	22.00		2.4		
14	22.02				
15	ca. 22.2†				

*Apparent trans coupling.

†Unresolved multiplets.

3. $IrH(CO)P_3/H_2$ in CD_2Cl_2 at 25°C (see Figure V-3a).

Chemical Shift (τ) (ppm ± .01ppm)			Coupling Constants (Hz ± .05Hz)		
Peak Number	Peak Shift	Center	J_{H-H}	$J_{H-P_{cis}}$	Assignments
1	19.85		] 4.8	] 16.6	
2	19.90				
6	20.03	20.06	] 4.8		7a
7	20.09			] 16.6	
10	(20.22)		]		
11	20.27				
3	19.97		] 2.4		
4	19.99		] 2.6	] 18.1	
5	20.02				
8	20.17		] 2.4		3d
9	20.20	20.20	] 2.1		
10	20.22			] 18.6	
13	(20.36)		]		
14	20.40		] 2.4		
15	20.43				
11	(20.27)		]	] 19.3	
12	20.33				7b
13	(20.36)				
16	20.49		] 4.4		
17	20.54	20.54		] 19.7	
18	(20.61)				
19	20.71		] 4.5		
20	20.76				
21	(20.81)				
13	20.36			] 21.9	
18	20.61			] 21.5	
22	20.85	20.73		] 21.0	27e
24	21.08				
18	(20.61)				
21	20.82		] 2.6	] 104.9*	
23	20.85	21.42		] 104.8*	3c
25	21.99		] 2.5		
26	22.02				
27	22.20				

*Apparent trans coupling.

4. IrD(CO) P_3/H_2 in CD_2Cl_2 at -20°C (see Figure V-3b).

Peak Number	Peak Shift (ppm ± .01ppm)	Center	J_{H-H} (Hz ± .25Hz)	$J_{H-P_{cis}}$ (Hz ± .25Hz)	Assignments
1	19.84		]4.8	]16.7	
2	19.89				
4	20.03	20.05	]4.6		28a
5	20.08			]16.5	
7	20.21		]4.6		
8	20.26				
3	19.99			]16.5	
6	20.17	20.17		]16.7	29a
10	20.35				
9	20.31		]4.3	]19.2	
10	(20.35)				
12	20.52	20.54	]4.5		28b
13	20.57			]19.3	
17	20.73		]4.3		
18	20.79				
14	20.65*			] 18.5	
19	20.85	21.43		]104.2†	30c
23	22.01			] 18.9	
24	22.22*				
11	20.48			]21.9	
16	20.72	20.84		]21.1	27e
20	20.96			]21.5	
22	21.20				

*Multiplet center.

†Apparent trans coupling.

5. $IrH(CO)P_3/D_2$ in CD_2Cl_2 at -20°C (see Figure V-3c).

Chemical Shift (ppm ± .01ppm)			Coupling Constants (Hz ± .25Hz)	Assignments
Peak Number	Peak Shift	Center	$J_{H-P_{cis}}$	
1	19.88			
3	20.06	20.06	16.6, 16.6	28'a
5	20.25			
2	20.03			
4	20.23	20.23	18.1, 18.1	30'd
7	20.43			
6	20.33			
9	20.54	20.54	19.3, 19.1	29'b
11	20.75			
8	20.47			
10	20.70	20.82	21.4, 21.4, 21.4	27e
12	20.94			
13	21.18			

B. ^{31}P N.m.r. Spectra of fac and mer $IrH_3(CO)P_2$ in CD_2Cl_2 at 25°C (see Figure II-5).

Peak Number	Chemical Shift (ppm ± .02ppm) Peak Shift	Center	Coupling Constants* (Hz ± 1Hz) $J_{H-P_{cis}}$	Assignments
1	15.95		11	
2	15.65	15.48	12	7
3	15.31		10	
4	15.04			
6	8.18			
7	7.81			
8	7.64			
9	7.47			
10	7.34	6.55		3
11	5.76			
12	5.60			
13	5.46			
14	5.26			
15	4.93			

*Partially decoupled values.

C. Calculated Spectra

Calculated Values[a]			Measured Values		
peak #[b]	frequency[c]	intensity	peak #[d]	frequency	intensity
1. fac-$IrH_3(CO)P_2$: ^1H spectrum					
1,2	52.5	2.0	23	52.1	2.0
5	77.4	.45			
6	66.4	.54	24[e]	64-72	.31
9	69.1	.51			
10	72.1	.49			
2. fac-$IrH_3(CO)P_2$: $^{31}P\{$phenyl protons$\}$spectrum					
	28.7	1.00	11	28.7	.99
	35.0	.56	12	34.8	.66
	40.6	1.00	13	39.7	1.00
	47.0	.89	14	47.0	.86
	59.2	.56	15	59.2	.43
3. mer-$IrH_3(CO)P_2$: $^{31}P\{$phenyl protons$\}$spectrum					
	-17.45	.50	1	-16.45	.49
	- 6.45	1.00	2	- 5.55	1.00
	- 4.45	.50	3[e]		
	4.45	.50	4[e]		
	6.45	1.00	5	6.65	1.00
	17.45	.50	6	16.45	.46

[a] The spectra were calculated using the program given in Appendix III and the parameters in Table II-2. In 1, J_{HH} = 5.0 and J_{PP} = 8.0 Hz.

[b] cf. Appendix III.

[c] Relative to resonance center. In 1 and 2, the multiplets are symmetrical; only the right portion of the multiplets is tabulated.

[d] cf. Figures V-3b (1) and II-5 (2,3).

[e] Unresolved shoulders.

APPENDIX III

COMPUTER PROGRAMS

A. KINCOR

The following program was used to analyze the kinetic data reported in Chapter IV. Two examples of the output of the program are shown in Appendix V. Kinetic data of all experiments processed by this program are tabulated in Appendix VII.

```
C
C     KINCOR
C
C          PROGRAM TO PROCESS KINETIC DATA
C     MEASURING THE ABSORBANCE OF REACTION PRODUCT
C     CONTAINING CORRECTIONS FOR TIME-MEASUREMENTS FROM CHART DISTANCE
C     AND FOR TIME MEASURED BY THE CLOCK
C     A LEAST-SQUARES SUBPROGRAM IS USED
C     THE PROGRAM WILL CORRECT FOR SOLVENT INDUCED DECOMPOSITION
C     AT LONG TIMES
C     ALL REACTIONS ARE ASSUMED TO BE FIRST ORDER
C     INITIAL RATES ARE CALCULATED BY FITTING THE DATA TO A POLYNOMIAL
C     (USING CURVFT), AND FINDING THE DERIVATIVE AT ZERO
C
C     INPUT DATA IS READ INTO MATRIX A
C     MATRIX A
C     COL   INFORMATION          FIELD  INPT CD OUTPUT SPACE
C     1     DATA PT NUM          F4.0   2-10    SAME   1
C     2     TIME(CM)             F6.2   11-21          1
C     3     TIME(HR-OCLK)        F4.0   22-30          1
C     4     TIME(MIN-OCLK)       F4.0   31-39          1
C     5     TIME (MIN)           F6.1   40-50          1
C     6     ABSORBANCE(RAW)      F6.3   51-61          1
C     7     ABSORBANCE (COR)
C     8     ORD FOR UNCOR RATE
C     9     ORD FOR DECOMP RATE
C     10    ORD FOR COR RATE
C
C     ORDER FOR INPUT CARDS
C     NUMBER OF RUNS IN PROGRAM
C     RUN IDENTIFICATION CARD
C     DATA CARDS FOR MATRIX A
C
C
0001          DIMENSION A(50,10),B(50,2),C(9),D(50),E(50),F(50),G(11),G(1),R(1)
0002          READ (5,101)NR
0003     101  FORMAT (I2)
0004          DO 16        II=1,NR
C
C     READ IN THE RUN IDENTIFICATION NUMBER, NUMBER OF POINTS IN THE
C     RUN, WHETHER CORRECTED (NC=1) OR UNCORRECTED (NC=2) FOR LONG
C     TERM DECOMPOSITION,THE HOUR (TZH) AND MINUTS (TZM) AT TIME ZERO,
C     AND THE BASELINE VALUE
C     IF NC = 3, THE INITIAL RXN RATE IS CALCULATED AFTER CORRECTING
C     FOR TIME AND ABSORBANCE VALUES; LOGS ARE NOT CALCULATED
C     IF NC = 4, ONLY THE INITIAL REACTION RATE IS CALCULATED; ABSORBANCE
C     VALUES ALONE ARE CORRECTED.
C     IF IRR = 1, THE INITIAL RATE IS OBTAINED AT CONCENTRATION OF ZERO.
C     IN THIS CASE, ABSORBANCE MUST BE SINGLE-VALUED OVER THE RANGE USED.
C     NS2 IS THE DATA PT NUMBER WHICH BEGINS THE 0-2 ABSORBANCE SCALE.
C
0005          READ (5,102)NIR,NP,NC,TZH,TZM,BL,IRR,NS2
0006     102  FORMAT (3(I2,2X),2(F4.0),F6.3,I2,I3)
0007          WRITE (6,103)NIR
0008     103  FORMAT (1H1,11HRUN NUMBER , I2)
0009          WRITE (6,104)NP
0010     104  FORMAT (1H , 10HTHERE ARE ,I2, 24H DATA POINTS IN THIS RUN)
0011          WRITE (6,105)TZH,TZM
0012     105  FORMAT(1H ,13HTIME ZERO IS ,F3.0,1H:,F3.0,8H O'CLOCK )
0013          WRITE (6,106)BL
0014     106  FORMAT (1H ,23HBASELINE ABSORBANCE IS , F6.3)
0015          IF (NC.EQ.1)WRITE(6,107)
0016     107  FORMAT (1HO,'  THIS PROGRAM IS CORRECTED FOR DECOMPOSITION AT LONG
            C REACTION TIMES BY AN ITERATIVE METHOD ')
```

```
0017            IF (NC.EQ.2)WRITE (6,108)
0018       108  FORMAT (1H0, 47HTHIS PROGRAM IS NOT CORRECTED FOR DECOMPOSITION)
0019            IF (NS2.NE.0) WRITE(6,121)NS2
0020       121  FORMAT (' SCALE 0-2 BEGINS AT POINT NUMBER ',I3)
                C
                C     READ DATA INTO MATRIX A
0021            DO 15       I2=1,NP
0022       15   READ(5,109)(A(I2,J),J=1,10)
0023       109  FORMAT (F4.0,1X,F6.2,1X,2(F4.0,1X),F6.1,1X,5(F6.3,1X))
0024            KK=NP
                C
                C     TO CORRECT FOR TIME AND ABSORBANCE
0025            IF (NS2.EQ.0) NS2=99
0026            S=1.
0027            DO 1        I3=1,NP
0028            IF (A(I3,1).GE.NS2)S=2.
0029            IF (NC.EQ.4)GO TO 1
0030            IF (A(I3,2).EQ.0.) GO TO 6
0031            A(I3,5)=2.*A(I3,2)
0032            GO TO 1
0033       6    TJ=A(I3,3)-TZM
0034            IF (TJ) 2,3,3
0035       2    TJ=TJ+12.
0036       3    TJ=TJ*60.
0037            A(I3,5)=TJ+A(I3,4)-TZM
0038            IF (A(I3,5).LT.0.) GO TO 2
0039       1    A(I3,7)=A(I3,6)*S-BL
0040            IF (NC.EQ.4)GO TO 22
                C
                C     TO FIND THE MAXIMUM ABSORBANCE VALUE
0041            IF(NC.EQ.3)GO TO 22
0042            IF (NC.EQ.2) GO TO 17
0043            AMAX=0.
0044            DO 5        I4=1,NP
0045            ADIFF=AMAX-A(I4,7)
0046            IF (ADIFF) 14,14,5
0047       14   AMAX=A(I4,7)
0048       5    CONTINUE
0049            GO TO 18
0050       17   AMAX=A(NP,7)
0051       18   WRITE(6,118)AMAX
0052       118  FORMAT (1H0,'THE MAXIMUM ABSORBANCE IS ',F6.3)
                C
                C      TO COMPUTE LOG (AMAX-A) FOR UNCORRECTED RATE
                C    KK IS THE VALUE FOR WHICH T IS LESS THAN 125 MINUITS
0053            KK=0
0054            DO 7        I5=1,NP
0055            IF (A(I5,5).GT.125.) GO TO 8
0056            AARG=AMAX-A(I5,7)
0057            IF (AARG.LE.0.)GO TO 8
0058            A (I5,8)=-ALOG(AARG)
0059       7    KK=KK+1
0060       8    CONTINUE
                C
                C     READ IN DATA TO B MATRIX TO CALCULATE LEAST SQUARES LINE
                C     RESULTS ARE IN C MATRIX
0061            DO 19       I6=1,KK
0062            B(I6,1)=A(I6,5)
0063       19   B(I6,2)=A(I6,8)
0064            NDP=KK
0065            CALL STRLN (B,C,NDP)
0066            WRITE(6,110)A(1,5),A(1,8),A(KK,5),A(KK,8),C(1),C(2),C(3),NDP
0067       110  FORMAT(1H0,38HLEAST SQUARES ANALYSIS OF POINTS FROM ,F6.1,
               C5H AND ,F10.6,10H TO POINTS,F6.1,5H AND , F10.6  /5X,9HSLOPE IS ,
               CF10.6,10X,27HCORRELATION COEFFICIENT IS ,F10.6,10X,
               C15HY-INTERCEPT IS , F10.6/5X,24HNUMBER OF DATA POINTS   ,I3)
0068            WRITE(6,400)
0069       400  FORMAT (9H ST DEV X,12X,8HST DEV Y,12X,10HST ERROR Y,10X,10HST DEV
               C SLP, 10X)
0070            WRITE (6,401)(C(ILL),ILL=4,7)
0071       401  FORMAT(1H ,6(F12.6,8X))
0072            WRITE (6,119)
0073       119  FORMAT(1H0,'THE FOLLOWING IS A PLOT OF THESE POINTS')
0074            DO 200      I20=1,NDP
0075            D(I20)=B(I20,1)
0076       200  E(I20)=B(I20,2)
0077            CALL PLOT1 (D,E,NDP,101)
0078            KPL=0
0079            IF (NC.EQ.1) GO TO 20
0080            WRITE (6,111)
0081       111  FORMAT (1H0,62HTHIS RATE IS UNCORRECTED FOR LONG TERM DECOMPOSITIO
               CN///)
0082            GO TO 22
0083       20   WRITE (6,112)
0084       112  FORMAT (1H0,'THIS RATE IS ONLY AN ESTIMATE AND MUST BE CORRECTED
               CFOR LONG TERM DECOMPOSITION'////////////)
                C
                C     TO FIND THE DATA POINT (KKK) WHERE THE RXN IS .01 FROM COMPLETION
0085            IF (KPL.GT.5)GO TO 21
0086            DO 9        I7=KK,NP
0087            DEV=EXP (-C(1)*A(I7,5))
0088            KKK=I7
0089            IF (DEV.LT.0.01) GO TO 10
0090       9    CONTINUE
0091       10   IF (KKK.EQ.NP) GO TO 21
                C
                C     TO COMPUTE THE DECOMPOSITION RATE, WHERE K4 IS THE NUMBER OF
                C     POINTS USED.
0092            K4=0
0093            DO 11       I8=KKK,NP
0094            A(I8,9)=-ALOG(A(I8,7))
0095            K4=K4+1
0096            B(K4,1)=A(I8,5)
0097       11   B(K4,2)=A(I8,9)
0098            NDP=K4
0099            WRITE (6,113)
0100       113  FORMAT (1H0,'THIS RATE IS THE LONG- TERM SOLVENT-INDUCED DECOMPOSI
               CTION RATE')
0101            CALL STRLN (B,C,NDP)
0102            WRITE (6,110)A(KKK,5),A(KKK,9),A(NP,5),A(NP,9),C(1),C(2),C(3),NDP
0103            IF (KPL.GT.0) GO TO 25
0104            WRITE (6,119)
0105            DO 201      I20=1,NDP
0106            D(I20)=B(I20,1)
0107       201  E(I20)=B(I20,2)
0108            CALL PLOT1 (D,E,NDP,101)
```

```
C     COMPUTATION OF CORRECTED RATE
30    KTST=KK+1
      IF (A(KTST,5).GT.125) GO TO 25
      KK=KTST
      IF (KTST.GT.50) STOP
      GO TO 30
25    AOPR=A(NP,7)/(EXP(-C(1)*A(NP,5)))
      DO 12          I9=1,KK
      AAPPR=           (EXP(-C(1)*A(I9,5))-A(I9,7)/AOPR)
      KN=I9
      IF (AAPPR.GT.0.) GO TO 31
      KN=KN-1
      A(I9,10)=0.
      GO TO 32
31    A(I9,10)=-ALOG(AAPPR)
      B(I9,1)=A(I9,5)
12    B(I9,2)=A(I9,10)
32    KK=KN
      NDP=KK
      KPL=KPL+1
      WRITE (6,122) AOPR
122   FORMAT(////' THE CORRECTED ABSORBANCE MAXIMUM, AOPR, IS',F7.3)
      WRITE (6,115)
115   FORMAT(1HO,'THIS RATE IS CORRECTED FOR LONG TERM DECOMPOSITION')
      CALL STRLN (B,C,NDP)
      WRITE (6,110)A(1,5),A(1,10),A(KK,5),A(KK,10),C(1),C(2),C(3),NDP
      DEV=EXP(-C(1)*A(KKK,5))
      IF (DEV.GT.0.01)GO TO 20
      WRITE (6,119)
      DO 202      I20=1,NDP
      D(I20)=B(I20,1)
202   E(I20)=B(I20,2)
      CALL PLOT1 (D,E,NDP,101)
      WRITE (6,120)
120   FORMAT (1H ,'THIS IS THE FINAL CORRECTED RATE')
      WRITE(6,400)
      WRITE (6,401)(C(ILL),ILL=4,9)
      GO TO 22
21    WRITE (6,114)
114   FORMAT (1HO,' ERROR: THE INITIAL RXN IS MORE THAN .01 FROM COMPLET
     CION')
C
C     PRINT TABLE OF DATA (ARRAY A)
22    WRITE(6,116)
116   FORMAT(1H1,6HPT.NO.,3X,10HTIME UNCOR, 19X,8HCOR.TIME,4X,10HABSORBA
     CNCE,11X,9HORDINATES/10X,2HCM,9X,2HHR,7X,3HMIN,6X,3HMIN,8X,3HRAW,
     C8X,3HCOR,8X,5HUNCOR,10X,6HDECOMP,9X,3HCOR/)
      DO 23       I10=1,NP
23    WRITE(6,117) (A(I10,J1),J1=1,10)
117   FORMAT(1H ,F4.0,5X,F6.2,5X,2(F4.0,5X),F6.1,5X,2(F6.3,5X),3(F10.6,
     C5X))
C
C  INTIAL RATE CALCULATION
      WRITE (6,300)
300   FORMAT (1H-,' CALCULATION OF INITIAL RATE'/'  THE FOLLOWING IS A P
     CLOT OF ABSORBANCE VERSUS TIME')
      DO 301      I21=1,KK
      D(I21)=A(I21,5)
301   E(I21)=A(I21,7)
      CALL PLOT1 (D,E,KK ,101)
      DATA F/40*1./
      M=10
      IF (KK.LT.12)M=KK-2
      CALL CURVFT (D,E,F,KK,1,M ,G,11,0.0,0,R)
      WRITE (6,303) G(2),G(1)
303   FORMAT (1HO,' THE SLOPE AT ZERO IS ',F10.5/'  THE Y-INTERCEPT IS',
     CF10.5)
      IF (IRF.NE.1) GO TO 16
      CALL CURVFT (E,D,F,KK,1,M ,G,11,0.0,0,R)
      RTIN=1./G(2)
      WRITE (6,304)RTIN
304   FORMAT (//' AT ZERO CONCENTRATION, THE INITIAL RATE IS ',F10.6)
      WRITE(6,303)G(2),G(1)
C
16    CONTINUE
      STOP
      END

      SUBROUTINE STRLN (B, C, NDP)
C
C  STPLN
C
C  THIS SUBPROGRAM WILL USE VALUES IN A TWO DIMENSIONAL MATRIX
C  AND CALCULATE THE SLOPE, Y-INTERCEPT, AND CORRELATION COEFFICIENT
C  BY THE LEAST SQUARES METHOD
C  INPUT IS MATRIX B, CONTAINING THE DATA POINTS
C  OUTPUT IS MATRIX C, WHERE C(1) IS THE SLOPE, C(2) IS THE CORRELATION
C  COEFFICIENT, AND C(3) IS THE Y-INTERCEPT
C  NDP IS THE NUMBER OF DATA POINTS, WHICH IS RECEIVED AS INPUT
C
      DIMENSION B(50,2), C(9)
      SX=0.
      SY=0.
      SXY=0.
      SX2=0.
      SY2=0.
      DO 50            I=1,NDP
      SX=B(I,1)+ SX
      SY=B(I,2) +SY
      SXY=B(I,1)*B(I,2)+SXY
      SX2=B(I,1)**2.+SX2
50    SY2=B(I,2)*B(I,2)+SY2
      PTN=NDP
      XAV=SX/PTN
      YAV=SY/PTN
      SIGX=SQRT(SX2/PTN-XAV**2.)
      SIGY=SQRT(SY2/PTN-YAV**2.)
      IF (SIGX.EQ.0.)STOP
      IF (SIGY.EQ.0.)STOP
      C(2)=(SXY/PTN-XAV*YAV)/(SIGX*SIGY)
      C(1)=C(2)*SIGY/SIGX
      C(3)=YAV-C(1)*XAV
      C(4)=SIGX
      C(5)=SIGY
      C(6)=SIGY*SQRT(1.-C(2)**2.)
      C(7)=C(6)/(C(4)*SQRT(PTN-2.))
      RETURN
      END
```

PROGRAM TITLE/PURPOSE AA'XX' Spectrum
PROGRAMMER W. J. Yorke
DATE Nov. 6, 1978

TI PROGRAMMABLE 57
PROGRAM RECORD

PROGRAM DESCRIPTION

The program computes the line frequencies and relative intensities of the A portion of an AA'XX' spectrum. The terminology is the same as in Becker, NMR Spectros pp. 167. The line positions are in Hz relative to the chemical shift of A. The intensities of lines 5 to 12 are calculated as 1/2 the incorrect value given by Becker. Lines 1 and 2 coincide, as do lines 3 & 4. Each pair has intensity 2. Together, they make up one-half the spectral intensity.
Memory 4 must be restored after each run.

HOW TO USE IT:

STEP	PRESS	DISPLAY/COMMENTS
	STORE in memory 1.	J_{AX}
	2.	$J_{AX'}$
	3.	$J_{AA'}$
	4	$J_{XX'}$
	7	−1
1	R/S	freq. of l.1, l.2 (= −l.3, l.4)
2	R/S	freq of l.5 (= −l.8)
3	R/S	intensity of l.5 (= int. of l.8)
4	R/S	intensity of l.6 (= int of l.7)
5	R/S	freq. of l.6 (= −l.7)
6	R/S	freq. of l.9 (= −l.12)
7	R/S	intensity of l.9 (= int. of l.12)
8	R/S	intensity of l.10 (= int. of l.11)
9	R/S	freq. of l.10 (= −l.11)

1014831 1
© 1977 TEXAS INSTRUMENTS INCORPORATED
TEXAS INSTRUMENTS

FLOW CHART/NOTES

"A" part of AA'XX':
a large doublet and two smaller quartets

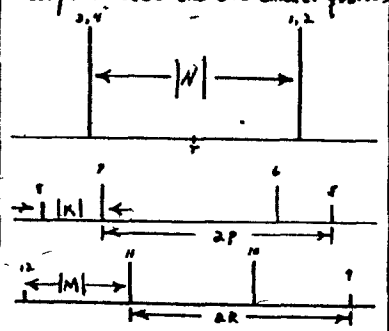

$K = J_{AA'} + J_{XX'}$
$L = J_{AX} - J_{AX'}$
$M = J_{AA'} - J_{XX'}$
$N = J_{AX} + J_{AX'}$
$2P = (K^2 + L^2)^{1/2}$
$2R = (M^2 + L^2)^{1/2}$

	MEMORIES		LABELS
0	■ L^2	n	0 LBL 0 (STEP 10)
1	J_{AX}	Σy	1 SBR 1
2	$J_{AX'}$	Σy'	2
3	$J_{AA'}$	Σx	3
4	$J_{XX'}$	Σx'	4
5	(AOS) K, M	Σxy	5
6	(AOS) 2P, 2R		6
7	(I) −1		7
			8
			9

TEXAS INSTRUMENTS

KEY	LOC	CODE	COMMENTS
RCL 1	00	33 1	
+	01	75	1/2 N
RCL 2	02	33 2	
SBR 1	03	61 1	
RCL 1	04	33 1	
−	05	65	
RCL 2	06	33 2	
=	07	85	L^2
x^2	08	23	
STO 0	09	32 0	
LBL 0	10	86 0	
RCL 3	11	33 3	
+	12	75	
RCL 4	13	33 4	K
=	14	85	
STO 5	15	32 5	
x^2	16	23	
+	17	75	
RCL 0	18	33 0	
=	19	85	2P
$\sqrt{x}$	20	24	
STO 6	21	32 6	
+	22	75	
RCL 5	23	33 5	LINE 5
SBR 1	24	61 1	
1	25	01	
−	26	65	
RCL 5	27	33 5	INT. 5
−	28	45	
RCL 6	29	33 6	
SBR 1	30	61 1	
−	31	65	
1	32	01	
=	33	85	INT. 6
|x|	34	40	
R/S	35	81	
RCL 6	36	33 6	
−	37	65	
RCL 5	38	33 5	LINE 6
SBR 1	39	61 1	
RCL 2	40	33 7	
PRD 7	41	39 7	K → M
GTO 0	42	61 0	
LBL 1	43	86 1	
=	44	85	
÷	45	45	SBR 1
2	46	02	
=	47	85	
R/S	48	81	
−SBR	49	−61	

APPENDIX IV

APPARATUS FOR THE MEASUREMENT OF REACTION KINETICS UNDER A CONSTANT PROPORTION OF GASES

The apparatus shown in Figure A-IV was used to prepare, maintain and sample solutions under an atmosphere of constant composition. The whole system could be evacuated and filled with the gas mixture in the proper proportions before dissolution of the solid complex. Sample solutions were forced out by means of the mercury pump. After equilibration to atmospheric pressure, the reaction flask K could be isolated from the system to eliminate evaporation. The detailed procedure is given below.

1. Weigh out the sample into the reaction flask K, and attach to the system.
2. Fill the solvent flask O, include a stirring bar, and degas the solvent.
3. Evacuate the entire system, keeping A, D, E and H closed.
4. With J and C closed, fill the system with the gases through E to atmospheric pressure. Open C and H, and let the solvent stirr for several minutes.
5. Transfer the proper amount of solvent by a syringe from solvent flask O to the reaction flask K, and start the timer.
6. To measure each sample, push the stainless-steel tubing through A into the solution and raise the height of the mercury reservoir M. Open B and fill the i.r. cell; then pull the tubing out of the solution, stopper the cell, close B, withdraw the tube and close A.
7. Step 6 must be repeated for each sample. The gas reservoir L may be refilled when necessary as in steps 3 and 4.

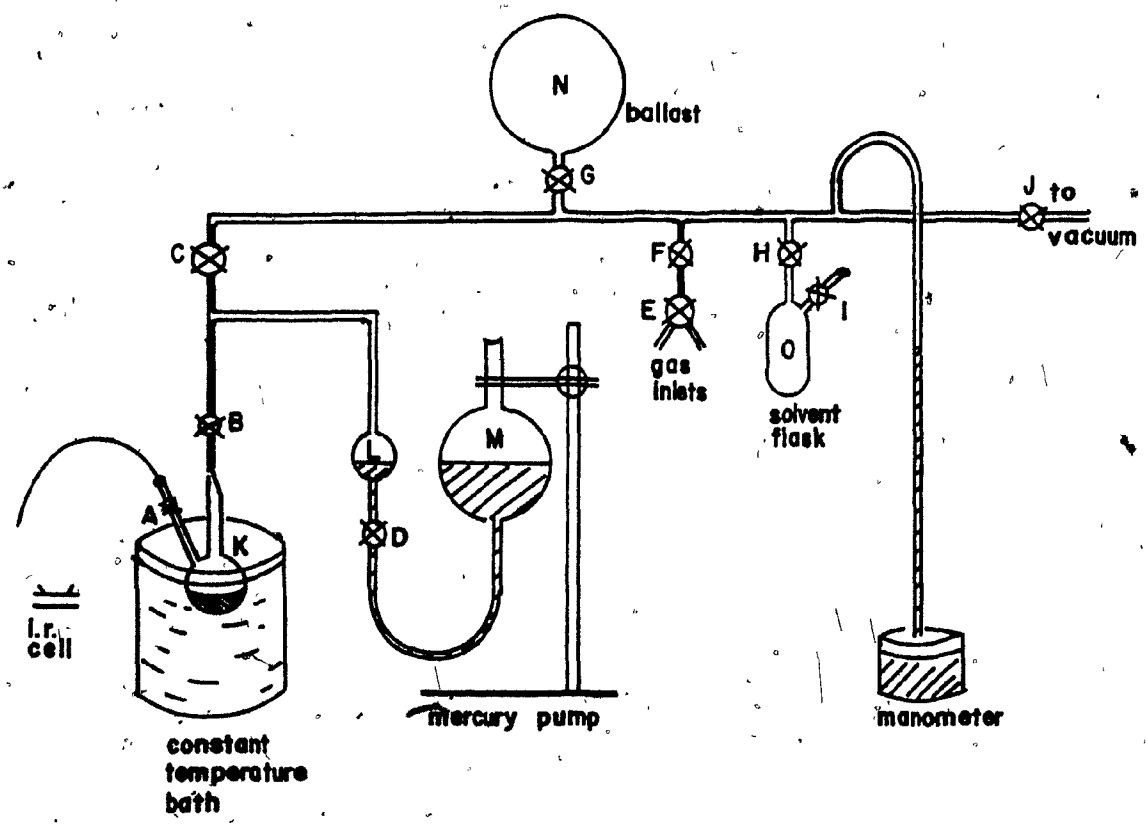

Figure A-IV. Apparatus for the measurement of reaction kinetics under a constant proportion of gases.

APPENDIX V

OUTPUT OF A KINETIC ANALYSIS

A. Reactions in Toluene

RUN NUMBER 24
THERE ARE 26 DATA POINTS IN THIS RUN
TIME ZERO IS 0.: 0. O'CLOCK
BASELINE ABSORBANCE IS 0.0

THIS PROGRAM IS NOT CORRECTED FOR DECOMPOSITION

THE MAXIMUM ABSORBANCE IS 0.629

LEAST SQUARES ANALYSIS OF POINTS FROM 7.5 AND 0.663588 TO POINTS 118.1 AND 2.617295
SLOPE IS 0.017657 CORRELATION COEFFICIENT IS 0.999420 Y-INTERCEPT IS 0.551224
NUMBER OF DATA POINTS 17

THE FOLLOWING IS A PLOT OF THESE POINTS

7.50000 ..X.. 118.100 .663588 ..Y.. 2.61730

PT.NO.	TIME UNCOR CM	HR	MIN	COR.TIME MIN	ABSORBANCE RAW	COR	ORDINATES UNCOR	DECOMP	COR
1.	3.75	0.	0.	7.5	0.114	0.114	0.663588	0.0	0.0
2.	4.65	0.	0.	9.3	0.124	0.124	0.683197	0.0	0.0
3.	5.45	0.	0.	10.9	0.145	0.145	0.725670	0.0	0.0
4.	6.55	0.	0.	13.1	0.164	0.164	0.765718	0.0	0.0
5.	8.55	0.	0.	17.1	0.198	0.198	0.841647	0.0	0.0
6.	10.50	0.	0.	21.0	0.232	0.232	0.923619	0.0	0.0
7.	13.75	0.	0.	27.5	0.290	0.290	1.081755	0.0	0.0
8.	16.20	0.	0.	32.4	0.314	0.314	1.195182	0.0	0.0
9.	19.15	0.	0.	38.3	0.337	0.337	1.331001	0.0	0.0
10.	22.05	0.	0.	44.1	0.370	0.370	1.490926	0.0	0.0
11.	25.65	0.	0.	51.3	0.402	0.402	1.648805	0.0	0.0
12.	29.85	0.	0.	59.7	0.430	0.430	1.814450	0.0	0.0
13.	33.90	0.	0.	67.8	0.456	0.456	1.984463	0.0	0.0
14.	41.00	0.	0.	82.0	0.492	0.492	1.987774	0.0	0.0
15.	48.55	0.	0.	97.1	0.523	0.523	2.244316	0.0	0.0
16.	52.70	0.	0.	105.4	0.540	0.540	2.419119	0.0	0.0
17.	59.05	0.	0.	118.1	0.556	0.556	2.617295	0.0	0.0
18.	65.50	0.	0.	131.0	0.571	0.571	0.0	0.0	0.0
19.	70.40	0.	0.	140.8	0.578	0.578	0.0	0.0	0.0
20.	76.20	0.	0.	152.4	0.586	0.586	0.0	0.0	0.0
21.	83.45	0.	0.	166.9	0.596	0.596	0.0	0.0	0.0
22.	92.40	0.	0.	184.8	0.605	0.605	0.0	0.0	0.0
23.	99.80	0.	0.	199.6	0.610	0.610	0.0	0.0	0.0
25.	116.20	0.	0.	232.4	0.623	0.623	0.0	0.0	0.0
27.	139.20	0.	0.	278.4	0.628	0.628	0.0	0.0	0.0
28.	170.00	0.	0.	340.0	0.629	0.629	0.0	0.0	0.0

CALCULATION OF INITIAL RATE
THE FOLLOWING IS A PLOT OF ABSORBANCE VERSUS TIME

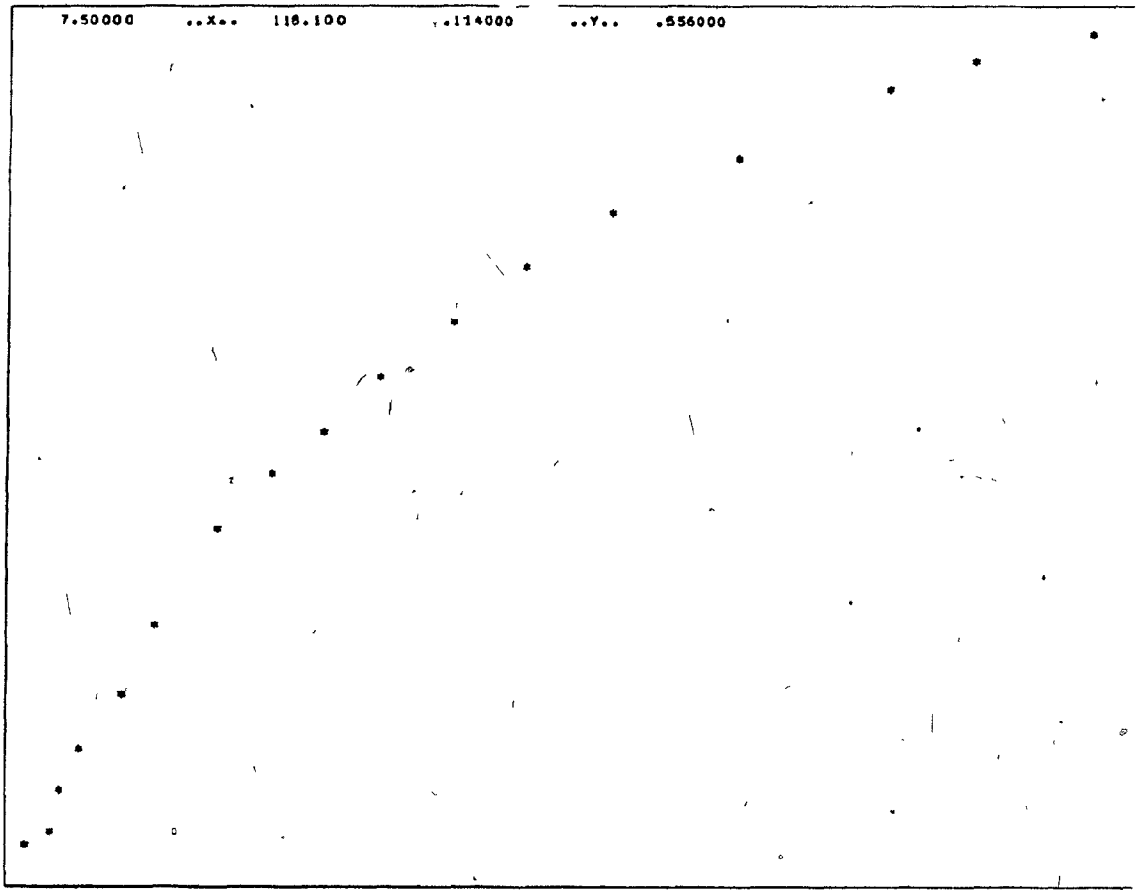

POLYNOMIAL CURVE FITTING

X	Y	F1	F2
0.7500000E+01	0.1140000E+00	0.1088293D+00	0.1088292D+00
0.9299999E+01	0.1240000E+00	0.1280211D+00	0.1280210D+00
0.1080000E+02	0.1450000E+00	0.1443783D+00	0.1443782D+00
0.1310000E+02	0.1640000E+00	0.1658351D+00	0.1658349D+00
0.1709999E+02	0.1980000E+00	0.2019585D+00	0.2019584D+00
0.2100000E+02	0.2320000E+00	0.2338684D+00	0.2338682D+00
0.2750300E+02	0.2900000E+00	0.2806071D+00	0.2806071D+00
0.3239999E+02	0.3140000E+00	0.3111859D+00	0.3111857D+00
0.3829999E+02	0.3370000E+00	0.3434866D+00	0.3434864D+00
0.4410001E+02	0.3700000E+00	0.3711575D+00	0.3711572D+00
0.5129999E+02	0.4020000E+00	0.4008930D+00	0.4008929D+00
0.5970001E+02	0.4300000E+00	0.4305022D+00	0.4305018D+00
0.6779999E+02	0.4560000E+00	0.4551388D+00	0.4551384D+00
0.8200000E+02	0.4920000E+00	0.4918206D+00	0.4918202D+00
0.9710001E+02	0.5230000E+00	0.5241214D+00	0.5241209D+00
0.1054000E+03	0.5400000E+00	0.5389636D+00	0.5389631D+00
0.1181000E+03	0.5560000E+00	0.5562323D+00	0.5562316D+00

SGMS0 0.231741390-01 0.187968460-02 0.132396530-03 0.250185480-04

SGMS0 0.175313080-04 0.189466490-04

MINIMUM SGMS0= 0.17501308D-04 FOR DEGREE 4

N= 4
A(0) = 0.1903931E-01
A(1) = 0.1308585E-01
A(2) = -0.1575352E-03
A(3) = 0.1043830E-05
A(4) = -0.3063826E-08

THE SLOPE AT ZERO IS 0.01309
THE Y-INTERCEPT IS 0.01910

B. Reactions in Methylene Chloride

```
RUN NUMBER 66
THERE ARE 36 DATA POINTS IN THIS RUN
TIME ZERO IS 11:13. O'CLOCK
BASELINE ABSORBANCE IS  0.0

  THIS PROGRAM IS CORRECTED FOR DECOMPOSITION AT LONG REACTION TIMES BY AN ITERATIVE METHOD
SCALE 0-2 BEGINS AT POINT NUMBER    1

THE MAXIMUM ABSORBANCE IS  0.514

LEAST SQUARES ANALYSIS OF POINTS FROM    6.7 AND   0.780886 TO POINTS 120.1 AND   2.995730
    SLOPE IS   0.019048          CORRELATION COEFFICIENT IS   0.997241          Y-INTERCEPT IS   0.581311
    NUMBER OF DATA POINTS    21
ST DEV X            ST DEV Y            ST ERROR Y
   33.934601            0.668584            0.049628

THE FOLLOWING IS A PLOT OF THESE POINTS
```

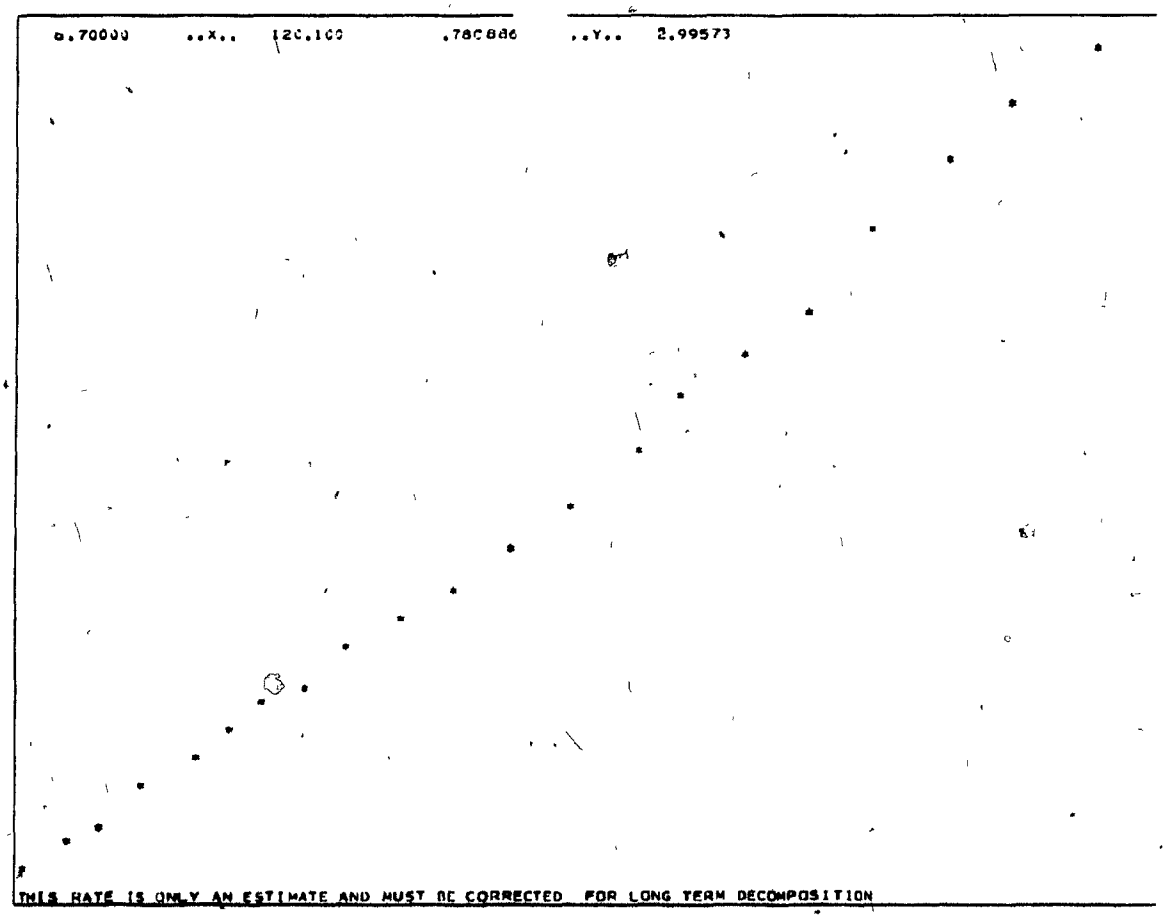


```
THIS RATE IS ONLY AN ESTIMATE AND MUST BE CORRECTED FOR LONG TERM DECOMPOSITION
```

```
THIS RATE IS THE LONG- TERM SOLVENT-INDUCED DECOMPOSITION RATE
THERE ARE LESS THAN 15 DEGREES OF FREEDOM; ERROR LIMITS ARE NOT CALCULATED

LEAST SQUARES ANALYSIS OF POINTS FROM  264.0 AND  0.681219 TO POINTS 602.0 AND  1.372994
    SLOPE IS   0.001207          CORRELATION COEFFICIENT IS   0.993841          Y-INTERCEPT IS   0.332464
    NUMBER OF DATA POINTS    18

THE FOLLOWING IS A PLOT OF THESE POINTS
```

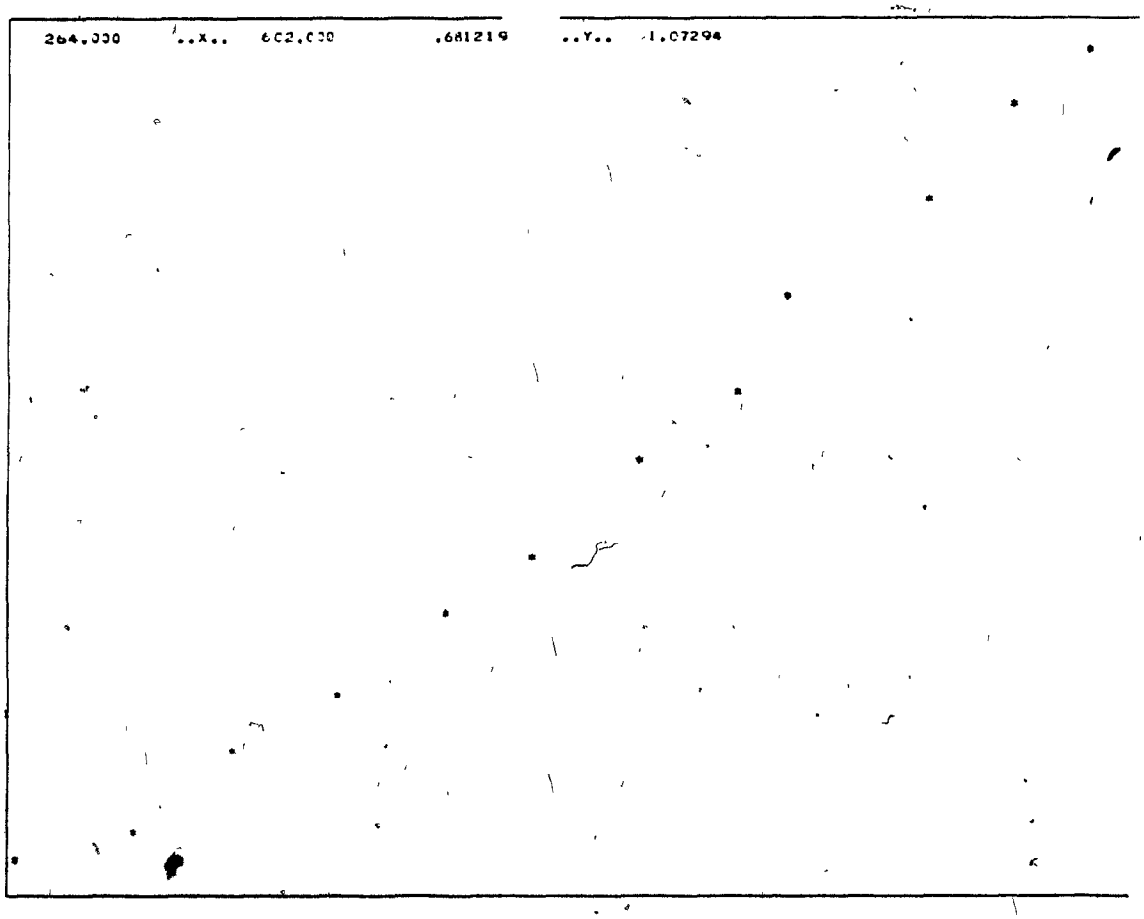

THE CORRECTED ABSORBANCE MAXIMUM, AOPR, IS 0.707

THIS RATE IS CORRECTED FOR LONG TERM DECOMPOSITION

LEAST SQUARES ANALYSIS OF POINTS FROM 6.7 AND 0.391285 TO POINTS 120.1 AND 1.565716
SLOPE IS 0.013146 CORRELATION COEFFICIENT IS 0.999642 Y-INTERCEPT IS -0.004591
NUMBER OF DATA POINTS 21

THIS RATE IS ONLY AN ESTIMATE AND MUST BE CORRECTED FOR LONG TERM DECOMPOSITION

THIS RATE IS THE LONG-TERM SOLVENT-INDUCED DECOMPOSITION RATE
THERE ARE LESS THAN 15 DEGREES OF FREEDOM; ERROR LIMITS ARE NOT CALCULATED

LEAST SQUARES ANALYSIS OF POINTS FROM 364.0 AND 0.763573 TO POINTS 602.0 AND 1.072944
SLOPE IS 0.021339 CORRELATION COEFFICIENT IS 0.997502 Y-INTERCEPT IS 0.264671
NUMBER OF DATA POINTS 9

THE CORRECTED ABSORBANCE MAXIMUM, AOPR, IS 0.706

THIS RATE IS CORRECTED FOR LONG TERM DECOMPOSITION

LEAST SQUARES ANALYSIS OF POINTS FROM 6.7 AND 0.085635 TO POINTS 120.1 AND 1.434649
SLOPE IS 0.011786 CORRELATION COEFFICIENT IS 0.999710 Y-INTERCEPT IS 0.009173
NUMBER OF DATA POINTS 21

THIS RATE IS ONLY AN ESTIMATE AND MUST BE CORRECTED FOR LONG TERM DECOMPOSITION

THIS RATE IS THE LONG- TERM SOLVENT-INDUCED DECOMPOSITION RATE
THERE ARE LESS THAN 15 DEGREES OF FREEDOM; ERROR LIMITS ARE NOT CALCULATED

LEAST SQUARES ANALYSIS OF POINTS FROM 400.0 AND 0.798568 TO POINTS 602.0 AND 1.072944
SLOPE IS 0.001383 CORRELATION COEFFICIENT IS 0.998140 Y-INTERCEPT IS 0.240952
NUMBER OF DATA POINTS 8

THE CORRECTED ABSORBANCE MAXIMUM, ADPR, IS 0.786

THIS RATE IS CORRECTED FOR LONG TERM DECOMPOSITION

LEAST SQUARES ANALYSIS OF POINTS FROM 6.7 AND 0.083857 TO POINTS 120.1 AND 1.359066
SLOPE IS 0.011398 CORRELATION COEFFICIENT IS 0.999735 Y-INTERCEPT IS 0.312421
NUMBER OF DATA POINTS 21

THIS RATE IS ONLY AN ESTIMATE AND MUST BE CORRECTED FOR LONG TERM DECOMPOSITION

THIS RATE IS THE LONG- TERM SOLVENT-INDUCED DECOMPOSITION RATE
THERE ARE LESS THAN 15 DEGREES OF FREEDOM; ERROR LIMITS ARE NOT CALCULATED

LEAST SQUARES ANALYSIS OF POINTS FROM 427.0 AND 0.830113 TO POINTS 602.0 AND 1.072944
SLOPE IS 0.001404 CORRELATION COEFFICIENT IS 0.997674 Y-INTERCEPT IS 0.229615
NUMBER OF DATA POINTS 7

THE CORRECTED ABSORBANCE MAXIMUM, ADPR, IS 0.796

THIS RATE IS CORRECTED FOR LONG TERM DECOMPOSITION

LEAST SQUARES ANALYSIS OF POINTS FROM 6.7 AND 0.083045 TO POINTS 120.1 AND 1.338955
SLOPE IS 0.011227 CORRELATION COEFFICIENT IS 0.999803 Y-INTERCEPT IS 0.013756
NUMBER OF DATA POINTS 21

THE FOLLOWING IS A PLOT OF THESE POINTS

6.70000 ..X.. 120.100 .830455E-01 ..Y.. 1.33895

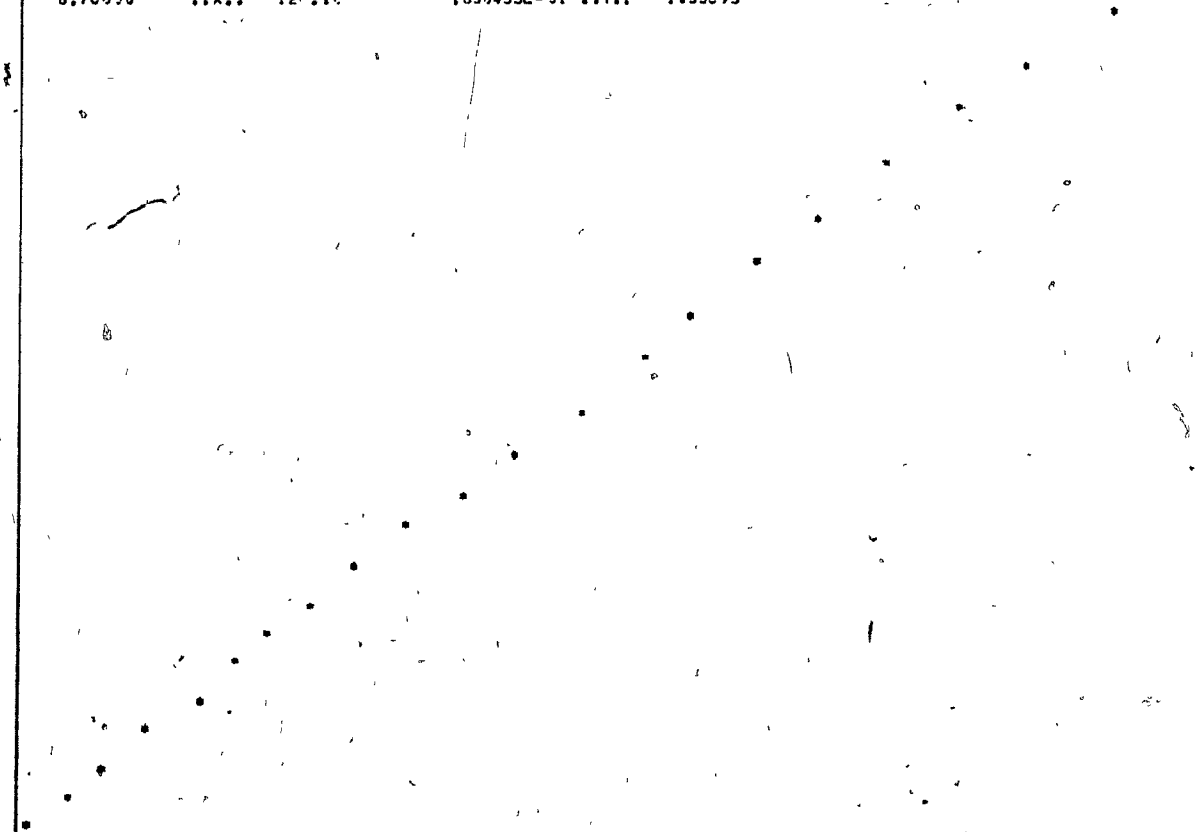

THIS IS THE FINAL CORRECTED RATE
ST DEV X ST DEV Y ST ERROR Y
0.036601 0.011135 0.009638

PT.NO.	TIME UNCOR CM	HR °	MIN	COR.TIME MIN	ABSORBANCE RAW	COR	ORDINATES UNCOR	DECOMP	COR
1.	3.35	0.	2.	6.7	0.028	0.056	0.780886	0.0	0.083045
2.	5.45	0.	3.	10.9	0.042	0.084	0.843970	0.0	0.126605
3.	7.30	0.	4.	14.6	0.054	0.108	0.901402	0.0	0.169510
4.	9.80	0.	5.	19.6	0.072	0.144	0.994252	0.0	0.233177
5.	12.20	0.	7.	24.4	0.085	0.170	1.067113	0.0	0.283919
6.	14.20	0.	8.	28.4	0.097	0.194	1.139434	0.0	0.332296
7.	16.35	0.	9.	32.7	0.111	0.222	1.231301	0.0	0.389888
8.	18.35	0.	10.	36.7	0.118	0.236	1.280133	0.0	0.425570
9.	20.45	0.	12.	41.0	0.131	0.262	1.378325	0.0	0.486001
10.	23.25	0.	13.	46.5	0.142	0.284	1.469675	0.0	0.544490
11.	25.95	0.	15.	51.7	0.150	0.300	1.541779	0.0	0.591982
12.	29.00	0.	17.	58.0	0.162	0.324	1.666730	0.0	0.663782
13.	32.40	0.	19.	64.8	0.172	0.344	1.771956	0.0	0.731836
14.	35.60	0.	21.	71.2	0.183	0.366	1.910542	0.0	0.809167
15.	37.90	0.	22.	75.8	0.192	0.384	2.040219	0.0	0.875152
16.	41.40	0.	24.	82.8	0.200	0.400	2.171556	0.0	0.946974
17.	44.90	0.	26.	89.8	0.206	0.412	2.282781	0.0	1.010225
18.	48.40	0.	28.	96.8	0.217	0.434	2.525728	0.0	1.115386
19.	52.00	0.	30.	104.0	0.223	0.446	2.688246	0.0	1.190603
20.	55.40	0.	32.	110.8	0.228	0.456	2.847310	0.0	1.261359
21.	60.35	0.	35.	120.7	0.232	0.464	2.995730	0.0	1.338955
22.	65.95	0.	38.	131.9	0.240	0.480	0.0	0.0	0.0
23.	76.50	0.	44.	153.0	0.248	0.496	0.0	0.0	0.0
24.	0.0	3.	24.	192.3	0.257	0.514	0.0	0.0	0.0
25.	0.0	4.	36.	264.0	0.253	0.506	0.0	0.681219	0.0
26.	0.0	5.	12.	300.0	0.251	0.503	0.0	0.693147	0.0
27.	0.0	5.	42.	330.0	0.240	0.480	0.0	0.733969	0.0
28.	0.0	6.	16.	364.0	0.233	0.466	0.0	0.763570	0.0
29.	0.0	6.	52.	400.0	0.225	0.451	0.0	0.798508	0.0
30.	0.0	7.	19.	427.0	0.218	0.436	0.0	0.830113	0.0
31.	0.0	7.	52.	460.0	0.208	0.416	0.0	0.877070	0.0
32.	0.0	8.	22.	490.0	0.202	0.404	0.0	0.906340	0.0
33.	0.0	8.	48.	508.0	0.193	0.386	0.0	0.951918	0.0
34.	0.0	9.	22.	550.0	0.184	0.368	0.0	0.999672	0.0
35.	0.0	9.	50.	578.0	0.176	0.352	0.0	1.044124	0.0
36.	0.0	10.	14.	602.0	0.171	0.342	0.0	1.072944	0.0

CALCULATION OF INITIAL RATE
THE FOLLOWING IS A PLOT OF ABSORBANCE VERSUS TIME

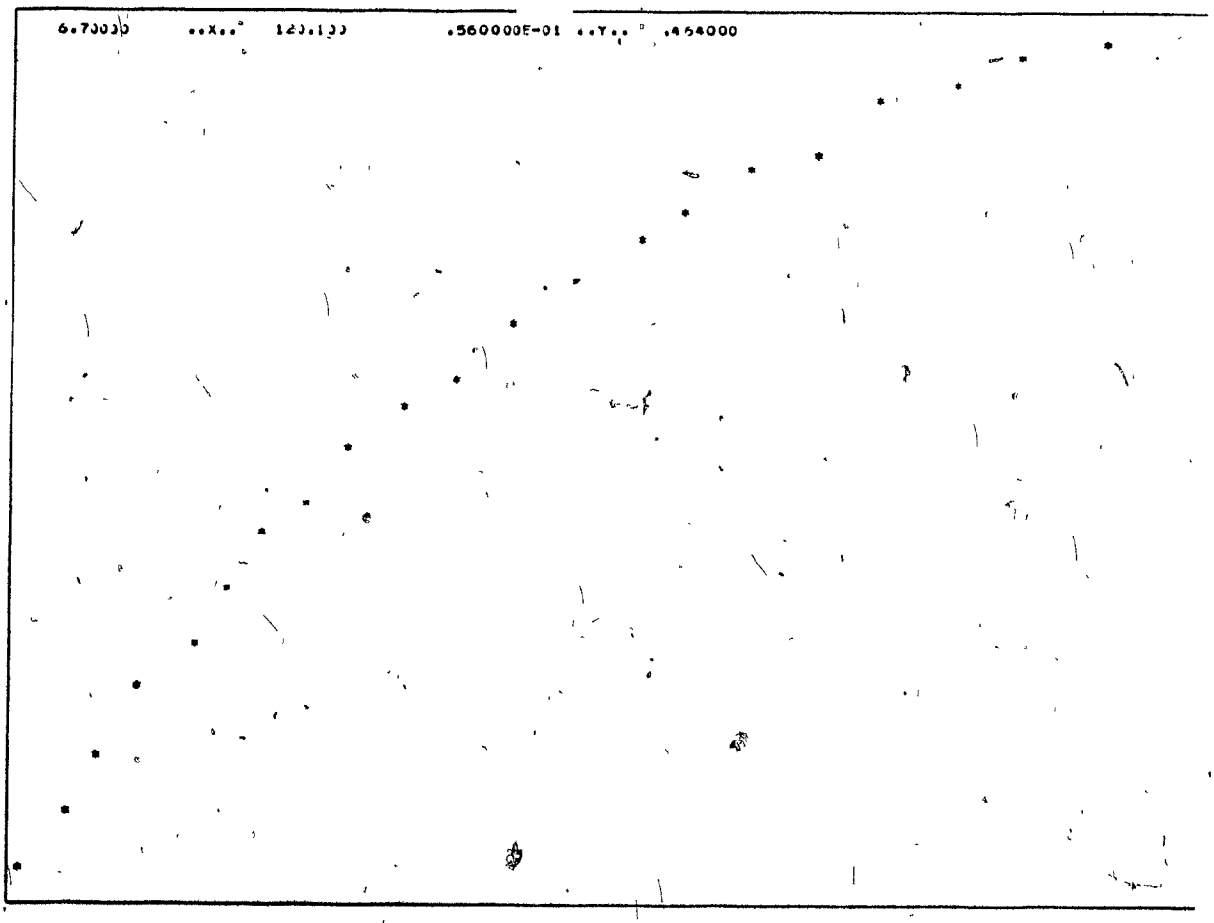

POLYNOMIAL CURVE FITTING

X	Y	F1	F2
0.4700001E+01	0.5600000E-01	0.5588396D-01	0.5588396D-01
0.1090000E+02	0.8399999E-01	0.8381716D-01	0.8381697D-01
0.1460000E+02	0.1080000E+00	0.1080771D+00	0.1080769D+00
0.1959999E+02	0.1440000E+00	0.1421374D+00	0.1421372D+00
0.2439999E+02	0.1700000E+00	0.1724534D+00	0.1724531D+00
0.2839999E+02	0.1940000E+00	0.1960711D+00	0.1960708D+00
0.3210000E+02	0.2220000E+00	0.2164399D+00	0.2164384D+00
0.3673000E+02	0.2359999E+00	0.2397563D+00	0.2397558D+00
0.4095999E+02	0.2620000E+00	0.2594676D+00	0.2594670D+00
0.4650000E+02	0.2740000E+00	0.2827021D+00	0.2827015D+00
0.5170001E+02	0.3000000E+00	0.3024622D+00	0.3024615D+00
0.5800000E+02	0.3240000E+00	0.3243869D+00	0.3243860D+00
0.6479999E+02	0.3440000E+00	0.3463218D+00	0.3463205D+00
0.7120001E+02	0.3660001E+00	0.3658383D+00	0.3658367D+00
0.7579999E+02	0.3839999E+00	0.3793171D+00	0.3793152D+00
0.8279999E+02	0.4000000E+00	0.3988753D+00	0.3988726D+00
0.8979999E+02	0.4119999E+00	0.4163916D+00	0.4168883D+00
0.9679999E+02	0.4340000E+00	0.4327054D+00	0.4327012D+00
0.1040000E+03	0.4460000E+00	0.4459721D+00	0.4459647D+00
0.1113800E+03	0.4560000E+00	0.4553782D+00	0.4553713D+00
0.1201000E+03	0.4640000E+00	0.4642488D+00	0.4642395D+00

SGMSQ 0.18613998D-01 0.8886340 4D-03 0.29135720D-04 0.13472784D-04

SGMSQ 0.10775921D-04 0.9624410 2D-05 0.91863304D-05 0.95542740D-05

MINIMUM SGMSQ= 0.91863304D-05 FOR DEGREE 6

N= 6
C 0 = 0.1595144E-01
C 1 = 0.5229169E-02
C 2 = 0.1419137E-03
C 3 = -0.5392239E-05
C 4 = 0.7523602E-07
C 5 = -0.4813310E-09
C 6 = 0.1159949E-11

THE SLOPE AT ZERO IS 0.00523
THE Y-INTERCEPT IS 0.01595

POLYNOMIAL CURVE FITTING

X	Y	F1	F2
0.5600000E-01	0.6700001E+01	0.6662198D+01	0.6662214D+01
0.8399999E-01	0.1090000E+02	0.1105826D+02	0.1105829D+02
0.1080000E+00	0.1460000E+02	0.1439656D+02	0.1439661D+02
0.1440000E+00	0.1959999E+02	0.1985538D+02	0.1985516D+02
0.1700000E+00	0.2439999E+02	0.2410886D+02	0.2410894D+02
0.1940000E+00	0.2839999E+02	0.2817354D+02	0.2817363D+02
0.2220000E+00	0.3210001E+02	0.3316579D+02	0.3316586D+02
0.2359999E+00	0.3670001E+02	0.3584756D+02	0.3584760D+02
0.2620000E+00	0.4095999E+02	0.4135347D+02	0.4135344D+02
0.2740000E+00	0.4650000E+02	0.4669201D+02	0.4669188D+02
0.3000000E+00	0.5170001E+02	0.5100052D+02	0.5100036D+02
0.3240000E+00	0.5800000E+02	0.5806804D+02	0.5806760D+02
0.3440000E+00	0.6479999E+02	0.6436169D+02	0.6436101D+02
0.3660001E+00	0.7120001E+02	0.7150517D+02	0.7150415D+02
0.3839999E+00	0.7579999E+02	0.7746005D+02	0.7745868D+02
0.4000000E+00	0.8279999E+02	0.8295281D+02	0.8295107D+02
0.4119999E+00	0.8979999E+02	0.8738743D+02	0.8738533D+02
0.4340000E+00	0.9679999E+02	0.9720407D+02	0.9720130D+02
0.4460000E+00	0.1040000E+03	0.1043135D+03	0.1043103D+03
0.4563000E+00	0.1113800E+03	0.1118251D+03	0.1118215D+03
0.4640000E+00	0.1201000E+03	0.1192682D+03	0.1192643D+03

SGMSQ 0.12091329D+04 0.61035572D+02 0.66509407D+01 0.26171831D+01

SGMSQ 0.22176434D+01 0.15962259D+01 0.11302876D+01 0.10543436D+01

SGMSQ 0.10837160D+01

MINIMUM SGMSQ= 0.10543436D+01 FOR DEGREE 7

N= 7
C 0 = -0.1971289E+02
C 1 = 0.9933347E+03
C 2 = -0.1520013E+05
C 3 = 0.1410197L+06
C 4 = -0.7245261E+06
C 5 = 0.2395343L+07
C 6 = -0.3160443E+07
C 7 = 0.1933661E+07

AT ZERO CONCENTRATION, THE INITIAL RATE IS 0.001007

THE SLOPE AT ZERO IS 9993.33469
THE Y-INTERCEPT IS -19.7128

APPENDIX VI

INFRA-RED MEASUREMENTS OF THE KINETICS OF THE ISOMERIZATION OF $IrH_3(CO)P_2$

C_o = initial absorbance of fac isomer.

A = absorbance of the mer isomer (measured absorbance - baseline absorbance at 1780 cm^{-1}).

$$X = \frac{A_o - A_{eq}}{A_o} \ln \left[\frac{A_o - A_{eq}}{A - A_{eq}} \right]$$

$$X' = \ln \left[\frac{A_{eq}}{A_{eq} - A} \right]$$

A_o, A_{eq} = initial or equilibrium absorbance of mer isomer.

N = number of points used in plots of X or X' vs t.

m = slope.

r = correlation coefficient.

b = intercept of X or X' at t = 0.

S.E.(y) = standard error in X or X'.

σ_m = standard deviation of slope

A. 100% H_2 in Feed Gas

$C_o = 0$			$A_o = 0$		
T = 25.5°C			T = 25.0°C		
t(min)	Ab	X	t(min)	Ab	X'
8	.237	.071	3.5	.023	.21
16	.220	.151	10.5	.036	.36
25	.205	.232	20.5	.050	.55
33	.190	.326	29.5	.061	.71
46	.168	.497	46.2	.083	1.17
60	.146	.737	60	.091	1.42
125	.113	1.533	97	.109	2.42
271	.103	2.613	127	.113	2.51
381	.101		245	.122	
593	.101		372	.120	
1440	.098		1260	.118	
A_o =	.254				
A_{eq} =	.101		A_{eq} =	.120	
N =	7			7	
m =	.0127			.0216	
b =	-.06			.104	
r =	.9986			.9988	
S.E. (y) =	.02473			.0322	
σ_m =	.0003			.0005	

B. 75% H_2/25% N_2 in Feed Gas

$C_o = 0$

$T = 25.5°C$

t(min)	Ab	X
5.5	.182	.098
16.2	.160	.245
30	.134	.490
49	.118	.718
78	.108	.925
127	.095	1.40

$A_o = 0$

$T = 25.3°C$

t(min)	Ab	X'
4.0	.023	.20
11.0	.031	.28
22.0	.055	.57
31.5	.063	.68
47	.082	1.05
61	.084	1.08
110	.103	1.68
152	.125	3.97
240	.126	
389	.127	

$A_o = .200$

$A_{eq} = .085$

$N = 6$

$m = .0104$

$b = .114$

$r = .9909$

$S.E.(y) = .0586$

$\sigma_m = .0009$

$A_{eq} = .127$

$N = 6$

.0167

.150

.9802

.0670

.0018

C. 50% H_2/50% N_2 in Feed Gas

$C_o = 0$

T = 25.5°C

t(min)	Ab	X
5.5	.195	.076
12.7	.169	.234
22.0	.153	.357
28.2	.138	.500
48.5	.126	.643
61.5	.117	.778
102	.100	1.159
234	.081	
1350	.075	

$A_o = .210$

$A_{eq} = .080$

N = 7

m = .0107

b = .106

r = .9883

S.E.(y) = .0514

σ_m = .0007

$A_o = 0$

T = 26.3°C

t(min)	Ab	X'
4.5	.019	.15
11.5	.040	.34
22.0	.062	.55
32.0	.077	.81
48.0	.096	1.19
62	.106	1.46
105	.125	2.33
125	.126	2.44
252	.137	4.9
349	.138	
1320	.126	

A_{eq} = .138

7

.0217

.093

.9989

.0324

.0005

D. 25% H_2/75% N_2 in Feed Gas

$C_o = 0$

$T = 25.5°C$

t(min)	Ab	X
7.5	.204	.116
13.0	.193	.177
21.5	.170	.330
29.5	.155	.456
50.7	.134	.692
67.2	.120	.923
95	.113	1.08
144	.093	2.32
269	.086	
384	.090	
1560	.089	

$A_o = .228$

$A_{eq} = .090$

$N = 7$

$m = .0115$

$b = .072$

$r = .9882$

$S.E.(y) = .0526$

$\sigma_m = .0008$

$A_o = 0$

$T = 26.2°C$

t(min)	Ab	X'
4.0	.032	.23
10.0	.047	.36
20.5	.068	.57
33.0	.090	.85
48.0	.108	1.16
64.0	.124	1.57
98	.137	2.09
127	.147	2.63
264	.153	3.57
369	.157	

$A_{eq} = .157$

7

.0196

.185

.9943

.0645

.0009

E. 100% N_2 in Feed Gas

$C_o = 0$

$T = 25.5°C$

t(min)	Ab	X
6	.234	.083
14	.210	.195
22	.182	.350
29	.166	.453
46	.133	.722
63	.122	.836
131	.077	1.62
244	.063	2.21
388	.050	
1260	.053	

$A_o = .254$

$[A_{eq} = .050]$*

$A_o = 0$

$T = 25.0°C$

t(min)	Ab	X'
3.7	.024	.35
9.0	.033	.53
19.5	.046	.84
30.0	.057	1.20
47.0	.077	2.96
62	.089	
95	.099	
124	.097	
228	.096	
382	.081	
1110	.060	

$[A_{eq} = .081]$*

*System not at equilibrium.

APPENDIX VII

KINETIC MEASUREMENTS OF THE ADDITION OF TRIPHENYLPHOSPHINE TO $IrH_3(CO)\,P_2$

The following tables report the absorbance of the product, $IrH(CO)\,P_3$, of the addition of triphenylphosphine to fac and mer $IrH_3(CO)\,P_2$ at various reaction times. The initial reaction rate and the reaction rate constants are reported in Tables IV-1 and IV-2, respectively. The initial conditions may be found for each experiment from the latter tables.

Rate constants were obtained as the slope of a least-squares line in a plot of ordinate versus time. The ordinates calculated for each experiment are listed in the third column of the following tables. For reactions in toluene, these values are equal to the left-hand-side of equation 43, using the maximum absorbance as E_{eq}. For reactions in methylene chloride, "corrected ordinates" were calculated as described in Chapter IV. In the latter cases, the values listed under "corrected ordinates" at long reaction times are those used to calculate the decomposition rate.

#22

COR.TIME MIN	ABSORB	ORDINATES UNCOR
6.5	0.064	0.599
8.0	0.083	0.634
10.4	0.117	0.701
12.5	0.137	0.742
15.7	0.162	0.796
20.5	0.204	0.994
25.9	0.243	0.994
31.2	0.279	1.096
36.8	0.313	1.203
43.0	0.348	1.316
50.0	0.378	1.448
58.5	0.411	1.599
66.8	0.442	1.786
80.8	0.479	2.009
96.1	0.508	2.253
104.3	0.528	2.465
117.0	0.542	2.645
129.9	0.556	0.0
139.9	0.563	0.0
151.0	0.573	0.0
183.6	0.588	0.0
215.0	0.599	0.0
252.2	0.608	0.0
340.0	0.613	0.0

#23

COR.TIME MIN	ABSORBANCE	ORDINATES UNCOR
7.2	0.054	0.621
8.8	0.077	0.665
10.7	0.100	0.711
12.9	0.126	0.765
16.7	0.155	0.830
22.1	0.203	0.946
26.8	0.229	1.016
32.0	0.266	1.123
37.5	0.295	1.217
43.7	0.330	1.343
50.8	0.360	1.465
59.2	0.395	1.629
67.5	0.421	1.771
81.5	0.453	1.980
96.6	0.487	2.263
105.0	0.503	2.430
117.7	0.518	2.617
130.3	0.531	0.0
139.9	0.542	0.0
150.9	0.546	0.0
184.4	0.564	0.0
215.4	0.582	0.0
252.8	0.588	0.0
340.0	0.591	0.0

#24

COR.TIME MIN	ABSORBANCE	ORDINATES UNCOR
7.5	0.114	0.663
9.3	0.124	0.683
10.9	0.145	0.725
13.1	0.164	0.765
17.1	0.198	0.841
21.0	0.232	0.923
27.5	0.290	1.081
32.4	0.314	1.155
38.3	0.337	1.231
44.1	0.370	1.350
51.3	0.402	1.482
59.7	0.430	1.614
67.8	0.456	1.754
82.0	0.492	1.987
97.1	0.523	2.244
105.4	0.540	2.419
118.1	0.556	2.617
131.0	0.571	0.0
140.8	0.578	0.0
152.4	0.586	0.0
186.9	0.596	0.0
184.8	0.605	0.0
199.6	0.610	0.0
232.4	0.623	0.0
278.4	0.628	0.0
340.0	0.629	0.0

#25

COR.TIME MIN	ABSORB	ORDINATES UNCOR
6.7	0.027	1.390
8.2	0.038	1.435
9.3	0.042	1.452
10.3	0.049	1.482
11.4	0.055	1.509
12.3	0.062	1.541
13.4	0.066	1.560
14.3	0.068	1.570
15.2	0.073	1.594
16.2	0.078	1.619
17.2	0.082	1.639
18.1	0.087	1.666
19.5	0.091	1.687
20.9	0.097	1.720
21.9	0.103	1.754
23.1	0.106	1.771
24.2	0.109	1.789
26.2	0.117	1.838
27.1	0.119	1.851
28.1	0.123	1.877
29.2	0.128	1.910
30.1	0.130	1.924
32.4	0.133	1.944
33.5	0.138	1.980
35.0	0.142	2.009
37.3	0.145	2.032
38.0	0.148	2.055
38.8	0.149	2.063
41.9	0.161	2.162
44.9	0.166	2.207
47.9	0.172	2.263
52.3	0.183	2.375
57.1	0.192	2.476
66.8	0.208	2.688
73.0	0.215	2.796
79.4	0.218	2.847
87.6	0.228	3.036
101.7	0.236	3.218
109.7	0.240	3.324
119.1	0.246	3.506
127.8	0.247	0.0
136.1	0.252	0.0
147.9	0.256	0.0
159.1	0.258	0.0
167.7	0.262	0.0
300.0	0.276	0.0

#26

COR.TIME MIN	ABSORBANCE	ORDINATES UNCOR
7.3	0.065	0.723
8.5	0.083	0.761
9.6	0.090	0.776
10.7	0.107	0.814
11.7	0.118	0.839
12.7	0.121	0.846
13.8	0.136	0.881
14.6	0.138	0.886
15.6	0.152	0.921
16.5	0.160	0.941
17.5	0.167	0.959
18.5	0.173	0.975
20.0	0.190	1.021
21.2	0.200	1.049
22.3	0.208	1.072
23.4	0.216	1.096
24.5	0.223	1.117
26.5	0.238	1.164
27.4	0.242	1.177
28.4	0.251	1.207
29.5	0.258	1.231
30.4	0.265	1.255
32.9	0.282	1.316
33.9	0.288	1.339
35.3	0.296	1.370
37.6	0.307	1.414
38.4	0.309	1.422
42.2	0.330	1.514
45.2	0.343	1.575
48.1	0.358	1.650
53.2	0.386	1.807
58.0	0.392	1.845
66.1	0.413	1.987
74.0	0.436	2.171
80.1	0.448	2.282
88.3	0.463	2.441
95.9	0.472	2.551
102.4	0.480	2.659
110.5	0.494	2.882
119.9	0.501	3.015
128.4	0.508	0.0
137.1	0.517	0.0
146.7	0.522	0.0
159.7	0.528	0.0
168.4	0.528	0.0
308.2	0.550	0.0

#27

COR.TIME MIN	ABSORBANCE	ORDINATES UNCOR
7.8	0.116	0.337
9.9	0.137	0.362
10.0	0.158	0.393
11.1	0.173	0.415
12.0	0.184	0.432
13.0	0.201	0.458
14.1	0.219	0.487
15.0	0.230	0.505
15.9	0.243	0.527
16.9	0.257	0.551
17.8	0.273	0.579
19.0	0.285	0.601
20.5	0.303	0.634
21.5	0.312	0.652
22.7	0.333	0.693
23.8	0.342	0.711
24.8	0.351	0.729
26.8	0.373	0.776
27.8	0.385	0.802
28.8	0.395	0.825
29.8	0.406	0.850
30.7	0.414	0.865
33.3	0.437	0.926
34.1	0.442	0.939
35.6	0.453	0.967
37.8	0.470	1.013
42.5	0.505	1.114
45.2	0.523	1.171
48.4	0.546	1.248
54.1	0.586	1.398
58.8	0.607	1.487
65.5	0.629	1.589
75.7	0.668	1.801
80.7	0.682	1.890
88.9	0.710	2.095
95.4	0.719	2.171
103.0	0.733	2.302
111.2	0.750	2.488
120.6	0.768	2.733
124.1	0.772	0.0
137.6	0.780	0.0
150.1	0.788	0.0
160.3	0.798	0.0
169.2	0.809	0.0
308.8	0.833	0.0

#31

COR.TIME MIN	ABSORBANCE OBS	COR
8.1	0.066	0.089
9.9	0.084	0.114
12.7	0.117	0.162
16.7	0.148	0.211
18.4	0.158	0.227
21.9	0.185	0.273
27.0	0.220	0.336
31.1	0.245	0.383
34.8	0.266	0.426
41.5	0.284	0.487
47.3	0.330	0.570
53.8	0.358	0.642
60.1	0.385	0.717
69.1	0.418	0.823
76.9	0.457	0.957
85.9	0.447	1.034
97.2	0.499	1.146
104.7	0.517	1.229
114.9	0.538	1.366
122.5	0.550	1.453
135.0	0.561	0.0
150.0	0.591	0.0
201.0	0.615	0.0
231.1	0.614	0.0
260.0	0.611	0.492
301.0	0.614	0.504
323.0	0.591	0.525
339.0	0.585	0.536
397.0	0.557	0.585
432.0	0.577	0.621
459.0	0.521	0.652
491.0	0.505	0.683
510.0	0.491	0.711

#32

COR.TIME MIN	ABSORB COR	ORDINATES COR
8.3	0.084	0.126
10.2	0.100	0.153
13.2	0.123	0.194
17.3	0.149	0.244
22.4	0.180	0.308
27.6	0.213	0.380
31.6	0.238	0.438
35.4	0.256	0.485
41.0	0.286	0.566
47.7	0.316	0.659
54.2	0.338	0.740
60.5	0.364	0.837
69.6	0.392	0.965
80.0	0.418	1.113
86.3	0.429	1.194
97.6	0.446	1.345
105.3	0.452	1.434
115.0	0.462	1.569
122.8	0.469	1.685
134.2	0.474	0.0
177.0	0.472	0.750
201.0	0.465	0.765
231.0	0.450	0.798
260.0	0.433	0.837
301.0	0.399	0.918
323.0	0.378	0.970
339.0	0.365	1.007
397.0	0.318	1.145
432.0	0.293	1.227
459.0	0.269	1.313
491.0	0.252	1.378
510.0	0.237	1.439

#33

COR.TIME MIN	ABSORB COR	ORDINATES COR
8.7	0.099	0.161
10.4	0.116	0.192
14.4	0.151	0.261
18.7	0.186	0.336
23.3	0.212	0.401
28.2	0.242	0.479
32.7	0.267	0.552
36.4	0.286	0.611
41.8	0.311	0.698
48.8	0.340	0.813
54.8	0.360	0.908
61.4	0.385	1.032
70.8	0.401	1.159
80.9	0.426	1.350
86.9	0.436	1.456
96.2	0.448	1.643
106.0	0.453	1.770
115.7	0.458	1.938
124.0	0.462	2.103
130.9	0.463	0.0
177.0	0.447	0.805
201.0	0.428	0.846
231.0	0.403	0.908
260.0	0.374	0.983
301.0	0.336	1.090
323.0	0.317	1.148
339.0	0.304	1.190
397.0	0.257	1.358
432.0	0.234	1.452
459.0	0.214	1.541
491.0	0.196	1.629
510.0	0.186	1.682

#34

COR.TIME MIN	ABSORB COR	ORDINATES COR
3.4	0.045	0.090
4.7	0.068	0.116
6.3	0.059	0.127
9.4	0.071	0.162
13.3	0.084	0.202
16.3	0.098	0.243
18.3	0.107	0.270
20.4	0.116	0.297
24.8	0.127	0.343
26.5	0.131	0.359
31.0	0.144	0.411
37.4	0.160	0.506
42.1	0.181	0.563
47.8	0.201	0.622
55.4	0.211	0.729
61.9	0.225	0.818
68.5	0.237	0.906
75.7	0.246	0.992
82.1	0.252	1.065
88.5	0.257	1.137
96.1	0.272	1.223
104.0	0.284	1.299
116.2	0.288	1.433
121.8	0.297	1.501
139.3	0.320	1.70
141.2	0.321	1.305
213.1	0.257	1.358
242.1	0.245	1.406
275.0	0.228	1.478
309.0	0.212	1.551
335.0	0.202	1.599
367.0	0.184	1.692
396.0	0.171	1.766
424.0	0.154	1.870
454.0	0.139	1.973
482.0	0.128	2.055

#35

COR.TIME MIN	ABSORB COR	ORDINATES COR
3.8	0.073	0.130
5.0	0.079	0.143
6.8	0.087	0.151
10.2	0.106	0.204
13.8	0.121	0.241
16.9	0.131	0.267
19.0	0.139	0.288
21.0	0.147	0.310
25.3	0.165	0.356
27.0	0.169	0.372
31.6	0.185	0.420
37.0	0.208	0.462
42.6	0.224	0.549
49.3	0.238	0.601
56.0	0.259	0.696
62.4	0.274	0.771
68.9	0.291	0.835
76.1	0.306	0.916
82.5	0.319	0.982
89.0	0.328	1.048
96.5	0.339	1.141
104.7	0.354	1.257
116.7	0.366	1.387
122.3	0.370	1.444
130.7	0.379	0.0
141.7	0.384	0.0
213.0	0.401	0.0
242.0	0.394	0.031
275.0	0.384	0.097
309.0	0.372	0.985
335.0	0.362	1.016
367.0	0.346	1.061
396.0	0.339	1.087
424.0	0.323	1.133
454.0	0.316	1.164
482.0	0.295	1.220

#36

COR.TIME MIN	ABSORB COR	ORDINATES COR
4.4	0.115	0.226
5.3	0.117	0.270
7.2	0.125	0.303
10.7	0.135	0.341
14.4	0.148	0.388
17.5	0.157	0.429
19.6	0.167	0.451
21.4	0.173	0.468
25.8	0.185	0.502
27.4	0.196	0.543
32.0	0.208	0.640
38.4	0.223	0.732
43.2	0.233	0.785
44.7	0.246	0.879
56.0	0.268	1.017
63.3	0.278	1.125
69.5	0.296	1.215
76.6	0.306	1.322
83.0	0.314	1.442
89.4	0.313	1.575
97.3	0.318	1.673
105.1	0.326	1.872
117.2	0.326	2.016
122.8	0.331	2.0
131.2	0.331	0.0
142.2	0.331	1.115
213.0	0.306	1.184
242.0	0.284	1.224
275.0	0.257	1.283
309.0	0.254	1.362
335.0	0.243	1.414
367.0	0.230	1.469
396.0	0.213	1.545
424.0	0.200	1.609
454.0	0.184	1.662
482.0	0.178	1.725

#37

COR.TIME MIN	ABSORB COR	ORDINATES COR
5.8	0.060	0.061
7.3	0.071	0.089
9.7	0.092	0.117
12.7	0.121	0.156
16.3	0.156	0.204
19.4	0.181	0.244
24.7	0.227	0.315
30.8	0.264	0.376
34.8	0.293	0.424
39.1	0.311	0.461
43.3	0.324	0.496
48.5	0.338	0.536
53.3	0.350	0.564
61.0	0.361	0.771
67.1	0.373	0.817
75.4	0.385	0.874
80.8	0.389	0.912
91.7	0.398	1.036
99.5	0.401	1.111
107.9	0.398	1.211
119.9	0.398	1.342
126.4	0.55	0.0
154.0	0.567	0.0
180.0	0.537	0.0
209.0	0.498	0.0
246.0	0.567	0.574
269.0	0.553	0.593
305.0	0.514	0.614
332.0	0.51	0.673
364.0	0.488	0.721
396.0	0.460	0.759
424.0	0.444	0.797
454.0	0.431	0.867
482.0	0.411	0.913
512.0	0.384	0.967
535.0	0.381	1.021

#38

COR.TIME MIN	ABSORB COR	ORDINATES COR
6.5	0.068	0.068
8.2	0.079	0.087
10.1	0.096	0.115
13.2	0.127	0.156
16.8	0.160	0.199
20.4	0.193	0.245
25.2	0.234	0.310
31.0	0.274	0.377
34.9	0.306	0.429
38.6	0.336	0.482
44.2	0.365	0.544
49.0	0.391	0.601
53.9	0.410	0.655
61.6	0.444	0.761
67.6	0.466	0.844
76.9	0.513	0.958
81.1	0.528	0.970
92.1	0.558	1.114
99.9	0.570	1.184
107.9	0.590	1.282
119.5	0.610	1.418
127.2	0.629	1.61
154.0	0.687	1.61
180.0	0.666	1.61
209.0	0.671	1.61
246.0	0.664	0.43
269.0	0.651	0.482
305.0	0.631	0.482
332.0	0.612	0.461
364.0	0.588	0.527
396.0	0.570	0.562
424.0	0.556	0.589
454.0	0.536	0.642
482.0	0.508	0.681
512.0	0.488	0.721
535.0	0.466	0.763

#39

COR.TIME MIN	ABSORB COR	ORDINATES COR
10.4	0.046	0.100
13.8	0.060	0.134
17.3	0.077	0.173
21.2	0.085	0.201
25.9	0.110	0.261
31.4	0.137	0.332
35.4	0.143	0.361
40.3	0.175	0.446
44.9	0.193	0.506
49.5	0.212	0.572
53.9	0.229	0.636
61.9	0.253	0.744
67.9	0.269	0.827
76.4	0.285	0.933
81.4	0.288	0.978
92.1	0.308	1.132
99.2	0.318	1.232
108.1	0.328	1.359
119.6	0.337	1.523
127.1	0.342	0.0
154.0	0.339	1.081
180.0	0.339	1.081
209.0	0.324	1.127
246.0	0.298	1.210
269.0	0.282	1.265
305.0	0.255	1.366
332.0	0.233	1.456
364.0	0.212	1.551
396.0	0.190	1.660
424.0	0.177	1.731
454.0	0.156	1.857
482.0	0.139	1.978
512.0	0.127	2.063
535.0	0.118	2.137

#40

COR.TIME MIN	ABSORB COR	ORDINATES UNCOR
7.4	0.096	0.012
8.8	0.127	0.043
10.4	0.142	0.059
13.4	0.187	0.108
17.9	0.244	0.174
21.5	0.283	0.221
26.5	0.340	0.295
30.9	0.390	0.365
36.9	0.440	0.440
42.6	0.490	0.520
48.8	0.542	0.612
54.8	0.589	0.703
61.8	0.644	0.820
68.2	0.686	0.921
74.2	0.729	1.035
82.3	0.786	1.210
90.5	0.815	1.313
100.3	0.856	1.478
107.6	0.890	1.639
117.6	0.920	1.807
124.9	0.936	1.910
131.8	0.948	0.0
151.0	0.988	0.0
177.0	1.026	0.0
207.0	1.052	0.0
239.0	1.060	0.0
261.0	1.080	0.0
309.0	1.086	0.0
337.0	1.086	0.0
359.0	1.088	0.0
377.0	1.084	0.0

#41

COR.TIME MIN	ABSORB COR	ORDINATES UNCOR
6.9	0.134	0.022
8.4	0.153	0.041
10.0	0.171	0.060
12.9	0.207	0.099
17.4	0.257	0.156
21.0	0.294	0.200
25.9	0.347	0.267
30.4	0.392	0.328
36.4	0.447	0.407
42.3	0.503	0.495
48.3	0.548	0.572
54.3	0.597	0.663
61.3	0.648	0.767
67.5	0.691	0.865
73.6	0.725	0.949
81.9	0.774	1.084
89.7	0.809	1.194
98.8	0.849	1.335
106.5	0.878	1.452
109.7	0.888	1.498
116.2	0.916	1.629
124.4	0.938	1.748
131.3	0.950	0.0
151.0	0.996	0.0
177.0	1.032	0.0
207.0	1.062	0.0
239.0	1.084	0.0
261.0	1.098	0.0
309.0	1.108	0.0
337.0	1.114	0.0
359.0	1.120	0.0
377.0	1.112	0.0

#42

COR.TIME MIN	ABSORB COR	ORDINATES UNCOR
7.8	0.039	-0.023
9.1	0.052	-0.010
10.9	0.077	0.014
14.1	0.113	0.051
18.5	0.164	0.106
22.2	0.212	0.161
27.0	0.257	0.215
31.5	0.305	0.277
37.4	0.357	0.348
43.3	0.413	0.430
49.7	0.470	0.522
55.3	0.518	0.606
62.3	0.567	0.701
68.8	0.608	0.787
74.9	0.648	0.879
82.9	0.697	1.005
90.7	0.733	1.108
99.3	0.768	1.220
106.9	0.801	1.339
108.2	0.817	1.402
116.9	0.847	1.532
124.0	0.867	1.629
130.7	0.891	0.0
151.0	0.931	0.0
177.0	0.975	0.0
207.0	1.005	0.0
239.0	1.023	0.0
261.0	1.041	0.0
309.0	1.051	0.0
337.0	1.061	0.0
359.0	1.061	0.0
177.0	1.063	0.0

#43

COR.TIME MIN	ABSORB COR	ORDINATES COR
[illegible]	[illegible]	[illegible]

#44

COR.TIME MIN	ABSORB COR	ORDINATES COR
[illegible]	[illegible]	[illegible]

#45

COR.TIME MIN	ABSORB COR	ORDINATES COR
5.9	0.048	0.133
7.1	0.054	0.152
10.8	0.078	0.219
13.9	0.083	0.253
18.1	0.099	0.314
22.5	0.117	0.387
25.9	0.128	0.436
29.9	0.141	0.498
33.9	0.149	0.543
38.6	0.173	0.667
46.5	0.183	0.737
52.0	0.198	0.842
58.3	0.213	0.958
64.3	0.228	1.088
71.0	0.234	1.170
76.2	0.242	1.265
83.4	0.254	1.423
92.3	0.260	1.556
100.2	0.264	1.673
107.8	0.269	1.815
113.8	0.269	1.879
120.9	0.274	0.0
127.7	0.270	0.0
133.4	0.274	1.294
169.0	0.274	1.294
197.0	0.263	1.335
226.0	0.253	1.374
264.0	0.243	1.414
286.0	0.231	1.465
355.0	0.203	1.594
387.0	0.189	1.666
421.0	0.178	1.725
453.0	0.163	1.814
485.0	0.151	1.890
516.0	0.144	1.937
544.0	0.135	2.002
569.0	0.125	2.079

#46

COR.TIME MIN	ABSORBANCE COR
3.3	0.103
4.6	0.110
5.5	0.119
7.9	0.132
9.8	0.145
12.8	0.166
15.6	0.192
17.6	0.203
21.3	0.228
24.1	0.243
27.4	0.267
31.4	0.293
35.0	0.313
39.7	0.337
43.7	0.360
46.0	0.383
52.0	0.402
56.8	0.423
61.9	0.446
67.6	0.473
73.4	0.492
77.3	0.507
83.9	0.508
91.8	0.552
99.8	0.572
108.4	0.593
114.6	0.608
118.4	0.616

#47

COR.TIME MIN	ABSORB COR
4.2	0.079
5.2	0.083
7.3	0.088
9.3	0.097
12.3	0.108
14.8	0.122
16.9	0.132
20.7	0.153
22.9	0.161
26.5	0.177
30.7	0.192
39.0	0.222
42.9	0.240
47.5	0.256
51.3	0.270
56.3	0.285
61.2	0.302
67.1	0.317
72.8	0.333
77.8	0.346
83.4	0.356
91.2	0.371
99.4	0.390
108.1	0.400
114.2	0.412
117.9	0.418

#48

COR.TIME MIN	ABSORBANCE COR
2.3	0.038
3.8	0.042
4.9	0.042
6.8	0.048
8.9	0.049
11.7	0.056
14.3	0.060
16.3	0.065
20.2	0.068
22.3	0.070
24.1	0.071
29.9	0.073
33.8	0.073
38.4	0.070
42.3	0.072
47.0	0.072
50.7	0.072
35.8	0.072
60.8	0.073
66.6	0.077
72.2	0.075
78.2	0.072
83.0	0.079
90.6	0.079
99.0	0.084
107.6	0.080
113.6	0.087
117.4	0.082

#49

COR.TIME MIN	ABSORBANCE COR
10.1	0.048
11.5	0.066
14.0	0.095
15.5	0.110
19.0	0.146
22.9	0.186
26.9	0.223
31.2	0.262
36.0	0.301
41.0	0.342
46.5	0.380
51.5	0.412
57.2	0.448
62.8	0.478
69.0	0.509
76.4	0.546
82.3	0.571
87.7	0.595
93.4	0.618
99.1	0.632
105.2	0.648
111.3	0.667
119.4	0.693
124.5	0.702

#50

COR.TIME MIN	ABSORBANCE COR
8.1	0.024
10.1	0.043
13.5	0.068
15.1	0.077
18.5	0.096
22.1	0.118
26.4	0.134
30.7	0.148
35.4	0.152
40.4	0.163
45.8	0.175
51.1	0.191
56.6	0.210
62.2	0.222
68.0	0.241
75.8	0.260
81.7	0.273
87.1	0.284
92.4	0.296
98.5	0.304
104.5	0.310
110.7	0.326
116.7	0.333
123.7	0.348

#51

COR.TIME MIN	ABSORBANCE COR
6.2	0.021
10.5	0.032
12.0	0.042
14.6	0.043
17.9	0.047
21.5	0.048
25.8	0.052
30.2	0.057
34.8	0.069
39.8	0.076
45.0	0.087
50.6	0.097
56.0	0.103
61.6	0.108
66.8	0.120
75.3	0.129
81.2	0.134
86.6	0.138
91.8	0.142
97.8	0.152
103.7	0.153
110.1	0.158
117.8	0.162
122.7	0.164

#52

COR.TIME MIN	ABSORBANCE COR
3.8	0.017
7.8	0.036
9.5	0.042
12.4	0.055
15.0	0.068
18.2	0.077
21.3	0.091
24.7	0.102
27.5	0.110
30.5	0.122
34.4	0.133
38.8	0.146
42.9	0.168
46.9	0.172
50.3	0.177
53.9	0.193
57.8	0.202
62.0	0.212
65.6	0.218
72.9	0.238
79.0	0.248
83.4	0.258
88.2	0.264
94.5	0.273
100.0	0.287
105.4	0.288
110.5	0.298
114.9	0.302
120.1	0.310
127.3	0.313

#53

COR.TIME MIN	ABSORBANCE COR
5.6	0.069
8.4	0.090
10.0	0.108
12.9	0.134
15.5	0.158
18.6	0.181
21.9	0.209
25.2	0.232
28.2	0.258
31.1	0.278
34.9	0.304
39.3	0.333
43.3	0.358
46.9	0.387
50.3	0.404
54.3	0.424
58.3	0.445
62.5	0.466
66.3	0.486
73.6	0.519
79.6	0.544
84.2	0.562
88.8	0.580
95.0	0.600
100.5	0.615
106.0	0.628
111.1	0.642
115.4	0.652
120.5	0.663
127.5	0.682

#54

COR.TIME MIN	ABSORBANCE COR
7.1	0.142
9.0	0.149
10.5	0.172
13.5	0.217
16.0	0.242
19.3	0.285
22.5	0.329
25.8	0.362
28.8	0.396
31.9	0.433
35.4	0.466
38.5	0.492
43.6	0.547
47.9	0.586
51.2	0.617
54.8	0.641
58.5	0.677
63.1	0.706
66.8	0.732
74.1	0.778
80.1	0.815
84.5	0.840
89.2	0.862
95.5	0.886
101.1	0.912
106.4	0.931
111.7	0.952
118.8	0.972
120.8	0.982
128.2	1.000

#55

COR.TIME MIN	ABSORB COR	ORDINATES COR
7.5	0.006	0.022
12.3	0.041	0.094
16.4	0.071	0.160
22.5	0.103	0.239
28.2	0.128	0.307
35.8	0.168	0.424
43.1	0.195	0.516
49.6	0.221	0.612
57.6	0.247	0.722
66.6	0.268	0.829
75.5	0.286	0.934
83.7	0.298	1.020
92.6	0.315	1.142
99.2	0.326	1.234
106.1	0.334	1.317
113.5	0.341	1.404
120.5	0.345	1.470
126.1	0.346	0.0
131.8	0.354	0.0
212.0	0.370	0.994
249.0	0.364	1.010
279.0	0.357	1.030
307.0	0.350	1.049
335.0	0.337	1.087
365.0	0.322	1.133
397.0	0.309	1.177
425.0	0.294	1.224
455.0	0.281	1.269
484.0	0.270	1.309
516.0	0.251	1.382
544.0	0.245	1.406

#56

COR.TIME MIN	ABSORB COR	ORDINATES COR
8.8	-0.014	0.001
13.0	0.004	0.056
17.2	0.024	0.119
23.3	0.050	0.210
29.0	0.077	0.309
36.6	0.096	0.403
43.9	0.117	0.511
50.5	0.135	0.614
60.3	0.160	0.781
67.1	0.164	0.845
75.9	0.174	0.960
84.2	0.184	1.062
93.1	0.194	1.225
99.7	0.207	1.392
106.7	0.205	1.447
114.2	0.202	1.499
121.0	0.206	1.617
126.5	0.202	1.1
132.3	0.205	0.0
212.0	0.190	1.660
249.0	0.172	1.760
279.0	0.165	1.801
307.0	0.150	1.897
335.0	0.135	2.002
365.0	0.122	2.103
397.0	0.114	2.171
425.0	0.100	2.302
455.0	0.088	2.430
484.0	0.082	2.531
516.0	0.070	2.659
544.0	0.063	2.764

#57

COR.TIME MIN	ABSORB COR	ORDINATES COR
9.5	-0.004	0.012
13.9	0.016	0.068
18.2	0.038	0.132
24.3	0.065	0.218
30.2	0.090	0.305
37.5	0.120	0.422
45.0	0.148	0.548
51.4	0.167	0.645
58.5	0.177	0.717
68.3	0.196	0.850
76.6	0.207	0.949
85.1	0.220	1.071
94.1	0.229	1.184
100.6	0.238	1.293
107.6	0.244	1.391
115.2	0.250	1.504
121.9	0.250	1.558
127.4	0.252	0.0
133.1	0.256	0.0
212.0	0.238	1.354
249.0	0.230	1.386
279.0	0.240	1.427
307.0	0.224	1.496
335.0	0.213	1.546
365.0	0.199	1.614
397.0	0.187	1.676
425.0	0.171	1.766
455.0	0.164	1.807
484.0	0.154	1.870
516.0	0.143	1.966
544.0	0.132	2.024

#58

COR.TIME MIN	ABSORB COR	ORDINATES COR
10.7	0.008	0.047
15.3	0.029	0.088
19.4	0.032	0.129
25.8	0.058	0.215
32.8	0.088	0.324
39.4	0.115	0.433
45.9	0.136	0.532
52.8	0.162	0.644
61.1	0.183	0.759
69.5	0.201	0.938
77.1	0.214	1.061
86.7	0.223	1.186
95.1	0.234	1.333
101.6	0.237	1.413
108.7	0.241	1.514
116.7	0.246	0.0
122.4	0.243	1.414
128.5	0.245	1.406
130.1	0.245	1.406
212.0	0.228	1.478
249.0	0.220	1.514
279.0	0.207	1.575
307.0	0.195	1.634
335.0	0.183	1.698
365.0	0.167	1.789
397.0	0.157	1.851
425.0	0.140	1.966
455.0	0.129	2.047
484.0	0.120	2.120
516.0	0.110	2.207
544.0	0.103	2.272

#59

COR.TIME MIN	ABSORB COR	ORDINATES COR
11.2	0.047	0.128
14.9	0.063	0.175
19.3	0.083	0.235
22.9	0.093	0.273
27.1	0.105	0.318
31.7	0.120	0.376
33.7	0.123	0.392
39.4	0.130	0.438
47.5	0.150	0.534
53.2	0.162	0.596
59.4	0.169	0.651
65.8	0.172	0.695
72.0	0.176	0.742
80.8	0.187	0.834
90.7	0.196	0.932
97.4	0.201	0.997
106.0	0.202	1.057
131.3	0.238	0.0
248.0	0.226	0.0
297.0	0.210	1.560
339.0	0.180	1.671
387.0	0.161	1.795
434.0	0.144	1.937
479.0	0.129	2.120
518.0	0.106	2.244

#62

COR.TIME MIN	ABSORB COR	ORDINATES COR
8.6	0.254	0.194
13.1	0.313	0.245
15.6	0.353	0.283
18.6	0.385	0.318
23.7	0.446	0.384
27.9	0.492	0.439
32.8	0.540	0.503
38.9	0.600	0.576
45.8	0.668	0.675
52.2	0.712	0.749
58.6	0.765	0.843
65.2	0.813	0.938
71.8	0.852	1.027
81.3	0.892	1.134
93.1	0.926	1.241
97.0	0.954	1.341
105.4	0.975	1.437
131.0	1.038	0.0
248.3	1.064	-0.062
297.0	1.016	-0.015
339.0	0.964	0.036
382.0	0.916	0.087
434.0	0.864	0.140
479.0	0.803	0.223
518.0	0.764	0.269

#63

COR.TIME MIN	ABSORB COR	ORDINATES COR
4.4	0.313	0.067
8.3	0.016	0.116
12.3	0.024	0.178
16.5	0.034	0.256
21.6	0.046	0.358
26.0	0.054	0.439
29.7	0.064	0.536
33.9	0.070	0.614
38.6	0.070	0.650
44.2	0.072	0.712
49.6	0.076	0.794
55.4	0.070	0.784
62.6	0.084	0.998
69.1	0.082	1.137
73.0	0.080	1.059
80.5	0.084	1.181
87.7	0.092	1.392
94.6	0.084	1.339
101.7	0.086	1.462
108.8	0.088	1.598
119.8	0.084	1.666
128.8	0.084	0.1
150.6	0.082	2.501
192.0	0.076	2.577
264.0	0.060	2.813
300.0	0.056	2.882
330.0	0.044	3.123
364.0	0.040	3.218
400.0	0.034	3.381
427.0	0.034	3.381
460.0	0.024	3.729
490.0	0.024	3.729
508.0	0.018	4.017
550.0	0.012	4.422
578.0	0.018	4.017
602.0	0.012	4.422

#64

COR.TIME MIN	ABSORB COR	ORDINATES COR
5.2	0.044	0.070
9.1	0.064	0.106
13.0	0.092	0.156
17.5	0.124	0.217
22.2	0.154	0.279
26.7	0.178	0.328
30.4	0.196	0.375
34.8	0.226	0.446
39.3	0.238	0.482
44.9	0.264	0.555
50.3	0.284	0.618
56.1	0.304	0.686
63.3	0.324	0.762
69.7	0.344	0.842
74.5	0.360	0.910
81.3	0.376	0.990
88.3	0.392	1.077
95.5	0.404	1.155
102.5	0.412	1.220
109.4	0.426	1.319
118.8	0.436	1.419
429.6	0.446	0.0
151.2	0.464	0.0
192.0	0.478	0.0
264.3	0.476	0.742
300.0	0.456	0.785
330.0	0.436	0.830
364.0	0.426	0.853
402.0	0.406	0.901
427.0	0.396	0.926
460.0	0.374	0.983
490.0	0.356	1.032
508.0	0.344	1.067
550.0	0.332	1.106
578.0	0.316	1.152
602.0	0.304	1.190

#65

COR.TIME MIN	ABSORB COR	ORDINATES COR
5.9	0.064	0.074
9.9	0.133	0.119
13.7	0.136	0.166
18.7	0.184	0.232
23.4	0.224	0.292
27.5	0.256	0.363
31.1	0.284	0.390
35.5	0.312	0.441
39.9	0.344	0.501
45.7	0.380	0.574
51.0	0.408	0.638
57.0	0.444	0.723
64.1	0.476	0.810
70.4	0.500	0.884
75.2	0.524	0.958
82.3	0.556	1.012
89.2	0.584	1.117
96.3	0.584	1.207
103.2	0.604	1.305
110.2	0.616	1.382
119.4	0.640	1.529
130.3	0.656	0.0
151.9	0.676	0.0
192.3	0.670	0.0
264.3	0.680	0.385
300.0	0.666	0.406
330.0	0.646	0.436
364.0	0.624	0.471
400.3	0.598	0.517
427.0	0.576	0.551
460.3	0.556	0.586
490.3	0.534	0.627
508.0	0.516	0.661
550.0	0.492	0.709
578.0	0.474	0.746
602.3	0.456	0.785

#66

COR.TIME MIN	ABSORB COR	ORDINATES COR
6.7	0.056	0.083
10.9	0.084	0.126
14.6	0.108	0.169
19.6	0.144	0.233
24.4	0.170	0.283
28.4	0.194	0.332
32.1	0.222	0.389
36.7	0.236	0.425
41.0	0.262	0.486
46.5	0.284	0.544
51.7	0.300	0.591
58.3	0.324	0.663
64.8	0.344	0.731
71.2	0.366	0.809
75.8	0.384	0.875
82.8	0.400	0.946
89.8	0.412	1.010
96.8	0.434	1.115
104.0	0.446	1.190
113.8	0.456	1.261
123.1	0.464	1.338
131.1	0.480	0.0
153.0	0.496	0.0
192.3	0.514	0.0
264.0	0.506	0.681
300.0	0.500	0.693
330.0	0.480	0.733
364.0	0.466	0.763
400.3	0.450	0.798
427.0	0.436	0.830
460.0	0.416	0.877
490.3	0.404	0.906
508.0	0.386	0.951
550.0	0.368	0.999
578.0	0.352	1.044
602.3	0.342	1.072

#67

COR.TIME MIN	ABSORB COR	ORDINATES COR
4.5	0.035	0.083
8.1	0.046	0.115
11.2	0.060	0.154
15.4	0.076	0.202
19.5	0.090	0.246
24.0	0.106	0.299
28.6	0.118	0.344
32.4	0.128	0.383
36.5	0.134	0.411
42.2	0.146	0.463
45.9	0.157	0.509
51.6	0.170	0.571
55.9	0.180	0.620
64.0	0.199	0.723
73.6	0.208	0.792
78.6	0.216	0.846
85.5	0.224	0.910
92.6	0.233	0.985
98.1	0.238	1.035
104.4	0.242	1.085
109.8	0.252	1.172
116.8	0.256	1.232
122.2	0.258	1.273
138.3	0.266	0.0
215.3	0.295	0.0
253.3	0.297	0.0
309.0	0.278	1.280
344.9	0.267	1.320
405.0	0.251	1.382
438.0	0.232	1.461
469.3	0.222	1.505
501.0	0.208	1.570
533.9	0.198	1.619
561.3	0.188	1.671

#68

COR.TIME MIN	ABSORB COR	ORDINATES COR
5.3	0.035	0.052
8.7	0.046	0.072
11.8	0.062	0.099
16.4	0.092	0.148
20.2	0.112	0.184
24.7	0.133	0.224
29.4	0.157	0.274
33.8	0.175	0.309
37.1	0.189	0.340
43.1	0.213	0.396
46.6	0.229	0.433
52.3	0.252	0.491
56.9	0.270	0.540
65.2	0.298	0.623
72.2	0.322	0.700
79.2	0.333	0.751
86.6	0.357	0.839
93.5	0.372	0.908
98.6	0.382	0.958
105.3	0.398	1.036
113.3	0.410	1.101
116.4	0.418	1.159
122.7	0.424	1.213
137.8	0.443	0.0
215.3	0.496	0.0
250.0	0.488	0.0
309.0	0.457	0.783
344.3	0.434	0.834
405.0	0.398	0.921
438.0	0.372	0.988
469.0	0.348	1.055
501.0	0.332	1.102
533.3	0.308	1.177
561.0	0.293	1.227

#69

COR.TIME MIN	ABSORB COR	ORDINATES COR
6.4	0.147	0.107
9.3	0.172	0.132
12.7	0.203	0.164
17.3	0.244	0.207
20.9	0.270	0.245
25.4	0.323	0.293
33.1	0.362	0.341
34.4	0.395	0.385
37.8	0.421	0.420
43.9	0.460	0.479
47.3	0.483	0.515
51.3	0.518	0.574
57.0	0.543	0.622
65.9	0.586	0.707
73.3	0.612	0.773
80.1	0.643	0.850
86.7	0.660	0.909
94.2	0.687	0.992
99.9	0.732	1.048
105.7	0.716	1.110
111.0	0.732	1.174
116.1	0.744	1.232
123.2	0.752	1.300
137.2	0.767	0.0
215.0	0.798	0.225
250.0	0.770	0.261
309.0	0.690	0.371
344.3	0.633	0.457
405.0	0.548	0.601
438.0	0.494	0.705
469.3	0.453	0.791
501.0	0.413	0.884
533.0	0.375	0.980
561.0	0.348	1.055

#70

COR.TIME MIN	ABSORB COR	ORDINATES COR
7.0	0.113	0.128
10.1	0.128	0.150
13.6	0.158	0.191
18.3	0.189	0.236
22.0	0.220	0.283
26.2	0.238	0.315
31.0	0.268	0.365
35.4	0.294	0.412
38.7	0.310	0.443
44.7	0.341	0.505
48.4	0.356	0.539
54.4	0.390	0.605
58.3	0.405	0.652
66.6	0.440	0.781
73.6	0.461	0.807
80.7	0.482	0.876
87.8	0.500	0.943
95.1	0.523	1.029
100.1	0.538	1.090
106.5	0.543	1.145
111.5	0.558	1.198
117.6	0.570	1.264
123.9	0.581	1.333
139.3	0.598	0.0
215.0	0.671	0.0
250.0	0.695	0.0
309.3	0.623	0.473
344.0	0.582	0.507
405.0	0.558	0.583
438.0	0.531	0.632
469.0	0.503	0.687
501.0	0.483	0.733
533.0	0.457	0.783
561.3	0.437	0.827

REFERENCES

1. A.P. Ginsberg, Transition Metal Chemistry, Vol. 1, ed. R.L. Carlin, Marcel Dekker, Inc., New York, 1965, p. 113.
2. J.P. Blackledge, Metal Hydrides, ed. W.M. Mueller, J.P. Blackledge, G.G. Libowitz, Academic Press, New York, 1968, p. 12.
3. A. Wurtz, Compt. Rend., 18 (1844) 702; cf. ref. 1.
4. D.T. Hurd, Chemistry of the Hydrides, John Wiley & Sons, Inc., New York, 1952, p. 44.
5. T. Graham, Philos. Trans. R. Soc. London (1866) 156 415.
6. T.B. Flanagan, W.A. Oates, Transition Metal Hydrides, ed. R. Bau, (Adv. in Chem., 167), American Chemical Society, Washington, D.C., 1978, p. 283.
7. Ref. 1, p. 114.
8. G. Wilkinson, J.M. Birmingham, J. Am. Chem. Soc., 77 (1955) 3421.
9. J. Chatt, L.A. Duncanson, B.L. Shaw, Proc. Chem. Soc. (1957) 343.
10. H.D. Kaesz, R.B. Saillant, Chem. Rev., 72 (1972) 231.
11. G.L. Geoffroy, J.R. Lehman, Adv. in Inorg. and Radiochem., Vol. 20, ed. H.J. Emeléus, A.G. Sharpe, Academic Press, New York, 1977, p. 189.
12. G.L. Geoffroy, M.G. Bradley, R. Pierantozzi, Transition Metal Hydrides, (ref. 6) p. 181.
13. G.G. Libowitz, The Solid-State Chemistry of Binary Metal Hydrides, W.A. Benjamin, Inc., New York, 1965, p. 94.
14. Ref. 2, pp. 3-5.
15. E.L. Muetterties, Transition Metal Hydrides, ed. E.L. Muetterties, Marcel Dekker, Inc., New York, 1971, p. 11.
16. K.M. Mackay, Hydrogen Compounds of the Metallic Elements, E. & F.N. Spon, Ltd., London, 1966, p. 85.
17. E.O. Wollan, J.W. Cable, W.C. Koehler, J. Phys. Chem. Solids, 24 (1963) 1141; cf. R.W. Broach, et al., ref. 6, p. 106.
18. Transition Metal Hydrides, ref. 6, pp. 302-381 and references therein.
19. K.M. Mackay, ref. 16, p. 47, and references therein.
20. See, for example, Transition Metal Hydrides (ref. 6), pp. 1, 11, 36, 61, 93 and 215.
21. J.P. Collman, W.R. Roper, Advances in Organometallic Chemistry, Vol. 7, ed. F.G.A. Stone and R. West, Academic Press, New York, 1968, p. 54.
22. A.P. Ginsberg, Transition Metal Hydrides (ref. 6) p. 201.
23. T.F. Koetzle, R.K. McMullan, R. Bau, D.W. Hart, R.G. Teller, D.L. Tipton, R.D. Wilson, ibid., p. 61.

24. E.L. Muetterties, Angewandte Chemie, 90 (1978) 577.
25. J.P. Jesson, Transition Metal Hydrides (ref. 15) p. 75.
26. D. Giusto, Inorg. Chem. Acta Rev., 6 (1972) 91.
27. Transition Metal Hydrides (ref. 15), chpts. 3, 4, and 5.
28. M.L.H. Green, D. Jones, Advances in Inorganic Chemistry and Radiochemistry, Vol. 7, ed. H. Emeléus and A. Sharpe, Academic Press, New York, 1965, p. 115.
29. J.P. McQue, Coord. Chem. Rev. (1973) 10 265.
30. D.M. Roundhill, Advances in Organometallic Chemistry, Vol. 13, ed. F.G.A. Stone and R. West, Academic Press, New York, 1975, p. 274.
31. J. Chatt, ibid., Vol. 12 (1974) p. 1.
32. J.L. Petersen, L.F. Dahl, J.M. Williams, Transition Metal Hydrides (ref. 6) p. 11.
33. M. Ciriano, M. Green, J. Howard, M. Murray, J.L. Spencer, F.G.A. Stone and C.A. Tsipis, ibid., p. 111.
34. M.R. Churchill, ibid., p. 42.
35. R.W. Baker, P. Pauling, J. Chem. Soc., (Chem. Comm.) (1969) 1495.
36. S. Datta, B. Dezube, J.K. Kouba, S.S. Wreford, J. Am. Chem. Soc., 100 (1978) 4404.
37. P.N. Rylander, Catalytic Hydrogenation over Platinum Metals, Academic Press, New York, 1967.
38. F.A. Cotton, G. Wilkinson, Advanced Inorganic Chemistry, 3rd ed., Interscience Publishers, New York, 1972, p. 792 and following pages.
39. R.F. Heck, Organotransition Metal Chemistry: A Mechanistic Approach, Academic Press, New York, 1974, p. 59.
40. B.R. James, Advances in Organometallic Chemistry, Vol. 17, ed. by F.G.A. Stone, R. West, Academic Press, New York, 1979, p. 319.
41. A.J. Chalk, J.F. Harrod, ibid., Vol. 6 (1968) p. 119.
42. J.L. Speier, ibid, Vol. 17 (1979) p. 407.
43. R.L. Pruett, ibid., p. 1.
44. J.F. Harrod, C.A. Smith, J. Am. Chem. Soc., 92 (1970) 2699.
45. J.F. Harrod, C.A. Smith, K.A. Than, ibid., 94 (1972) 8321.
46. A.J. Chalk, J.F. Harrod, J. Am. Chem. Soc., 87 (1965) 16.
47. A.J. Maeland, Transition Metal Hydrides, ref. 6, p. 302.
48. G.G. Libowitz, Critical Material Problems in Energy Production, ed. C. Stein, Academic Press, New York, 1976, p. 825; cf. ref. 6, p. 303.
49. Transition Metal Hydrides, ref. 6, pp. 302-382.
50. Ibid., p. 303 and 366.
51. L. Vaska, M.F. Werneke, Trans. New York Acad. Sci., 33 (1971) 70.
52. G.L. Geoffroy, H.B. Gray, G.S. Hammond, J. Am. Chem. Soc., 97 (1975) 3933.
53. G.L. Geoffroy, R. Pierantozzi, J. Am. Chem. Soc., 98 (1976) 8054.

54. K. Elmit, M.L.H. Green, R.A. Forder, F. Jefferson, K. Prout, J. Chem. Soc. (Chem. Comm.) (1974) 747.
55. C. Grannotti, M.L.H. Green, ibid. (1972) 1114.
56. L. Farrugia, M.L.H. Green, ibid. (1975) 416.
57. C. Masters, Advances in Organometallic Chemistry, ref. 40 (1979) p. 61.
58. J.M. Lehn, J.P. Sauvage, Nouveau Journal de Chimie, 1 (1977) 449 and references therein.
59. J.M. Lehn, J.P. Sauvage, R. Ziessel, ibid, 3 (1979) 423.
60. G. Sprintschnik, H.W. Sprintschnik, P.P. Kirsch, D.G. Whitten, J. Am. Chem. Soc., 99 (1977) 4947.
61. G.L. Gaines, Jr., P.E. Behnken, S.J. Valenty, ibid., 100 (1978) 6549.
62. G.M. Brown, B. Brunschwig, C. Creutz, J. Endicott, N. Sutin, ibid., 101 (1979) 1300.
63. T. Yoschida, Y. Ueda, S. Otsuki, J. Am. Chem. Soc., 100 (1978) 3941.
64. T. Yoschida, T. Matsuda, T. Okano, T. Kitani, S. Otsuka, J. Am. Chem. Soc., 101 (1979) 2027.
65. W. Hieber, H. Schulten, B. Marin, Z. Anorg. Allg. Chem., 240 (1939) 261; cf. ref. 28.
66. See R.A. Schunn, Transition Metal Hydrides, ref. 15, p. 209, 210 and 212.
67. Ibid., p. 232.
68. T.J. Marks, J.R. Kolb, Chem. Rev., 77 (1977) 263.
69. J. Chatt, R.S. Coffey, B.L. Shaw, J. Chem. Soc., (1965) 7391.
70. H. Yamazaki, M. Takesada, N. Hagehara, Bull. Chem. Soc. Japan, 42 (1969) 275.
71. L. Vaska, J. Am. Chem. Soc., 88 (1966) 5325.
72. G. Parshall, Acc. Chem. Res., 3 (1970) 139; J. Dehaud, M. Pfeffer, Coord. Chem. Rev., 18 (1976) 327.
73. H.C. Clark, K.R. Dixon, W.J. Jacobs, J. Am. Chem. Soc., 91 (1969) 1346.
74. H.C. Clark, W.J. Jacobs, Inorg. Chem., 9 (1970) 1229.
75. J. Powell, B.L. Shaw, J. Chem. Soc. (A) (1968) 617.
76. J.P. Yesinowski, T.L. Brown, Inorg. Chem., 10 (1971) 1097; ref. 38.
77. F. Basolo, R.G. Pearson, Mechanisms of Inorganic Reactions, 2nd ed., John Wiley & Sons, Inc., New York, 1968, p. 375; ref. 207.
78. D.H. Gerlach, W.G. Peet, E.L. Muetterties, J. Am. Chem. Soc., 94 (1972) 4545; ref. 10 and 11.
79. G.B. Young, G.M. Whitesides, ibid., 100 (1978) 5808.
80. L. Malatesta, G. Caglio, M. Angoletta, J. Chem. Soc. (1965) 6974.
81. Ref. 142, 143; ref. 11, p. 196.
82. See ref. 28 and references therein.
83. L. Vaska, J.W. DiLuzio, J. Am. Chem. Soc., 83 (1961) 2784.
84. J. Halpern, Acc. Chem. Res., 3 (1970) 386.
85. L. Vaska, ibid., 1 (1968) 335.

86. J.P. Collman, ibid., 1 (1968) 136.
87. B.R. James, Homogeneous Hydrogenation, John Wiley & Sons, Inc., New York, 1973.
88. Inorganic Reaction Mechanisms, Specialist Periodical Reports, The Chemical Society, London, published yearly since 1969.
89. J.P. Collman, Acc. Chem. Res., 10 (1977) 265.
90. F. Basolo, B.M. Hoffmann, J.A. Ibers, ibid., 8 (1975) 384.
91. L. Vaska, ibid., 9 (1976) 175.
92. A.D. Allen, F. Bottomley, ibid., 1 (1968) 360.
93. J. Chatt, J. Organomet. Chem., 100 (1975) 17.
94. A. Sacco, M. Rossi, J. Chem. Soc. (Chem. Comm.) (1967) 316.
95. H.F. Schaefer, III, Acc. Chem. Res., 10 (1977) 287.
96. L. Vaska, J.W. DiLuzio, J. Am. Chem. Soc., 84 (1962) 679.
97. P. Chock, J. Halpern, J. Am. Chem. Soc., 88 (1966) 3511.
98. E.M. Miller, B.L. Shaw, J. Chem. Soc. (Dalton) (1974) 480.
99. B.L. Shaw, J. Organomet. Chem., 94 (1975) 251.
100. E.M. Hyde, B.L. Shaw, J. Chem. Soc. (Dalton) (1975) 765.
101. R. Ugo, A. Pasini, A. Fusi, S. Cenini, J. Am. Chem. Soc., 94 (1972) 7364.
102. N.E. Burke, A. Singhal, M.J. Hintz, J.A. Ley, H. Hui, L.R. Smith, D.M. Blake, J. Am. Chem. Soc., 101 (1979) 74, and references therein.
103. B.L. Shaw, R.E. Stainbank, J. Chem. Soc. (Dalton) (1972) 224.
104. A.J. Deeming, B.L. Shaw, J. Chem. Soc. (A) (1969) 1128.
105. M.S. Fraser, W.H. Baddley, J. Organomet. Chem., 36 (1972) 377.
106. M.S. Fraser, G.F. Everitt, W.H. Baddley, ibid., 35 (1972) 403.
107. J. Chatt, J.M. Davidson, J. Chem. Soc. (1965) 843.
108. G.W. Parshall, Acc. Chem. Res., 8 (1975) 113.
109. See ref. 53, 72 and 190 for examples.
110. D.M. Blake, M. Kubota, Inorg. Chem., 9 (1970) 989.
111. R.G. Pearson, W.R. Muir, J. Am. Chem. Soc., 92 (1970) 5511.
112. R.W. Johnson, R.G. Pearson, J. Chem. Soc. (Chem. Comm.) (1970) 986.
113. J.A. Labinger, R.J. Braus, D. Dolphin, J.A. Osborn, ibid., 612.
114. G.M. Whitesides, D.J. Boschetto, J. Am. Chem. Soc., 93 (1971) 1529.
115. F.R. Jenson, B. Knickel, ibid., 6339.
116. J.A. Labinger, A.V. Kramer, J.A. Osborn, ibid., 95 (1973) 7908.
117. J.P. Fawcett, J.F. Harrod, Can. J. Chem., 54 (1976) 3102.
118. D.H. Gerlach, A.R. Kane, G.W. Parshall, J.P. Jesson, E.L. Muetterties, J. Am. Chem. Soc., 93 (1971) 3543.
119. J.F. Harrod, G. Hamer, W. Yorke, J. Am. Chem. Soc., 101 (1979) 3987 and references therein.
120. R.G. Pearson, Acc. Chem. Res., 4 (1971) 1952.

121. M.L. Tobe, Inorganic Reaction Mechanisms, Thomas Nelson and Sons, Ltd., London, 1972.
122. J.P. Collman, C.T. Sears, Inorg. Chem., 7 (1968) 27.
123. R.N. Haszeldine, R.V. Parish, J.H. Setchfield, J. Organomet. Chem., 57 (1973) 279.
124. B. Longato, F. Morandini, S. Bresadola, Inorg. Chem., 15 (1976) 650.
125. See, for example, M.D. Fryzuk, B. Bosnich, J. Am. Chem. Soc., 101 (1979) 3043.
126. Ref. 38, p. 776.
127. J. Halpern, M. Pribanić, Inorg. Chem., 9 (1970) 2616; C.S. Sokol, C.H. Brubaker, J. Inorg. Nucl. Chem., 30 (1968) 3267.
128. P.C. Ford, R.G. Rinker, C. Ungermann, R.M. Laine, V. Landis, S. Moya, J. Am. Chem. Soc., 100 (1978) 4595.
129. C.K. Brown, W. Mowat, G. Yagupsky, G. Wilkinson, J. Chem. Soc. (A) (1971) 850.
130. G. Yagupsky, G. Wilkinson, ibid. (1969) 725.
131. L. Vaska, Inorg. Nucl. Chem. Lett., 1 (1965) 89.
132. M.G. Burnett, R.J. Morrison, J. Chem. Soc. (A) (1971) 2325.
133. M.G. Burnett, R.J. Morrison, C.J. Strugnell, J. Chem. Soc. (Dalton) (1973) 701; (1974) 1663.
134. M.G. Burnett, R.J. Morrison, ibid. (1973) 632.
135. M.G. Burnett; C.J. Strugnell, J. Chem. Res. (1977) (S) 250, (M) 2935.
136. C. O'Connor, G. Wilkinson, J. Chem. Soc. (A) (1968) 2665.
137. L. Vaska, M.E. Tadros, J. Am. Chem. Soc., 93 (1971) 7099.
138. R.A. Schunn, Inorg. Chem., 9 (1970) 2567.
139. M. Martelli, S. Schravon, S. Zecchin, G. Pilloni, Inorg. Chim. Acta, 15 (1975) 217.
140. J.A. van Doorn, C. Masters, C. van der Woude, J. Organomet. Chem., 141 (1977) 231.
141. J.A. van Doorn, C. van der Woude, J. Chem. Soc. (Dalton) (1978) 1213.
142. B.E. Mann, C. Masters, B.L. Shaw, J. Inorg. Nucl. Chem., 33 (1971) 2195.
143. B.E. Mann, C. Masters, B.L. Shaw, J. Chem. Soc. (Chem. Comm.) (1970) 846.
144. B.L. Shaw, R.E. Stainbank, J. Chem. Soc. (Dalton) (1972) 2108.
145. W.R. Roper, K.G. Town, J. Chem. Soc. (Chem. Comm.) (1977) 781.
146. R. Zanella, F. Canziani, R. Ros, M. Groziani, J. Organomet. Chem., 67 (1974) 449.
147. J.J. Levison, S.D. Robinson, J. Chem. Soc. (A) (1970) 2947.
148. R. Bau, W. Carroll, D. Hart, R. Teller, T. Koetzle, Transition Metal Hydrides (ref. 6) p. 73, and references therein.
149. M. Angoletta, G. Caglio, Gazz. Chim. Ital., 99 (1969) 46.

150. F. Canziani, F. Zinglaes, Red. Inst. Lombardo Sci. Lettere A, 96 (1962) 513. Chem. Abs., 62: 11401.
151. J.M. Jenkins, B.L. Shaw, J. Chem. Soc. (A) (1966) 1407.
152. A. Araneo, F. Bonati, G. Minghetti, J. Organomet. Chem., 25 (1970) C25.
153. S.S. Bath, L. Vaska, J. Am. Chem. Soc., 85 (1963) 3500. An alternate preparation was reported by L. Malatesta at the same time (cf. ref. 153).
154. G. Wilkinson, R.A. Schunn, W.G. Peet, Inorg. Syn., 13 (1972) 126-129.
155. J.F. Harrod, D.F.R. Gilson, R. Charles, Can. J. Chem., 47 (1969) 1431.
156. Personal observations.
157. S.J. LaPlaca, J.A. Ibers, J. Am. Chem. Soc., 85 (1963) 3501.
158. J.J. Levison, S.D. Robinson, J. Chem. Soc. (Dalton) (1972) 2013.
159. J.F. Harrod, D.F.R. Gilson, R. Charles, Can. J. Chem., 47 (1969) 2205.
160. C.K. Brown, D. Georgion, G. Wilkinson, J. Chem. Soc. (Dalton) (1973) 929.
161. R. Mason, I. Søtofte, S.D. Robinson, M.F. Uttley, J. Organomet. Chem., 46 (1972) C61.
162. P.L. Bellon, C. Benedicenti, G. Caglio, M. Manassero, J. Chem. Soc. (Chem. Comm.) (1973) 946.
163. M. Angoletta, G. Caglio, Red. Inst. Lombardo Sci. Lettere A, 97 (1963) 823.
164. References 11, 28, 154; L.M. Venanzi, Platinum Group Metals and Compounds, American Chemical Society, Washington, D.C., 1971, Adv. in Chem. Ser. 98; W.P. Griffith, The Chemistry of the Rarer Platinum Metals, Interscience Publishers, New York, 1967; S.E. Livingstone, Comprehensive Inorganic Chemistry, Vol. 3, Pergamon Press, New York, 1973, p. 1262; S.C. Tripathi, S.C. Scrivastava, R.P. Mani, A.K. Shrimal, Inorg. Chim. Acta, 17 (1976) 257.
165. C. O'Connor, G. Yagupsky, D. Evans, G. Wilkinson, J. Chem. Soc. (Chem. Comm.) (1965) 420.
166. J.P. Collman, F. Vastine, W.R. Roper, J. Am. Chem. Soc., 90 (1968) 2282.
167. M. Ciechanowicz, A.C. Skapski, P.G.H. Troughton, Acta Crystallog., B32 (1976) 1673.
168. B.E. Mann, C. Masters, B.L. Shaw, J. Chem. Soc. (Chem. Comm.) (1970) 703.
169. D. Evans, G. Yagupsky, G. Wilkinson, J. Chem. Soc. (A) (1968) 2660 and 2665.
170. R. Poddar, U. Agarwada, J. Inorg. Nucl. Chem., 36 (1974) 575.
171. A.J. Chalk, J. Chem. Soc. (Chem. Comm.) (1969), 1207.

172. J.P. Fawcett, J.F. Harrod, J. Organomet. Chem., 113 (1976) 245.
173. E.D. Becker, High Resolution NMR, Academic Press, New York, 1969.
174. F.A. Bovey, Nuclear Magnetic Resonance Spectroscopy, Academic Press, New York, 1969.
175. R.C. Taylor, J.F. Young, G. Wilkinson, Inorg. Chem., 5 (1966) 20.
176. A.J. Deeming, B.L. Shaw, J. Chem. Soc. (A) (1968) 1887. See ref. 141 for trans Cl configuration.
177. R.J. Abraham, The Analysis of High Resolution NMR Spectra, Elsevier Publishing Co., New York, 1971, p. 87 and 311.
178. E.J. Rosenbaum, Physical Chemistry, Appelton-Century-Crofts, Inc., 1970.
179. L. Vaska, R.E. Rhodes, J. Am. Chem. Soc., 87 (1965) 4970.
180. P. Meakin, E.L. Muetterties, J.P. Jesson, J. Am. Chem. Soc., 95 (1973) 75, and references therein.
181. P. Meakin, L.J. Guggenberger, W.G. Peet, E.L. Muetterties, J.P. Jesson, ibid., 1467.
182. J.S. Miller, K.G. Caulton, ibid., 97 (1975) 1067.
183. R.K. Pomeroy, W.A.G. Graham, ibid., 94 (1972) 274.
184. L. Vaska, W.V. Miller, B.R. Flynn, J. Chem. Soc. (Chem. Comm.) (1971) 1615.
185. L. Vaska, J. Am. Chem. Soc., 88 (1966) 4100.
186. A.J. Deeming, B.L. Shaw, J. Chem. Soc. (Chem. Comm.) (1968) 751.
187. B. Longato, S. Bresadola, Inorg. Chim. Acta, 33 (1979) 189.
188. M.F. Hawthorne, T.E. Berry, P.A. Wegner, J. Am. Chem. Soc., 87 (1965) 4746.
189. L. Vaska, J. Chem. Soc. (Chem. Comm) (1966) 614.
190. F. Morandini, B. Longato, S. Bresadola, J. Organomet. Chem., 132 (1977) 291.
191. G.W. Parshall, Collected Accounts of Transition Metal Chemistry, Vol. 1, American Chemical Society, Washington, D.C., 1973, p. 209.
192. W.W. Paudler, Nuclear Magnetic Resonance, Allyn and Bacon, Inc., Boston, 1971, p. 84.
193. J. Ronayne, D.H. Williams, J. Chem. Soc. (Chem. Comm.) (1966) 712.
194. H. Batiz-Hernandez, R.A. Bernheim, Progress in NMR Spectroscopy, ed. Esmley, Feeney and Sutcliff, Vol. 3, Pergamon Press, Oxford, 1967, p. 63.
195. Nuclear Magnetic Resonance, Specialist Periodical Reports, Vol. 5, The Chemical Society, London, 1976, p. 45.
196. G.M. Ford, L.G. Robinson, G.B. Savitsky, J. Mag. Res., 4 (1970) 109.
197. F.H. Köhler, W. Prössdorf, J. Am. Chem. Soc., 100 (1978) 5970.

198. H.S. Gutowsky, J. Chem. Phys., 31 (1959) 1683.
199. C.R. Lassigne, E.J. Wells, J. Mag. Res., 31 (1978) 195.
200. C.J. Jameson, J. Chem. Phys., 66 (1977) 4977, 4983.
201. T.G. Appelton, H.C. Clark, L.E. Manzer, Coord. Chem. Rev., 10 (1973) 335.
202. R. Crabtree, J. Quirk, T. Khan-Fillebeen, G. Morris, J. Organomet. Chem., 157 (1978) C13.
203. Quoted by Paudler, ref. 192, p. 76, from H.S. Gutowsky, C.H. Holm, J. Chem. Phys., 25 (1956) 1228.
204. N. Serpone, D.G. Bickley, Inorganic Reaction Mechanisms, Part II, ed. J.O. Edwards, Vol. 17 of Progress in Inorganic Chemistry, Interscience Publishers, New York, 1972, p. 391.
205. D.J. Darensbourg, Inorg. Chem., 18 (1979) 14.
206. P.R. Hoffman, J.S. Miller, C.B. Ungermann, K.G. Caulton, J. Am. Chem. Soc., 95 (1973) 7902.
207. C. Langford, H.B. Gray, Ligand Substitution Reaction Processes, W.A. Benjamin, Inc., New York, 1966; cf. ref. 76.